GA-A13453
UC-77

GAMMA SPECTROSCOPIC EXAMINATION OF PEACH BOTTOM HTGR CORE COMPONENTS

by

J. F. HOLZGRAF, F. McCORD, and C. F. WALLROTH

Prepared under
Contract EY-76-C-03-0167
Project Agreement No. 56
for the San Francisco Operations Office
Department of Energy and the
Electric Power Research Institute

GENERAL ATOMIC PROJECT 3238
DATE PUBLISHED: APRIL 1978

GENERAL ATOMIC COMPANY

DISCLAIMER

DISCLAIMER

Printed in the United States of America
Available from
National Technical Information Service
U.S. Department of Commerce
5285 Port Royal Road
Springfield, Virginia 22161
Price: Printed Copy $8.00; Microfiche $3.00

180
6-29-78

Dr. 215

GA-A13453
UC-77

MASTER

GAMMA SPECTROSCOPIC EXAMINATION OF PEACH BOTTOM HTGR CORE COMPONENTS

by

J. F. HOLZGRAF, F. McCORD, and C. F. WALLROTH

Prepared under
Contract EY-76-C-03-0167
Project Agreement No. 56
for the San Francisco Operations Office
Department of Energy and the
Electric Power Research Institute

DATE PUBLISHED: APRIL 1978

GENERAL ATOMIC COMPANY

FOREWORD

Peach Bottom Atomic Power Station Unit No. 1 was the first installation of a High-Temperature Gas-Cooled Reactor (HTGR) in the United States. Power operation began in January 1967 and commercial operation on June 1, 1967. The plant was operated successfully through October 31, 1974, when it was shut down for decommissioning.

In March 1975, the Peach Bottom End-of-Life Program, cosponsored by ERDA and EPRI, was initiated. The prime objective of this program is to validate specific HTGR design codes and predictions by comparison of actual and predicted physics, thermal, fission product, and materials behavior in the Peach Bottom reactor. These design methods verifications, to be completed in CY-78, utilize the data determined during three consecutive phases of the program, together with the data determined in a complementary program of Peach Bottom driver fuel element postirradiation examinations at ORNL. The three phases are (1) nondestructive fuel and circuit gamma scanning at the Peach Bottom site, (2) removal of Peach Bottom steam generator and primary circuit components, and (3) laboratory examinations of removed components.

This report covers the gamma spectroscopic examinations of Peach Bottom reactor core components sponsored by General Atomic and by ERDA and EPRI under the Peach Bottom End-of-Life Program. Associated analyses and design methods verifications are also included.

ABSTRACT

During discharge of Core 2 from the Peach Bottom High-Temperature Gas-Cooled Reactor (HTGR), 55 driver elements, 21 test elements, three reflector elements, and one control rod with sleeve were axially gamma scanned with a high-resolution Ge(Li) detector. The purpose of the exercise was to determine fission product distributions for use in burnup calculations, power profile determinations, and fission product release and redistribution studies. The results showed that the predicted and measured burnups had a ±7% root mean square deviation on an element-to-element basis and were within ±0.7% (1σ) on a core average basis. The element-to-element variation of ±7% is within the generally stated ±3% to 8% accuracy for nuclear predictions.

The only isotopes detected that redistributed within the elements were Cs-137 and Cs-134. This redistribution was characterized by release in the high-temperature upper portion of some driver elements, movement down the purge stream, and buildup on both sleeve and compact surfaces in the cooler portions of the element; the core average Cs-137 loss via migration through the sleeve into the coolant was undetectable within the measurement uncertainty of ±0.4% (1σ). The scanning of the reflectors and control rods showed low Cs-137 and Cs-134 contamination and some pronounced cesium buildup for the control rod sleeve. Cesium redistribution was found to vary with core position; elements on the periphery of the core exhibited less redistribution than elements near the center owing to higher temperatures.

Measured Pa-233 profiles were found to be slightly different in shape from predicted thorium absorption rates. Radial power factors and their time history were reasonably well modeled. This conclusion was reached from activity measurements for total fuel elements at various radial core locations: long-lived isotopes followed the predicted time-averaged power

distributions, whereas short-lived isotopes were approaching the end-of-life power predictions. Both end-of-life and time-averaged distributions enveloped the isotopic distributions of short- to long-lived nuclides. Axial power profiles were compared with short- and long-lived isotopes. The Cs-137 profiles verified the calculated time-averaged power profiles, and Zr-95 combined with La-140 adequately presented the predicted end-of-life axial power shape. Analysis of single-channel strip charts showed axial expansion of the driver fuel stacks as predicted and accounted for by the fuel element design.

CONTENTS

FIGURES

TABLES

1. INTRODUCTION

The final shutdown of the Peach Bottom HTGR on October 31, 1974, presented a unique opportunity to measure the isotopic distribution of gamma ray emitting radionuclides in about 10% of the fuel elements. Fifty-five fuel driver elements, 21 fuel test elements, three reflector elements, and a control rod and sleeve were axially gamma scanned. A description of the core components is given in Ref 1. The first scanning operation took place from November 24 to December 18, 1974, to measure short-half-lived isotopes; the second phase was between May 28 and June 8, 1975, to detect long-lived isotopes. The elements in Phase I and II scanning operations are listed in Tables 1 and 2, respectively, and are shown in core maps in Figs. 1 and 2.* Phase I was privately funded by General Atomic (GA), and the program was merged with the EPRI/ERDA-sponsored Peach Bottom End-of-Life Program for the Phase II measurements.

The raw spectra of all the gamma scanning were stored on GA SIGMA II tapes (see Table 1). Analysis of these spectra was performed using a spectra integration program (PBGST) and a special data reduction program (PBEOLGS), which are discussed in Section 2.3. The objectives as outlined in the gamma scanning test plan (Ref. 2) are to determine:

1. Axial and radial power distributions.

2. Relative and absolute burnup.

3. Fission product distributions.

---

*Figures and tables appear in Appendixes A and B, respectively.

4. Axial and radial thorium absorption rate distributions near end of life (EOL).

5. Fuel column length changes during irradiation.

The feasibility of gamma spectroscopic examination of HTGR fuel elements had been demonstrated by the Dragon Project (Ref. 3). The methodology for the evaluation of the Peach Bottom EOL gamma scan examination was developed with the analysis of FTE-6 (Ref. 4).

Ten different isotopes, which are listed in Table 3 together with their nuclear constants, were chosen to establish the following types of information:

Isotope	Application
Cs-137 (absolute inventory)	Composite FIMA and Cs-137 loss
La-140 (relative) Zr-95 (relative)	Normalized power distribution for last 50 to 200 days* of reactor operation
Cs-137 (relative)	Normalized time-averaged power distribution**
Cs-134/Cs-137 (relative)	Normalized time-averaged thermal fluence distribution**
Pa-233 (relative)	Normalized Th-232 absorption rates
Cs-137/Zr-95 Ce-141/Zr-95 Ce-144/Zr-95 I-131/Zr-95 Ru-103/Zr-95	Fission product release and redistribution within the element

*Three half-lives assumed.
**Assuming fuel loadings and no cesium migration.

Strip charts of single-channel scans were analyzed to determine the change in fuel stack lengths during irradiation by comparison with preirradiation data.

2. EXPERIMENTAL DESCRIPTION

2.1. EQUIPMENT

The general arrangement of the gamma scanning equipment at Peach Bottom is outlined in Figs. 3 through 5. The major components were a collimator, a charge machine, a Ge(Li) gamma spectrometer, and associated electronic data acquisition equipment.

The Peach Bottom charge machine was outfitted with a gamma scan port that penetrated nearly through its wall; a 12.7-mm steel plate separated the end of the collimator from the charge machine cavity (see Figs. 3 and 4 and Ref. 2). With an element positioned in the charge machine cavity, the collimator system allowed the measurement of gamma ray emissions from a fixed volume of fuel. The collimator geometry and the scanning paths of the two collimators that were used on the majority of the scans are shown in Fig. 6.

The charge machine driver mechanism was modified to slow movement of the element past the collimator slit (Fig. 4). Attached to the driver mechanism shaft were a meter and a single-turn potentiometer, which were calibrated (Ref. 8) and used to visually and electronically monitor the position of the element relative to the collimator system. Additionally, a switch was installed on the driver mechanism shaft and was activated once during each revolution of the shaft. When the switch was activated, a pulse signal was sent for graphical recording, which provided a log of element position as a function of time.

The gamma rays passing through the collimator slit were monitored using a high-resolution Ge(Li) detector. The detector was isolated in a lead case to reduce background activity to a minimum. The signal from the detector was transmitted to two monitoring systems: (1) a pulse height multichannel analyzer (MCA) and (2) a series of single-channel analyzers (SCAs) (Fig. 5). The MCA-accumulated gamma ray spectra were stored on magnetic tape for computer analysis and data processing at GA. The SCA activity data of selected nuclide peaks and their backgrounds were graphically recorded continuously as a function of time on X-Y plotters and at 1-min intervals with scalers and a teletype unit.

2.2. SCANNING PROCEDURE

Two types of measurements were performed on each element: (1) measuring activities while the element was slowly moved past the collimator system (axial scans) and (2) measuring activities at a specified location with the element stationary (static scans). The sequence of each element scan was as follows:

1. Calibration (Cs-137, Co-60 source).
2. Background measurements.
3. Axial scans.
4. Static scans on selected fuel locations.
5. Trap scan.
6. Second calibration (Cs-137, Co-60 source).

2.2.1. Axial Scans

For the axial scans, the element was moved at a constant speed (∿70 mm/min) past the collimator system with all gamma ray monitoring systems operating, i.e., (1) MCA-magnetic tape, (2) SCA-ratemeter-recorder, and (3) SCA-scaler-teletype. The axial scans were generally started 0.6 m and 0.3 m below the start of the fuel column for Phases I and II, respectively, and ended above the top of the fuel column in both Phase I and II scanning. The MCA was operated in a LIVE-TIME mode with a 50-s count time. During the magnetic tape recording operation, no spectrum was being accumulated in the analyzer (∿4.3-s dead-time). The SCA-ratemeter output was continuously graphically recorded along with the pulse signals from the drive mechanism locations and magnetic tape and teletype record pulses. The scalar count times were 60 s with a dead-time of ∿6 s during the teletype record time.

2.2.2. Static Counts

Measurements were made with the elements stationary using both the MCA and SCA scalar systems. The MCA was operated in a LIVE-TIME mode with a count time of 5 min; simultaneously, five 60-s counts were made at each scan location on the element with the SCA scalar systems.

Static counts were made in the top, middle, and bottom sections of the driver fuel column (usually at the center of compacts 5, 16, and 25), in the trap area of the element, and in the graphite portion of the element for background. For test elements, static counts were made at the center of each fuel body and in the trap area. Additional static counts were made on fuel elements selected for destructive postirradiation examination (PIE) or at locations where unusual activity was noted from the SCA graphs.

2.3. DATA PROCESSING

On an average, 50 to 60 spectra were measured for each element and recorded on magnetic tape.

The raw spectra collected at Peach Bottom were transcribed and analyzed using the SIGMA II computer PBGST program at GA (Ref. 7). This program identified the isotope peaks, integrated the area under each peak, subtracted out the background, and calculated the 2σ counting error (Ref. 9). In addition, the program decayed the counts-per-minute (CPM) back to EOL of Core 2 (October 31, 1974, 15.35 hr) and corrected the counts for the relative detector efficiency, absolute intensity, attenuation of the 12.7-mm steel plate, and approximate attenuation of the fuel bodies. These corrections (see Table 3) gave a modified CPM value which is approximately proportional to the disintegration rate of the various isotopes. These corrections were not used in the following analysis because of an absolute calibration technique described in Section 2.4; however, comparison with absolute values showed the relative corrections to be within measurement errors (Ref. 7).

The processed SIGMA II tape was then translated to the UNIVAC-1110 (Ref. 10) for data analysis. Tabulation of element scans, calculations of absolute CPM and composite FIMA values, and comparisons and plots of isotope profiles were all done using the PBEOLGS program (Ref. 11). The entire PBEOLGS data package for element E14-01 is presented in Appendix C as an example. The tables and calculations are described in Sections 2.3.1 through 2.3.7.

2.3.1. Isotope CPM Table

The first table (see Appendix C) lists the CPM of the ten selected isotopes and their associated 1σ counting errors, core position, identity, and scan interval. The scans are listed in chronological order except for the static counts, calibrations, and miscellaneous scans that are tabulated separately. In the driver elements, the automatic scans were also separated into three strata, which represent the bottom graphite section, fuel section, and upper graphite section; the static scans were listed as one stratum in each element scan. In the test elements, the scans were stratified on a body-to-body basis. The strata information was then included in the weighted mean and associated statistical information, which is explained by the following algorithms:

$$\text{WT MEAN CPM} = \sum W_i \ \text{CPM}_i = \overline{\text{CPM}} \quad , \qquad (1)$$

$$W_i = \frac{\ell_i}{\Sigma \ell_i} \quad , \qquad (2)$$

where W_i = weighting factor,

ℓ_i = scan interval,

CPM_i = CPM for each individual scan, WT MEAN CPM = mean CPM weighted with scan interval;

$$\text{WT MEAN 1 SIGMA} = \left(\sum W_i \; S_i^2\right)^{1/2} , \tag{3}$$

where S_i = standard error for each individual scan (1σ);

$$\text{WT RMS} = \left[\sum W_i \; (CPM_i - \overline{CPM})^2\right]^{1/2} ; \tag{4}$$

$$\text{WT ERROR} = \left[\sum W_i^2 (S)_i^2\right]^{1/2} . \tag{5}$$

2.3.2. Isotope Ratio Table

The isotope ratio gives the calculated CPM ratios of various isotopes for each scan from the CPM table (Section 2.3.1). The following statistical algorithms apply:

$$\text{RATIO} = R_i = \frac{CPM_A}{CPM_B} , \tag{6}$$

$$\text{1 SIGMA ERROR} = R_i \left[\left(\frac{S_A}{CPM_A}\right)^2 + \left(\frac{S_B}{CPM_B}\right)^2\right]^{1/2} = S_{Ri} , \tag{7}$$

$$\text{WT MEAN RATIO} = \sum W_i \; R_i = \overline{R_i} , \tag{8}$$

$$\text{WT MEAN 1 SIGMA} = \left(\sum W_i \; S_{Ri}^2\right)^{1/2} , \tag{9}$$

$$\text{WT RMS} = \left[\sum W_i \; (R_i - \overline{R_i})^2\right]^{1/2} , \tag{10}$$

$$\text{WT ERROR} = \left(\sum W_i^2 \; R_i^2\right)^{1/2} . \tag{11}$$

2.3.3. Normalized Isotope Ratio Table

The normalized isotope ratio table shows the CPM of various isotopes normalized to the total weighted mean of all strata containing fuel. The following algorithms apply (Ref. 4):

$$N_i = \frac{CPM_i}{\overline{CPM}} \quad , \tag{12}$$

where N_i = normalized ratio,

CPM_i = CPM for each scan (see Section 2.3.1),

$\overline{CPM}$ = weighted mean of all fuel sections (total strata mean);

$$\text{1 SIGMA ERROR} = \frac{CPM_i}{\overline{CPM}} \left[\left(\frac{S_{CPM_i}}{CPM_i} \right)^2 \left(1 - \frac{2}{N} \frac{CPM_i}{\overline{CPM}} \right) + \left(\frac{S_{\overline{CPM}}}{\overline{CPM}} \right)^2 \right]^{1/2} \quad , \tag{13}$$

where S_{CPM_i} = 1 SIGMA counting error of isotope i on each scan,

$S_{\overline{CPM}}$ = 1 SIGMA counting error on mean CPM along the fuel element (of any preselected strata) (see Eq. 5).

The WT MEAN, RATIO, WT MEAN 1 SIGMA, WT RMS, and WT ERROR are all calculated from Eqs. 6 through 11 in Section 2.3.2.

2.3.4. Absolute Isotope Concentrations

The quantitative isotope concentrations and composite fissions per initial metal atom (FIMA) using Cs-137 and Ru-106 are shown in the next table (see Appendix C). The calculations of the curies and FIMA are explained in Section 3.3. For convenience, the reported curie value at each axial location is for an equivalent compact at that position (see Section

2.4 for a detailed discussion of calibration). This allows the direct comparison of results using different collimators and gamma scanning of fuel compacts at ORNL without the need for complicated scanning geometry corrections. The error analysis of these calculations is discussed in detail in Ref. 4. Reduction of the strata information is done with the algorithms outlined in Section 2.3.1.

2.3.5. Interpolation Table

The interpolation linearly interpolates the CPM and ratios to any set of axial locations. The centerlines of all compacts are used for interpolation points for the fuel driver elements. Because the scan interval is equal by definition, the algorithm can be simplified:

$$\overline{X} = \frac{1}{n} \sum X_i \quad , \tag{14}$$

$$S_{\overline{x}} = \left(\frac{1}{n} \sum S_x{}^2 \right)^{1/2} \quad , \tag{15}$$

$$RMS = \left[\frac{1}{n} \sum (R_i - \overline{R})^2 \right]^{1/2} \quad , \tag{16}$$

$$ERROR = \left(\frac{1}{n^2} \sum S_x{}^2 \right)^{1/2} \quad . \tag{17}$$

2.3.6. Statistical Test Table

The statistical test table is designed to compare any stratified measured information with predictions or equivalent measured information for statistical significance. The relative difference between the two values for comparison calculated with an associated error and a statistical individual agreement test is applied to the comparison. These tests and the method of calculation are outlined in Section 3.1.

2.3.7. Plot Package

Any strata information can be plotted against the axial core location of the particular scan along the fuel element.

2.4. CALIBRATIONS

To calculate absolute curie and FIMA values for the driver elements it was necessary to calibrate the scanning geometry at Peach Bottom. This was achieved for Phase I by cross-calibrating the results determined from ORNL on individual driver element compacts from element E14-01 (Ref. 12) and the *in situ* scanning of E14-01 at the Peach Bottom site. E14-01 was chosen as a calibration element because it did not show significant cesium transport (Ref. 12). If an element with cesium transport had been used for calibration, it would have been impossible in the Peach Bottom scans to separate the detected cesium activity in the compact from that built up on the graphite components. This would have caused an erroneous comparison with individual compact activities determined at ORNL, which do not contain the accumulated cesium activity of the sleeve and center spine cross sections seen in the Peach Bottom scans (see Fig. 6). However, this problem can be overcome by composition of activity measurements at ORNL for compact and graphite components, as described in Section 3.4.

In the calibration procedure, four static scans were taken from E14-01 which corresponded to the mean activities of the four compacts measured at ORNL. Using the absolute isotope activities measured at ORNL for each compact and the relative activity in CPM observed at Peach Bottom, the absolute counting efficiency of the Phase I Peach Bottom gamma scanning geometry (17.47-mm x 0.254-mm collimator) can be determined using the following equation for each particular nuclide gamma energy peak:

$$CE = \frac{CPM}{DPM * A.I.} , \quad (18)$$

where CE = absolute counting efficiency,

CPM = counts per minute measured at Peach Bottom for about 76.2 mm (3 in.) of axial fuel element length,

DPM = disintegrations per minute measured at ORNL for a single fuel compact of 76.2-mm (3-in.) length,

A.I. = absolute intensity of a particular isotope.

This expression includes all the geometry and attenuation effects associated with the Peach Bottom scans. All driver fuel spectra were converted to an equivalent axial fuel element section of 76.2 mm (3 in.) at the axial midpoint of each scan. This calibration does not fully account for relative depletion or enrichment of a mobile isotope along the scanning geometry due to radial and axial migration compared with nonmobile isotopes within the scanned volume. For the releasing element F03-01, the measured Cs-137 inventory was close to that predicted (see Section 3.4), which indicates that the geometry effects described above still allowed the determination of axial Cs-137 and Cs-134 activity within the accuracy of the calibration.

The counting efficiency was calculated for all the isotope energy peaks except La-140 and I-131, which were too short-lived to be detected at ORNL. The counting efficiency of these two isotopes and all other isotopes was determined from the logarithmic first-order fit through the counting efficiency versus energy data of peaks greater than 300 keV (Fig. 7).

Because the counting efficiency changes with each geometry, it was also necessary to determine the counting efficiency for the gamma scanning of Phase II driver elements, which were measured with a 6.35-mm x 1.27-mm collimator. All of the driver elements scanned at ORNL were from Phase I; therefore, the calibration procedure used for Phase I was not applicable for Phase II gamma scanning. To correct for this, several collimators used on E14-02 and E03-01 were intercompared to determine a factor that could be multiplied by the Phase I counting efficiencies to give appropriate results for the Phase I scans. Element E14-02 was scanned with the 0.254-mm x 17.475-mm and 0.254-mm x 23.876-mm collimators, and E03-01 was scanned with the 0.254-mm x 23.876-mm and 1.270-mm x 0.635-mm collimators. The relationship between the various CPM values seen by each collimator is as follows:

$$\frac{B}{A} * \frac{C}{B} = \frac{C}{A} = 5.025 \quad , \tag{19}$$

where A = (0.254 mm x 17.475 mm) Phase I driver elements,

B = (0.254 mm x 23.876 mm) Phase I and II driver elements,

C = (1.270 mm x 0.635 mm) Phase II driver elements.

The counting efficiency of each isotope used in the analysis of Phase II was determined by multiplying the counting efficiency determined for the Phase I collimator by 5.025. Both calibration curves are shown in Fig. 7. Certain elements in both Phase I and Phase II could not be calibrated for quantitative results. The nonfueled components including reflectors (A18-08, D18-12, and D17-12), a guide sleeve (E08-01G), and a control rod (E08-01) had no calibration. In Phase I, FPTE-3 (E14-08) and FTE-18 (E06-01) (Ref. 9) were not calibrated because of unusual fueled geometries and can presently only be evaluated in relative terms. Some isotope calibration data may become available from PIEs at the Atomic Energy Research Establishment (AERE), Harwell, Great Britain, and Kernforschungsanlage (KFA), Jülich, West Germany. In Phase II, F01-01, F07-06, F09-08, F10-09, F14-13, and F12-11 did not yield quantitative results because of collimator or detector problems during scanning,* which were not recognized until the fuel elements were sealed for final disposal in Idaho.

Several of the driver elements were scanned twice for reproducibility. Specifically, the double scanning of A17-11 and C02-01 (FTE-6) showed

*F01-01 lost collimator identity; F07-06, F09-08, F10-09, and F12-11 had collimator or detector problems; and F14-13 was inadvertently scanned with a lead shield in place.

measurements of all the isotopes to be well within the 2σ counting errors as shown below:

Element	Pa-233 Activity Scan 1 (CPM ± 2σ)	Scan 2 (CPM ± 2σ)
A17-11	49,224 ± 902	49,441 ± 900
C02-01 (FTE-6)		
Body 1	168 ± 12	171 ± 13
Body 2	341 ± 25	302 ± 23
Body 3	349 ± 30	341 ± 28

The counting efficiency of the test element gamma scans was calculated using the same methodology applied to the driver elements. The source terms in both the six- and eight-hole teledial configurations came from FTE-15 (Ref. 13) and FTE-6 (Ref. 4) hot cell gamma scanning at GA. By calculating the volume percent of each fuel rod scanned in the collimator path (see Fig. 6), the total absolute activity of each of the major isotopes was determined from calibrated GA hot cell scans on individual fuel rods. Using these calibrated disintegrations per minute (DPM) values and the CPM values seen in the Peach Bottom scanning of FTE-6 and FTE-15, the counting efficiency was calculated using Eq. 18. The absolute curie values quoted in the analysis section for the fuel test elements are for the volume of fuel and graphite seen by the collimator in Fig. 6 over the nominal length of a standard equivalent fuel rod (49.28 mm or 63.5 mm for the eight- or six-hole teledial configuration, respectively) which has its midpoint at the centerline of each Peach Bottom scan. The difference between the driver and test element calibration is the corresponding fuel and graphite volume, which is the equivalent of one fuel compact inclusive spine and sleeve section, whereas test element inventories are representative for the fraction of fuel rods (about 3 and 3.5 fuel rods for six- and eight-hole teledial configurations, respectively) and graphite within the collimator path shown in Fig. 6.

3. RESULTS

3.1. FUEL STACK LENGTHS

One of the goals of the Peach Bottom EOL gamma scanning program was to determine the *in situ* fuel stack lengths of various driver and test elements from Phase I and Phase II. Using the single-channel strip charts of various nuclides and the calibrated Veeder-Root location system, the fuel stack lengths were determined for each fuel element scanned. Figure 8 shows a typical strip chart from driver element E14-01. In most cases, several nuclide strip charts were available for each fuel element; therefore, the mean, $\bar{x}$, and standard deviation on the mean, $S_{\bar{x}}$, were calculated when applicable.

The statistical tests used for the comparison of the methods were the individual values agreement test, the group agreement test, and the group goodness-of-fit test (Ref. 4). The null hypothesis, i.e., that there is no difference, is accepted at the 0.05 significance level for the individual value agreement test if

$$|dj| = \left|\frac{Z_j}{S_{Zj}}\right| \leq 1.96 \quad , \tag{20}$$

where Z_j = relative difference,

S_{Zj} = error on the relative difference.

The group agreement test is passed if

$$|\sqrt{m}\ \bar{d}| \leq 1.96 \quad , \tag{21}$$

where m = number of measured values or tests,

$\bar{d}$ = average of $Z_j/|S_{Zj}|$ for the m values.

The group goodness-of-fit test is accepted if

$$\frac{1}{m} \sum \left(\frac{S_j}{S_{Z_j}} \right)^2 \leq \frac{\chi^2_{0.95}}{m} \quad , \tag{22}$$

where $\chi^2_{0.95}$ = upper 95 percentile point for the chi-squared distribution with m degrees of freedom.

The axial variability is within the uncertainty of the measurements if

$$\frac{m \ RMS^2}{df \ \ \sigma^2} \leq \frac{\chi^2_{0.95}}{df} \quad , \tag{23}$$

where df = degree of freedom (usually m - 1),

$\sigma^2 = 1/m \sum S^2_{Z_j}$ mean measurement error,

$RMS^2 = 1/m \sum (Z_j - \bar{Z})^2$ root mean square deviation (axial variability).

Comparison of fuel body stack lengths from the destructive PIEs and the Peach Bottom EOL gamma scanning of FTE-6 (Ref. 4) was used to qualify the accuracy of the gamma scanning method. As shown in Table 4, there are no significant differences in the two measurements. This permits the confident use of stack lengths for elements where no direct postirradiation measurements are available.

For the Phase I element, FTE-18 (Ref. 9), single-channel isotope plots were analyzed for fuel body and total stack lengths. A comparison of the lengths as derived from metrology and gamma scanning is shown in Table 5. The following conclusions can be drawn:

1. When comparing total fuel body stack length information determined from gamma scanning and metrology, a bias of $\hat{b} = 8 \pm 2$ mm was detected for the Peach Bottom scan length over all six fuel bodies.

However, this is a small relative error of 0.4 ± 0.1 (1σ)% over a total length of 2083 mm (82.01 in.).

2. The associated error with the Peach Bottom scan-derived fuel body strain data can be as large as the measured effect. Therefore, for strain information, metrology data are preferred. On the average, the bias was $\hat{b}$ = 54 ± 17 (1σ) (relative %) between the two methods of strain measurements.

3. The hot cell scan data give an accumulative EOL fuel length of 2051 mm (80.75 in.), which results in an accumulative fuel-free length of 32 mm (1.26 in.). This is a revision of the information presented in Ref. 9, which results from the recent calibration of the gamma scanner drive mechanism at the GA hot cell (change from 0.04 in./rev to 0.04167 in./rev).

4. By application of the metrology-derived stack strain, the accumulative beginning-of-life (BOL) fuel length was 2063 mm (81.25 in.) rather than 2036 mm (80.16 in.) nominal; i.e., the fuel-free zones at the ends of each fuel body averaged 2.7 mm (0.11 in.) rather than 5 mm (0.2 in.).

5. Significant differences between metrology-derived and Peach Bottom gamma-scan-derived length measurements were detected at the 95% confidence level by application of statistical test methods. However, the absolute differences are small and are acceptable for length determination. For reliable strain information, precision metrology is the preferred method.

Results of the relative change of <u>in situ</u> stack lengths for Phase I and Phase II driver elements are presented in Table 6. Table 7 shows the results of the test elements scanned in Phase I. The driver element strains are compared with mean fast fluence and time-averaged fuel temperatures in

Figs. 9 and 10. The following conclusions can be drawn from the results of the Phase I and Phase II gamma-scan-derived fuel stack lengths:

1. Fuel stack lengths of driver elements had an average expansion of 0.7% with a standard deviation on the mean of ±0.2%. The fuel stack expansion tended to increase with both fast fluence and temperature. The data were found to best follow the computer-derived relationship (see Fig. 10)

$$d\ell/\ell = \frac{2.45 \times 10^{-4}\ \phi T}{10^{25}\ \text{cm}^{-2}\ {}^{\circ}\text{C}}\ (\%) \quad , \qquad (24)$$

where ϕ = fast fluence (10^{25} n/cm^2),
T = element and time-averaged temperature (°C),
$d\ell/\ell$ = strain of fuel stack length (%).

2. Fuel stack lengths in the test elements all decreased. All elements containing TRISO-BISO or TRISO-TRISO* fuel with the exception of FTE-9 showed approximately 1% shrinkage. Element FTE-9 showed shrinkage of 3.5% for a TRISO-BISO fuel, which is significantly more than expected and is believed to be a measurement error. Element FBTE-1 with BISO-BISO fuel shrank about 3%, and blended beds in FBTE-5 had about 2% shrinkage.

3.2. POWER PROFILES

Short- and long-lived isotope profiles were used to verify, respectively, axial and radial EOL and time-averaged power profiles. Normalized profiles for La-140 and Zr-95 were used to test the power during the last 50 to 200 days, and Cs-137 and Cs-134/Cs-137 normalized profiles were used in the comparison of calculated time-averaged power profiles and thermal fluence profiles, respectively.

---

*Gamma spectroscopy only detects the fuel stack envelope, i.e., the stack with the least shrinkage; consequently, TRISO-TRISO fuel is usually detected.

3.2.1. Axial Profiles

In the axial power profile comparison, two qualifications were necessary in the use of the isotope profiles. The first was that only elements with insignificant cesium migration could be used in the time-averaged power profile comparison. The other was that the loading of each element was assumed to be constant along its length; this assumption was necessary to allow the use of the Cs-134/Cs-137 ratio, which is not related to the power if the fuel loading changes and is more representative of the thermal fluence distribution in any case.

In the Peach Bottom scans, Zr-95 and La-140 profiles showed insignificant differences for unperturbed elements two or more locations away from control rods. This suggests little difference in the relative power profile for the last 50 to 200 days. Figure 11 shows the close agreement in these two isotope profiles for E14-01, which was not influenced by control rods. In driver elements that were near control rod banks which were gradually withdrawn toward EOL, the isotope profiles are different because of a significant change in the axial power profile distribution with time. Figure 12 shows an example of this for F03-01.

E14-01 was used in the comparison of FEVER-calculated isotope-derived power profiles. In Fig. 13 the E14-01 time-averaged profiles show good agreement between measurements and predictions except for the bottom of the core, where apparently more thermal neutron reflections occurred than was predicted. The E14-01 EOL power profiles are also compared with FEVER-calculated values in Fig. 14; in this case the profile flattened as predicted, but the shift in the peak to the top of the element was not obvious. When 14 unperturbed elements were grouped together, the average La-140 activity was found to follow the same trends as it did in E14-01 when compared with the FEVER EOL power (see Fig. 15).

3.2.2. Radial Profiles

Using the mean activity of La-140, Zr-95, and Cs-137 in driver elements not influenced by control rods, the radial core distribution of these isotopes was compared with the GAUGE-predicted EOL and time-averaged radial power profiles. Figures 16 and 17 show the predicted EOL profile and the normalized isotope activities of both La-140 and Zr-95 for Phase I from 15 unrodded fuel elements (as identified in Table 8*) and Zr-95 for Phase II from 15 unrodded elements (see Table 9*). In both cases the normalized isotope profiles appeared somewhat flatter than the predicted EOL, with the Zr-95 profile being further away from the predicted EOL power shape than the La-140 profile.

The Cs-137 profile is also compared with the time-averaged power profile in Figs. 18 and 19 for Phase I and Phase II, respectively. In both Phase I and Phase II driver elements, the relatively flat predicted time-averaged power profile was substantiated by the measured Cs-137 activity.

In Fig. 20, a summary of the calculated radial power profiles and measured isotope profiles shows some interesting trends:

1. There appears to be an area around core radial position 9 or 10 with no change in the relative radial power production.

2. With increasing time, the relative power production became higher in the center and lower at the periphery, which makes the control rod removal pattern visible.

3. Owing to the fact that the predicted EOL and time-averaged power distributions envelope the short-, medium-, and long-life isotopic distributions on either side, it is concluded that the radial power factors and their time histories are reasonably well modeled.

---

*Except A03-03 for Phase I and E03-01, E14-02, and F05-04 for Phase II because of different irradiation exposure (A03-03) or arbitrary reduction toward the same sample size between Phase I and Phase II for statistical purposes.

3.3. COMPOSITE BURNUP

Ru-106 and Cs-137 can be used to establish a composite burnup which is defined as the number of fissions occurring per initial heavy metal atom (FIMA).

The burnup can be calculated by

$$FIMA_c = \frac{DPM}{(U_o + Th_o)\lambda\, y} \quad , \tag{25}$$

where
- $FIMA_c$ = composite burnup,
- DPM = disintegrations/minute of isotope at EOL,
- λ = isotope decay constant (min^{-1}),
- y = fractional fission yield of isotope from U-235),*
- Th_o = number of atoms of thorium at BOL,
- U_o = number of atoms of uranium at BOL.

A rigorous analysis requires the calculation of the decay of the isotope during the life of the reactor. When long-lived isotopes are used, the power fluctuations of the reactor become more insignificant and it can be assumed in most cases that the reactor operated at constant power for the life of the core. In this case the decay during life can be approximated by

$$N' = N \left(\frac{1 - e^{-\lambda t}}{\lambda t}\right) \quad , \tag{26}$$

where
- N' = atoms of isotope corrected for decay during life,
- N = atoms of isotope at EOL,
- λ = isotope decay constant (s^{-1}),
- t = time of irradiation (s).

---

*Assume the same for U-233.

There was gross redistribution of Cs-137 in the majority of the elements, as discussed in Section 3.4. Substitution of Ru-106 as a fission monitor in cases of cesium loss or movement was not possible because of its low yield and consequently large counting error.

In cases where Cs-137 was redistributed in the element but not lost, the total Cs-137 inventory can be used in the calculation of an element average FIMA and compared with GAUGE predictions. (GAUGE is a two-dimensional depletion code in an r-Θ geometry.) It is felt to be a reasonable assumption in light of an approximate loss of 65 Ci (Ref. 14) into the primary circuit, which is 2×10^{-4} of the total Cs-137 inventory of the core.

Table 8 summarizes the FIMA comparison between all the driver elements and several test elements that had constant axial fuel loadings. In all cases the calculated and measured absolute FIMA were within ±15% of each other.

To demonstrate the agreement of the calculated and measured FIMA on a core average basis, all the fuel driver elements except for F07-06, F09-08, F10-09, and F12-11, which showed scanning problems, and F01-01, which had no calibration, were averaged. The results are as follows:

	FIMA (n=48)		Relative Difference	
	Calculated (at. %)	Measured (at. %)	$(C/M-1)=\bar{Z}$	$S_{\bar{Z}}$ (1σ)
Mean	7.53	7.59	-0.004	±0.007
RMS	±1.45	±1.54	±0.068	--
Error (1σ)	--	±0.05	±0.048[a]	--

(a) Mean relative measurement error for individual driver elements.

This analysis shows a -0.4% ± 0.7% (1σ) higher FIMA than that predicted by GAUGE. Using an individual agreement test discussed in Section 3.1, 14 out of 48 of the driver elements showed differences between the calculations and the measurements that could not be attributed to the measurement error. On a group basis (Eq. 21), the agreement showed that there was no difference at the 0.05 significance level between the measured and calculated values. Consequently, there was no significant difference between the calculated and measured burnup on a core average within the uncertainty of ±0.7%. (The established bias of -0.4% is well within the uncertainty of ±0.7% and can therefore be ignored.) The root mean square deviations, RMS, for the calculated and measured FIMA values were within ±5% of each other, which is evidence that the element-to-element variation was well predicted for the core. The measured RMS is higher than the predicted, which is partially due to a superposition of counting errors in addition to the true element-to-element variability.

As mentioned above, several of the fuel elements showed significant differences between the calculated and measured FIMA values. Using the element-to-element variation test (Eq. 20), the difference between the calculated and measured burnups on a core basis was found to be significant, with ±6.8% versus a mean counting error of ±4.8%. The observed range was between +14% and -15%, which covers the 2σ range of the observed RMS deviation. From a statistical viewpoint, the deviations for all the 48 driver elements participating in the test were within the 2σ range and therefore acceptable for the test.

In summary, it is concluded that the core average power was predicted within ±0.7% (1σ) and that the element-to-element variation between predicted and measured local power was within ±6.8% (1σ). This is even better than the commonly stated uncertainty of ±3% to ±8% for nuclear depletion calculations (Ref. 15).

Several test elements with uniform axial fuel loadings are compared with GAUGE-calculated values in Table 8. The comparison of the eight test elements with a mean element FIMA is shown below:

	FIMA (n=8)		Relative Difference	
	Calculated (at. %)	Measured (at. %)	$(C/M-1)=\overline{Z}$	$S_{\overline{Z}}$ (1σ)
Mean	7.82	9.10	-0.125	±0.022
RMS	±2.22	±3.05	±0.122	--
Error (1σ)	--	±0.22	±0.062[a]	--

(a) Mean relative measurement error for individual fuel test elements

On an individual element basis, four of the eight test elements showed significant differences between the measured and calculated values. On a group level, the bias between the calculated and measured values could not be explained by measurement errors. A possible explanation for the bias is the complicated scanning geometry (see Fig. 6). Because the amount of fueled volume can change with azimuthal movement, the confidence in the scanning configuration of the fuel test elements is less than for driver fuel elements, where rotation and off-axis effects of the element within the fuel handling machine had less effect on the scanned geometry. The lowering of the fuel elements from the fuel handling machine into storage cans was occasionally monitored with a television system. Very slight rotation and pendulum effects were observed during these operations.

The alternative explanation is an obvious underprediction of time-averaged power for this group of test elements. This is not necessarily representative for the total group of 33 test elements; however, the RMS deviation of ±12% between predicted and obtained test element power may be indicative of the achievable accuracy in lack of any other information (e.g., destructive burnup measurements). The observed deviations ranged between +10% and -24%.

3.4. FISSION PRODUCT RELEASE AND REDISTRIBUTION

One of the major goals of the EOL gamma scanning exercise was to determine the release and redistribution of relative fission products within the driver and test elements and possible migration through the sleeves into the primary circuit.

The total measured cesium inventory at EOL in each of the driver elements in both Phase I and Phase II is compared with the predicted Cs-137 inventory in Tables 10 and 11. The predicted Cs-137 inventory was derived from the GAUGE FIMA and Eq. 19. Because of the direct relationship between FIMA and the Cs-137 inventory, the bias between the calculated and measured mean Cs-137 inventory was similar to the FIMA biases in Tables 8 and 9 on both an element-to-element basis and a core average basis. Because of the smaller uncertainty in the Cs-137 activity compared with deduced burnup values, there were 21 out of 48 elements which showed significant differences at the 0.05 level between measured and calibrated values using the individual agreement test (Eq. 20) as compared with the burnup comparison, where 14 out of 48 elements showed disagreement. On a core average basis, the group agreement test showed no difference between the measured and calculated values on the 0.05 significance level.

The following values were obtained:

	Cs-137 Inventory (n=48)		Relative Difference	
	Calculated (Ci)	Measured (Ci)	$(C/M-1)=\bar{Z}$	$S_{\bar{Z}}$ (1σ)
Mean	391	395	-0.006	±0.004
RMS	±48	±55	±0.066	--
Error (1σ)	--	±1	±0.025[(a)]	--

(a) Mean relative measurement error for individual driver elements.

The numerical conclusions are that on a core average basis, the cesium inventory is predicted within ±0.4% (the established bias of -0.5% is within the 2σ limit of the progressed measurement error and therefore is ignored). The element-to-element variation was established with ±6.6%, which again is larger than the mean relative measurement error of ±2.5%. The measurement uncertainty on the cesium inventory represents a fraction of $\pm 3.5 \times 10^{-3}$, which is a factor of 18 larger than the estimated core release (Ref. 14) of 2×10^{-4}* into the primary circuit.

An assumption in the measurement of the Cs-137 activity from the Peach Bottom gamma scans is that the Cs-137 inventory is contained within the compact in a homogeneous manner. In reality, this is not true because the regions where Cs-137 is lost from the compacts or built up on the sleeve and spine would be different from the calibrated geometry of a fuel compact with a homogeneous isotopic distribution. The impact of this effect is shown by the full element scanning of F03-01 at Peach Bottom and individual compact, sleeve, and spine scanning at ORNL. If the effect were large, the difference in the ORNL and Peach Bottom scans would be significant. In Table 12, the activity of each compact and the adjacent sleeve and spine sections as determined at ORNL are compared with FISS-PROD** predicted Cs-137 inventories and inventories determined from the Peach Bottom gamma scans, which were calibrated with the E14-01 inventory measurements at ORNL. The results are summarized below:

Method	Cs-137 Inventory (Ci)	Measurement Error (Ci)
GAUGE	383.8	ND
FISS-PROD**	394.6	ND
Peach Bottom	404.8	±7.1 (1σ)
ORNL	404.2	±3.2 (1σ)

*Reference 14 assesses 65 Ci of cesium released into the primary circuit, which represents a fraction of 2×10^{-4} assuming a total core inventory of 3.2×10^{5} Ci, based on the mean inventory per element times 804 elements. Some additional cesium was accumulated at reflector and control rod components, which was not accounted for in the 65-Ci estimate.

**FISS-PROD is a one flux group depletion code.

The good agreement between the ORNL and Peach Bottom determinations confirms the precision of the E14-01 and F03-01 inventory measurements at ORNL.

The axial distribution of the Cs-137 was also found to be in good agreement for the ORNL and Peach Bottom scans, as shown in Fig. 21. This comparison demonstrates that the Peach Bottom scanning accurately measured the cesium activity in elements that had significant cesium redistribution.

Reflector and control rod components were also gamma scanned and showed low Cs-137 contamination as follows:

Element I.D.	Element Type	Cs-137 Activity Above Background		Cs-134 Activity Above Background	
		Mean (CPM)	Error (%) (1σ)	Mean (CPM)	Error (%) (1σ)
A18-08	Reflector	12.6	±4.3	<0.1	--
D18-12	Reflector	<0.3		<0.1	--
E17-16	Reflector	13.6	±5.2[a]	<0.1[a]	--
E08-01G	Control rod guide sleeve	24.9	±4.6	37.4	±1.2
F08-01A	Control rod	8.1	±5.7	1.8	±0.4

(a) Using average background from A18-08 and D18-12.

The control rod sleeve (E08-01G) had the highest cesium levels above the background. Because there is no quantitative calibration for the scanning of these reactor components, an assessment of the magnitude of the cesium accumulation cannot be made until some calibration has been done on reflector A18-08, which was shipped to ORNL for PIE. On a semiquantitative basis the buildup would be small, because 20 CPM of Cs-137 corresponds to <1% of the activity seen in a standard driver element, which is ∿5 Ci.

Low release was also evident from the scan of the fission product trap in each of the driver elements (see Tables 10 and 11). In all cases except two, the cesium activity in the trap was only slightly above the background. In E04-02 and E09-02, the activity in the trap was an order of magnitude higher than for the rest of the elements. Using the detector calibration for the fuel scanning, there was a 7- to 9-Ci buildup of both Cs-137 and Cs-134 in each trap. This corresponds to approximately 2% of the total cesium inventory in these two particular elements; however, these values have to be confirmed by inventory measurements for specific fission product traps at ORNL.

The redistribution of mobile fission products in the elements is characterized by the predicted and measured profiles of these isotopes. In the case of Cs-137, the predicted values from the FISS-PROD (Ref. 16) calculations are a good representation of the non-distributed profile because the long half-life of Cs-137 (30.1 yr) is not seriously affected by the detailed power history of the element.

Only the Cs-137 was calculated with FISS-PROD owing to the simplicity of this one-dimensional depletion code, which does not accurately predict short-lived isotopes. All other isotopes will be analyzed qualitatively by their profiles and in comparison with non-releasing isotopes. The FISS-PROD determined relationship between fluence and Cs-137 activity produced is shown in Fig. 22.

The redistribution of Cs-137 within the driver elements appears to correlate with core location, which is explainable by the fuel element temperature. The difference in Cs-137 redistribution is illustrated graphically in Fig. 23. These plots show the measured and predicted Cs-137 inventory for E01-01, E03-02, E06-02, E09-01, E11-01, and E14-01, which covered the radius of the core. In Tables 13 through 18, the quantitative difference between the measured and calculated Cs-137 inventories is given. From the comparison of the six elements it is obvious that the Cs-137 distribution is similar in all elements. Generally, the highest Cs-137 loss occurs in the upper portion of the element near compacts 18 through 22, and thus Cs-137 is subsequently transported downward by the purge stream until it accumulates on cooler surfaces. The maximum accumulation occurred between compacts 2 through 8 in the six fuel elements analyzed. To show that this behavior is consistent for other radial sections through the core, the plots of Cs-137 activity of F02-01, F04-03, and F15-14 are given in Fig. 24. Again, the Cs-137 redistribution is seen to increase with locations nearer the center of the core. The three plots in Fig. 24 also show the measured activity of Cs-134. It is obvious from the profiles that both isotopes of cesium redistribute themselves in the elements in a similar fashion.

To further illustrate the core location* effect and Cs-137 loss in the upper high-temperature region of the driver elements, a plot of core locations versus maximum Cs-137 loss is shown in Fig. 25. With few exceptions, increasing Cs-137 release was found for compacts 15 through 22 with decreasing distance from the core center.

Cs-137 redistribution data for E01-01, E03-02, E06-02, E09-01, E11-01, and E14-01 from Tables 13 through 18 were used in a correlation of Cs-137 release to fuel temperature within the element. The time-averaged SURVEY (Ref. 17) calculated fuel temperatures (Table 19) for several of the compacts in each element are plotted against the relative Cs-137 difference in that compact in Fig. 26. This plot shows a noticeable loss of Cs-137 from the compacts starting at approximately 1060°C (time-averaged temperature). Above this temperature the magnitude of the loss increased but appeared to be somewhat random. The scatter in the data is attributed to the uncertainty in the measurements and in the SURVEY-calculated temperatures, which have an intrinsic error and are not fully representative of the diffusive release of Cs-137; in fact, the activation-energy time-weighted temperature should be used in the comparison of the Cs-137 diffusive process as explained in Ref. 4. The time-weighted temperature is used only for illustrative purposes in this particular analysis.

*Core radial location is defined by the first two digits of the element identity. For example, the core location for F06-02 is 06. This number is directly related to the distance from the center of the core, which varied between 01 to 17.

Another analysis was performed on all the driver elements to summarize the effect of Cs-137 redistribution within the core. For all driver elements, the maximum Cs-137 buildup and release areas were determined and related to the time-averaged temperatures in Tables 20 and 21. Several conclusions were drawn from this analysis:

1. Maximum Cs-137 plateout occurred in compacts 5 to 14, and maximum Cs-137 loss occurred in compacts 15 to 25.

2. The time-averaged temperature of the fuel where Cs-137 loss was greatest was 1100°C with an RMS of ±30°C for 37 driver elements that showed Cs-137 loss. This generally corresponded to the location of peak fuel temperature of the elements (see Fig. 26).

3. The Cs-137 plateout occurred in regions with fuel temperatures of 936°C ±81°C (RMS) and maximum EOL sleeve temperatures of 652°C ±46°C (RMS).

The redistribution and loss of other radionuclides were also considered; specifically, cesium, ruthenium, and iodine isotopes were tested for mobility. The mobility tests were performed in fuel elements using several non-releasing fuel elements as internal standards. The criterion for loss or movement was deduced from a comparison of isotopic ratios between a mobile and a non-mobile isotope; Zr-95 was chosen as a non-mobile isotope. A description of the test statistic is given in Ref. 4.

FISS-PROD calculations of the isotopic inventories of a fuel compact at various thermal fluence exposures showed that the isotopic ratios changed from 5% to 20% within the thermal fluence exposure of the fuel driver elements. Therefore, a correlation of thermal fluence versus isotopic ratios can be established when comparing a non-releasing element with elements suspected of release.

The ratios chosen for the initial analysis were Ce-141/Zr-95, Ru-103/Zr-95, and I-131/Zr-95. Ru-106 and Ce-144 were not chosen for mobility tests because of the low fission yield of Ru-106 and because of the low absolute gamma ray intensity for Ce-144, which resulted in low activities and high counting errors. E01-01 was the element used for a test of mobility of the three isotopes in question, because it was one of the Cs-137 redistributing elements scanned first during Phase I. The short cooldown time for this element allowed good discrimination for short half-lived isotopes, especially I-131. During Phase II of the gamma scanning, I-131 and Ce-141 activity was not detected owing to their short half-lives and consequently low activity levels after a 7-month decay.

E14-01 was considered to be a non-releasing element from gamma scanning evidence at ORNL (Ref. 12) and the Peach Bottom gamma scanning, which indicated no cesium loss or redistribution (see Section 3.4); it was therefore used to determine the relationship between fluence and isotopic ratios. A14-14 and E13-01 were also chosen from Phase II gamma scanning to add additional data to the Ru-103/Zr-95 ratio versus thermal fluence data. I-131 and Ce-141 distribution profiles were limited to data for these isotopes from Phase I gamma scanning, which had only E14-01 as a non-releasing element with the standard fuel loading (45.792 g Th, 8.318 g U). The high-thorium-loaded (Th:U atomic ratio of 18.5:1) fuel elements in Phase I did not show Cs-137 redistribution, but were not analyzed for other isotopic movement.

The data of GAUGE/FEVER calculated thermal fluence versus the various isotopic ratios from E04-01, A14-14, and E03-01 are shown in Figs. 27 through 29. A least squares fit was determined for each set of data, and this was used for the non-releasing base lines of Ce-141/Zr-95, I-131/Zr-95, and Ru-103/Zr-95. The 95% confidence limits on this linear regression were determined via algorithms described in Ref. 4.

Using these ratio-fluence relationships, the non-releasing base lines with their 95% confidence levels are compared with the measured ratios in

Figs. 30(a) and 31(a) for E01-01, which was shown to be a high-releasing element, as discussed in Section 3.4.

In all cases the measured and non-releasing base lines were within the 95% confidence levels of each other. The conclusion is that within the 2σ uncertainties of the counting errors, Ce-141, Ru-103, and I-131 isotopes were not mobile in the Peach Bottom driver elements. The absolute isotopic profiles of these three elements, which are shown in Figs. 30(b) through 32(b), were relatively smooth with no major perturbations, which is further evidence of no fission product mobility of Ce-141, Ru-103, or I-131.

3.5. THORIUM ABSORPTION RATES

Mathematically, the Pa-233 concentration is shown to be related to the thorium absorption by

$$\frac{dN_{Pa-233}}{dt} = -\lambda' N_{Pa-233} + \sigma_a N_{Th-232} \phi , \qquad (27)$$

where ϕ = neutron flux,

N_{Pa-233} = number of nuclei of Pa-233 formed,

$\sigma_a N_{Th-232} \phi$ = absorption rate of Th-232,

σ_a = microscopic cross section for absorption reactions in Th-232,

$\lambda' = \lambda + \sigma_a \phi$,

λ = decay constant of Pa-233 .

All the Pa-233 normalized profiles in the fuel driver elements were smooth and had small counting errors. The GAUGE/FEVER calculated normalized absorption rate for E14-01 is compared with the Pa-233 normalized profile in Fig. 33. The measured and calculated profiles agree closely except for a shift in peak toward the bottom of the core.

The radial distribution of Pa-233 in the core was also compared with the GAUGE-calculated EOL thorium absorption rate for driver elements that were located away from the control rods. Figures 34 and 35 show the calculated and measured comparison for Phase I and Phase II driver elements, respectively. In both cases the measured radial profiles of Pa-233 were flatter than the predicted profile, which may be explainable by the shift in radial power distribution toward EOL due to control rod withdrawal, as discussed in Section 3.2.2.

4. CONCLUSIONS

The Peach Bottom EOL gamma scanning exercise of driver elements, test elements, reflector elements, and a control rod with sleeve was done to provide a data base of information on fission product distribution in the Peach Bottom core for use in validating nuclear physics and thermal performance and fission product release codes. The analysis of the gamma spectroscopic data allows conclusions about burnup, power and thorium absorption profiles, fission product release and redistribution trends, and fuel stack length dimensional changes. The conclusions from these findings are summarized below:

1. Fuel stack dimensional changes of the fuel driver elements showed an average increase of 0.7% in length, which is within the design criterion of the elements. This stack expansion tended to increase with both higher temperatures and fast fluences. Most of the fuel test elements showed a shrinkage in their fuel stacks of -0.5% to -2%.

2. Normalized axial and radial Cs-137 profiles in the core properly predicted the corresponding axial and radial time-averaged power distributions.

3. The shape and peak shift in the FEVER-calculated EOL axial power profiles were reasonably well predicted by the normalized Zr-95 and La-140 distributions. Radial EOL power profiles were also approached by the normalized radial La-140 and Zr-95 profiles.

4. The influence of control rod withdrawal on the EOL power shape of nearby elements was reflected in different La-140 and Zr-95 axial profiles.

5. Measured burnup from the Cs-137 inventory and GAUGE-calculated burnups of the driver and test elements were within ±6.8% (1σ) of each other on an element-to-element basis. This agreement is better than the generally stated accuracy of ±10% for nuclear predictions. The relative difference of the measured and calculated burnups on a core average basis for 48 driver elements was within the progressed uncertainty of the measurements [+0.7% (1σ)].

6. Cesium inventory measurements resulted in agreement with predictions within ±0.4% on a core average basis and within ±6.6% on an element-to-element basis. The measured cesium inventory was associated with a relative error of $\pm 3.5 \times 10^{-3}$, which is above the estimated fractional release (excluding accumulation of cesium in reflector and control rod components) of 2×10^{-4} into the primary circuit; i.e., the cesium release was undetectable within the sensitivity of the measurement method.

7. Ten isotopes were systematically analyzed, and only Cs-137 and Cs-134 were found to be released and redistributed within the element. In the case of Cs-137 there was no detectable release from the driver elements within the measurement uncertainties, although Cs-137 and Cs-134 did redistribute within the fuel elements. This was characterized by release in the locations of high fuel temperatures in the upper portions of the driver element and movement down the purge stream to the cooler sleeve, spine, and compact surfaces where accumulation occurred.

8. Of the non-fueled components scanned (i.e., reflectors, control rod, and control rod sleeve), only the control rod sleeve showed some Cs-137 and Cs-134 contamination. The activity on this sleeve was approximated to be <1% of total activity in one driver element, or <5 Ci.

9. The Pa-233 normalized activity profile was found to follow the predicted GAUGE/FEVER thorium absorption profiles except for a slight shift of the peak toward the bottom of the core. Measured radial core Pa-233 profiles were found to be flatter than the calculated EOL thorium absorption rates, which may be related to the change in power distribution toward EOL due to control rod removal.

5. ACKNOWLEDGMENTS

The authors would like to acknowledge the support and advice of all the individuals involved with this report. Special thanks go to Paul Love and Andy Valenciano for their patience and overtime efforts to complete the PBEOLGS data reduction program that made this report possible. John Saurwein is also thanked for his helpful discussions and data input; Frank Dyer, ORNL, is acknowledged for the calibration work (Ref. 12), which formed the basis for the quantitative analysis in this report; and Art Mehner is thanked for the coordination of the data collection at the site. Other contributors are as follows:

Data Collection

V. Orphen, V. Rodger, J. MacKenzie, A. Wyman, and D. Bryan of the Intelcom Rad Tech staff; W. Birely and associated Philadelphia Electric staff at Peach Bottom; L. Mayweather, D. Harmston, R. DeNooy, K. Buthe, J. Graves, A. Wyman, J. Renauld

Data Reduction

E. Anderson, D. Hill, A. Bagierek, R. Archibald, W. Lefler, M. Scott

Report Preparation

D. Novak, J. Baker, J. Weaver and staff

6. REFERENCES

1. Philadelphia Electric Company, "Final Hazards Summary Report, Peach Bottom Atomic Power Station," Vol. II, 1964.
2. Mehner, A. S., "Test Plan for Gamma Scanning Peach Bottom Test and Driver Elements," General Atomic Company, unpublished data.
3. Hick, H., and J. York, "Metallic Fission Product Behavior in Dragon Fuel Elements as Observed from Gamma-Spectrometric Examination," Dragon Report DPTN/5-13, November 5, 1973.
4. Wallroth, C. F., J. F. Holzgraf, and D. D. Jensen, "Postirradiation Examination and Evaluation of Peach Bottom Fuel Test Element FTE-6," ERDA Report GA-A13943, September 1977.
5. Meek, M. E., and B. F. Rider, "Compilation of Fission Product Yields," Vallecitos Nuclear Center Report NEDO-12154-1, 1974.
6. Evaluated Nuclear Data File Library, ENDF/B, Version IV, Brookhaven National Laboratory.
7. Anderson, E. E., "Method of Data Reduction for Peach Bottom Gamma Scan," General Atomic Company, unpublished data.
8. Scheffel, W. J., et al., "Peach Bottom 150 Full-Power Day Core Examinations," General Atomic Report GAMD-8703, December 1968.
9. Wallroth, C. F., et al., "Postirradiation Examination and Evaluation of Peach Bottom Molded Fuel Test Element FTE-18," General Atomic Report GA-A13699, June 1, 1976.
10. Archibald, R., General Atomic Company, private communication, February 1976.
11. Love, P., and A. Valenciano, "PBEOLGS, A Program for Peach Bottom EOL Gamma Scan Analysis," General Atomic Company, unpublished data.
12. Wichner, R. P., et al., "Distribution of Fission Products in Peach Bottom HTGR Fuel Element E14-01," ERDA Report ORNL/TM 5730, Oak Ridge National Laboratory, August 1977.

13. Holzgraf, J. F., et al., "Postirradiation Examination and Evaluation of Peach Bottom Fuel Test Elements FTE-14 and 15," General Atomic Report GA-A13944, to be published.

14. Hanson, D. L., N. L. Baldwin, and W. E. Selph, "Gamma Scanning the Primary Circuit of the Peach Bottom HTGR," General Atomic Report GA-A14161, October 31, 1976.

15. "Reactor Burn-up Physics," in Proceedings of a Panel on Reactor Burn-up Physics, a Conference Organized by the International Atomic Energy Agency and Held in Vienna, July 12-16, 1971, IAEA, Vienna 1973.

16. Crockett, T., General Atomic Company, private communication, June 1977.

17. Saurwein, J. J., "Peach Bottom Test Element Thermal Analyses with TREVER Code," General Atomic Company, unpublished data.

APPENDIX A

FIGURES

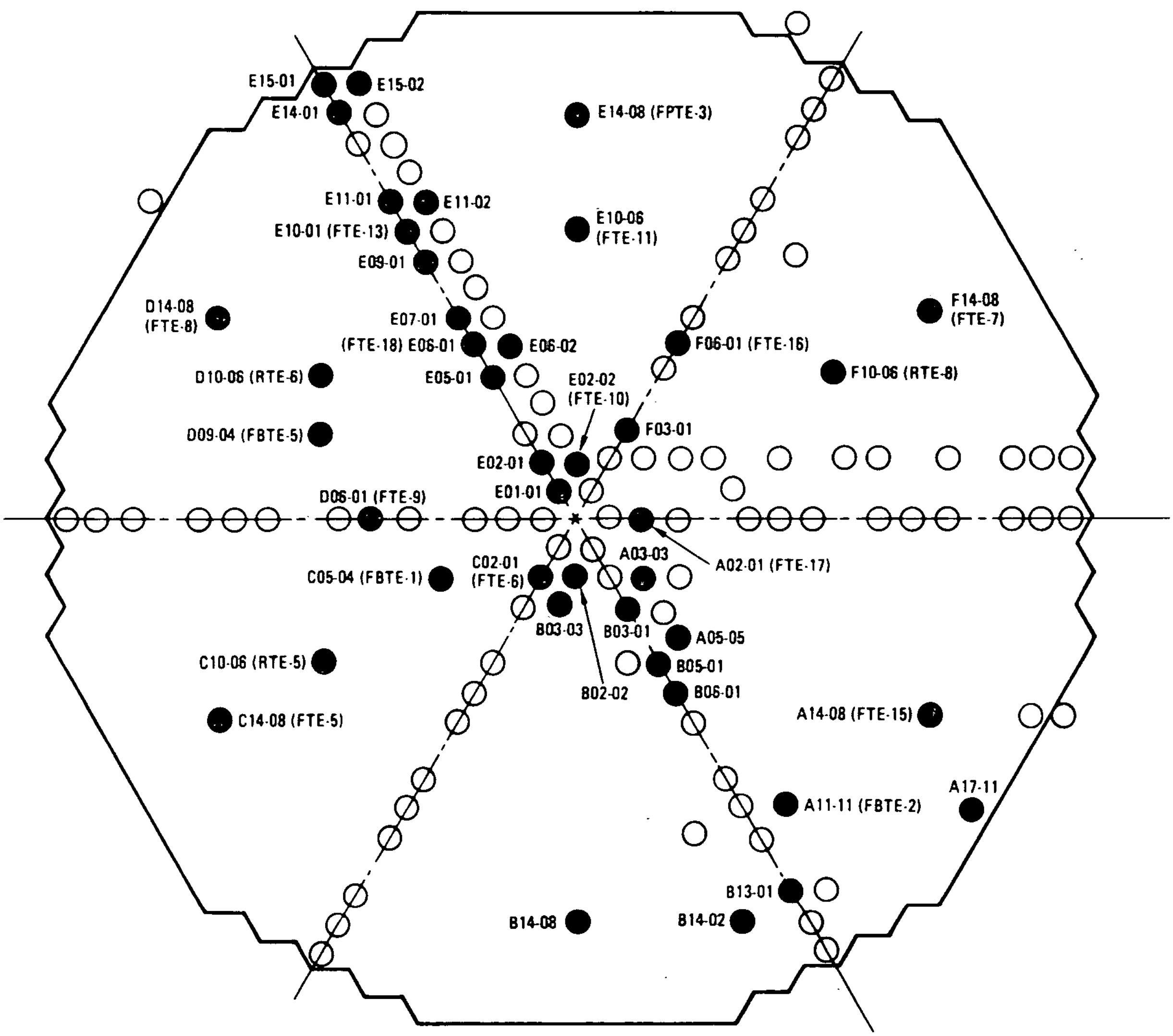

Fig. 1. Peach Bottom elements scanned during Phase I

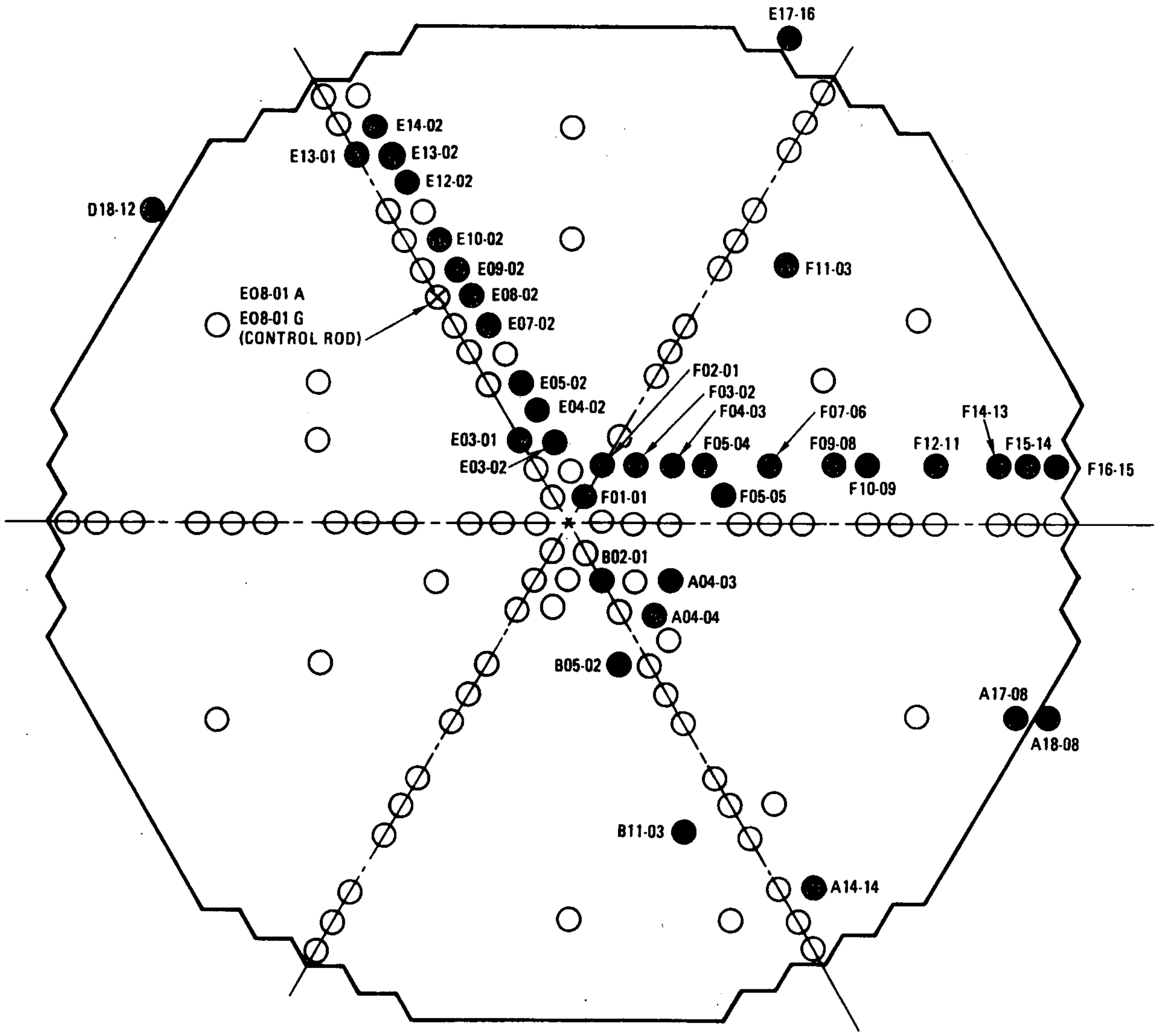

Fig. 2. Peach Bottom elements scanned during Phase II

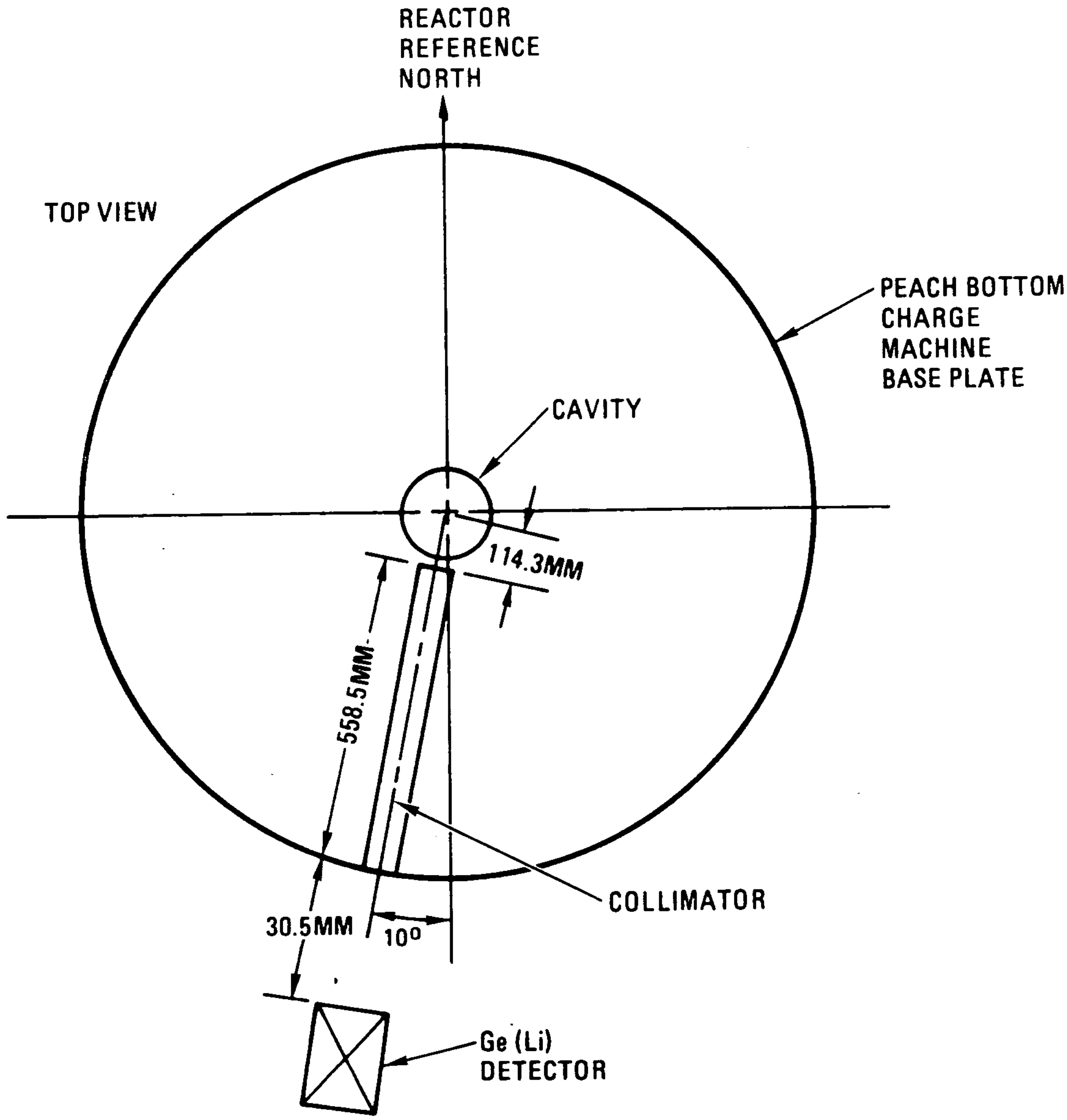

Fig. 3. Collimator geometry in Peach Bottom charge machine

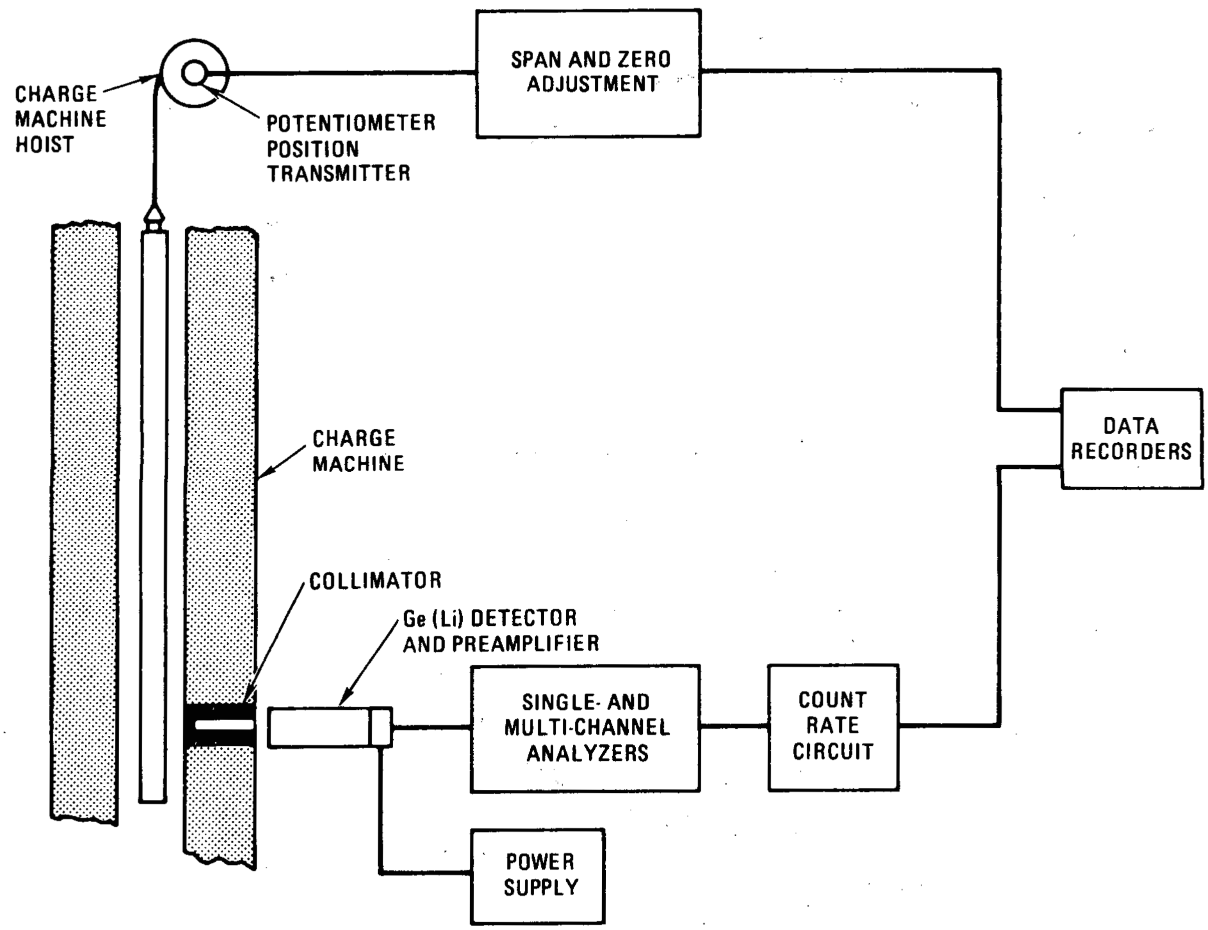

Fig. 4. Test arrangement for gamma scanning Peach Bottom test and driver fuel elements

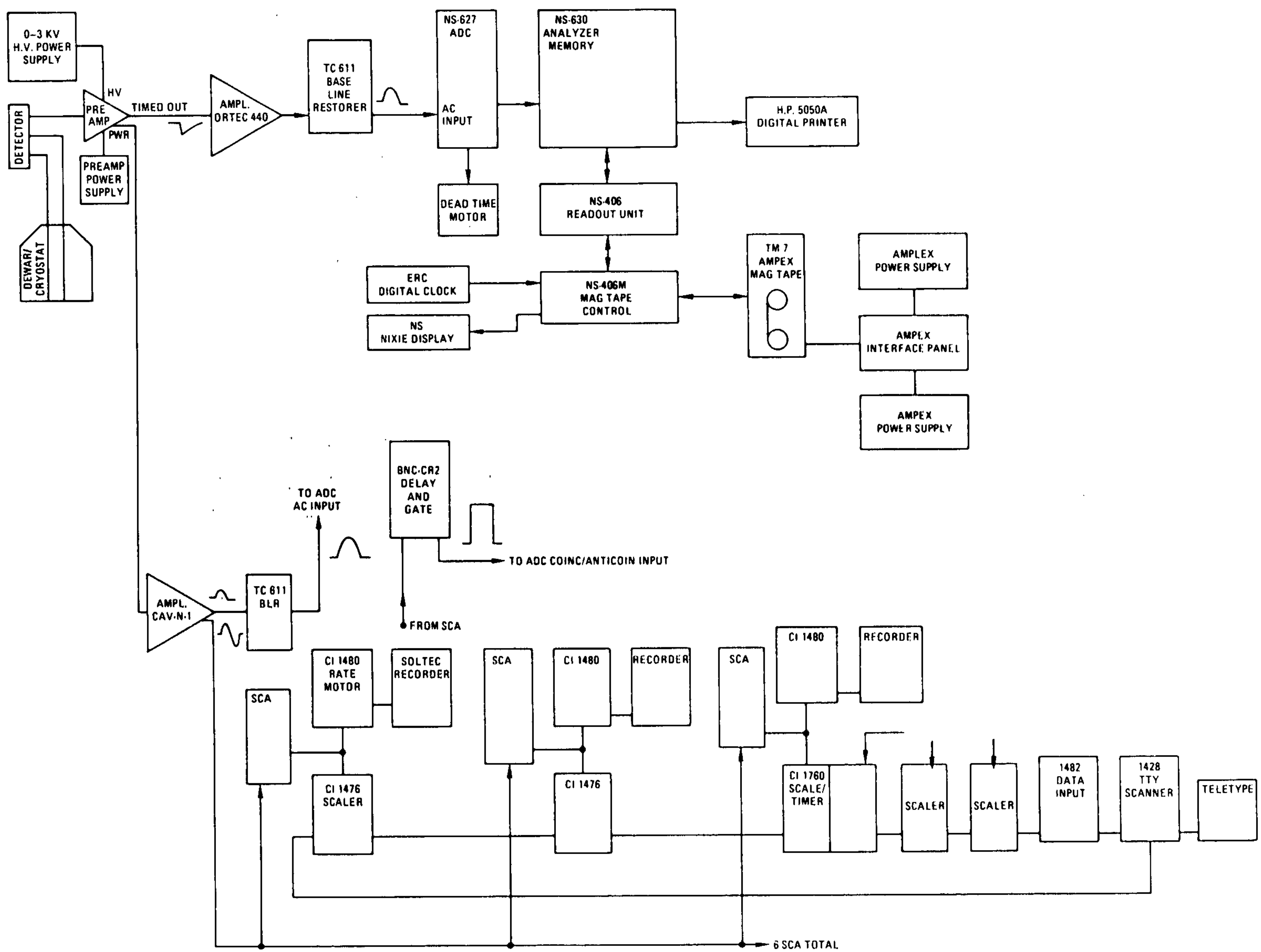

Fig. 5. Electrical schematic of Peach Bottom gamma scanning equipment

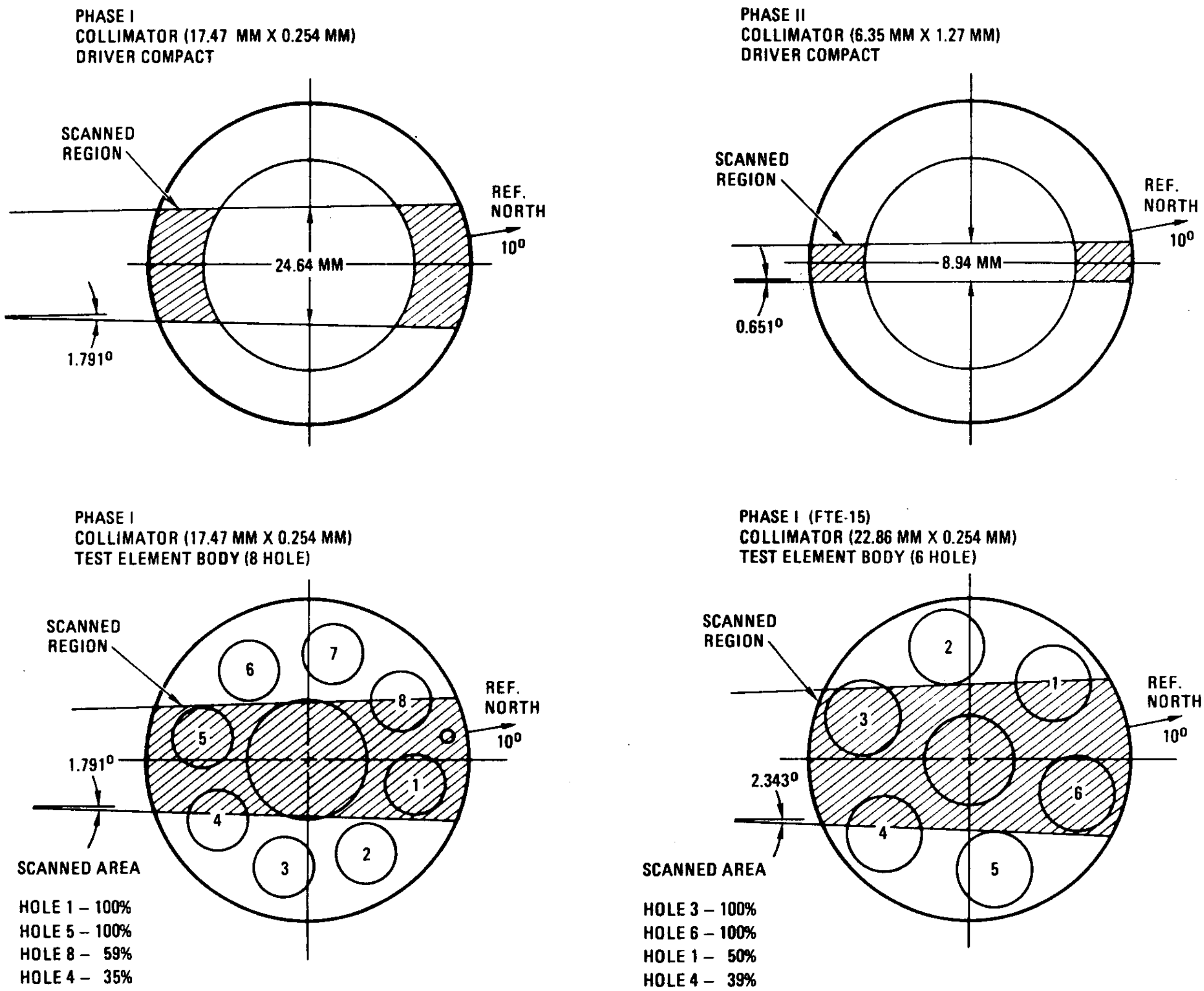

Fig. 6. Effective scanning paths of Peach Bottom EOL gamma scanning

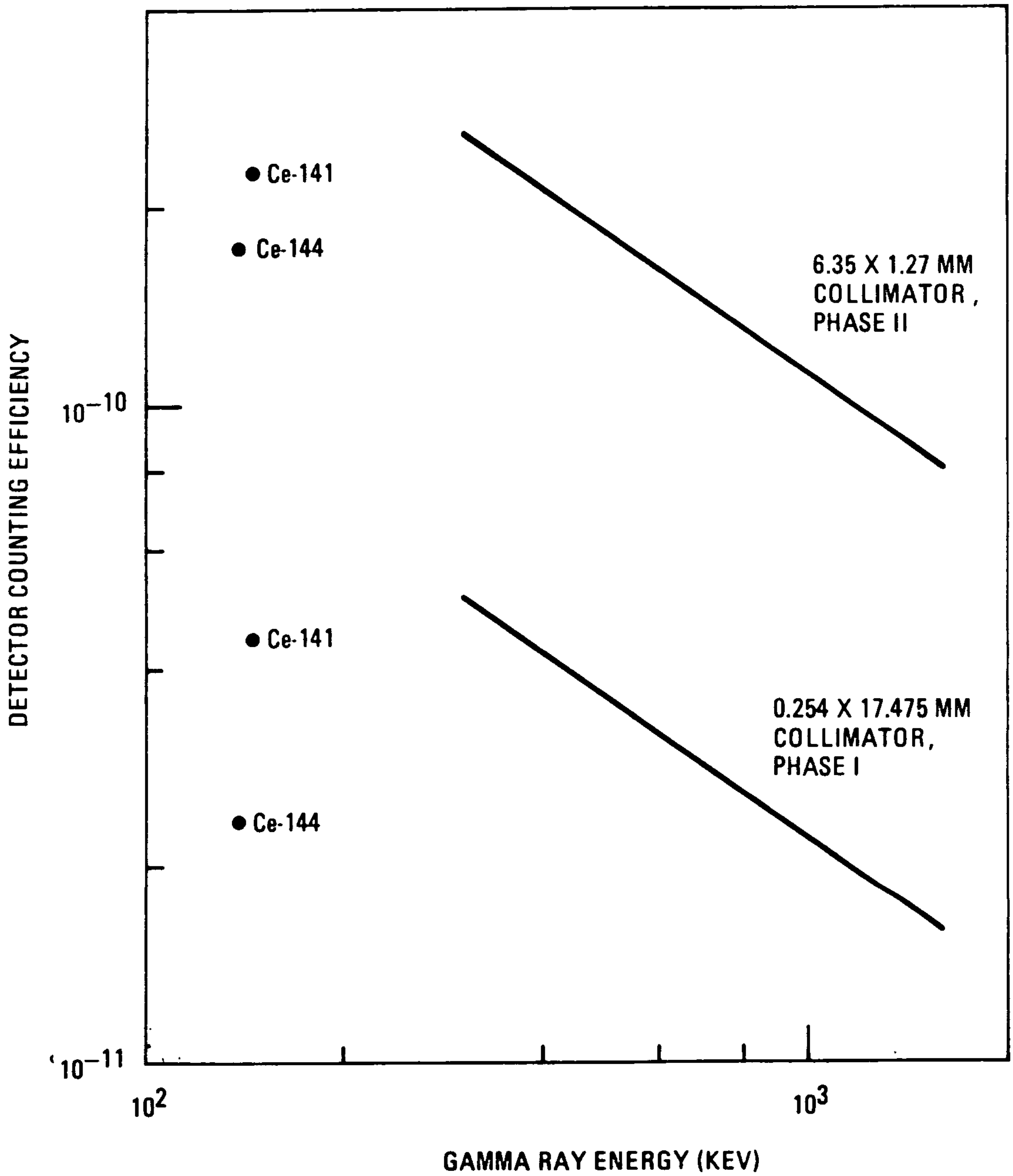

Fig. 7. Detector counting efficiency for Phase I and Phase II gamma scanning

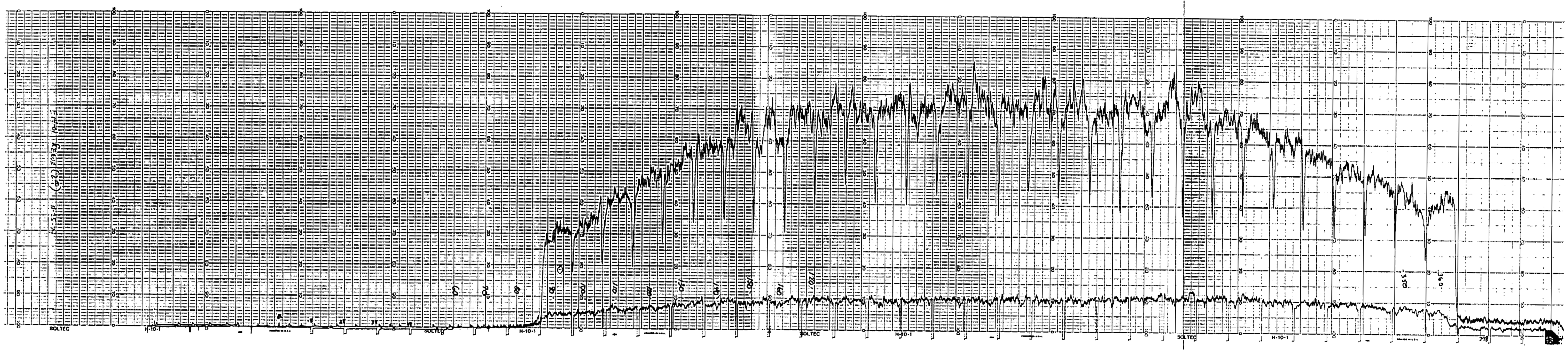

Fig. 8. E14-01 strip chart recording of Cs-137

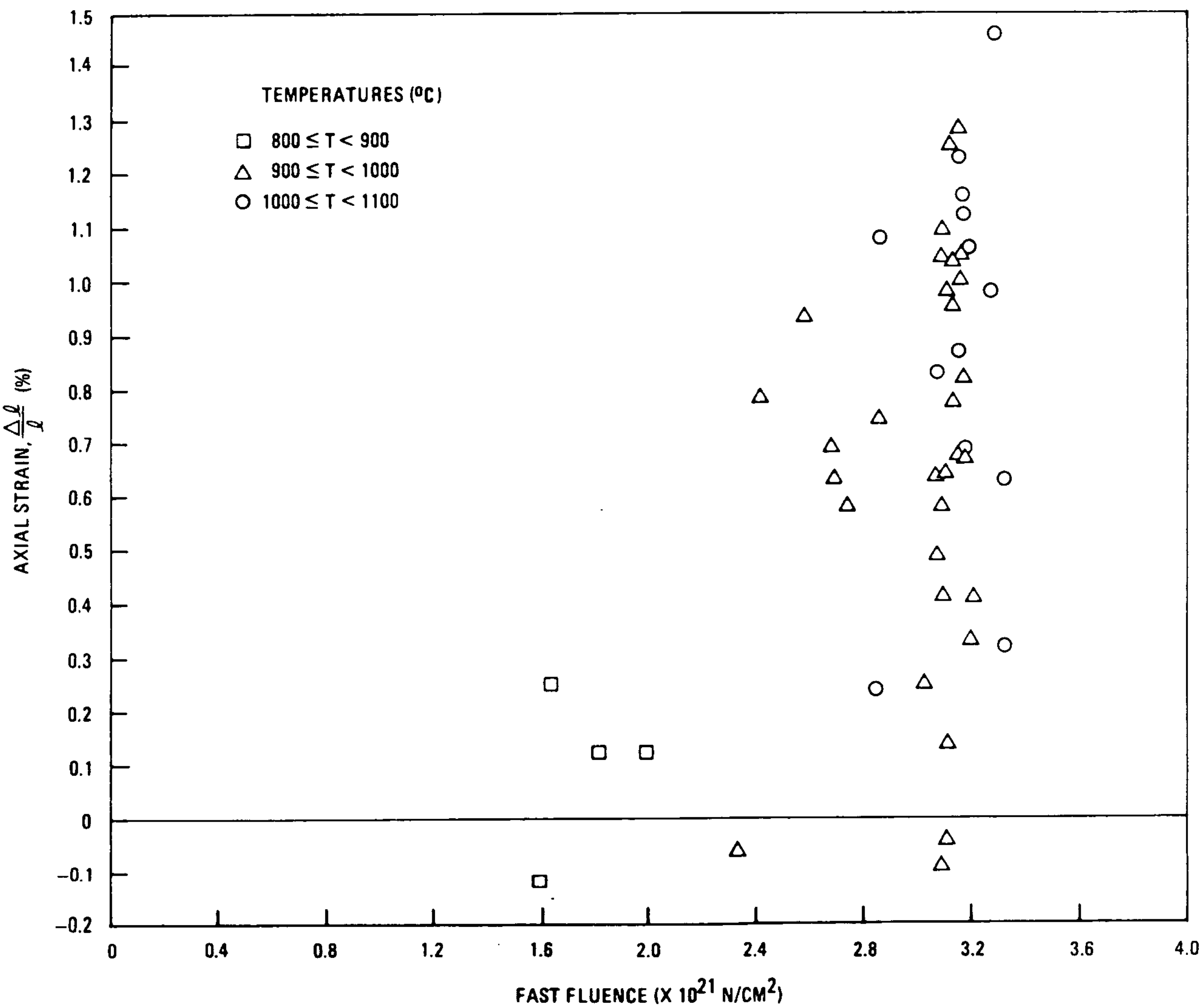

Fig. 9. Measured axial strain versus fast fluence at various time-averaged temperature ranges

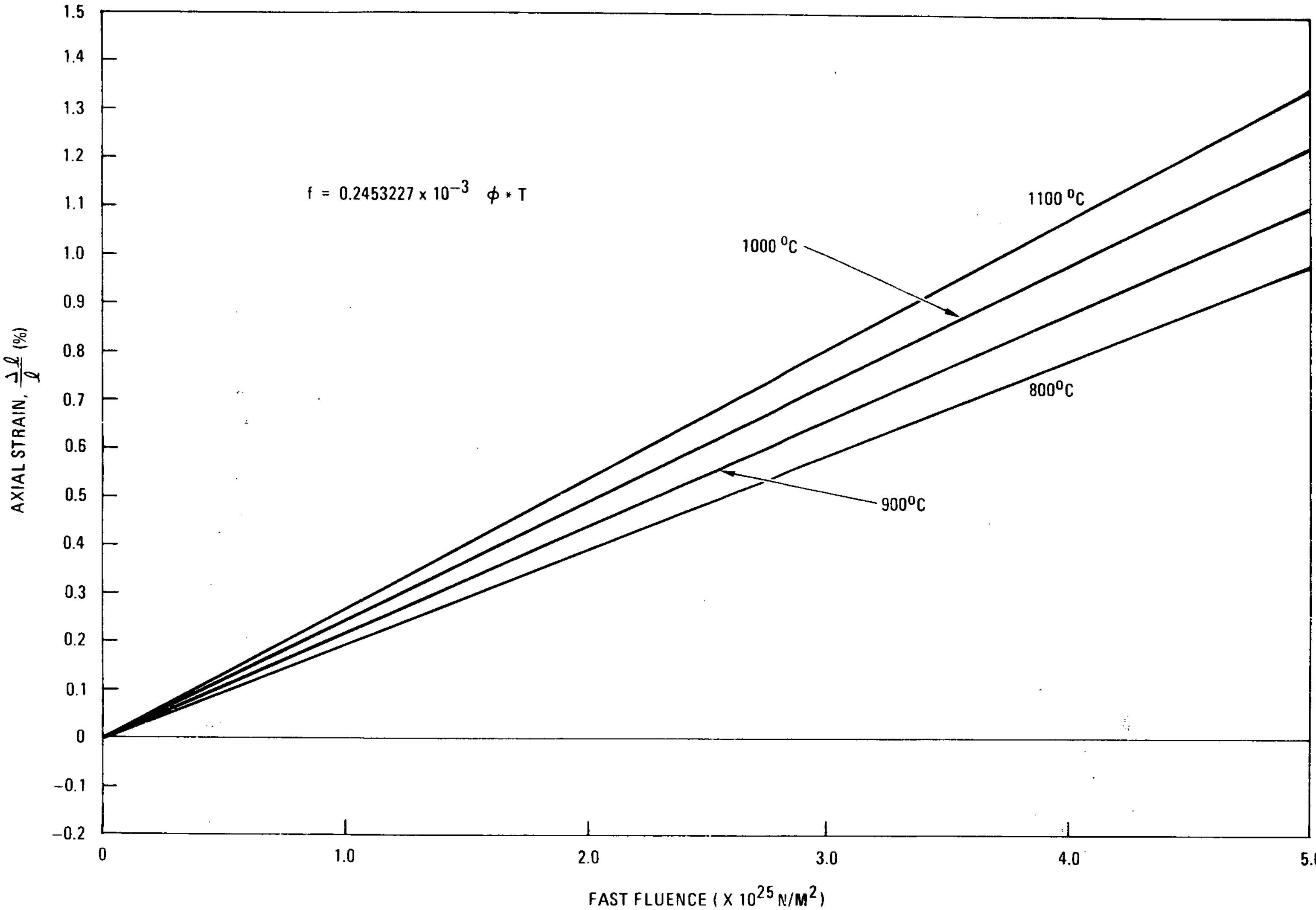

Fig. 10. Fitted axial strain versus fast fluence at various temperatures

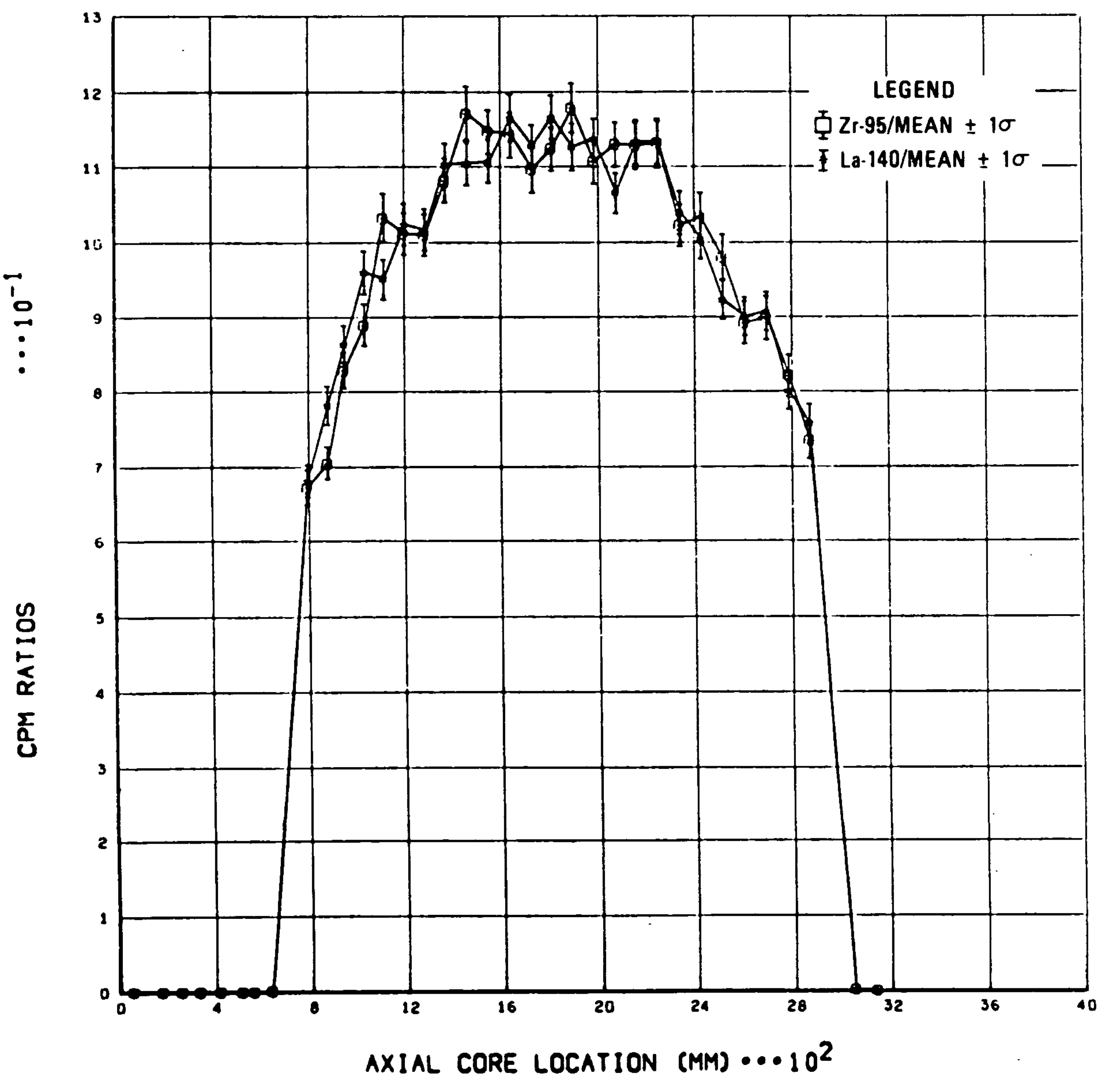

Fig. 11. Normalized nuclide CPM ratio axial profiles of Zr-95 and La-140 for E14-01

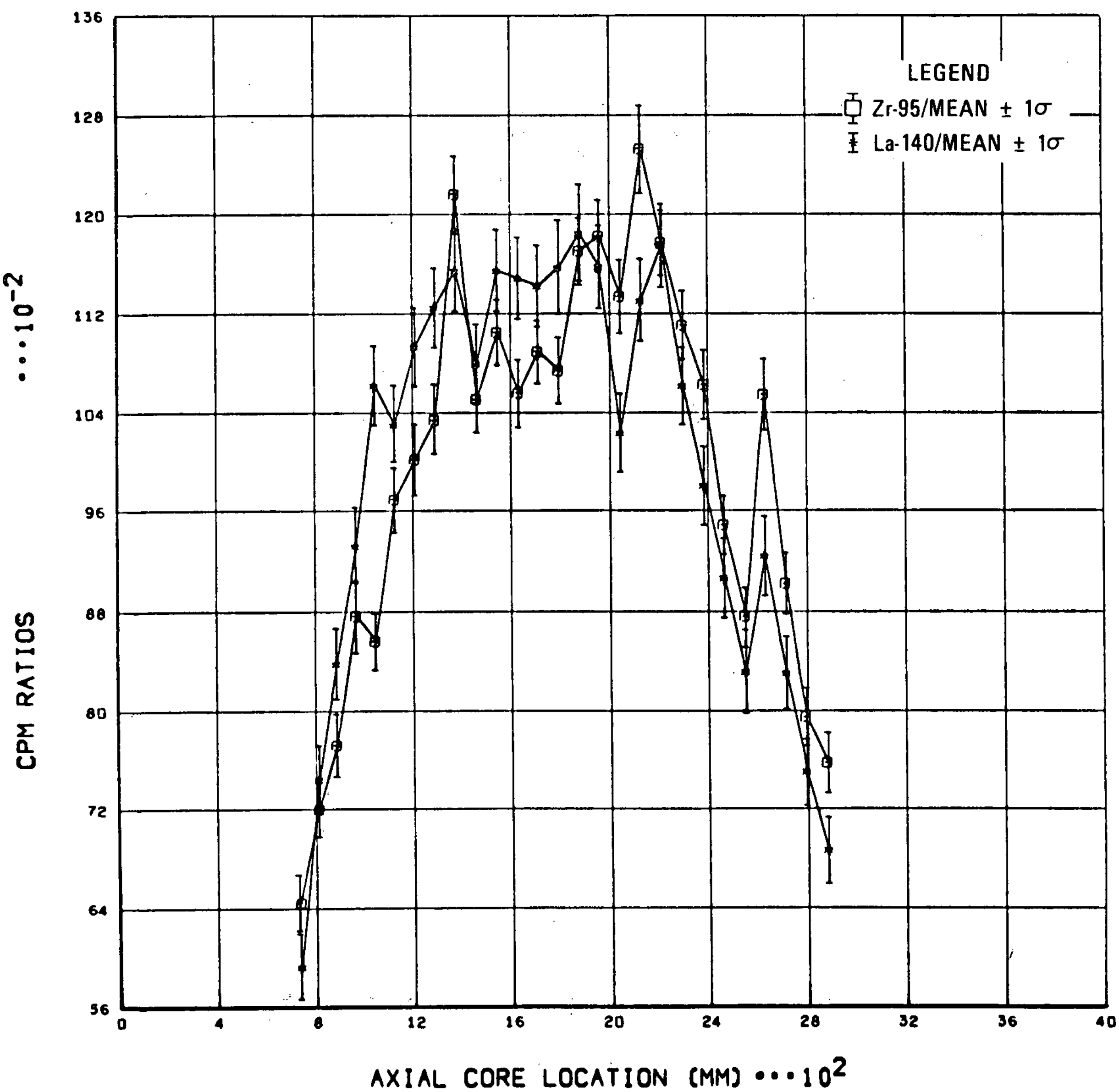

Fig. 12. Normalized nuclide CPM ratio axial profiles of Zr-95 and La-140 for F03-01

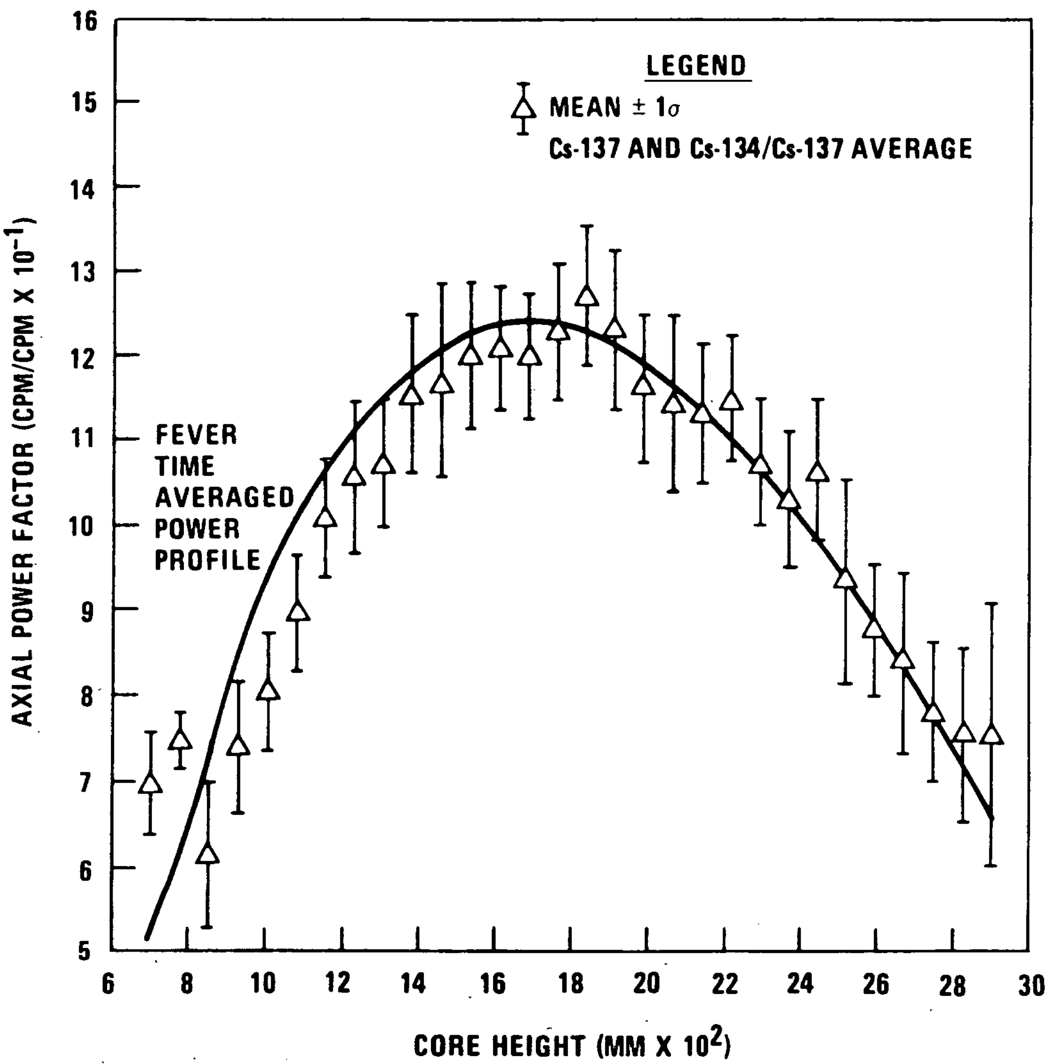

Fig. 13. FEVER time-averaged power profile comparison for E14-01

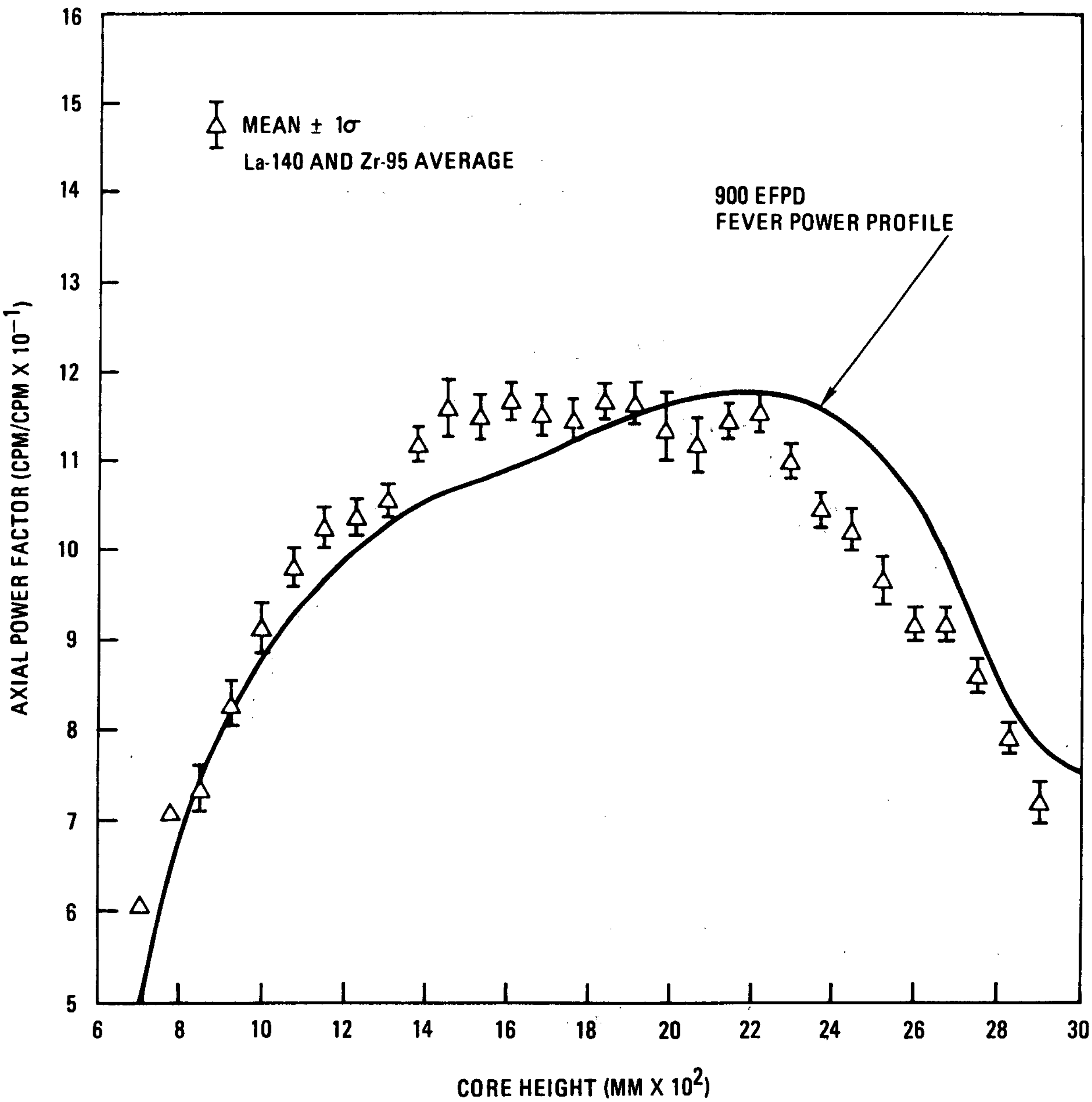

Fig. 14. FEVER calculated EOL power profile comparison for E14-01

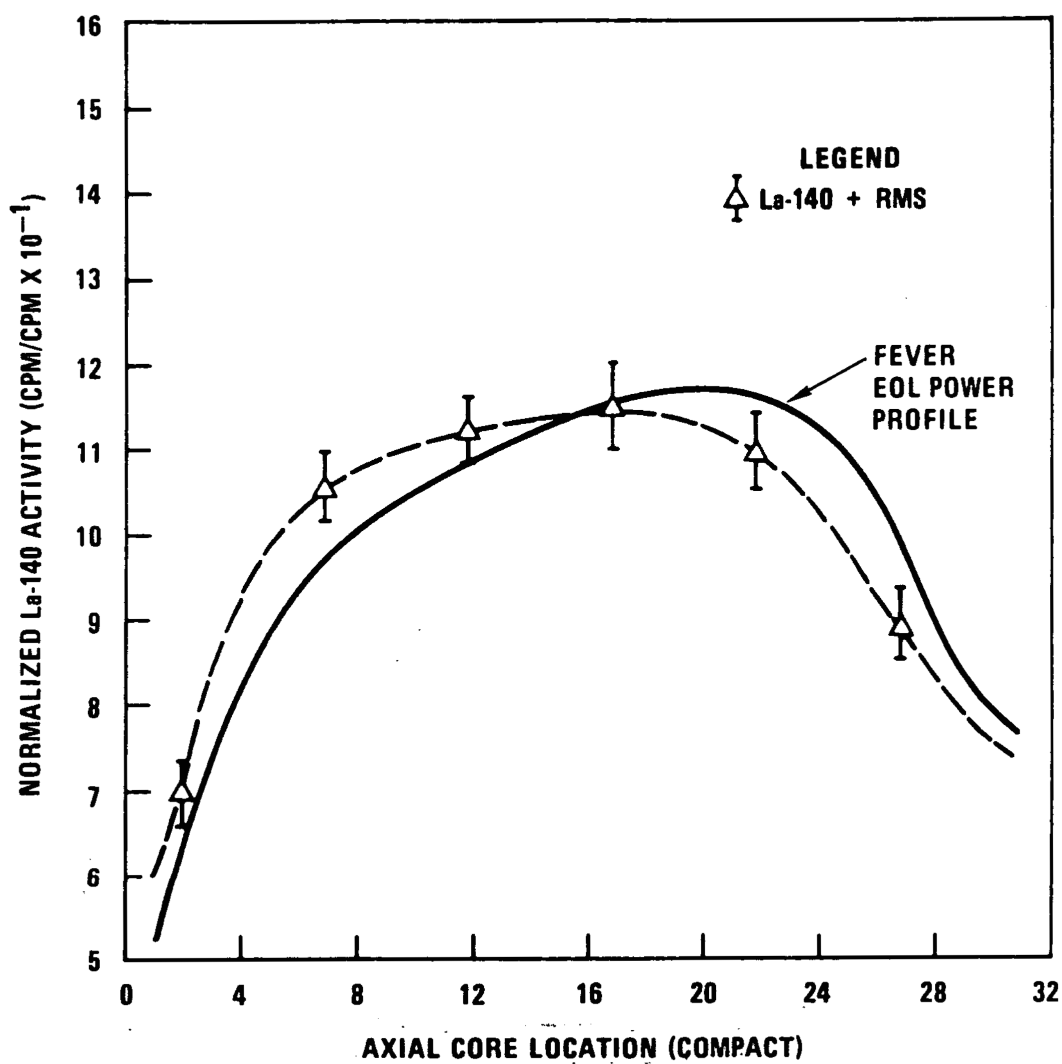

Fig. 15. EOL axial power profile comparison for 14 Phase I unperturbed elements

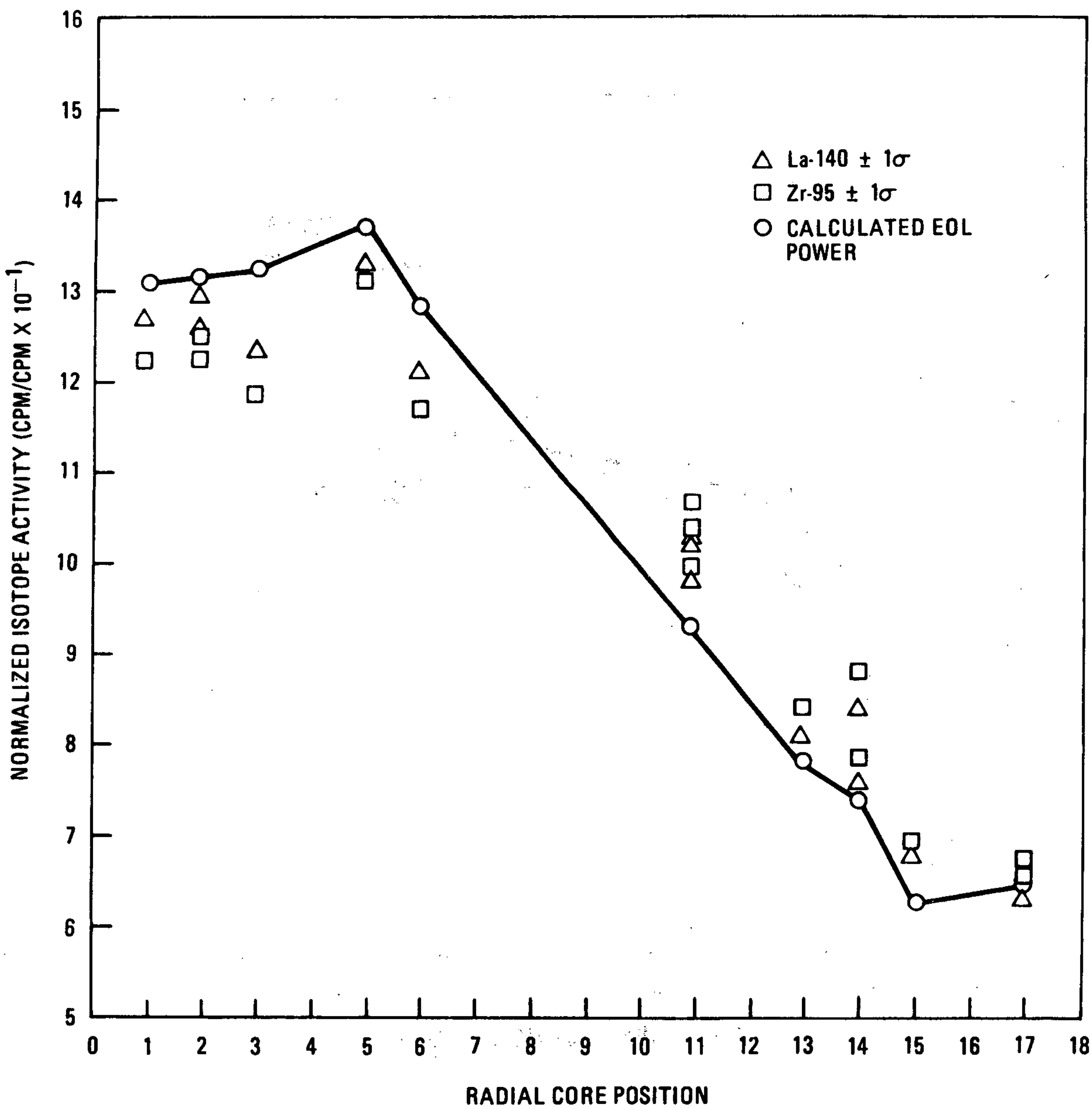

Fig. 16. Normalized radial distribution of La-140 and Zr-95 in Phase I driver elements

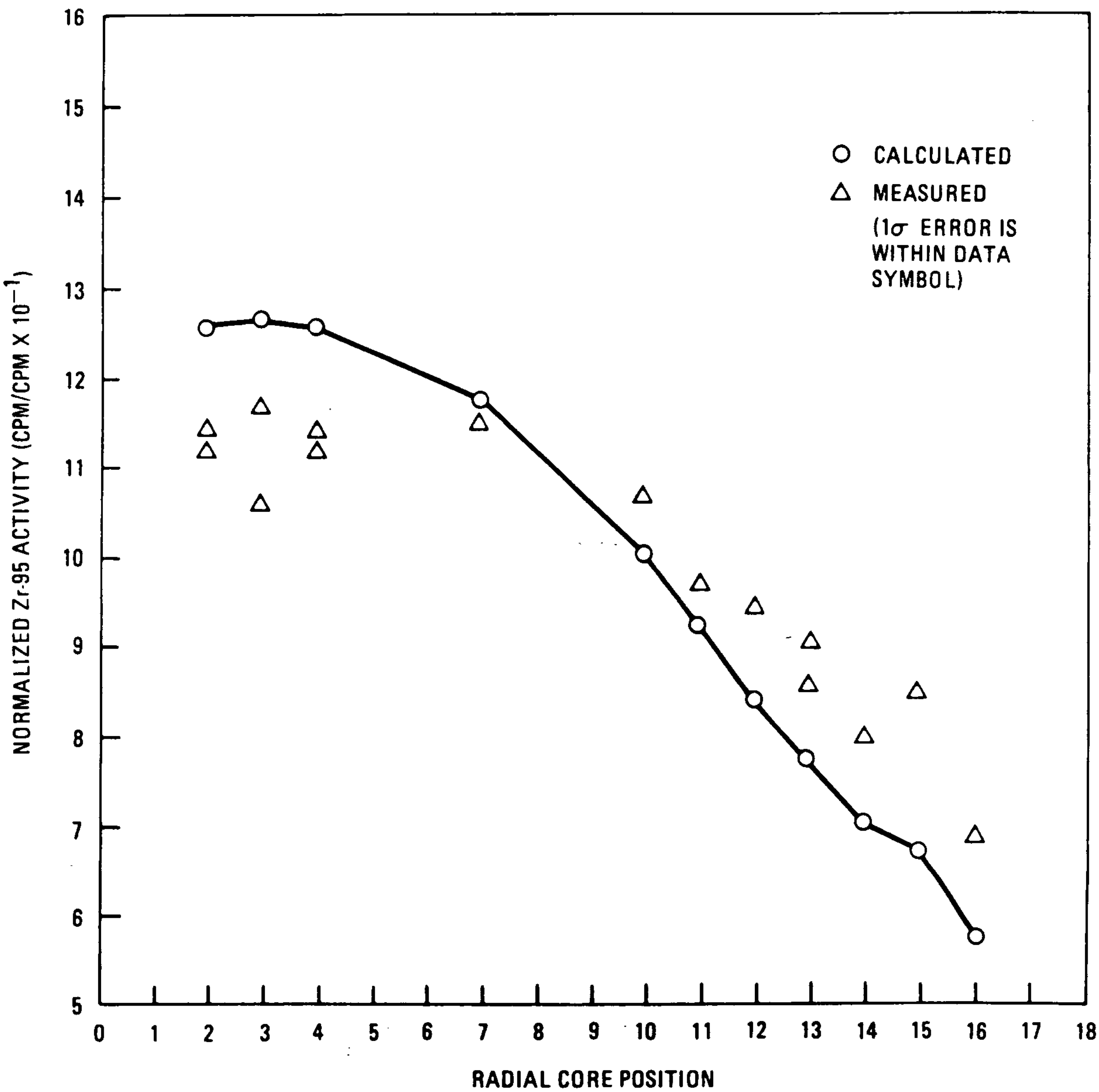

Fig. 17. Normalized radial distribution of Zr-95 in Phase II driver elements

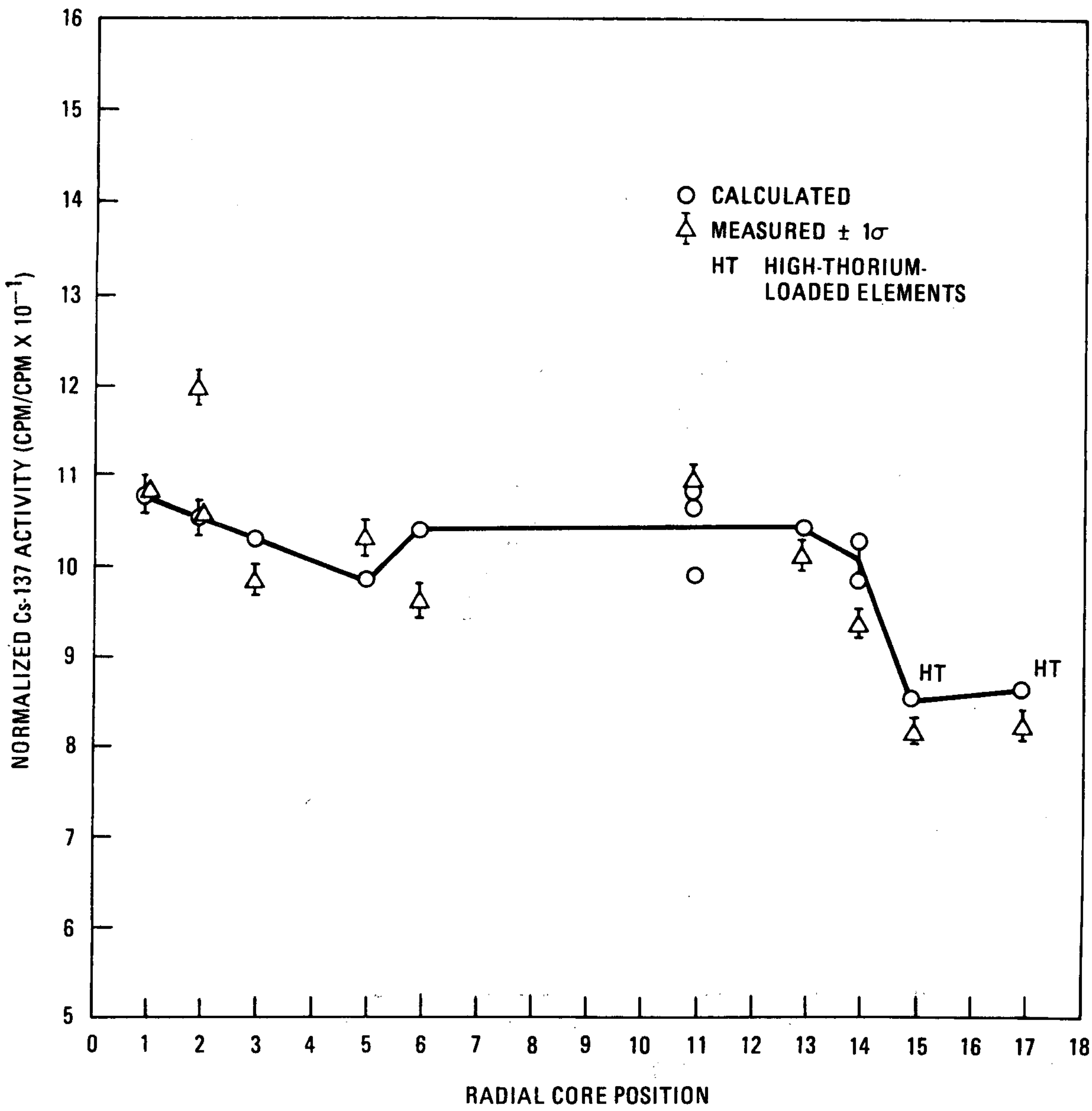

Fig. 18. Normalized radial distribution of Cs-137 in Phase I driver elements

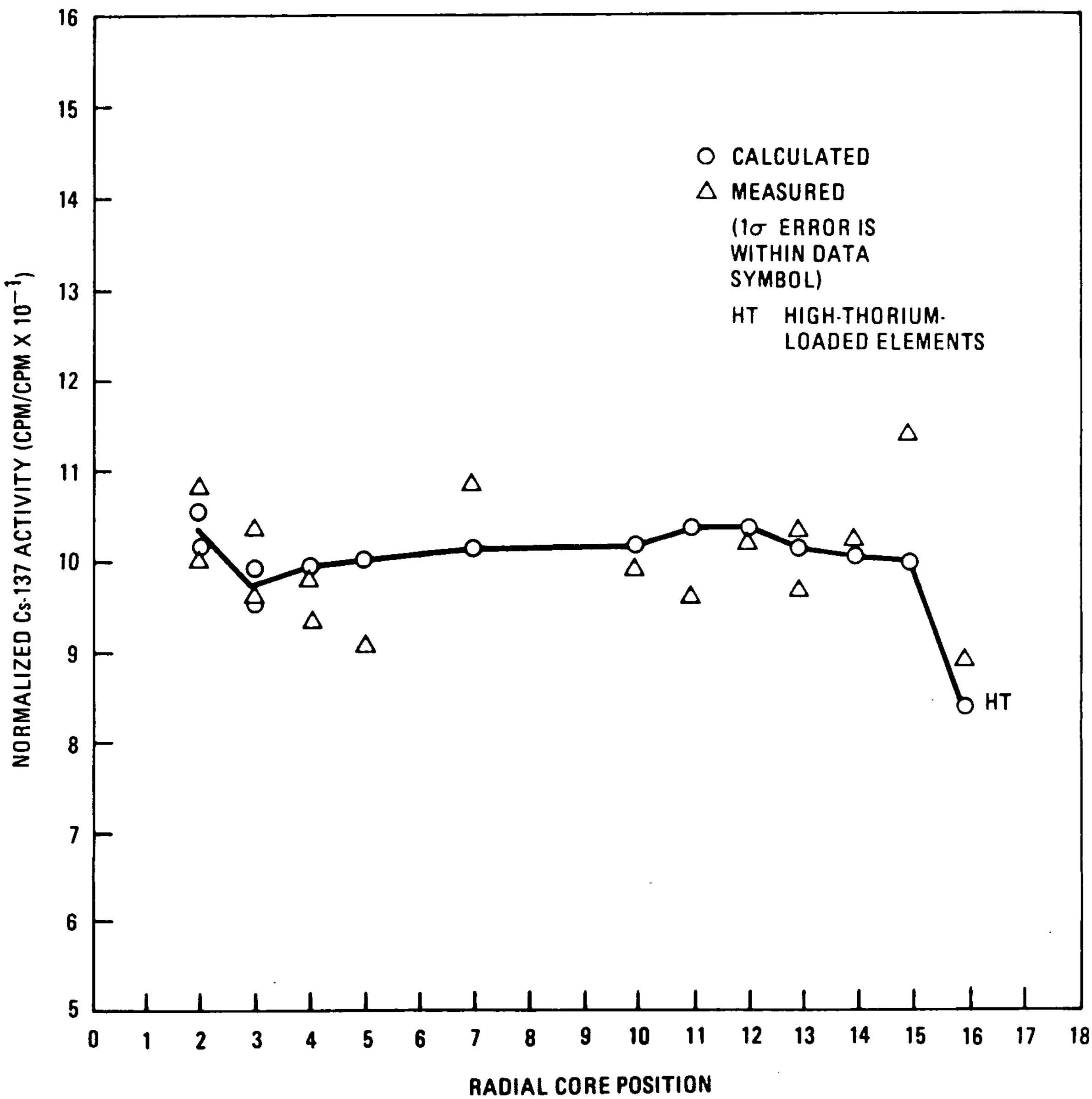

Fig. 19. Normalized radial distribution of Cs-137 in Phase II driver elements

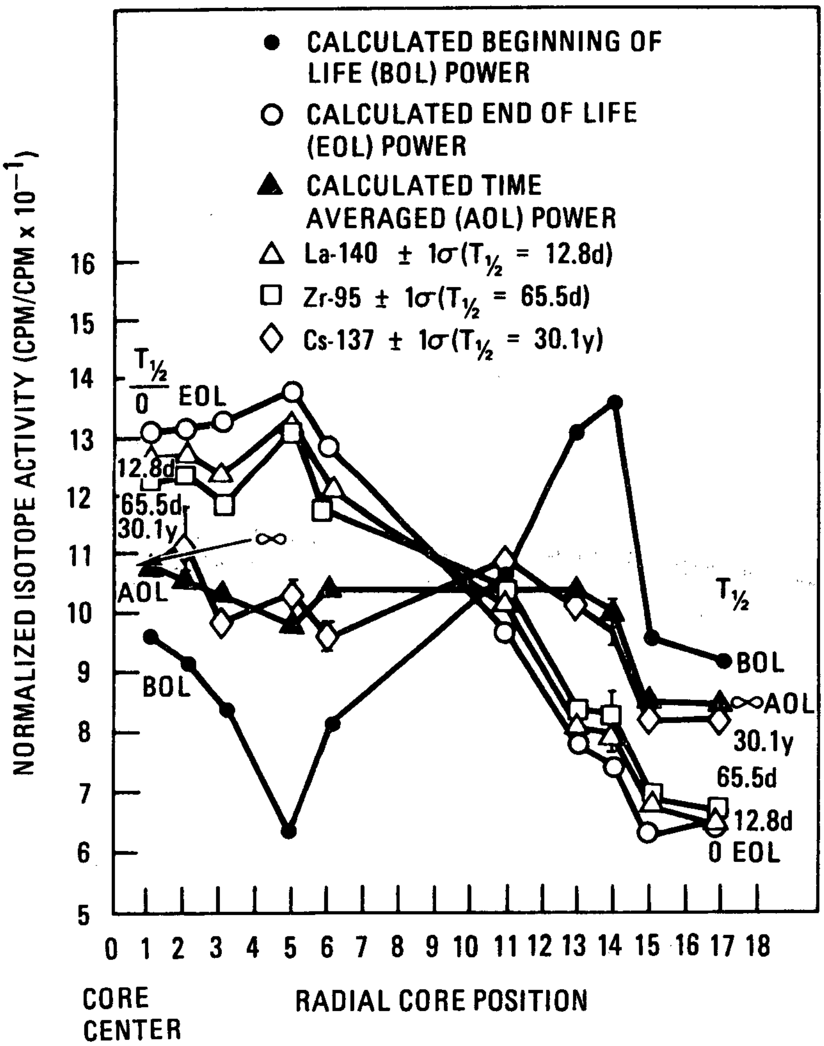

Fig. 20. Normalized radial isotope distribution summary for Phase I

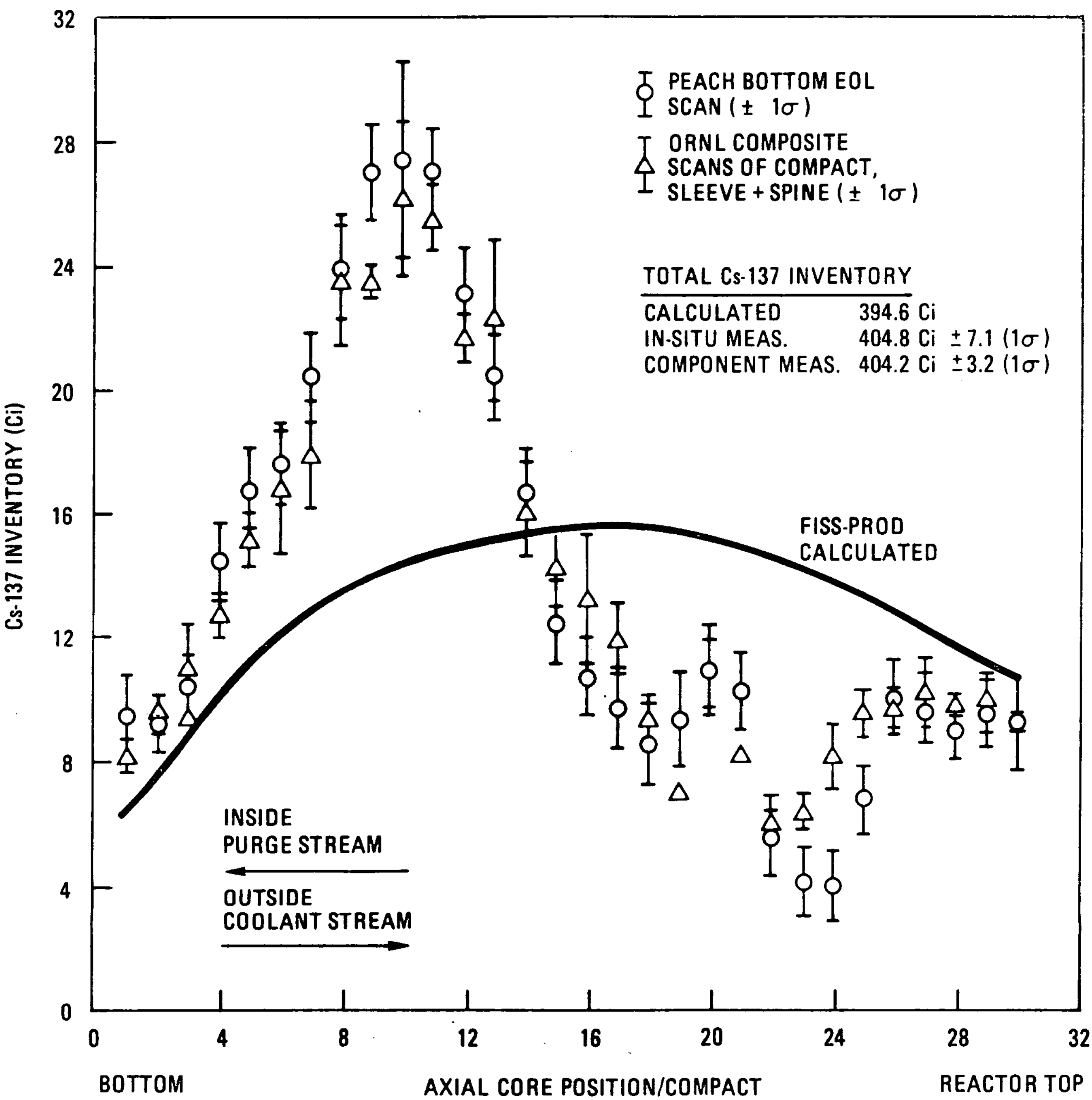

Fig. 21. Cs-137 inventory versus axial core position for F03-01

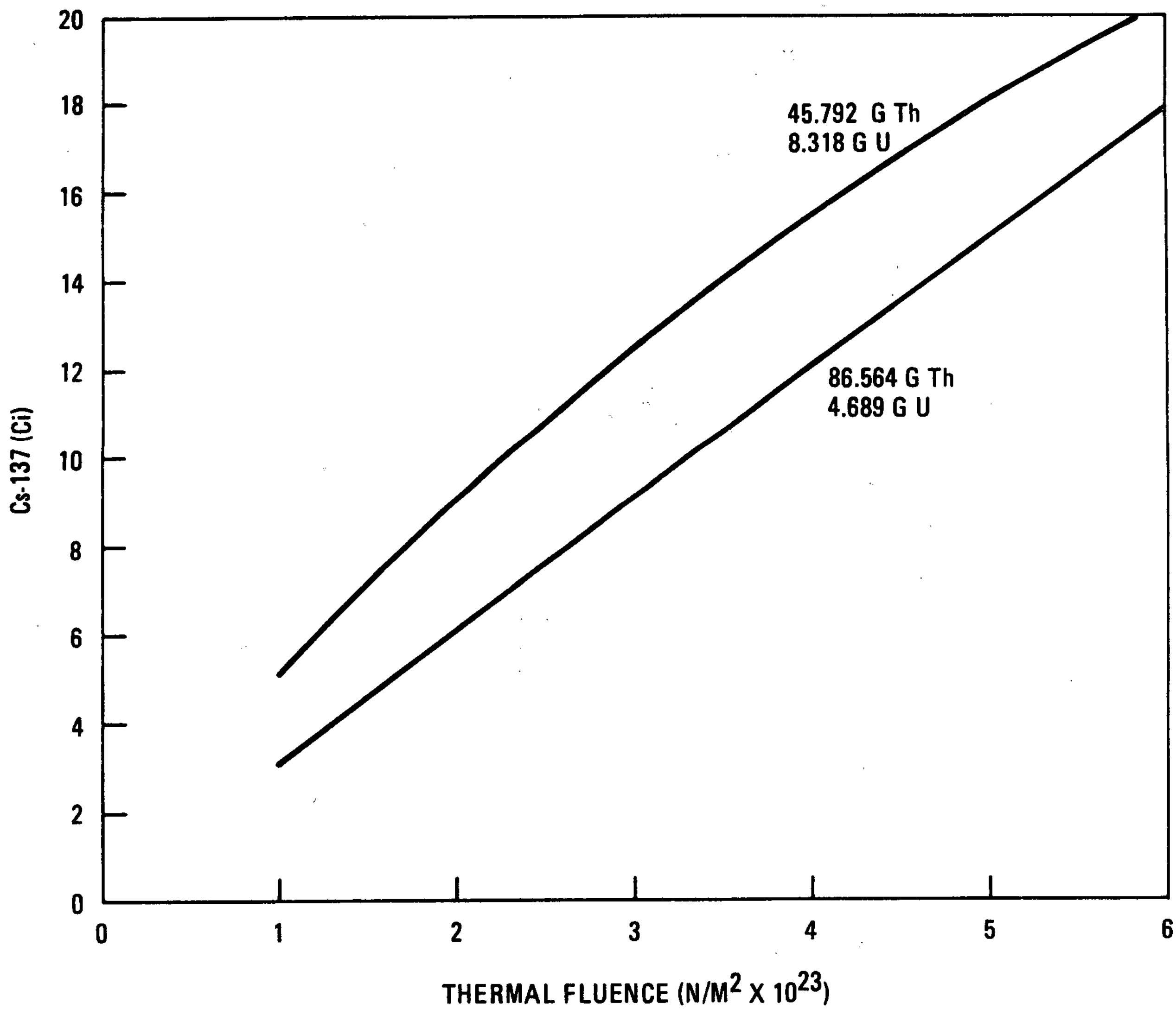

Fig. 22. FISS-PROD calculated Cs-137 inventories for Peach Bottom driver elements

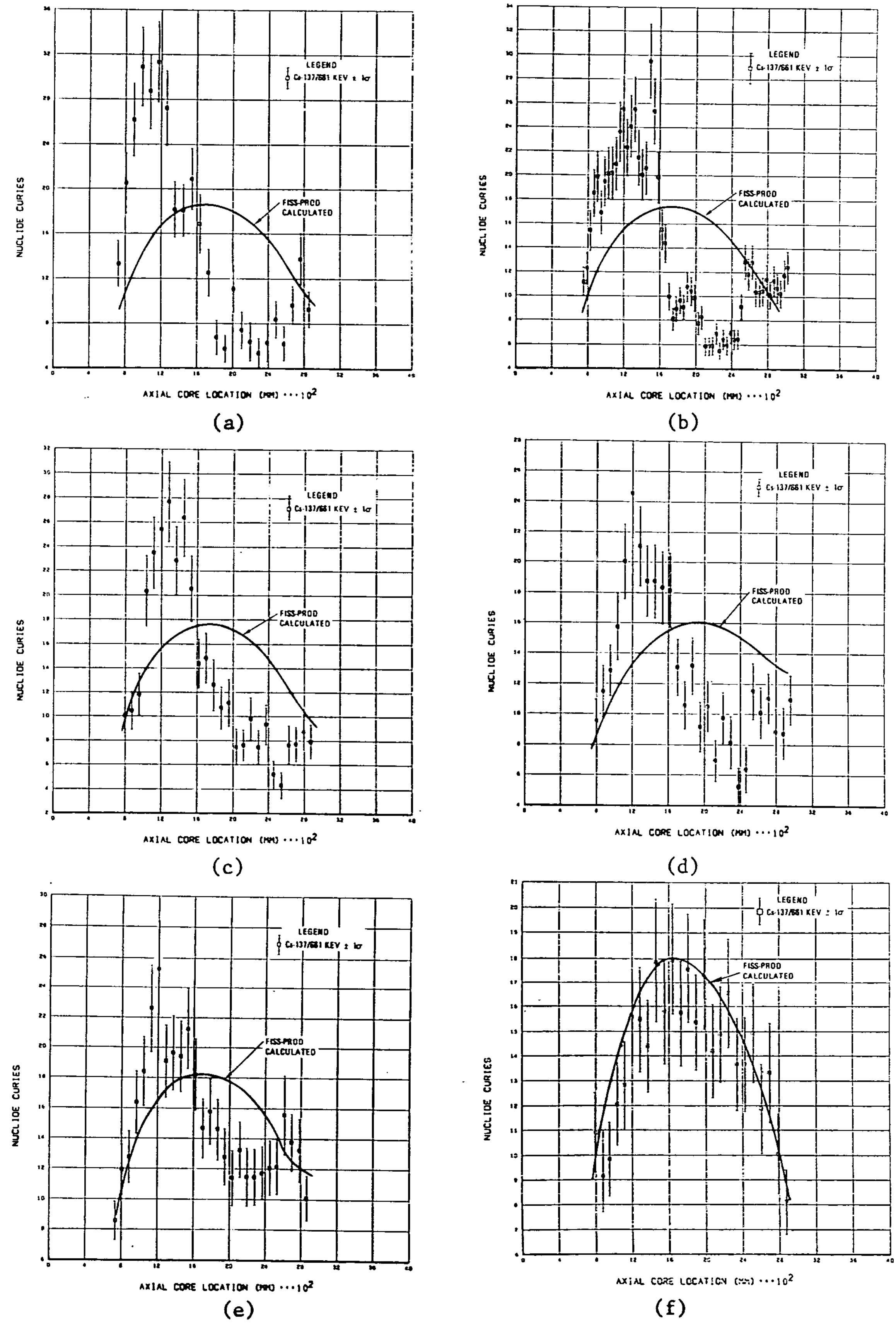

Fig. 23. Absolute cesium nuclide activities for (a) E01-01, (b) E03-02, (c) E06-02, (d) E09-01, (e) E11-01, and (f) E14-01

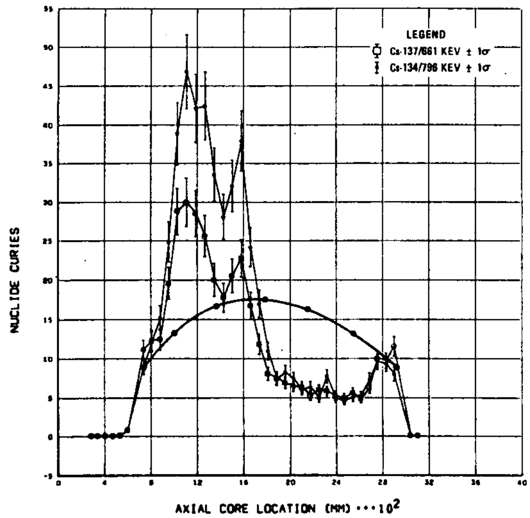

(a)

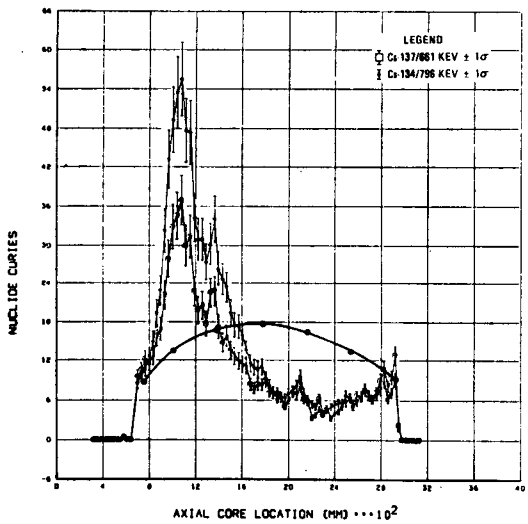

(b)

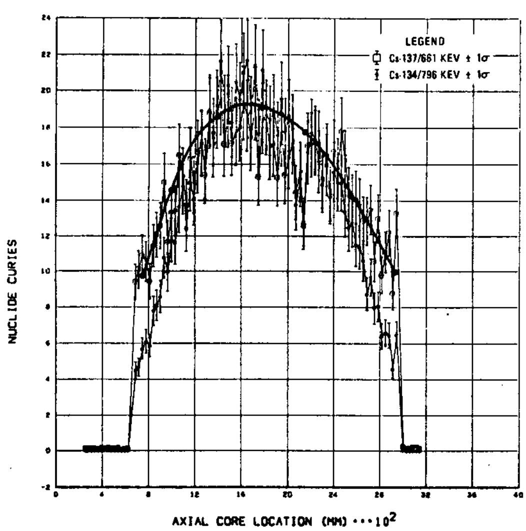

(c)

Fig. 24. Absolute cesium nuclide activities for (a) F02-01, (b)F04-03, and (c) F15-14. Solid curves are FISS-PROD calculations.

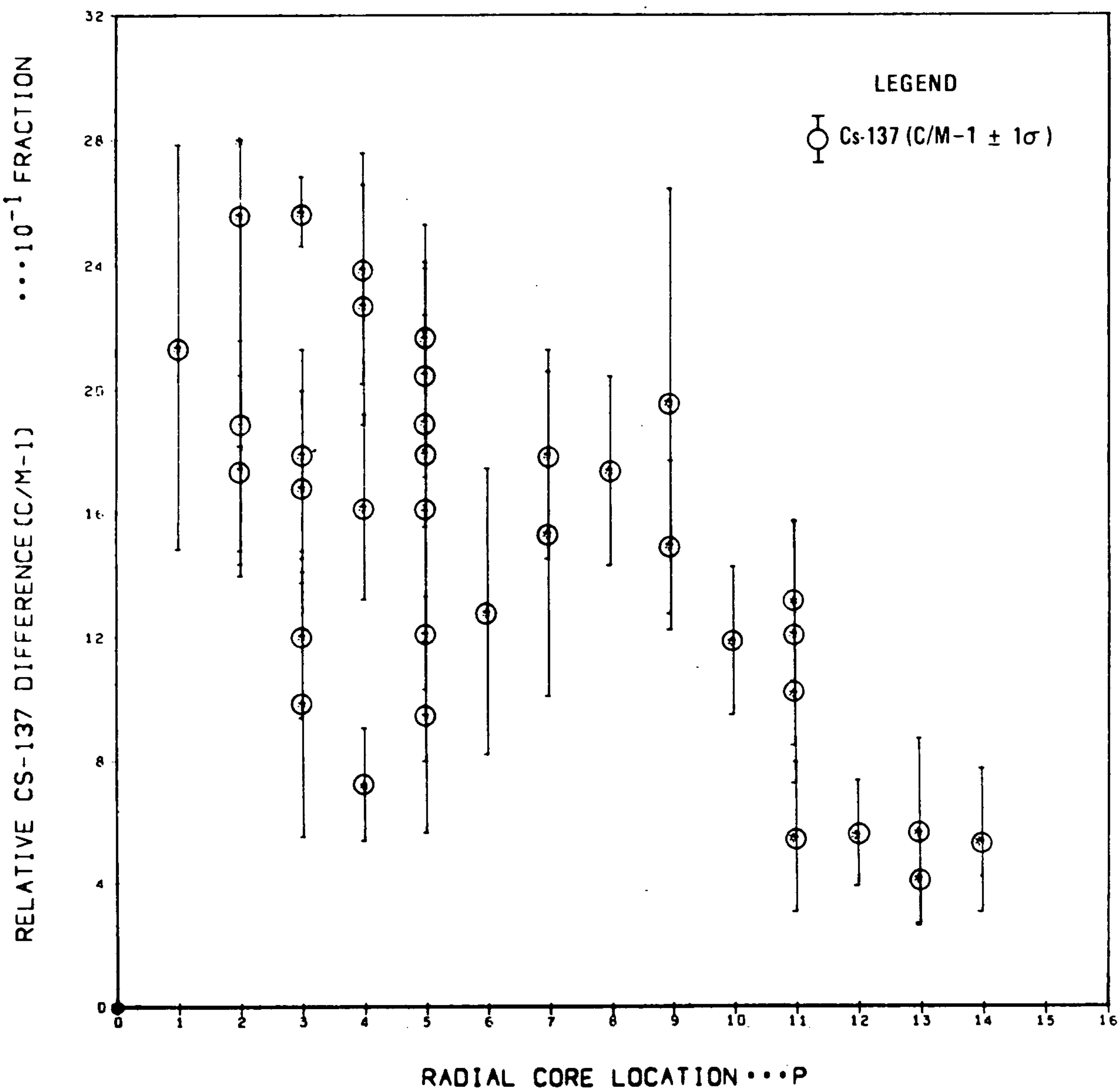

Fig. 25. Relative Cs-137 difference versus core location

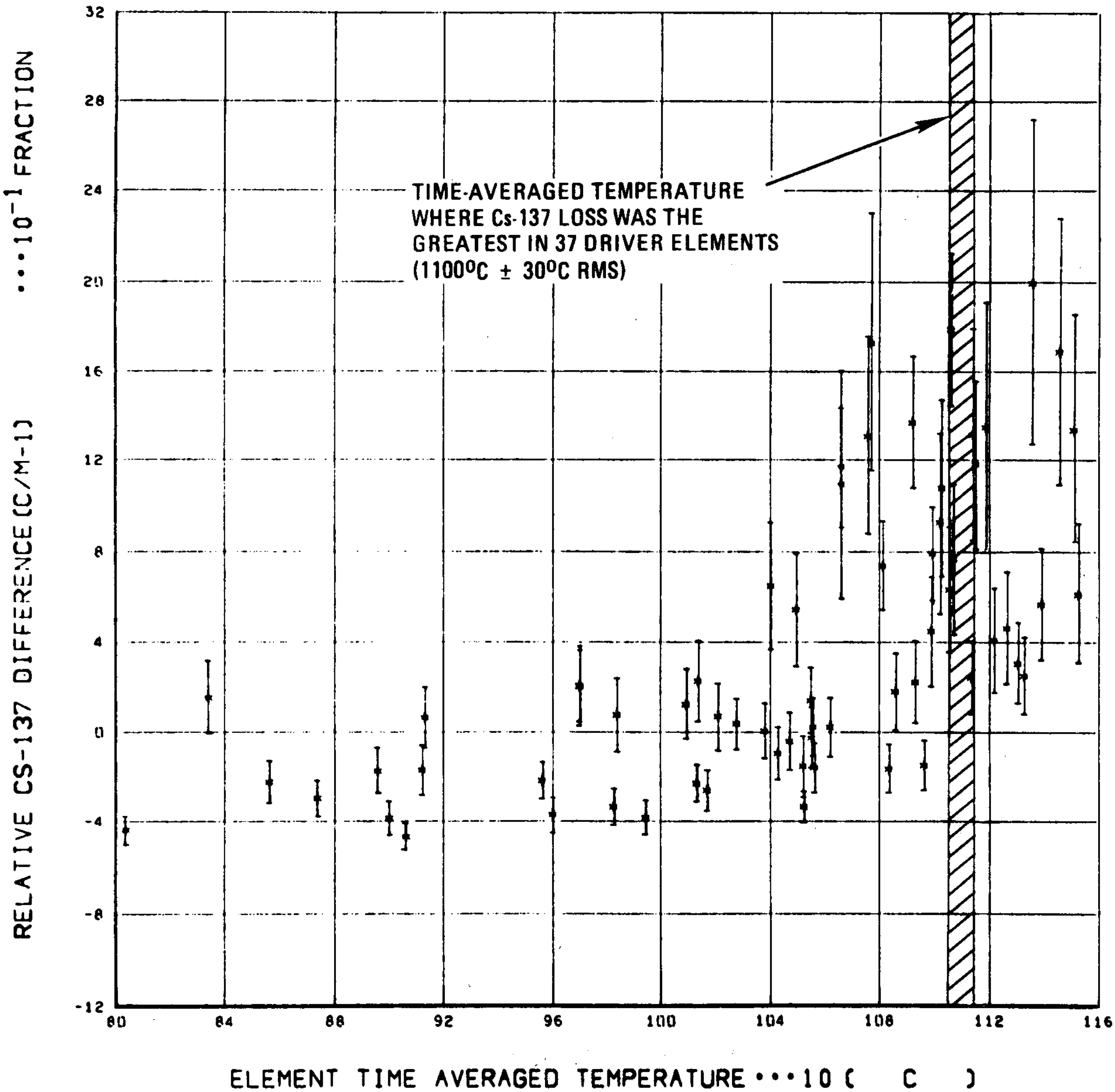

Fig. 26. Relative Cs-137 difference versus mean element temperature

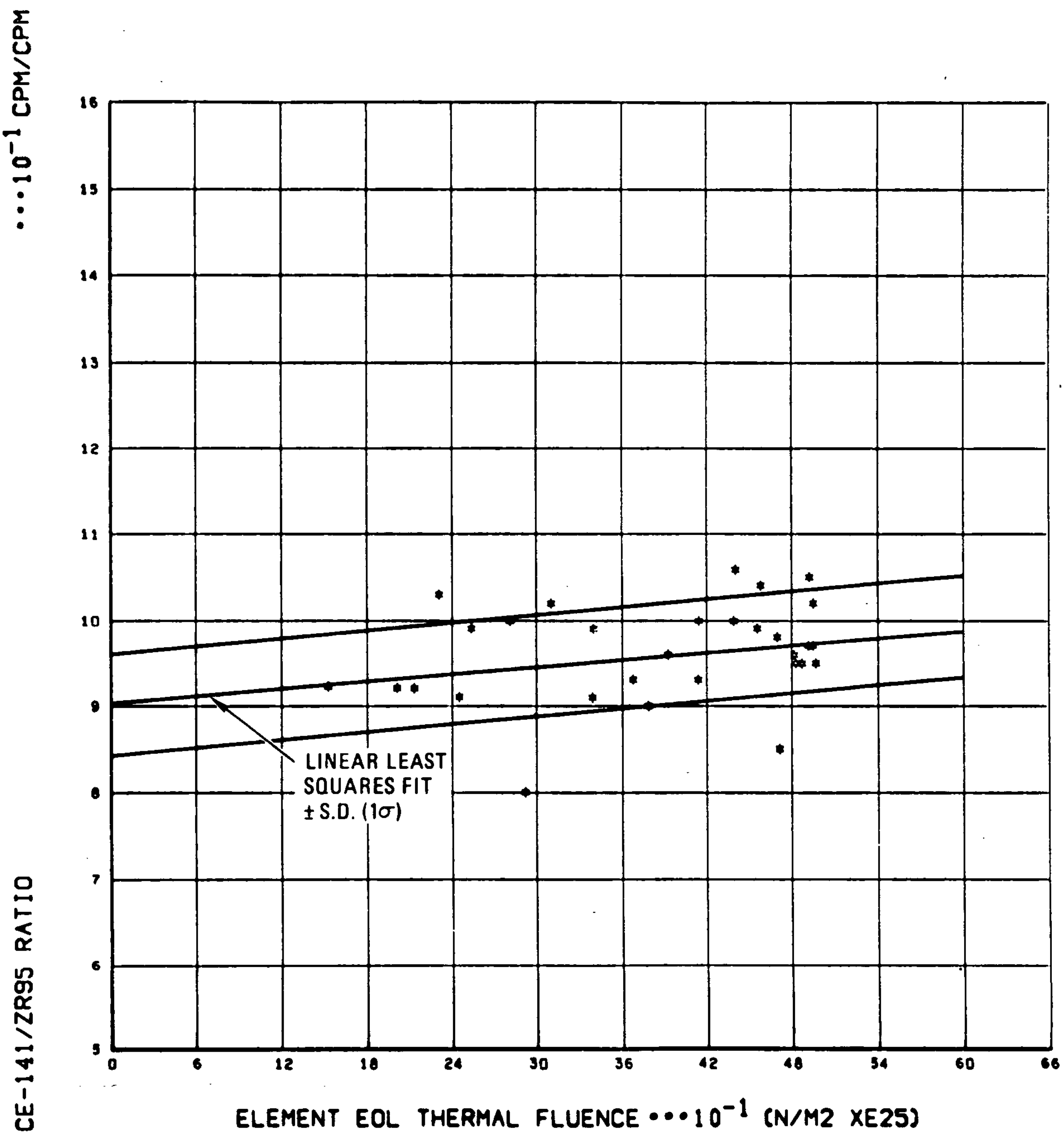

Fig. 27. Ce-141/Zr-95 CPM ratio versus thermal fluence

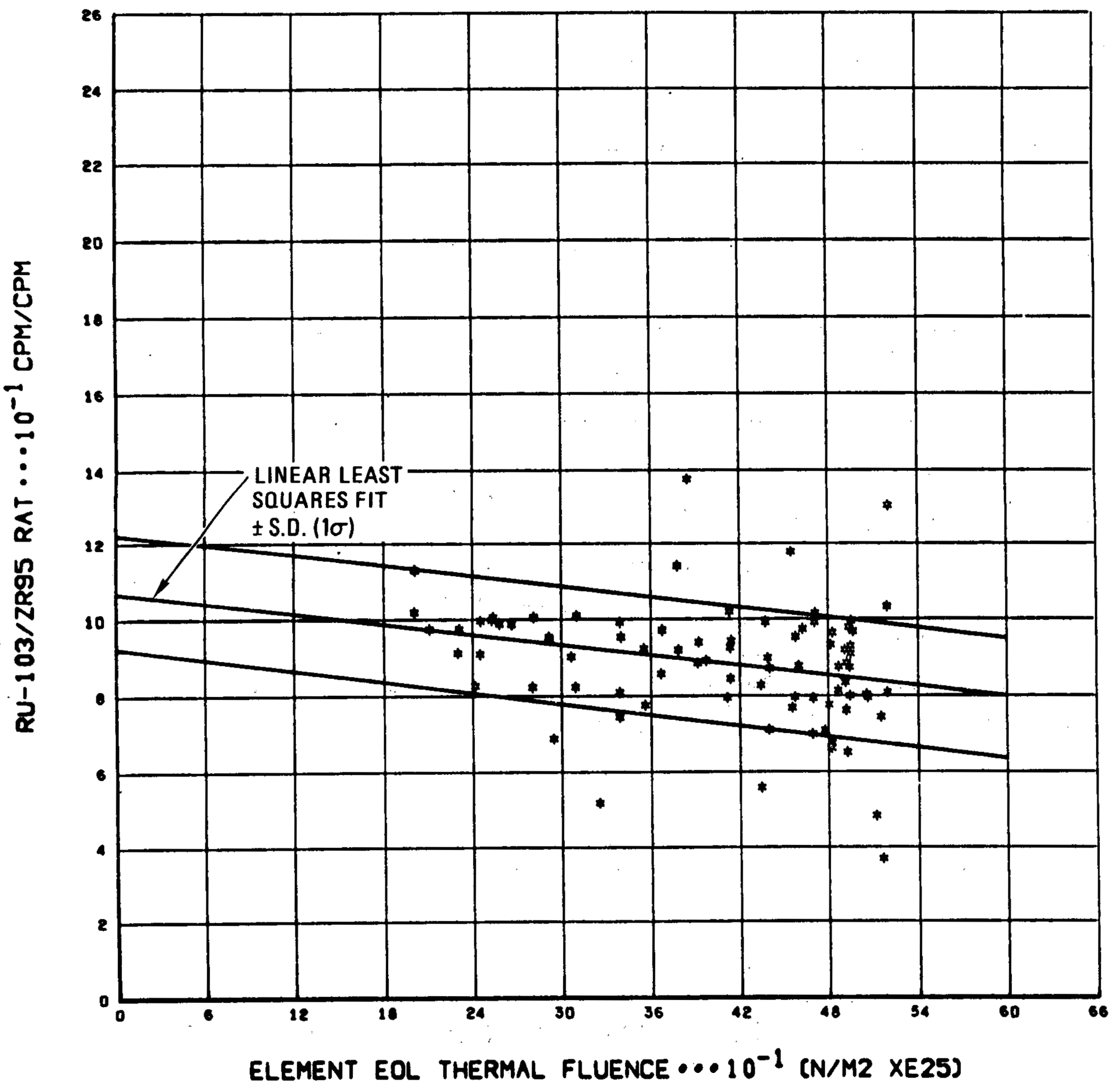

Fig. 28. Ru-103/Zr-95 CPM ratio versus thermal fluence

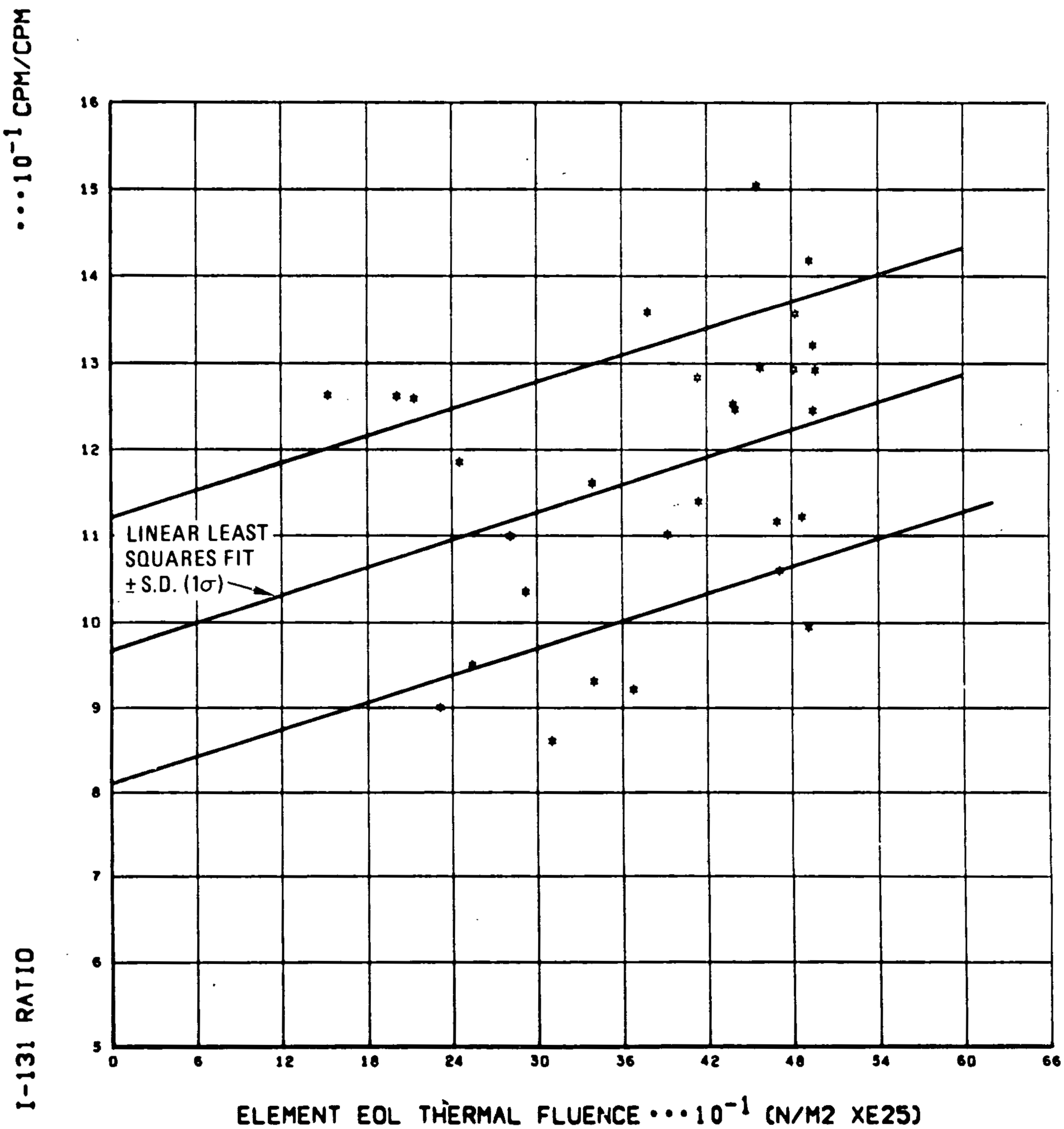

Fig. 29. I-131/Zr-95 CPM ratio versus thermal fluence

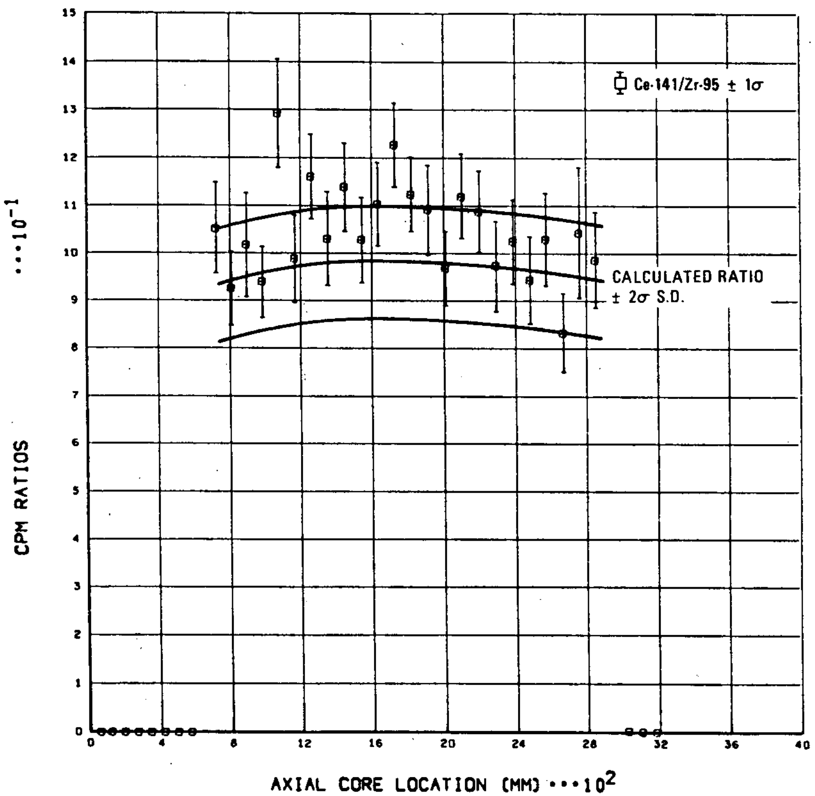

Fig. 30(a). Cerium/zirconium nuclide CPM ratios for E01-01

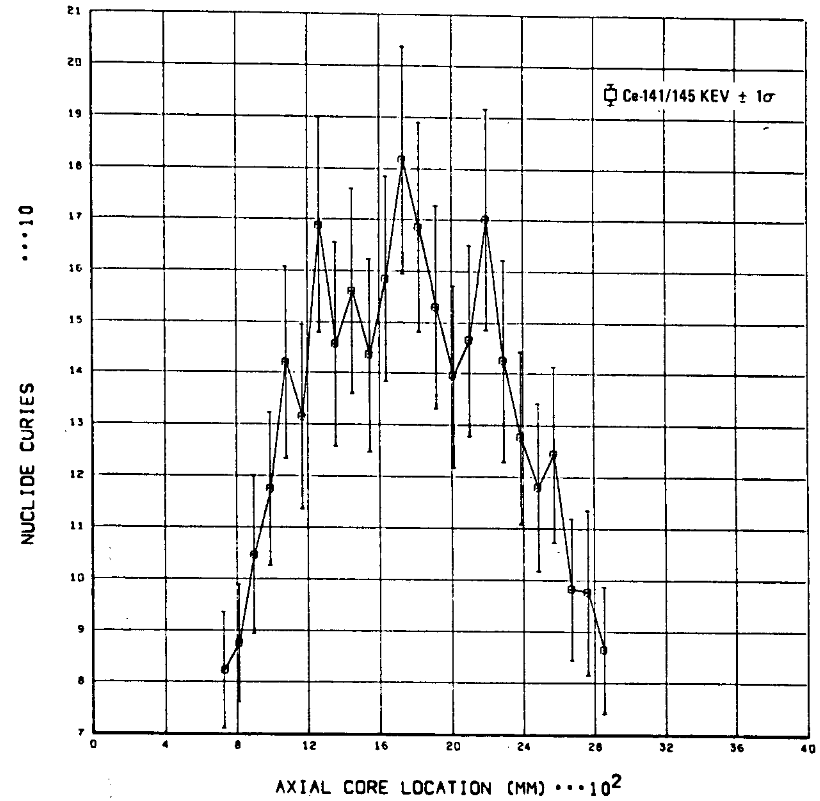

Fig. 30(b). Absolute cerium nuclide activities for E01-01

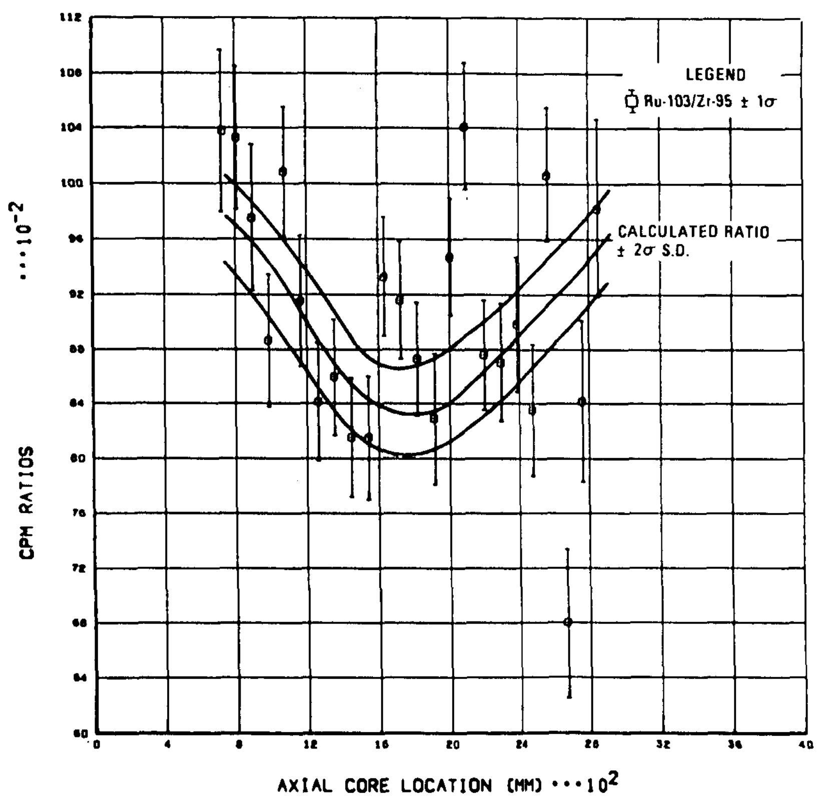

Fig. 31(a). Ruthenium/zirconium nuclide CPM ratios for E01-01

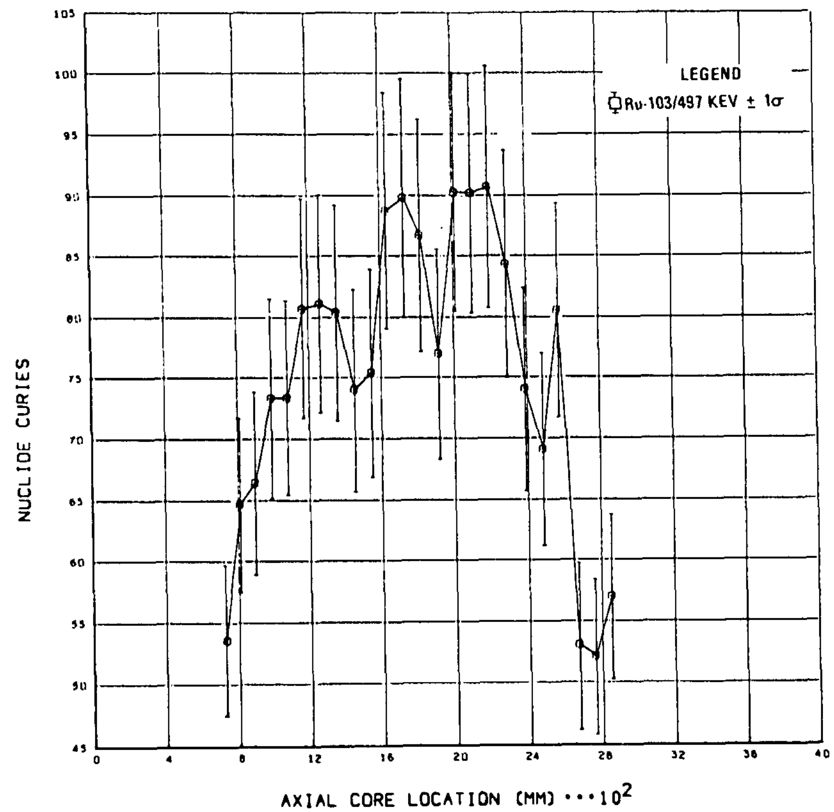

Fig. 31(b). Absolute ruthenium nuclide activities for E01-01

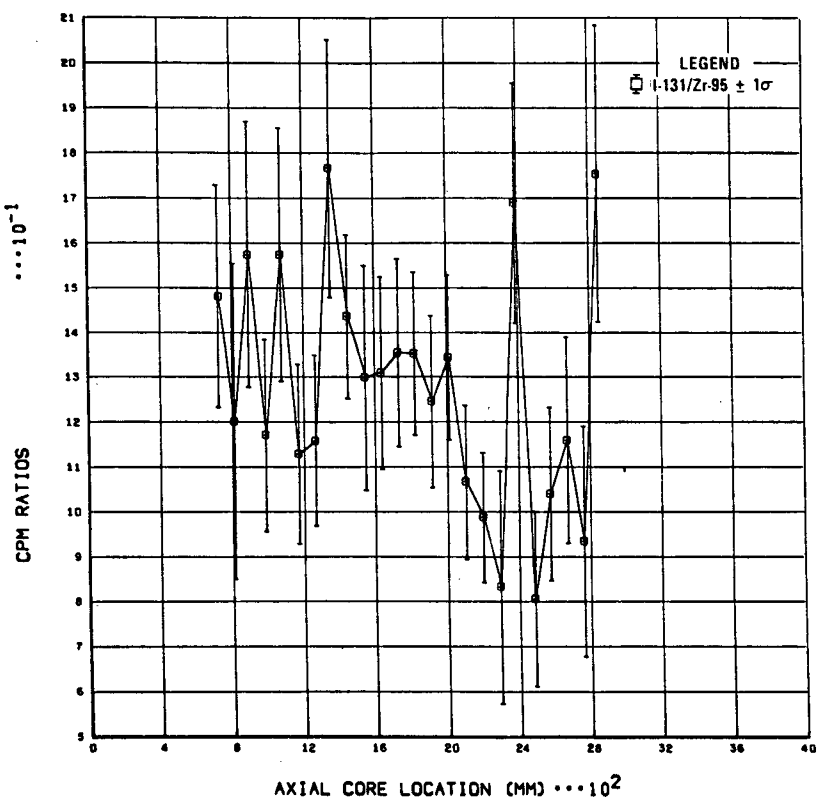

Fig. 32(a). Iodine/zirconium nuclide CPM ratios for E01-01

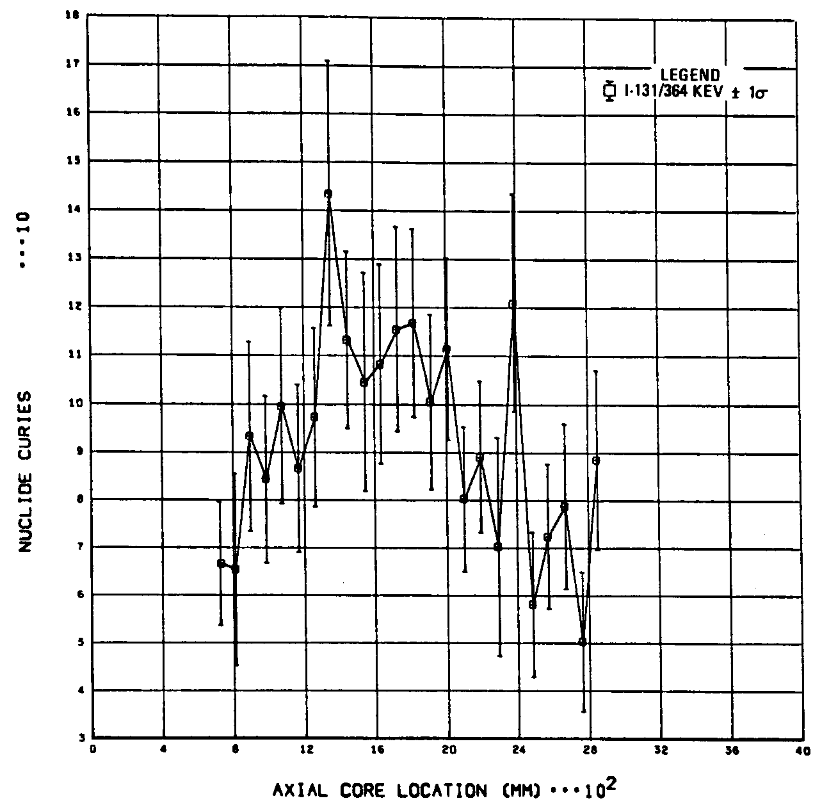

Fig. 32(b). Absolute iodine nuclide activities for E01-01

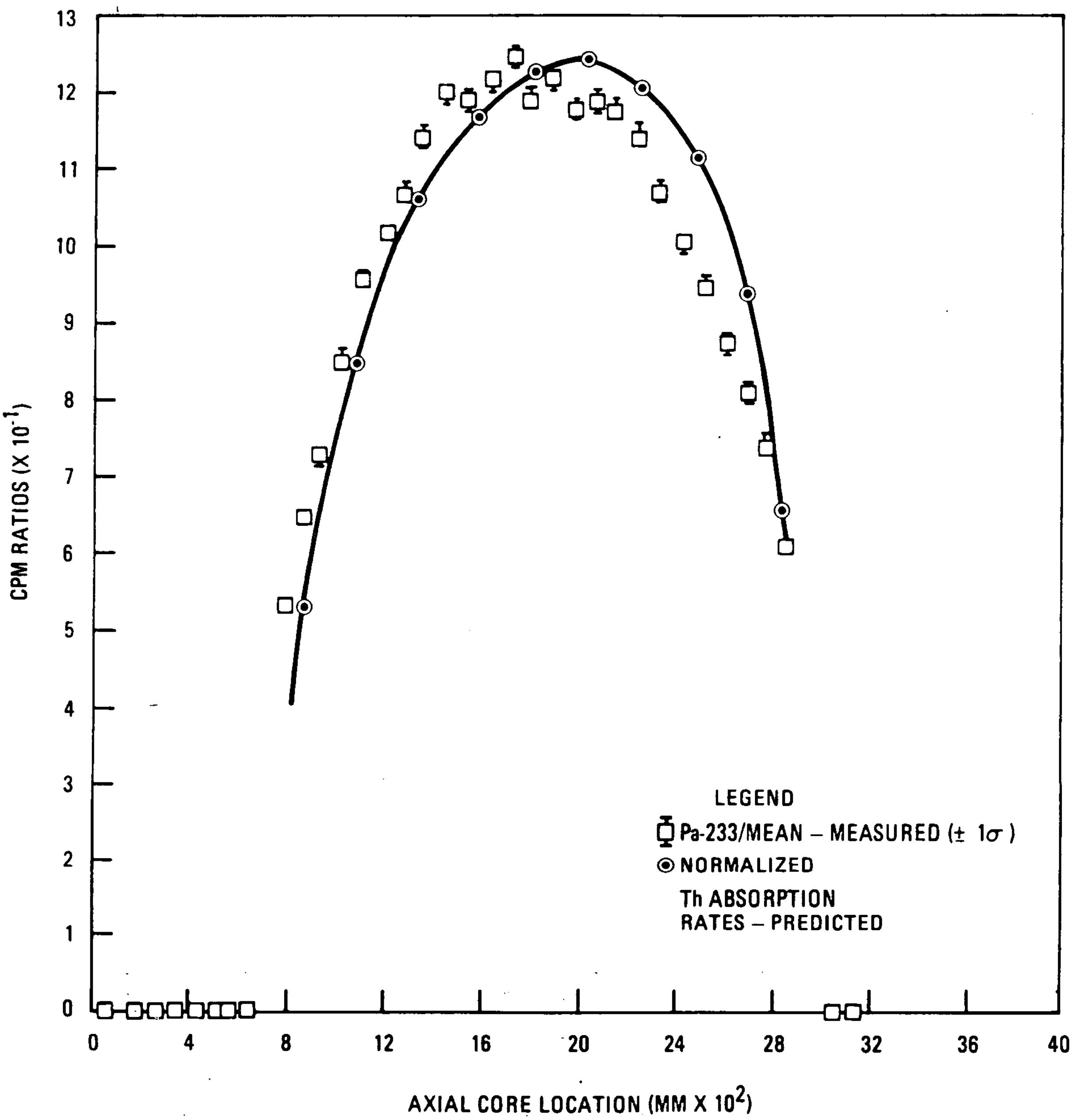

Fig. 33. Normalized protactinium CPM ratios for E14-01

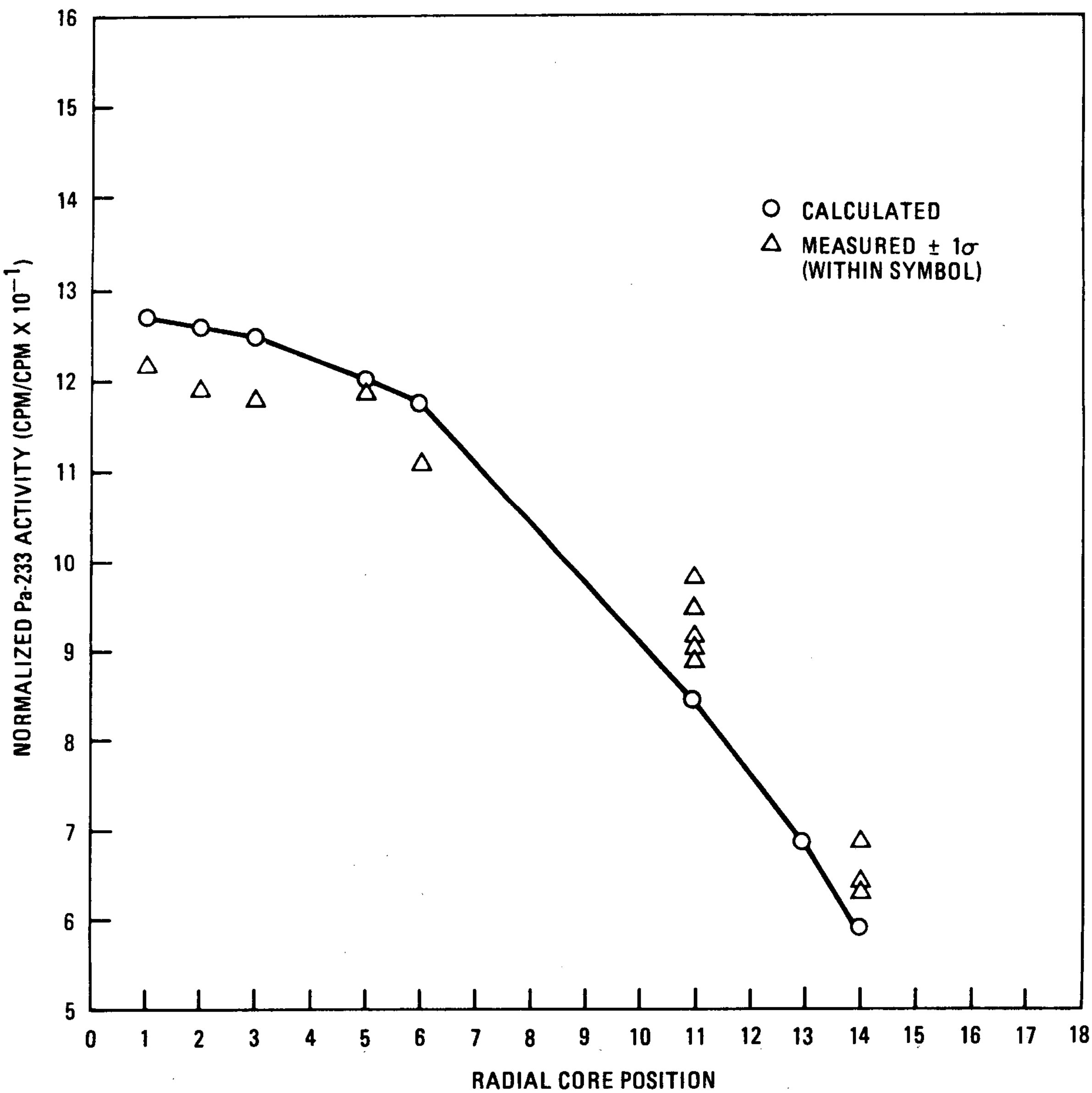

Fig. 34. Normalized radial distribution of Pa-233 in Phase I driver elements

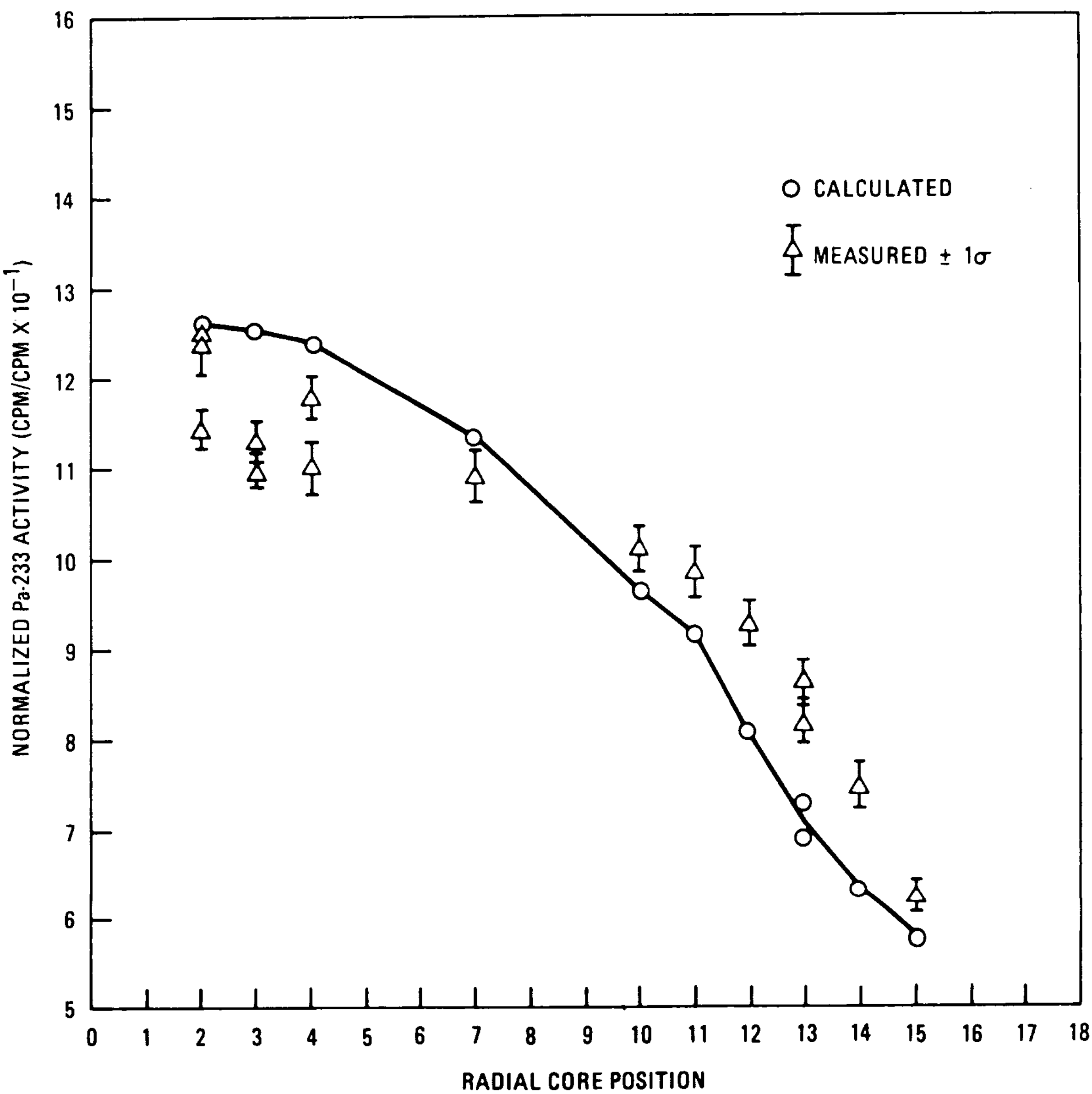

Fig. 35. Normalized radial distribution of Pa-233 in Phase II driver elements

APPENDIX B

TABLES

TABLE 1
PEACH BOTTOM ELEMENTS GAMMA SCANNED DURING PHASE I

Element I.D.	Element Type[a]	Date Scanned	Collimator[b] (mm)	Scans (GA Tag No. 15)	UNIVAC Tape Storage Tape No.	UNIVAC Tape Storage File No.
A17-11	D	11/24/74	17.475 x 0.254	1-105	2530	1
E14-01	ID	11/24/74		106-191		2
C02-01	FTE-6	11/25/74		192-267		3
E01-01	ID	11/26/74		268-343		4
E02-02	ID	11/27/74		344-386		5
E06-01	FTE-18	11/27/74		387-468		6
E09-01	ID	11/29/74		469-515		7
E11-01	ID	11/29/74		516-574		8
E15-01	ID	11/29/74		575-621		9
D14-08	FTE-8	11/30/74		622-668		10
E10-01	FTE-13	11/30/74		669-717		11
E07-01	ID	11/30/74		718-764		12
E06-02	D	12/1/74		765-811		13
E05-01	ID	12/1/74		812-859		14
E15-02	D	12/2/74		860-907		15
D10-06	RTE-6	12/2/74		908-957		16
B13-01	ID	12/2/74		958-1010		17
A03-03	D	12/2/74		1011-1056		18
D06-01	FTE-9	12/3/74		1057-1102		19
B02-02	ID	12/3/74		1103-1148		20
E02-01	FTE-10	12/3/74		1149-1195		21
C10-06	RTE-5	12/3/74		1196-1257		22
E11-02	D	12/4/74		1258-1306		23
A05-05	D	12/4/74		1307-1353		24
C14-08	FTE-5	12/5/74		1354-1407		25
A02-01	FTE-17	12/5/74		1408-1462		26
B03-01	D	12/5/74		1463-1507		27
C05-04	FBTE-1	12/5/74		1508-1555		28
B14-02	D	12/5/74		1556-1605		29
D09-04	FBTE-5	12/6/74		1606-1652		30
F10-06	RTE-8	12/6/74		1655-1707		31
A11-11	FBTE-2	12/7/74		1708-1759		32
B06-01	FTE-12	12/7/74		1760-1809		33
B14-08	FBTE-3	12/7/74		1810-1857		34
B03-03	D	12/7/74		1858-1904	↓	35
B05-01	D	12/7/74		1905-1955	2530	36
F03-01	D	12/8/74		1958-2004	2555	1
F06-01	FTE-16	12/8/74		2005-2054		2
F05-05	D	12/8/74		2055-2101		3
A17-08	D	12/8/74	↓	2102-2169		4
F11-03	D	12/8/74	17.475 x 0.254	2170-2231		5
A14-08	FTE-15	12/9/74	22.86 x 0.254	2232-2303		6
E14-08	FPTE-3	12/18/74	17.475 x 0.254	2304-2432		7
C17-08	D	12/6/74		2433-2450		8
E10-06	FTE-11	12/6/74	↓	2451-2508	↓	8
F14-08	FTE-7	12/6/74	17.475 x 0.254	2509-2559	2555	9

[a] D - driver
ID - instrumented driver
FTE - final test element
RTE - recycle test element
FBTE - fuel bed test element
FPTE - fuel pin test element

[b] Cross section dimensions.

TABLE 2
PEACH BOTTOM ELEMENTS GAMMA SCANNED DURING PHASE II

Element I.D.	Element Type[a]	Date Scanned	Collimator[b] (mm)	Scans (GA Tag No. 15)	UNIVAC Tape Storage	
					Tape No.	File No.
E03-01	ID	5/28/75	17.475 x 0.254	1-83, 480-510	1784	1
E03-01	ID	5/29/75	1.27 x 6.35	84-170		2
E14-02	ID	5/27/75	17.475 x 0.254	171-277		3
E14-02	ID	5/27/75	23.876 x 0.254	278-369		37
F01-01	ID	5/27/75	23.876 x 0.254	371-479		4
E03-02	ID	5/29/75	1.27 x 6.35	515-602		5
E09-02	ID	5/30/75		603-695		6
E04-02	ID	5/30/75		696-789		7
E13-02	ID	5/31/75		801-888		38
E05-02	ID	5/31/75		890-975		8
E12-02	ID	5/31/75		976-1106		39
E07-02	ID	6/1/75		1108-1194		9
E07-02	ID	6/1/75		1195-1272		10
E10-02	ID	6/2/75		1273-1362		11
E13-01	ID	6/2/75		1364-1448		12
E08-02	ID	6/2/75		1449-1548		13
A04-03	D	6/3/75		1549-1647		14
A04-04	D	6/4/75		1648-1738		15
A14-14	ID	6/4/75		1739-1828		16
B05-02	D	6/4/75		1829-1956		17
F03-02	D	6/6/75		1957-2051		18
F04-03	D	6/6/75		2052-2155		19
F15-14	D	6/9/75		2156-2301		20
F16-15	D	6/10/75		2303-2398		21
B11-03	D	6/5/75		2399-2506		22
B11-03	D	6/5/75		2507-2563		23
F02-01	D	6/5/75		2564-2699		40
D18-08	Reflector	6/12/75		2700-2766		24
D18-12	Reflector	6/13/75		2767-2820		25
E17-16	Reflector	6/13/75		2821-2871		26
F05-04	D	6/7/75		2872-2971		27
F07-06	D	6/7/75		2972-3086		28
F09-08	D	6/7/75		3087-3189		29
F10-09	D	6/8/75	1.27 x 6.35	3190-3295		30
F14-13	D	6/9/75	Lead	3296-3398		31
F14-13	D	6/9/75	Shield	3399-3499		32
B02-01	D	6/10/75	1.27 x 6.35	3520-3540		33
E08-01G	Guide sleeve	6/16/75		3591-3647		34
F08-01A	Control rod	6/19/75	1.27 x 6.35	3648-3800	1784	35

[a] D - driver
ID - instrumented driver

[b] Cross section dimensions.

TABLE 3
NUCLEAR CONSTANTS FOR ISOTOPES USED IN PEACH BOTTOM EOL GAMMA SCANNING

Isotope I.D.	Gamma Energy Peak (keV)	Decay Constant λ[a] (sec^{-1})	Half-Life[a]	Thermal Fission Yield[b] U-233 (%)	Thermal Fission Yield[b] U-235 (%)	Absolute Intensity[b]	Precursor	PBGST Factors[c]
Ce-144	133	2.821×10^{-8}	284.4 days	4.64	5.46	0.030		5.1
Ce-141	145	2.466×10^{-7}	32.5 days	6.58	5.89	0.480		0.536
Pa-233	312	2.967×10^{-7}	27.5 days	--	--	0.0033		0.446
I-131	364	6.723×10^{-7}	8.1 days	--	--	0.820		0.215
Ru-103	497	2.026×10^{-7}	39.6 days	1.70	3.14	0.890		0.220
Ru-106	512	2.174×10^{-8}	369.0 days	0.257	0.392	0.210		0.933
Cs-137	662	7.302×10^{-10}	30.1 years	6.80	6.27	0.846		0.252
Zr-95	724	1.225×10^{-7}	65.5 days	6.25	6.46	0.436		0.518
Cs-134	796	1.067×10^{-8}	762.9 days	1.36×10^{-3}	4.5×10^{-5}	0.961	Xe-133	0.279
La-140[d]	1596	6.268×10^{-7}	12.8 days	6.43	6.32	0.956	Ba-140	0.291

[a] Data taken from Ref. 5.

[b] Data taken from Ref. 6

[c] Corrected to CPM for relative detector efficiency, attenuation, and absolute intensity (Ref. 7).

[d] Precursor Ba-140 is the direct fission yield isotope, measured through its daughter La-140. Direct yield La-140 is decayed at time of gamma scan because of a short half-life of 40.2 hr.

TABLE 4
FTE-6 COMPARISON OF FUEL STACK LENGTH

Body	EOL Fuel Stack Length: Metrology $\bar{x}_1$ (mm)	Metrology $S_{\bar{x}_1}$ (mm)	Peach Bottom Gamma Scan $\bar{x}_2$ (mm)	Peach Bottom Gamma Scan $S_{\bar{x}_2}$[(a)] (mm)	Relative Difference $Z = \bar{x}_2/\bar{x}_1 - 1$ (%)	Relative Difference S_Z (%)	Test 1 $D = Z/S_Z$	Test 1 Results	Test 2 D^2
1	679.8	±2.7	677.4	±3.3	-0.35	±0.63	-0.56	0.56 < 1.96 Insignificant	0.31
2	677.0	±3.0	678.9	±2.8	+0.28	±0.60	+0.47	0.47 < 1.96 Insignificant	0.22
3	676.5	±3.1	677.0	±2.2	+0.07	±0.56	+0.12	0.12 < 1.96 Insignificant	0.02
Mean $\bar{\bar{x}}$, $\bar{S}_{\bar{x}}$	677.8	±2.9	677.8	±2.8	0.0	±0.60	0.01		0.18
RMS, $S_{\bar{\bar{x}}}$	±1.4	±1.7	±0.8	±1.6	0.0	±0.34			
Test results							0.017 < 1.96 Insignificant		0.18 < 2.6 Insignificant

(a) $S_{\bar{x}}$ from three single-channel analyzer strip charts.

TABLE 5

FTE-18 COMPARISON OF FUEL BODY AND STACK LENGTHS DERIVED FROM METROLOGY AND GAMMA SCANNING

	BOL Body Length		EOL PIE Body Length		Peach Bottom EOL γ Scan Body Length[a]		Hot Cell EOL γ Scan: Fuel Length	Hot Cell EOL γ Scan: Unfueled Length	Relative Change from Metrology (Method 1)		Relative Change from Peach Bottom γ Scan (Method 2)		Relative Difference Between Methods 2 and 1	
Body I.D.	$\bar{x}_1$ (in.)	s_1 (in.)	$\bar{x}_2$ (in.)	s_2 (in.)	$\bar{x}_3$ (in.)	s_3 (in.)	$\bar{x}_4$[b] (in.)	$\bar{x}_2 - \bar{x}_4$ (in.)	$u_1 = \frac{\bar{x}_2}{\bar{x}_1} - 1$ (%)	s_{u_1} (%)	$u_2 = \frac{\bar{x}_3}{\bar{x}_1} - 1$ (%)	s_{u_2} (%)	$Z = \frac{u_2}{u_1} - 1$	s_Z
Body 1	13.7761	±0.0021	13.6886	±0.0020	13.71	±0.016	13.50	0.19	-0.6349	±0.0210	-0.480	±0.117	-0.24	±0.19
Body 2	13.7769	±0.0024	13.7051	±0.0020	13.58	±0.028	13.50	0.20	-0.5215	±0.0226	-1.429	±0.204	+1.74	±0.41
Body 3	13.7826	±0.0036	13.7109	±0.0020	13.61	±0.026	13.42	0.29	-0.5204	±0.0300	-1.252	±0.190	+1.41	±0.39
Body 4	13.7800	±0.0034	13.7128	±0.0020	13.95	±0.042	13.58	0.13	-0.4881	±0.0284	+1.234	±0.306	-3.53	±0.64
Body 5	13.6286	±0.0033	13.5284	±0.0020	13.65	±0.040	13.29	0.24	-0.7353	±0.0283	+0.157	±0.295	-1.21	±0.40
Body 6	13.7767	±0.0032	13.6654	±0.0020	13.82	±0.026	13.46	0.21	-0.8079	±0.0275	+0.314	±0.190	-1.39	±0.24
Total stack	82.5209	±0.0075	82.0112	±0.0049	82.32	±0.076	80.75[c]	1.26	-0.6177	±0.0261	-0.243	±0.267	-0.61	±0.43
Mean $\bar{\bar{x}}$, $\bar{s}_{\bar{x}}$	13.7535	±0.0030	13.6685	±0.0020	13.72	±0.031	13.46	0.21	-0.6180	±0.0265	-0.243	±0.267	-0.54	±0.41
RMS, $s_{\bar{x}}$	0.0559	±0.0012	0.0647	±0.0008	0.13	±0.013	0.09	0.05	±0.1196	±0.0108	±0.925	±0.093	±1.79	±0.17

(a) Determined from five strip chart examinations.

(b) Measurement error assumed to be ±0.04 in.

(c) BOL composite fuel length of 81.25 in. concluded.

TABLE 6
PHASE I AND PHASE II FUEL STACK LENGTH COMPARISON FOR DRIVER ELEMENTS

Element I.D.	Preirradiation Stack Length,[a] x_1 (mm)	Postirradiation Stack Length, x_2 (mm)	$S_{\bar{x}_2}$ (mm)	Difference $\bar{x}_2 - x_1$ (mm)	$Z = \bar{x}_2/x_1 - 1$ (%)	S_Z (%)	Fast Fluence (10^{25} n/m^2)	Fuel Temp.[b] (°C)
				PHASE I				
E14-01[c]	2290.8	2289.3	±2.3	- 1.5	-0.06	±0.17	2.3	945
E01-01[c]	2276.5	2304.6	±2.6	+28.1	+1.23	±0.18	3.2	1024
F03-01[c]	2289.2	2303.9	±3.6	+14.7	+0.64	±0.21	3.1	940
F05-05	2276.5	2300.0	±0.9	+23.5	+1.03	±0.11	3.1	969
E02-02	2295.5	2311.2	±2.6	+15.7	+0.68	±0.18	3.2	1007
E09-01	2297.1	2296.1	±2.3	- 1.0	-0.04	±0.17	3.1	950
E11-01	2287.6	2306.6	± 0	+19.0	+0.83	±0.14	3.1	1011
E15-01	2289.2	2286.4	±2.6	- 2.8	-0.12	±0.18	1.6	827
E07-01	2290.8	2293.9	±0.7	+ 3.1	+0.14	±0.14	3.1	949
E05-01	2297.1	2306.6	± 0	+ 9.5	+0.41	±0.14	3.1	958
E15-02	2292.4	2295.2	±5.8	+ 2.8	+0.12	±0.29	2.0	828
B13-01	2289.2	2294.8	±1.8	+ 5.6	+0.24	±0.16	2.8	1011
A03-03	2263.8	2267.6	±2.8	+ 3.8	+0.17	±0.19	0.8	N.D.
B02-02	2265.4	2289.5	±1.4	+24.1	+1.06	±0.16	3.2	1010
E11-02	2287.6	2307.4	±0.5	+19.8	+0.87	±0.14	3.1	1007
A05-05	2278.1	2300.5	±0.8	+22.4	+0.98	±0.15	3.1	949
B03-01	2282.8	2296.0	±1.3	+13.2	+0.58	±0.15	3.1	950
B14-02	2274.9	2289.2	±0.7	+14.3	+0.63	±0.14	3.1	999
B03-03	2260.6	2289.5	±0.7	+28.9	+1.28	±0.15	2.7	987
B05-01	2293.9	2318.9	±1.6	+25.0	+1.09	±0.16	3.1	939
A17-08	2279.7	2282.4	±0.6	+ 2.7	+0.12	±0.14	1.8	861
F11-03	2293.1	2315.6	±0.5	+22.5	+0.98	±0.14	3.3	1024
				PHASE II				
E14-02	2287.6	2308.9	±3.4	+21.3	+0.93	±0.20	2.6	951
F01-01	2281.2	2307.7	±1.9	+26.5	+1.16	±0.16	3.1	1023
E03-01	2271.7	2282.8	±8.1	+11.1	+0.49	±0.38	3.1	960
E03-02	2287.6	2309.4	±3.2	+21.8	+0.95	±0.20	3.1	986
E09-02	2282.8	2300.3	±6.3	+17.5	+0.77	±0.31	3.1	947
E04-02	2282.8	2304.5	±1.2	- 2.1	-0.09	±0.15	3.1	957
E13-02	2290.8	2307.8	±0.6	+17.0	+0.74	±0.14	2.9	980
E05-02	2298.7	2313.3	±1.9	+14.6	+0.64	±0.16	3.1	963
E12-02	2284.4	2290.1	±10.5	+ 5.7	+0.25	±0.48	3.0	1000
E07-02	2292.4	2299.9	±1.4	+ 7.5	+0.33	±0.15	3.2	993
E10-02	2292.4	2307.8	±2.0	+15.4	+0.67	±0.16	3.2	995
E13-01	2290.8	2304.2	±2.9	+13.4	+0.58	±0.19	2.7	967
E08-02	2292.4	2307.8	±1.2	+15.4	+0.67	±0.15	3.1	948
A04-03	2279.7	2302.4	±3.3	+22.7	+1.00	±0.20	3.2	987
A04-04	2282.8	2306.6	± 0	+23.8	+1.04	±0.14	3.1	948
A14-14	2290.8	2306.5	±0.1	+15.7	+0.69	±0.14	2.7	995
B05-02	2278.1	2306.5	± 0	+28.4	+1.25	±0.14	3.1	950
B11-03[c]	2273.3	2306.6	± 0	+33.3	+1.46	±0.14	3.3	1029
F02-01	2289.2	2308.0	±0.9	+18.8	+0.82	±0.15	3.2	997
F03-02	2282.8	2306.6	±0.1	+23.8	+1.04	±0.14	3.1	986
F04-03	2260.6	2286.2	±2.2	+25.6	+1.13	±0.17	3.2	984
F05-04	2284.4	2293.7	±1.3	+ 9.3	+0.41	±0.15	3.2	994
F09-08	2284.4	2298.9	±2.7	+14.5	+0.63	±0.18	3.3	1018
F10-09	2290.8	2298.2	±4.6	+ 7.4	+0.32	±0.24	3.3	1020
F14-13	2279.1	2303.7	±1.4	+24.6	+1.08	±0.15	2.9	1002
F15-14	2308.4	2309.4	±0.5	+20.2	+0.88	±0.14	2.4	992
F16-15	2304.3	2304.5	±6.7	+ 5.8	+0.25	±0.32	1.6	860
B02-01	2310.0	2311.5	±1.4	+25.5	+1.12	±0.15	3.2	1004
Mean $\bar{x}$, $\bar{S}_x$, $S_{\bar{x}}$	2285.7	2300.8	±3.0	+15.6	+0.68	±0.19	2.9	971
RMS, $S_{\bar{x}}$	±10.6	±9.8	±0.4	± 9.2	±0.40	±0.03	±0.5	±46

[a] An $S_{\bar{x}_1}$ of 3.2 mm is assumed for preirradiation stack lengths.

[b] Time and volume averaged.

[c] Scanned at ORNL.

TABLE 7
COMPARISON OF STACK LENGTH OF TEST ELEMENTS

Element I.D.	Preirradiation Stack Length,[a] x_1 (mm)	Postirradiation Stack Length, x_2 (mm)	$S_{\bar{x}_2}$ (mm)	Difference $\bar{x}_2 - x_1$ (mm)	$Z = \bar{x}_2/x_1 - 1$ (%)	S_Z (%)	Fast Fluence (10^{25} n/m^2)	Fuel Temp.[b] (°C)	Fuel Geometry
F06-01, FIE-18[b]	2063.8	2051.1	±0.2	-210.3	-0.62	±0.03	1.9	NA	Molded bed
D14-08, FTE-8	2275.8	2257.7	±0.8	- 18.1	-0.80	±0.14	2.1	NA	Rods
E10-01, FTE-13	2290.8	2269.5	±0	- 21.3	-0.93	±0.14	1.8	NA	Rods
D06-01, FTE-9	2337.5	2257.0	±0.1	- 80.5	-3.44	±0.13	2.3	939	Rods
E02-01, FTE-10	2273.3	2253.4	±0.6	- 19.9	-0.88	±0.14	3.2	NA	Rods
C14-08, FTE-5	2287.6	2269.5	--	- 18.1	-0.79	±0.14	3.0	965	Rods
A02-01, FTE-17	2279.7	2269.5	±1.2	- 10.5	-0.46	±0.15	1.8	NA	Rods
F06-01, FTE-16	2275.6	2262.6	±0.3	- 13.0	-0.57	±0.14	1.8	NA	Rods
A14-08, FTE-15	2287.5	2269.1	±2.4	- 18.4	-0.80	±0.17	1.7	1064	Rods
D10-06, RTE-6	2294.7	2274.4	±0.9	- 20.3	-0.88	±0.14	3.3	1010	Rods
C10-06, RTE-5	2290.3	2275.5	±0.6	- 14.8	-0.65	±0.14	3.3	1005	Rods
F10-06, RTE-8	2300.1	2287.5	±8.0	- 12.6	-0.55	±0.37	3.3	991	Rods
C05-04, FBTE-1	2298.7	2227.7	±0.9	- 71.0	-3.09	±0.14	3.1	NA	Rods
D09-04, FBTE-5	2277.7	2236.6	±0.7	- 41.1	-1.80	±0.14	3.3	NA	Blended bed
A11-11, FBTE-2	2281.2	2263.2	±2.4	- 22.4	-0.98	±0.17	3.1	NA	Rods
B14-08, FBTE-3	2276.0	2252.3	±1.3	- 23.7	-1.04	±0.15	3.1	NA	Rods
E14-08, FPTE-3[b]	2234.7	2226.9	±1.4	- 7.8	-0.35	±0.16	2.2	NA	Compacts
Mean $\bar{x}$	2284.9	2248.5	±2.3	- 36.7	-29.2	±0.17	2.6	996	
RMS, $S_{\bar{x}}$	±19.35	±46.83	±0.57	±47.64	±2.08	±0.041	±0.6	±39	

[a] A preirradiation $S_{\bar{x}_1}$ of 3.2 mm is assumed, except for FTE-18 with S_{x_1} = ±0.1 mm (see Table 6).

[b] Element time-weighed average fuel temperature.

[c] Scanned at GA hot cell.

TABLE 8

BURNUP COMPARISON FOR DRIVER AND TEST ELEMENTS SCANNED DURING PHASE I OF PEACH BOTTOM EOL PROGRAM

Element I.D.	GAUGE Position (Patch/Hex.)	Total FIMA: GAUGE, C (%)	Total FIMA: Meas., M (%)	Total FIMA: $S_M(1\sigma)$ (%)	Relative Difference, (C/M-1)=Z: Z	Relative Difference, (C/M-1)=Z: $S_Z(1\sigma)$	Comparison: Test 1 $D=Z/S_Z$	Comparison: Test 2 D^2	Cs-137 Movement	Remarks[(a)]
PHASE I DRIVER ELEMENTS										
A17-11	106/7	4.06	4.00	±0.19	+0.015	±0.048	0.311	0.097	No	High Th loading.
E14-01	126/1	7.80	8.35	±0.52	-0.066	±0.058	-1.132	1.282	No	
E01-01	1/7	8.58	8.89	±0.43	-0.035	±0.047	-0.747	0.558	Yes	
E02-02	2/4	8.39	8.70	±0.60	-0.036	±0.066	-0.536	0.287	Yes	
E09-01	61/6	7.87	7.60	±0.49	+0.036	±0.067	0.532	0.283	Yes	Next to control rod.
E11-01	90/4	8.52	9.03	±0.54	-0.056	±0.056	-1.001	1.002	Yes	
E15-01	126/2	4.07	4.00	±0.25	+0.018	±0.064	0.275	0.076	No	High Th loading.
E07-01	37/1	7.84	8.19	±0.54	-0.043	±0.063	-0.677	0.458	Yes	Next to control rod.
E06-02	8/6	8.25	7.94	±0.54	+0.039	±0.071	0.553	0.305	Yes	
E05-01	19/3	7.77	8.52	±0.55	-0.088	±0.059	-1.495	2.236	Yes	
F15-02	126/3	3.96	3.94	±0.25	+0.005	±0.064	0.080	0.006	No	High Th loading, next to control rod.
B13-01	108/5	8.29	8.37	±0.50	-0.010	±0.059	-0.162	0.026	Yes (Small)	
A03-03	4/3	2.69	2.88	±0.33	-0.066	±0.107	-0.616	0.380	N.D.	No temp. avail., low Th and U loading.
B02-02	5/4	8.39	9.90	±0.63	-0.153	±0.054	-2.828	8.000	Yes	
E11-02	61/2	7.87	8.92	±0.52	-0.118	±0.051	-2.289	5.238	Yes	
A05-05	13/1	7.69	7.98	±0.50	-0.036	±0.060	-0.602	0.362	Yes	Next to control rod.
B03-01	5/6	7.63	8.46	±0.58	-0.098	±0.062	-1.587	2.518	Yes	Next to control rod.
B14-02	108/4	8.16	8.13	±0.47	+0.004	±0.058	0.064	0.004	Yes (Small)	
B03-03	5/3	8.16	8.14	±0.55	+0.002	±0.068	0.036	0.001	Yes	
B05-01	13/3	7.59	8.41	±0.52	-0.098	±0.056	-1.747	3.053	Yes	Next to control rod.
F03-01	3/6	7.63	8.11	±0.51	-0.059	±0.059	-1.000	1.001	Yes	Next to control rod.
F05-05	11/1	7.87	7.87	±0.49	0.000	±0.062	0.000	0.000	Yes	Next to control rod.
A17-08	105/6	4.06	4.02	±0.23	+0.010	±0.058	0.172	0.030	No	High Th loading.
F11-03	41/3	8.46	4.07	±0.53	-0.067	±0.055	-1.234	1.523	Yes	
Mean $\bar{x}$, $\bar{S}_x$		7.150	7.476	±0.485	-0.0375	±0.0623	-0.651	1.197		
RMS, $S_{\bar{x}}$		±1.776	±1.969	±0.099	±0.0498	±0.0127	±0.879	±1.879		
Test					0.67<1.52 insignificant		3.19>1.96 significant	1.20<1.52 insignificant		
PHASE I TEST ELEMENTS										
C02-01 (FTE-6)	6/5	8.25	7.48	±0.57	+0.103	±0.084	1.220	1.490		
D14-08 (FTE-8)	88/1	9.32	10.42	±0.71	-0.106	±0.061	-1.732	3.000		
C14-08 (FTE-5)	88/1, 83/1	9.31	11.01	±0.66	-0.155	±0.051	-3.057	9.343		
A02-01 (FTE-17)	4/5	4.11	5.44	±0.43	-0.244	±0.060	-4.094	16.760		
E05-04 (FBTE-1)	17/6	10.22	10.91	±0.74	-0.063	±0.064	-1.000	1.000		
F14-08 (FTE-7)	68/1	5.82	7.12	±0.46	-0.183	±0.053	-3.474	12.066		
A11-11 (FBTE-2)	34/5	10.17	14.87	±0.89	-0.316	±0.041	-7.714	59.509		
F06-01 (FTE-12)	22/5	5.39	5.57	±0.40	-0.032	±0.070	-0.460	0.211		
Mean $\bar{x}$, $\bar{S}_x$		7.824	9.103	±0.629	-0.125	±0.062	-2.539	12.922		
RMS, $S_{\bar{x}}$		±2.225	±3.049	±0.222	±0.122	±0.022	±2.545	±18.479		
Test										

(a) All elements are unperturbed except where noted.

TABLE 9
BURNUP COMPARISON OF DRIVER ELEMENTS SCANNED DURING PHASE II OF PEACH BOTTOM EOL PROGRAM

Element I.D.	GAUGE Position (Patch/Hex.)	Total FIMA: GAUGE, C (%)	Total FIMA: Meas., M (%)	Total FIMA: $S_M(1\sigma)$ (%)	Relative Difference: (C/M-1)=Z	Relative Difference: $S_Z(1\sigma)$	Comparison: Test 1 $D=Z/S_Z$	Comparison: Test 2 D^2	Cs-137 Movement	Remarks[(a)]
PHASE II DRIVER ELEMENTS										
E03-01	2/6	7.85	8.20	±0.24	-0.043	±0.028	-1.523	2.321	Yes	
E14-02	126/4	8.11	8.78	±0.42	-0.076	±0.044	-1.727	2.983	No	
F01-01	1/2	8.54	Not Determined						Yes	No calibration.
E03-02	2/1	8.16	8.19	±0.24	-0.004	±0.029	-0.125	0.016	Yes	
E09-02	61/5	7.86	7.13	±0.21	+0.102	±0.032	3.153	9.943	Yes	Next to control rod.
E04-02	2/7	7.80	7.54	±0.24	+0.034	±0.033	1.047	1.097	Yes	Next to control rod.
E13-02	91/7	8.31	7.67	±0.20	+0.083	±0.029	2.954	8.723	No	
E05-02	8/5	7.87	6.99	±0.20	+0.126	±0.032	3.908	15.273	Yes	Next to control rod.
E12-02	91/6	8.44	8.07	±0.21	+0.046	±0.027	1.685	2.838	Yes	
E07-02	37/4	8.25	8.50	±0.18	-0.029	±0.021	-1.431	2.048	Yes	
E10-02	61/1	8.29	7.85	±0.21	+0.056	±0.028	1.984	3.936	Yes	
E13-01	126/5	8.24	8.17	±0.22	+0.009	±0.027	0.315	0.100	No	
E08-02	37/3	7.86	6.94	±0.20	+0.133	±0.033	4.062	16.496	Yes	Next to control rod.
A04-03	4/2	8.06	7.80	±0.23	+0.033	±0.030	1.094	1.197	Yes	
A04-04	13/5	7.63	8.05	±0.22	-0.052	±0.026	-2.014	4.057	Yes	Next to control rod.
A14-14	108/6	8.16	8.11	±0.21	+0.006	±0.026	0.237	0.056	No	
B05-02	5/4	7.69	7.79	±0.22	-0.013	±0.028	-0.460	0.212	Yes	Next to control rod.
F03-02	3/1	8.05	7.60	±0.19	+0.059	±0.026	2.236	5.000	Yes	
F04-03	3/2	8.06	7.39	±0.19	+0.091	±0.028	3.233	10.453	Yes	
F15-14	101/3	8.13	9.03	±0.18	-0.100	±0.018	-5.554	30.842	No	
B10-15	139/5	4.05	4.19	±0.09	-0.033	±0.020	-1.609	2.590	No	
B11-03	49/3	8.46	7.62	±0.20	+0.110	±0.029	3.783	14.311	Yes	
F02-01	3/5	8.23	7.71	±0.19	+0.067	±0.026	2.564	6.574	Yes	
F05-04	11/6	8.17	7.19	±0.17	+0.136	±0.027	5.073	25.738	Yes	
F07-06	24/4	3.04	Not Determined						-	No calibration.
F09-08	44/5	8.38	Not Determined						Yes	No calibration.
F12-09	44/1	8.37	Not Determined						Yes	No calibration.
F14-13	101/4	8.12	Not Determined						-	No calibration.
B02-01	5/5	8.23	8.57	±0.21	-0.040	±0.024	-1.686	2.842	Yes	
F12-11	70/6	8.34	Not Determined						-	No calibration.
Mean $\bar{x}$, $\bar{S}_x$		7.915	7.712	±0.218	+0.0292	±0.028	0.883	7.069		
RMS, $S_{\bar{x}}$		±0.834	±0.904	±0.044	±0.0674	±0.0058	±2.508	± 8.044		
Test					6.05>1.52 Significant		4.33>1.96 Significant	7.07>1.52 Significant		
PHASE I & PHASE II DRIVER ELEMENTS										
Total $\bar{x}$, $S_{\bar{x}}$		7.533	7.594	±0.376	-0.0042	±0.0478	0.116	4.133		
RMS, $S_{\bar{x}}$		±1.439	±1.537	±0.054	±0.0680	±0.0069	±2.030	±6.537		
Test					3.95>1.35 Significant		0.80<1.96 Not Significant	4.13>1.35 Significant		

(a) All elements are unperturbed except where noted.

TABLE 10
Cs-137 INVENTORY COMPARISON OF PHASE I DRIVER ELEMENTS

Element I.D.	GAUGE Position (Patch/Hex.)	Cs-137 Inventory			Relative Difference		Comparison		Fission Product Trap Activity		Cs-137 Movement
		GAUGE, C (Ci)	MEAS., M (Ci)	$S_M(1\sigma)$ (Ci)	(C/M-1)= Z	$S_Z(1\sigma)$	$D = Z/S_Z$	D^2	Cs-137 (Ci ± 1σ)	Cs-134 (Ci ± 1σ)	
PHASE I DRIVER ELEMENTS											
A17-11	106/7	344.7	339.0	±9.3	0.017	±0.028	0.60	0.36	NA	NA	No
E14-01	126/1	392.1	420.0	±10.4	-0.066	±0.023	-2.87	8.26	0.5 ± 0.1	<0.1	No
E01-01	1/7	431.4	447.0	±13.1	-0.035	±0.028	-1.23	1.52	0.4 ± 0.1	0.2 ± 0.1	Yes
E02-02	2/4	421.8	438.0	±12.6	-0.037	±0.028	-1.34	1.78	0.4 ± 0.1	<0.1	Yes
E09-01	61/6	395.7	381.0	±10.4	0.039	±0.028	1.36	1.85	0.5 ± 0.1	0.2 ± 0.1	Yes
E11-01	90/4	428.4	453.0	±11.5	-0.054	±0.024	-2.26	5.12	0.5 ± 0.1	<0.1	Yes
E15-01	126/2	345.6	339.0	±9.3	0.019	±0.028	0.70	0.49	0.4 ± 0.2	<0.1	No
E07-01	37/1	394.2	411.0	±11.5	-0.041	±0.027	-1.52	2.32	0.5 ± 0.2	<0.1	Yes
E06-02	8/6	414.8	399.0	±11.5	0.040	±0.030	1.32	1.75	0.6 ± 0.1	<0.1	Yes
E05-01	19/3	390.7	429.0	±12.0	-0.089	±0.025	-3.51	12.28	0.5 ± 0.1	<0.1	Yes
E15-02	126/3	336.2	333.0	±8.8	0.010	±0.027	0.36	0.13	0.4 ± 0.1	<0.1	No
B13-01	108/5	416.8	420.0	±11.0	-0.008	±0.026	-0.27	0.09	0.5 ± 0.2	<0.1	Yes (Small)
A03-03	4/3	100.5	108.0	±6.6	-0.069	±0.057	-1.22	1.48	0.3 ± 0.1	<0.1	N.D.
B02-02	5/4	421.8	498.0	±14.2	-0.153	±0.024	-6.34	40.14	<0.1	<0.1	Yes
E11-02	61/2	395.7	450.0	±11.5	-0.121	±0.022	-5.37	28.83	0.5 ± 0.2	<0.1	Yes
A05-05	13/1	386.6	402.0	±11.0	-0.038	±0.026	-1.46	2.12	0.4 ± 0.1	0.2 ± 0.1	Yes
B03-01	5/6	383.6	426.0	±12.0	-0.100	±0.025	-3.92	15.40	0.3 ± 0.1	0.1 ± 0.1	Yes
B14-02	108/4	410.3	408.0	±10.4	0.006	±0.026	0.22	0.05	0.5 ± 0.1	0.1 ± 0.1	Yes (Small)
B03-03	5/3	410.3	408.0	±12.0	0.006	±0.026	0.22	0.05	0.4 ± 0.1	<0.1	Yes
B05-01	13/3	381.6	423.0	±11.5	-0.098	±0.025	-3.99	15.93	0.4 ± 0.1	<0.1	Yes
F03-01	3/6	383.6	404.8	±11.0	-0.060	±0.025	-2.36	5.57	0.4 ± 0.1	<0.1	Yes
F05-05	11/1	395.7	396.0	±11.0	-0.001	±0.028	-0.03	0.01	0.5 ± 0.1	<0.1	Yes
A17-08	105/6	344.7	342.0	±8.8	0.008	±0.026	0.30	0.09	0.5 ± 0.1	<0.1	No
F11-03	41/3	425.4	456.0	±11.5	-0.067	±0.024	-2.85	8.14	0.5 ± 0.1	<0.1	Yes
Mean $\bar{x}$, $\bar{S}_x$		381.3	397.8	±11.1	-0.038	±0.028	-1.48	6.41	0.43 ± 0.12	0.035 ± 0.05	
RMS, $S_{\bar{x}}$		±64.5	±69.4	±2.3	±0.050	±0.006	±2.06	±9.82	±0.12 ± 0.025	±0.07 ± 0.01	
Test					3.08 < 1.52 Significant		4.46 > 1.96 Significant	6.41 > 1.52 Significant			

TABLE 11
Cs-137 INVENTORY COMPARISON OF PHASE I AND II DRIVER ELEMENTS

Element I.D.	GAUGE Position (Patch/ Hex.)	Cs-137 Inventory			Relative Difference		Comparison		Fission Product Trap Activity		Cs-137 Movement
		GAUGE, C (Ci)	Meas., M (Ci)	$S_M(1\sigma)$ (Ci)	(C/M-1) = Z	$S_Z(1\sigma)$	$D = Z/S_Z$	D^2	Cs-137 (Ci ± 1σ)	Cs-134 (Ci ± 1σ)	
PHASE II DRIVER ELEMENTS											
E03-01	2/6	394.6	411.0	±9.3	-0.040	±0.022	-1.84	3.37	0.2 ± <0.1	0.1 ± <0.1	Yes
E14-01	126/4	407.8	441.0	±9.6	-0.075	±0.020	-3.74	13.99	0.7 ± 0.1	0.1 ± <0.1	No
F01-01	1/2	Not Determined									Yes
E03-02	2/1	410.3	411.0	±8.8	-0.002	±0.021	-0.08	0.01	1.6 ± 0.2	1.9 ± 0.2	Yes
E09-02	61/5	395.2	357.0	±7.7	0.107	±0.024	4.48	20.08	9.7 ± 1.0	9.8 ± 1.0	Yes
E04-02	2/7	392.1	378.0	±8.2	0.037	±0.023	1.66	2.75	7.1 ± 0.7	8.8 ± <0.1	Yes
E13-02	91/7	417.9	387.0	±7.7	0.080	±0.021	3.72	13.81	NA	NA	No
E05-02	8/5	395.7	351.0	±7.7	0.127	±0.025	5.15	26.52	0.3 ± <0.1	0.2 ± <0.1	Yes
E12-02	91/6	424.3	405.0	±8.2	0.048	±0.021	2.25	5.05	NA	NA	Yes
E07-02	37/4	414.8	429.0	±9.3	-0.033	±0.021	-1.58	2.49	2.2 ± 0.2	2.9 ± 0.3	Yes
E10-02	61/1	416.8	393.0	±8.2	0.061	±0.022	2.74	7.49	0.2 ± <0.1	0.1 ± <0.1	Yes
E13-01	126/3	414.3	411.0	±8.2	0.008	±0.020	0.40	0.16	0.2 ± <0.1	<0.1	No
E08-02	37/3	395.2	348.0	±7.7	0.136	±0.025	5.40	29.14	0.9 ± 0.1	0.9 ± 0.1	Yes
A04-03	4/2	405.3	393.0	±8.2	0.031	±0.022	1.45	2.12	0.2 ± <0.1	<0.1	Yes
A04-04	13/5	383.6	405.0	±8.8	-0.053	±0.021	-2.57	6.59	0.6 ± 0.1	0.7 ± 0.1	Yes
A14-14	108/6	410.3	408.0	±8.2	0.006	±0.020	0.28	0.08	0.2 ± <0.1	0.1 ± <0.1	No
B05-02	5/4	386.6	393.0	±8.2	-0.016	±0.021	-0.79	0.63	0.2 ± <0.1	0.1 ± <0.1	Yes
F03-02	3/1	404.7	381.0	±8.2	0.062	±0.023	2.72	7.40	0.5 ± <0.1	0.5 ± 0.1	Yes
F04-03	3/2	405.3	372.0	±8.8	0.090	±0.026	3.47	12.06	0.2 ± <0.1	<0.1	Yes
F15-14	101/3	408.8	453.0	±8.8	-0.098	±0.018	-5.57	30.98	0.1 ± <0.1	<0.1	No
F16-15	139/5	343.9	354.0	±7.1	-0.031	±0.019	-1.60	2.56	NA	NA	No
B11-03	49/3	425.4	384.0	±7.7	0.108	±0.022	4.85	23.56	0.5 ± 0.1	0.5 ± 0.1	Yes
F02-01	3/5	387.7	387.0	±8.8	0.002	±0.023	0.08	0.01	0.2 ± <0.1	0.1 ± <0.1	Yes
F05-04	11/6	373.8	348.1	±7.7	0.074	±0.024	3.11	9.66	2.6 ± 0.3	3.2 ± 0.3	Yes
F07-06	24/4	Not Determined									
F09-08	44/5	Not Determined									Yes
F10-09	44/1	Not Determined									Yes
F14-13	101/4	Not Determined									
B02-01	5/5	413.8	432.0	±8.8	-0.042	±0.020	-2.16	4.66	1.1 ± 0.1	1.0 ± 0.1	Yes
F12-11	70/6	Not Determined									
Mean $\bar{x}$, $\bar{S}_x$		401.2	393.5	±8.4	±0.024	±0.022	0.91	9.38	1.40 ± 0.29	1.48 ± 0.313	
RMS, $S_{\bar{x}}$		±17.6	±28.0	±1.7	±0.064	±0.045	±2.93	±9.62	±2.40 ± 0.062	±0.70 ± 0.068	
Test					8.83 > 1.52 Significant		4.46 > 1.96 Significant	9.38 > 1.52 Significant			
PHASE I & II DRIVER ELEMENTS											
Total $\bar{x}$, $\bar{S}_x$		391.3	395.4	±9.8	-0.0064	±0.0249	-0.28	7.89	0.92 ± 0.076	±0.723 ± 0.22	
RMS, $S_{\bar{x}}$		±48.3	±54.9	±1.4	±0.0657	±0.0036	±2.80	±9.84	± 1.73 ± 0.033	±2.00 ± 0.033	
Test					7.05 > 1.35 Significant		1.94 < 1.96 Insignificant	7.89 > 1.35 Significant			

TABLE 12
F03-01 Cs-137 INVENTORY COMPARISON

Compact I.D.	FISS-PROD Calc. Cs-137 Inventory (Ci)	ORNL Scans								Peach Bottom Scan (Total Ci)	
		Compact (Ci)		Sleeve (Ci)		Spine (Ci)		Total (Ci)			
		Meas.	±1σ(a)	Meas.	±1σ(b)	Meas.	±1σ(b)	Meas.	±1σ(b)	Meas.	±1σ
1	6.4	8.20	0.21	0.0032	0.00008	0.0080	0.0002	8.21	0.21	9.50	1.30
2	7.7	9.43	0.24	0.0066	0.00017	0.067	0.0017	9.50	0.24	9.23	0.87
3	8.8	10.70	0.62	0.0108	0.0006	0.154	0.0089	10.86	0.63	10.43	1.01
4	10.0	12.50	0.28	0.0233	0.0005	0.201	0.0045	12.72	0.28	14.47	1.26
5	11.2	14.90	0.35	0.0352	0.0008	0.223	0.0052	15.19	0.36	16.84	1.29
6	12.2	16.40	0.80	0.0811	0.0040	0.250	0.012	16.73	0.82	17.62	1.31
7	13.0	17.40	0.69	0.2653	0.011	0.257	0.010	17.92	0.71	20.39	1.45
8	13.6	22.20	0.86	0.9841	0.038	0.378	0.015	23.56	0.91	23.84	1.51
9	14.0	20.70	0.21	2.195	0.022	0.622	0.006	23.52	0.24	27.03	1.53
10	14.4	23.70	1.02	1.753	0.075	0.774	0.033	26.23	1.13	27.44	1.57
11	14.6	22.50	0.43	2.222	0.042	0.887	0.017	25.61	0.49	26.99	1.48
12	14.9	17.50	0.31	3.308	0.058	0.887	0.016	21.70	0.38	23.11	1.48
13	15.2	18.90	1.06	2.536	0.142	0.793	0.044	22.23	1.24	20.43	1.38
14	15.4	13.50	0.62	2.032	0.093	0.646	0.030	16.18	0.74	16.63	1.46
15	15.4	11.30	0.46	2.253	0.092	0.553	0.023	14.11	0.57	12.52	1.38
16	15.6	10.30	0.88	2.328	0.199	0.618	0.053	13.25	1.13	10.77	1.24
17	15.6	8.26	0.46	2.930	0.163	0.745	0.041	11.94	0.66	9.72	1.30
18	15.6	5.99	0.21	3.003	0.105	0.370	0.013	9.36	0.33	8.71	1.42
19	15.4	4.88	0.09	1.987	0.037	0.178	0.003	7.05	0.13	9.35	1.51
20	15.3	7.92	0.46	2.518	0.146	0.429	0.025	10.87	0.63	10.96	1.45
21	15.1	5.77	0.09	1.985	0.031	0.480	0.007	8.24	0.13	10.28	1.23
22	14.7	4.73	0.16	1.106	0.037	0.220	0.007	6.06	0.21	5.64	1.25
23	14.3	5.50	0.22	0.787	0.031	0.119	0.004	6.41	0.26	4.16	1.12
24	13.9	7.35	0.42	0.803	0.046	0.037	0.002	8.19	0.47	4.06	1.11
25	13.4	8.82	0.30	0.703	0.024	0.052	0.002	9.58	0.33	6.79	1.09
26	12.9	9.35	0.26	0.378	0.011	0.026	0.0007	9.75	0.27	10.13	1.18
27	12.3	10.10	0.45	0.130	0.006	0.0035	0.0002	10.23	0.46	9.77	1.09
28	11.7	9.79	0.13	0.047	0.0006	0.0010	0.00001	9.84	0.13	9.17	1.01
29	11.2	9.89	0.38	0.011	0.0004	0.0005	0.00002	9.90	0.38	9.61	1.07
30	10.8	9.23	0.13	0.0078	0.0001	0.0004	0.000006	9.24	0.13	9.20	1.40
Total	394.60	357.71	±2.77	36.43	±0.40	9.98	±0.11	404.18	±3.16	404.79	±7.14
Mean $\overline{X}$, S_x	13.15	11.91	±0.51	1.21	±0.07	0.33	±0.019	13.47	±0.58	±13.49	±1.30
RMS, $S_{\overline{x}}$	±2.43	±5.48	±0.09	±1.10	±0.013	±0.29	±0.004	±5.94	±0.11	±6.78	±0.24

(a) Standard deviation/$\sqrt{6}$, where 6 is the number of scans taken on each compact.

(b) Error assumed to be the same fractional error reported on compact scans.

TABLE 13

E01-1 COMPARISON OF CALCULATED AND MEASURED AXIAL Cs-137 INVENTORY

Compact I.D.	Core Height[(a)] (mm)	Cs-137 Inventory Per Compact: Calc., C (%)	Meas., M (%)	S_M (1σ) (%)	Relative Difference (C/M-1) = Z: Z	S_Z (1σ)	Comparison: Test 1 D = Z/S_Z	Test 2 D^2	GAUGE/FEVER Thermal Fluence ($n/m^2 \times 10^{25}$) (E < 0.38aJ)	Time-Avg. SURVEY Fuel Temp. (°C)
2	775	9.2	20.6	±2.7	-0.553	±0.059	-9.45	89.38	2.07	632.7
4	927	12.5	26.2	±3.3	-0.523	±0.060	-8.70	75.72	3.01	790.6
6	1080	15.2	28.7	±3.3	-0.470	±0.061	-7.72	59.66	3.90	905.8
8	1232	16.9	27.2	±3.3	-0.379	±0.075	-5.02	25.24	4.53	994.7
10	1384	17.8	18.2	±2.5	-0.022	±0.134	-0.16	0.03	4.85	1055.4
12	1537	17.9	20.9	±2.7	-0.144	±0.111	-1.29	1.68	5.01	1096.8
14	1689	18.3	12.5	±2.1	0.464	±0.246	1.89	3.56	5.09	1127.0
16	1842	18.3	6.8	±1.5	1.691	±0.594	2.85	8.13	5.09	1145.8
18	1994	17.9	11.1	±2.1	0.613	±0.305	2.01	4.03	4.96	1152.5
20	2146	17.4	7.4	±1.6	1.351	±0.508	2.66	7.07	4.68	1151.1
22	2299	16.2	5.4	±1.3	2.000	±0.722	2.77	7.67	4.27	1135.8
24	2451	14.8	8.4	±1.6	0.762	±0.336	2.27	5.15	3.78	1107.1
26	2604	13.0	6.2	±1.5	1.097	±0.507	2.16	4.67	3.18	1065.8
28	2756	11.2	13.8	±2.3	-0.188	±0.135	-1.39	1.94	2.61	1011.1
30	2908	9.8	9.3	±1.6	0.054	±0.181	0.30	0.09	2.20	980.7
Mean $\bar{x}$, $S_{\bar{x}}$		15.09	15.00	±0.61[(b)]						
RMS		±3.08	±7.88							

(a) From "0" Ref., Drawing 33-FT-2.

(b) $S_{\bar{x}} = \left[\frac{1}{n^2}\sum(1\sigma)^2\right]^{1/2}$.

TABLE 14
E03-02 COMPARISON OF CALCULATED AND MEASURED AXIAL Cs-137 INVENTORY

Compact I.D.	Mean Core Height[a] (mm)	Cs-137 Inventory Per Compact			Relative Difference (C/M-1) = Z		Comparison		GAUGE/FEVER Thermal Fluence ($n/m^2 \times 10^{25}$) (E < 0.38aJ)	Time-Avg. SURVEY Fuel Temp. (°C)
		Calc., C (%)	Meas., M (%)	S_M (1σ) (%)	Z	S_Z (1σ)	Test 1 $D = Z/S_Z$	Test 2 D^2		
2	775	8.7	12.3	±1.3	-0.293	±0.075	-3.92	15.33	1.90	619.3
4	927	11.7	19.9	±2.1	-0.412	±0.062	-6.64	44.11	2.75	766.9
6	1080	14.2	20.2	±2.1	-0.297	±0.084	-3.56	12.65	3.57	873.4
8	1232	15.9	22.3	±2.4	-0.213	±0.082	-2.60	6.77	4.15	956.1
10	1384	16.6	21.5	±2.3	-0.228	±0.083	-2.76	7.61	4.44	1013.4
12	1537	17.0	25.4	±27	-0.331	±0.071	-4.65	21.61	4.59	1052.6
14	1689	17.2	9.9	±1.1	0.737	±0.193	3.82	14.59	4.66	1081.3
16	1842	17.2	9.6	±1.1	0.792	±0.205	3.86	14.87	4.66	1099.6
18	1994	17.0	9.8	±1.1	0.735	±0.195	3.77	14.24	4.54	1106.7
20	2146	16.2	5.8	±0.7	1.793	±0.337	5.32	28.29	4.29	1106.1
22	2299	15.2	6.4	±0.8	1.375	±0.297	4.63	21.45	3.91	1092.4
24	2451	13.9	6.4	±0.8	1.172	±0.271	4.32	18.63	3.46	1066.1
26	2604	12.2	11.8	±1.3	0.034	±0.114	0.30	0.09	2.91	1027.6
28	2756	10.4	10.4	±1.2	0.000	±0.115	1.00	0.00	2.39	976.3
30	2908	9.1	10.7	±1.2	-0.150	±0.095	-1.57	2.46	2.01	947.0
Mean $\bar{x}$, $S_{\bar{x}}$		14.17	13.49	±0.42[b]						
RMS		±2.93	±6.29							

(a) From "0" Ref., Drawing 33-FT-2.

(b) $S_{\bar{x}} = \left[\frac{1}{n^2} \sum (1\sigma)^2\right]^{1/2}$.

TABLE 15

E06-02 COMPARISON OF Cs-137 AXIAL INVENTORY

Compact I.D.	Core Height(a) (mm)	Cs-137 Inventory Per Compact: Calc., C (%)	Cs-137 Inventory Per Compact: Meas., M (%)	Cs-137 Inventory Per Compact: S_M (1σ) (%)	Relative Difference (C/M-1) = Z: Z	Relative Difference (C/M-1) = Z: S_Z (1σ)	Comparison: Test 1 $D = Z/S_Z$	Comparison: Test 2 D^2	GAUGE/FEVER Thermal Fluence ($n/m^2 \times 10^{25}$) (E < 0.38aJ)	Time Avg. SURVEY Fuel Temp. (°C)
2	775	8.9	10.1	±1.5	-0.109	±0.132	-0.08	0.68	1.95	624.9
4	927	11.9	11.8	±1.8	0.008	±0.154	0.06	0.00	2.83	774.7
6	1080	14.5	23.5	±2.9	-0.383	+0.076	-5.03	25.30	3.67	899.5
8	1232	16.1	25.5	±3.2	-0.369	±0.079	-4.66	21.65	4.26	960.2
10	1384	16.9	22.8	±2.8	-0.259	±0.091	-2.84	8.08	4.56	1017.1
12	1537	17.3	20.5	±2.7	-0.156	±0.111	-1.40	1.97	4.71	1056.6
14	1689	17.5	14.8	±2.1	0.182	±0.170	1.09	1.18	4.79	1086.3
16	1842	17.5	10.7	±1.8	0.636	±0.275	2.31	5.34	4.78	1105.8
18	1994	17.2	7.4	±1.5	1.324	±0.471	2.81	7.90	4.66	1114.4
20	2146	16.6	7.6	±1.3	1.184	±0.374	3.17	12.05	4.40	1115.2
22	2299	15.4	7.4	±1.4	1.081	±0.394	2.75	7.54	4.01	1102.7
24	2451	14.2	5.2	±1.1	1.731	±0.578	3.00	8.98	3.55	1077.1
26	2604	12.5	7.6	±1.6	0.645	±0.281	2.29	5.25	2.99	1040.1
28	2756	10.6	8.7	±1.4	0.218	±0.196	1.11	1.24	2.45	989.2
30	2908	9.3	7.9	±1.4	0.177	±0.209	0.85	0.72	2.07	960.0
Mean $\bar{x}$, $S_{\bar{x}}$		14.43	12.77	±0.52(b)						
RMS		±2.96	±6.65							

(a) From "0" Ref., Drawing 33-FT-2.

(b) $S_{\bar{x}} = \left[\frac{1}{n^2} \sum (1\sigma)^2\right]^{1/2}$.

TABLE 16

E09-01 COMPARISON OF MEASURED AND CALCULATED Cs-137 AXIAL INVENTORY

Compact I.D.	Core Height[a] (mm)	Cs-137 Inventory Per Compact: Calc., C (%)	Meas., M (%)	$S_M(1\sigma)$ (%)	Relative Difference (C/M-1) = Z: Z	$S_Z(1\sigma)$	Comparison: Test 1 $D = Z/S_Z$	Test 2 D^2	GAUGE/FEVER Thermal Fluence ($n/m^2 \times 10^{25}$) (E <0.38aJ)	Time Avg. SURVEY Fuel Temp. (°C)
2	775	8.0	9.5	±1.4	-0.158	±0.124	-1.27	1.62	1.72	579.4
4	927	10.3	12.9	±1.7	-0.202	±0.105	-1.92	3.67	2.34	669.0
6	1080	12.3	20.1	±2.5	-0.388	±0.076	-5.10	26.00	2.94	739.7
8	1232	13.8	24.6	±2.9	-0.439	±0.066	-6.64	44.07	3.42	803.3
10	1384	14.6	18.8	±2.3	-0.223	±0.095	-2.35	5.53	3.69	856.3
12	1537	15.2	18.3	±2.4	-0.169	±0.109	-1.56	2.42	3.92	912.0
14	1689	15.8	13.1	±1.9	0.206	±0.175	1.18	1.39	4.12	970.1
16	1842	16.2	13.2	±1.9	0.227	±0.177	1.29	1.66	4.25	1014.0
18	1994	16.2	10.5	±1.7	0.543	±0.250	2.17	4.72	4.27	1049.8
20	2149	16.0	6.9	±1.3	1.319	±0.437	3.02	9.11	4.20	1076.2
22	2299	15.6	8.1	±1.7	0.926	±0.404	2.29	5.25	4.05	1102.6
24	2451	15.1	6.4	±1.5	1.360	±0.553	2.46	6.04	3.87	1119.4
26	2604	14.6	10.1	±1.7	0.446	±0.243	1.83	3.35	3.71	1099.3
28	2756	13.6	8.8	±1.5	0.545	±0.263	2.07	4.29	3.39	1120.9
30	2908	12.9	8.7	±1.7	0.483	±0.290	1.07	2.78	3.16	1103.8
Mean $\bar{x}$, $S_{\bar{x}}$		14.01	12.67	±0.50[b]						
RMS		±2.26	±5.25							

(a) From "0" Ref., Drawing 33-FT-2.

(b) $S_{\bar{x}} = \left[\frac{1}{n^2} \sum (1\sigma)^2\right]^{1/2}$

TABLE 17

E11-01 COMPARISON OF Cs-137 AXIAL INVENTORY

Compact I.D.	Core Height[(a)] (mm)	Cs-137 Inventory Per Compact: Calc., C (%)	Meas., M (%)	$S_M(1\sigma)$ (%)	Relative Difference (C/M-1) = Z: Z	$S_Z(1\sigma)$	Comparison: Test 1 $D = Z/S_Z$	Test 2 D^2	GAUGE/FEVER Thermal Fluence ($n/m^2 \times 10^{25}$) (E <0.38aJ)	Time-Avg. SURVEY Fuel Temp. (°C)
2	775	9.2	11.9	±1.7	-0.227	±0.110	-2.03	4.22	2.08	627.2
4	927	12.5	16.4	±2.1	-0.238	±0.098	-2.44	5.94	3.02	782.4
6	1080	15.2	18.4	±2.3	-0.174	±0.103	-1.68	2.84	3.92	895.4
8	1232	16.9	25.3	±3.1	-0.332	±0.082	-4.06	16.46	4.56	982.7
10	1384	17.8	19.6	±2.5	-0.092	±0.116	-0.79	0.63	4.88	1042.9
12	1537	17.9	21.3	±2.7	-0.160	±0.107	-1.50	2.25	5.04	1083.9
14	1689	18.3	14.7	±1.9	0.245	±0.161	1.52	2.32	5.12	1114.0
16	1842	18.3	14.6	±2.0	0.253	±0.172	1.48	2.18	5.12	1132.9
18	1994	17.9	11.4	±1.8	0.570	±0.248	2.30	5.29	4.99	1139.3
20	2146	17.4	13.3	±1.8	0.308	±0.177	1.74	3.03	4.71	1130.7
22	2299	16.2	11.5	±1.9	0.409	±0.233	1.756	3.08	4.29	1122.1
24	2451	14.8	12.1	±1.8	0.223	±0.182	1.226	1.50	3.80	1093.4
26	2604	13.2	15.6	±2.6	-0.154	±0.141	-1.09	1.19	3.20	1052.0
28	2756	11.2	13.2	±2.1	-0.152	±0.135	-1.12	1.26	2.62	998.0
30	2908	9.8	10.1	±1.5	-0.030	±0.144	-0.20	0.04	2.21	968.1
Mean $\bar{x}$, $S_{\bar{x}}$		15.11	15.29	±0.56[(b)]						
RMS		±3.07	±4.11							

(a) From "0" Ref., Drawing 33-FT-2.

(b) $S_{\bar{x}} = \left[\frac{1}{n^2} \sum (1\sigma)^2\right]^{1/2}$.

TABLE 18
E14-01 COMPARISON OF MEASURED AND CALCULATED Cs-137 AXIAL INVENTORY

Compact I.D.	Core Height(a) (mm)	Cs-137 Inventory Per Compact			Relative Difference (C/M-1) = Z		Comparison		GAUGE/FEVER Thermal Fluence ($n/m^2 \times 10^{25}$) (E <0.38aJ)	Time-Avg. SURVEY Fuel Temp. (°C)
		Calc., C (%)	Meas., M (%)	$S_M(1\sigma)$ (%)	Z	$S_Z(1\sigma)$	Test 1 $D = Z/S_Z$	Test 2 D^2		
2	775	9.1	10.9	±1.6	-0.165	±0.123	1.35	1.82	2.02	598.8
4	927	12.3	9.8	±1.5	0.255	±0.192	1.33	1.76	2.93	734.8
6	1080	14.8	12.8	±1.8	0.156	±0.163	0.96	0.92	3.80	833.6
8	1232	16.6	15.6	±2.0	0.064	±0.136	0.47	0.22	4.41	913.3
10	1384	17.4	14.4	±1.9	0.208	±0.159	1.31	1.71	4.72	970.1
12	1537	17.8	15.8	±2.2	0.127	±0.157	0.81	0.65	4.88	1009.3
14	1689	18.0	17.9	±2.2	0.006	±0.124	0.05	0.00	4.96	1038.1
16	1842	18.0	17.6	±2.2	0.023	±0.128	0.18	0.03	4.96	1056.1
18	1994	17.6	17.2	±2.2	0.023	±0.131	0.18	0.03	4.83	1062.4
20	2146	17.0	14.9	±1.9	0.141	±0.145	0.97	0.94	4.56	1054.8
22	2299	15.9	16.5	±2.2	-0.040	±0.128	0.28	0.08	4.15	1047.2
24	2451	14.6	13.7	±1.9	0.070	±0.148	0.44	0.20	3.68	1020.9
26	2604	12.8	11.9	±1.8	0.076	±0.163	0.47	0.22	3.10	983.6
28	2756	10.9	10.0	±1.6	0.090	±0.174	0.52	0.27	2.54	935.6
30	2908	9.5	8.1	±1.3	0.173	±0.188	0.92	0.84	2.14	911.6
Mean $\bar{x}$, $S_{\bar{x}}$		14.82	13.81	±0.49(b)						
RMS		±3.05	±2.99							

(a) From "0" Ref., Drawing 33-FT-2.

(b) $S_{\bar{x}} = \left[\frac{1}{n^2} \sum (1\sigma)^2\right]^{1/2}$.

TABLE 19
SURVEY TEMPERATURE PREDICTIONS FOR PEACH BOTTOM DRIVER ELEMENTS

Element I.D.	GAUGE Location (Patch/ Column)	Predicted Time- and Volume-Averaged Temperatures for Even-Numbered Fuel Compacts (°C)															
		Bottom 2	4	6	8	10	12	14	16	18	20	22	24	26	28	Top 30	$\bar{x}$	RMS[a]
F01-01	1/2	632	790	905	994	1055	1097	1127	1146	1152	1151	1136	1106	1065	1010	980	1023	126
E01-01	1/7	632	790	905	994	1055	1096	1127	1145	1152	1151	1135	1107	1065	1011	980	1023	127
E03-02	2/1	619	767	873	956	1013	1052	1081	1099	1106	1106	1092	1066	1027	976	947	985	118
E02-02	2/4	626	780	892	979	1038	1079	1108	1126	1133	1132	1117	1089	1048	995	965	1007	123
E03-01	2/6	611	752	851	928	982	1020	1048	1066	1075	1075	1064	1040	1004	956	927	960	111
E04-02	2/7	610	750	848	924	978	1015	1044	1062	1070	1071	1059	1036	1000	952	924	956	110
F03-02	3/1	616	764	873	958	1016	1056	1084	1102	1108	1106	1091	1064	1024	972	942	985	119
F04-03	3/2	617	765	872	955	1013	1052	1081	1099	1105	1104	1090	1063	1024	973	943	984	118
F02-01	3/5	621	772	883	970	1029	1069	1098	1116	1122	1120	1105	1077	1036	983	953	997	122
F03-01	3/6	576	693	786	866	926	974	1016	1044	1062	1074	1071	1055	1031	992	971	940	128
A04-03	4/2	618	767	874	958	1016	1055	1084	1102	1109	1108	1093	1066	1027	976	946	987	124
B03-03	5/3	619	768	875	958	1016	1055	1084	1102	1109	1108	1094	1067	1028	977	947	987	118
B02-02	5/4	627	781	894	981	1041	1082	1111	1129	1136	1134	1119	1091	1050	996	966	1010	124
B02-01	5/5	624	777	889	976	1036	1076	1105	1124	1130	1128	1113	1084	1043	990	959	1004	123
B03-01	5/6	579	697	791	873	933	982	1023	1052	1070	1082	1079	1063	1038	999	977	949	129
E05-02	8/5	613	755	853	929	983	1020	1049	1068	1077	1078	1067	1043	1008	960	931	962	111
E06-02	8/6	624	774	879	960	1017	1056	1086	1105	1114	1115	1102	1077	1040	989	960	993	118
F05-05	11/1	615	758	858	935	990	1028	1057	1076	1084	1085	1073	1049	1013	964	936	968	113
F05-04	11/6	623	773	881	964	1022	1061	1090	1109	1116	1116	1102	1076	1037	985	955	994	119
A05-05	13/1	579	697	790	872	927	980	1022	1051	1069	1081	1078	1063	1039	1000	978	949	129
B05-01	13/3	576	692	783	862	921	969	1010	1039	1056	1069	1067	1052	1029	991	970	939	127
A04-04	13/5	578	696	790	871	931	980	1021	1050	1068	1080	1077	1062	1037	998	976	948	129
B05-02	14/5	579	697	791	873	933	982	1023	1052	1070	1082	1080	1065	1040	1001	979	950	130
E05-01	19/3	612	752	848	922	976	1013	1042	1061	1071	1072	1062	1039	1005	957	928	957	110
E07-01	37/1	578	669	739	802	855	910	968	1012	1048	1079	1101	1117	1135	1117	1100	949	158
E08-02	37/3	577	668	738	801	853	909	967	1011	1046	1077	1099	1115	1133	1115	1098	947	158
E07-02	37/4	624	774	878	959	1015	1055	1085	1106	1113	1114	1102	1077	1039	989	959	993	118
F11-03	41/3	632	792	909	998	1059	1100	1130	1148	1155	1145[b]	1136	1107	1064	1009	977	1024	127
F10-09	44/1	632	791	904	991	1051	1092	1122	1141	1148	1140[b]	1132	1103	1062	1008	976	1019	125
F09-08	44/5	633	790	903	989	1048	1089	1119	1139	1146	1139[b]	1131	1103	1063	1009	978	1018	124
B11-03	49/3	634	795	913	1003	1065	1106	1136	1155	1161	1151[b]	1142	1111	1068	1012	980	1029	128
E10-02	61/1	623	789	880	963	1021	1061	1090	1109	1117	1110[b]	1103	1078	1038	986	956	995	118
E11-02	61/2	626	780	892	978	1037	1077	1107	1126	1133	1125[b]	1117	1088	1047	994	964	1006	123
E09-02	61/5	577	667	737	800	853	908	966	1010	1046	1072[b]	1098	1114	1133	1115	1098	946	157
E09-01	61/6	578	669	739	803	856	912	970	1014	1049	1076[b]	1102	1119	1138	1120	1103	950	159
F12-11	70/6	631	790	907	997	1057	1098	1128	1146	1152	1142[b]	1133	1103	1060	1004	973	1021	126
E11-01	90/4	627	782	895	982	1042	1083	1114	1132	1139	1130[b]	1122	1093	1052	998	968	1011	124
E12-02	91/6	622	774	885	972	1031	1072	1101	1119	1126	1117[b]	1108	1080	1039	985	956	999	122
E13-02	91/7	613	760	869	954	1013	1053	1082	1100	1105	1097[b]	1088	1059	1019	939	938	979	119
F15-14	101/3	613	761	873	963	1025	1067	1098	1116	1121	1111[b]	1101	1071	1029	976	951	992	124
F14-13	101/4	619	772	887	977	1039	1080	1110	1127	1132	1121[b]	1111	1080	1037	983	954	1002	126
A17-08	105/6	564	679	761	828	877	912	938	955	961	955[b]	949	927	895	855	837	861	91
A17-11	106/7	562	677	758	825	874	908	934	950	957	951[b]	944	922	891	851	833	858.	92
B14-02	108/4	616	768	882	973	1036	1078	1107	1124	1129	1118[b]	1108	1077	1034	980	951	999	125
B13-01	108/5	622	777	894	986	1049	1091	1120	1138	1142	1132[b]	1121	1090	1046	991	962	1011	127
A14-14	108/6	615	765	879	969	1031	1073	1102	1119	1124	1114[b]	1103	1072	1030	976	948	995	124
E14-01	126/1	598	734	833	913	970	1009	1038	1056	1062	1054[b]	1047	1020	983	935	911.	.944	111
E15-01	126/2	550	658	733	794	839	872	897	913	919	915[b]	910	891	863	862	811	826	85
E15-02	126/3	550	661	737	799	845	877	901	916	922	917[b]	911	890	860	822	803	828	85
E14-02	126/4	600	739	840	922	979	1018	1046	1064	1070	1061[b]	1053	1025	987	938	912	950	113
E13-01	126/5	607	750	855	939	997	1036	1065	1082	1088	1080[b]	1071	1043	1004	953	925	966	117
F16-15	139/5	562	677	759	826	876	911	938	954	961	955[b]	949	927	896	857	840	859	94

(a) $RMS = \left[\frac{1}{n} (x_i - \bar{x})^2\right]^{1/2}$.

(b) Interpolated value.

TABLE 20
POSITION AND MAGNITUDE OF MAXIMUM Cs-137 RELEASE IN DRIVER ELEMENTS

Element I.D.	Axial Location (mm)	Maximum Cs-137 Loss: Calc., C (%)	Maximum Cs-137 Loss: Meas., M (%)	Maximum Cs-137 Loss: S_M (1σ) (%)	Relative Difference (C/M-1) = Z: Z	Relative Difference (C/M-1) = Z: S_Z (1σ)	Comparison: Test 1 $D=Z/S_Z$	Comparison: Test 2 D^2	Compact I.D.	GAUGE/FEVER Thermal Fluence ($n/m^2 \times 10^{25}$) (E <0.38aJ)	Time-Avg. SURVEY Fuel Temp. (°C)
E03-01	1991	16.1	7.3	±0.9	1.205	±0.272	4.43	19.66	18	4.26	1075
E14-02	Smooth Profile										
E03-02	2109	16.2	5.8	±0.7	1.793	±0.337	5.32	28.29	20	4.29	1106
E09-02	2000	16.0	6.4	±0.7	1.500	±0.273	5.49	30.01	18	4.22	1046
E04-02	1660	16.4	9.5	±1.0	0.726	±0.182	4.00	15.98	15	4.34	1053
E13-02	Smooth Profile										
E05-02	2266	14.8	5.1	±0.6	1.902	±0.341	5.57	31.04	21-22	3.78	1067
E12-02	2236	16.7	10.7	±1.2	0.561	±0.175	3.21	10.26	21	4.45	1113
E07-02	2248	16.2	5.8	±0.7	1.793	±0.337	5.32	28.29	21	4.25	1109
E10-02	2333	16.2	7.4	±0.8	1.189	±0.237	5.02	25.25	21	4.29	1107
E13-01	2192	16.7	11.8	±1.3	0.415	±0.156	2.66	7.09	20-21	4.46	1080
E08-02	2511	14.8	5.4	±0.6	1.741	±0.304	5.72	32.68	25	3.80	1125
A04-03	2415	13.9	5.3	±0.6	1.623	±0.297	5.47	29.87	24	3.44	1067
A04-04	2070	15.6	4.6	±0.5	2.391	±0.368	6.49	42.08	19	4.04	1074
A14-14	Smooth Profile										
B05-02	2106	16.8	5.3	±0.6	2.170	±0.359	6.05	36.56	20	4.51	1083
F03-02	2028	16.4	6.1	±0.7	1.688	±0.309	5.47	29.96	19	4.37	1108
F04-03	1971	16.7	5.1	±0.6	2.275	±0.385	5.91	34.86	18	4.48	1106
F15-14	Smooth Profile										
B11-03	2211	16.7	7.2	±0.8	1.319	±0.258	5.12	26.21	21	4.47	1147
F02-81	2470	14.1	5.0	±0.6	1.820	±0.338	5.38	28.93	24	3.53	1077
F05-04	2014	16.8	5.5	±0.6	2.055	±0.333	6.17	38.02	19	4.47	1117
B02-01	1996	17.3	6.3	±0.7	1.746	±0.305	5.72	32.75	18	4.68	1130
A17-11	Smooth Profile										
E14-01	Smooth Profile										
E01-01	1917	18.2	5.8	±1.2	2.138	±0.649	3.29	10.84	27	5.05	1149
E02-02	2255	16.4	4.6	±1.5	2.565	±1.163	2.21	4.87	21	4.33	1125
E09-01	2379	15.4	5.2	±1.2	1.962	±0.683	2.87	8.24	23	3.95	1111
F11-01	2035	17.7	11.4	±1.8	0.553	±0.245	2.25	5.08	19	4.85	1135
F15-01	Smooth Profile										
E07-01	1988	16.0	6.3	±1.3	1.540	±0.524	2.94	8.63	19	4.22	1064
E06-02	2038	16.9	7.4	±1.5	1.284	±0.463	2.77	7.69	19	4.54	1114
E05-01	1979	16.0	8.2	±1.6	0.951	±0.381	2.50	6.24	18	4.22	1071
E15-02	Smooth Profile										
B13-01	2083	17.9	11.4	±2.2	0.570	±0.303	1.88	3.54	19	4.94	1137
A03-03	Smooth Profile										
B02-02	1998	17.5	4.6	±1.1	2.804	±0.910	3.08	9.50	18	4.77	1136
F11-02	1979	17.7	8.0	±1.3	1.213	±0.360	3.37	11.37	18	4.88	1133
A05-05	2236	15.4	5.9	±1.3	1.610	±0.575	2.80	7.84	21	3.91	1080
B03-01	1963	15.7	7.9	±1.7	0.987	±0.428	2.31	5.33	18	4.09	1070
B14-02	2204	17.1	11.1	±1.7	0.541	±0.236	2.29	5.25	21	4.62	1131
B03-03	1914	17.1	2.7	±1.0	5.333	±2.346	2.27	5.16	17	4.62	1106
B05-01	1984	15.4	5.5	±1.2	1.800	±0.610	2.95	8.68	18	3.99	1057
F03-01	2384	14.3	4.0	±1.2	2.575	±0.107	2.40	5.76	23	3.60	1063
F05-05	1730	16.6	7.5	±1.4	1.213	±0.413	2.94	8.62	15	4.44	1066
A17-08	Smooth Profile										
F11-03	1770	18.2	9.0	±1.3	1.022	±0.292	3.50	12.24	15	5.06	1113
Mean $\bar{x}$											1110
RMS											±29

TABLE 21
POSITION AND MAGNITUDE OF MAXIMUM Cs-137 PLATEOUT IN DRIVER ELEMENTS

Element I.D.	Axial Location (mm)	Calc., C (%)	Maximum Cs-137 Plateout: Meas., M (%)	Maximum Cs-137 Plateout: S_M (1σ) (%)	Relative Difference (C/M-1) = Z: Z	Relative Difference (C/M-1) = Z: S_Z (1σ)	Comparison: Test 1 $D=Z/S_Z$	Comparison: Test 2 D^2	Compact I.D.	GAUGE/FEVER Thermal Fluence ($n/m^2 \times 10^{25}$) (E <0.38aJ)	Time-Averaged SURVEY Temperatures: Compact (°C)	Time-Averaged SURVEY Temperatures: EOL Max. Sleeve (°C)
E03-01	1266	15.2	28.7	±3.0	-0.473	±0.055	-8.50	72.19	8	3.90	928	690
E14-02	Smooth Profile											
E03-02	1494	17.0	29.5	±3.1	-0.424	±0.061	-7.00	48.96	11-12	4.56	1053	740
E09-02	1361	14.4	24.8	±2.6	-0.419	±0.061	-6.89	47.46	10	8.65	853	668
E04-02	1327	15.4	24.8	±2.6	-0.379	±0.065	-5.82	33.90	9	4.01	952	706
E13-02	Smooth Profile											
E05-02	1250	15.2	25.7	±2.7	-0.409	±0.062	-6.58	43.23	8	3.92	929	683
E12-02	1329	17.3	22.4	±2.4	-0.228	±0.083	-2.75	7.57	9	4.66	1002	575
E07-02	1237	16.2	25.5	±2.7	-0.365	±0.067	-5.42	29.4	8	4.28	959	652
E10-02	1492	17.4	24.4	±2.6	-0.287	±0.076	-3.78	14.25	11	4.72	1041	646
E13-01	1550	17.7	18.0	±1.9	-0.017	±0.104	-0.16	0.26	12	4.87	1037	578
E08-02	1090	13.4	21.7	±2.3	-0.382	±0.065	-5.84	34.15	6	3.28	738	614
A04-03	1195	15.4	27.0	±2.8	-0.429	±0.059	-7.26	52.76	7-8	3.98	959	668
A04-04	1334	14.2	32.7	±3.4	-0.566	±0.045	-12.53	157.00	9	3.54	902	727
A14-14	Smooth Profile											
B05-02	1392	17.2	24.1	±2.6	-0.286	±0.077	-3.72	13.83	10	4.67	934	709
F03-02	1196	15.0	32.3	±3.3	-0.536	±0.047	-11.29	127.43	7	3.86	916	662
F04-03	1075	14.1	37.0	±3.8	-0.619	±0.039	-15.81	250.07	6	3.53	872	637
F15-14	Smooth Profile											
B11-03	1425	17.8	21.6	±2.3	-0.176	±0.088	-2.00	4.02	11	4.91	1086	622
F02-01	1108	15.4	30.0	±3.1	-0.487	±0.053	-9.17	84.18	7	3.98	927	658
F05-C4	1006	13.2	24.8	±2.6	-0.468	±0.056	-8.38	70.26	5	3.23	828	650
B02-01	1084	14.5	25.6	±2.7	-0.434	±0.060	-7.26	52.68	6	3.68	889	638
A17-11	Smooth Profile											
E14-01	Smooth Profile											
E01-01	986	14.0	30.9	±3.5	-0.547	±0.051	-10.66	113.58	5	3.49	848	612
E02-02	1137	15.7	30.9	±3.6	-0.492	±0.059	-8.31	69.06	7	4.10	936	655
E09-01	1198	13.5	24.6	±2.9	-0.451	±0.065	-6.97	48.65	7-8	3.32	803	630
E11-01	1216	17.0	23.0	±2.8	-0.261	±0.090	-2.90	8.41	8	4.56	983	572
E15-01	Smooth Profile											
E07-01	1393	14.5	26.7	±3.4	-0.457	±0.069	-6.61	43.66	10	3.67	855	695
E06-02	1280	16.4	27.7	±3.3	-0.408	±0.071	-5.78	33.45	8-9	4.34	960	664
E05-01	1042	13.4	26.9	±3.2	-0.502	±0.059	-8.47	71.72	6	3.32	849	645
E15-02	Smooth Profile											
B13-01	1680	18.5	20.9	±2.5	-0.115	±0.106	-1.08	1.18	14	5.21	1121	594
A03-03	Smooth Profile											
B02-02	1144	15.8	42.3	±4.7	-0.626	±0.042	-15.09	227.86	7	4.10	938	654
E11-02	1176	16.0	28.2	±3.3	-0.433	±0.066	-6.52	42.46	7	4.19	935	568
A05-05	1303	14.2	24.9	±2.9	-0.430	±0.066	-6.47	41.86	9	3.55	902	721
B03-01	1505	15.0	36.0	±4.6	-0.583	±0.053	-10.96	120.05	12	3.86	982	682
B14-02	1500	18.4	19.8	±2.5	-0.071	±0.117	-0.60	0.36	12	5.14	1078	563
B03-03	1154	15.2	43.8	±4.9	-0.652	±0.039	-16.82	282.88	7	3.90	917	694
B05-01	1229	13.4	33.3	±3.9	-0.598	±0.047	-12.68	160.79	8	3.31	863	704
F03-01	1375	14.2	27.5	±3.2	-0.484	±0.060	-8.05	64.79	9-10	3.55	897	
F05-05	1227	15.3	29.4	±3.4	-0.480	±0.060	-7.97	63.52	8	3.94	936	680
A17-08	Smooth Profile											
F11-03	1365	17.6	28.7	±3.4	-0.387	±0.073	-5.32	28.34	10	4.80	1059	613

APPENDIX C

E14-01 DATA PACKAGE

DISC HAS 15 PLOT FRAMES

0 ERRORS WERE DETECTED

EXIT LOC041071

@XQT,0 PBEOLGS

NUMBER OF RECORDS FOR THIS FILE = 86

MISC. SCANS STRATAS

106	107	108	115
153	153	117	141
190	191	143	144
0	0	145	152
0	0	0	0
0	0	0	0
0	0	0	0
0	0	0	0
0	0	0	0
0	0	0	0
0	0	0	0
0	0	0	0
0	0	0	0
0	0	0	0
0	0	0	0

FIRST RECORD # 3 LAST RECORD # 47

STRATA	START	END	TOTALS	REC/STR
1	3	10	0	6
2	12	36	1	25
3	38	39	0	2
4	40	47	0	8

SPECTRUM I.D. GA.TAG NO.	CORE LOCATION PARAMETERS AXIAL CORE LOC. CP (MM)	SCAN INTERVAL / FUEL ELEMENT I.D.	CE-144 133 KEV	CE-141 145 KEV	PA-233 312 KEV	I-131 364 KEV	RU-103 497 KEV	RU-106 512 KEV	CS-137 661 KEV	ZR-95 724 KEV	CS-134 796 KEV	LA-140 1596 KEV
			NUCLIDE CPM + / - 1 SIGMA COUNTING ERROR									
* * *	BEGIN STRATA # 1 * * *											
108	49.21	81.66	.0	27.1	.0	.0	3.7	12.6	21.3	.0	.0	.0
		AUTO #1 E14-01	.0	22.0	.0	.0	2.7	4.1	17.4	.0	.0	.0
109	178.50	68.05	.0	.0	22.1	.0	9.3	.0	20.4	.0	.0	.0
		AUTO #2 E14-01	.0	.0	10.6	.0	4.2	.0	5.1	.0	.0	.0
110	254.72	68.05	.0	.0	43.1	.0	5.6	.0	25.2	.0	.0	.0
		AUTO #3 E14-01	.0	.0	10.1	.0	3.3	.0	5.6	.0	.0	.0
111	328.90	69.41	.0	.0	.0	.0	13.0	.0	10.5	.0	11.1	.0
		AUTO #4 E14-01	.0	.0	.0	.0	5.0	.0	17.0	.0	3.8	.0
112	416.00	93.91	.0	.0	.0	112.4	.0	5.0	18.0	.0	.0	.0
		AUTO #5 E14-01	.0	.0	.0	34.6	.0	2.6	4.7	.0	.0	.0
113	507.17	80.30	.0	.0	.0	.0	7.4	7.5	18.0	.0	1.2	.0
		AUTO #6 E14-01	.0	.0	.0	.0	3.8	3.1	4.7	.0	1.3	.0
114	556.86	68.05	.0	.0	42.0	375.7	.0	.0	14.4	.0	.0	.0
		AUTO #7 E14-01	.0	.0	27.8	137.0	.0	.0	4.2	.0	.0	.0
115	629.00	76.22	.0	.0	.0	.0	16.0	.0	17.3	4.7	.0	.0
		AUTO #8 E14-01	.0	.0	.0	.0	11.0	.0	6.6	2.8	.0	.0
* * *	STRATA # 1 E14-01 TOTALS * * *											
MEAN =	365.04	WT MEAN CPM =	.0	27.1	35.8	223.0	9.1	8.2	18.2	4.7	5.8	.0
RMS =	186.18	WT MEAN 1SIGMA=	.0	22.0	18.1	92.6	5.7	3.3	9.7	2.8	2.7	.0
MIDPT=	339.11	WT RMS =	.0	.0	9.6	129.9	4.3	3.2	4.0	.0	4.9	.0
RANGE=	656.00	WT ERROR =	.0	22.0	10.5	61.0	2.4	1.9	3.5	2.8	1.9	.0
116	706.58	78.94	364.0	1403.0	8282.8	2210.7	1566.1	.0	322.7	1595.1	115.0	2632.9
		AUTO #9 E14-01	164.3	172.0	203.7	426.0	104.3	.0	44.1	92.9	26.6	129.9
* * *	BEGIN STRATA # 2 * * *											
117	792.31	81.66	277.3	2596.6	18779.7	3864.5	2732.4	.0	610.6	2947.1	189.2	4970.1
		AUTO #10 E14-01	177.8	223.6	295.0	661.8	154.2	.0	62.8	110.0	44.9	169.3
118	879.42	81.66	.0	2849.7	22696.8	3476.3	3181.5	.0	511.4	3084.9	268.9	5706.4
		AUTO #11 E14-01	.0	243.4	361.2	702.0	163.9	.0	61.2	95.1	37.0	197.0
119	946.78	91.19	614.2	2758.6	25458.4	3637.3	3347.3	136.7	550.5	3630.2	398.9	6301.2
		AUTO #12 E14-01	275.3	260.7	407.6	855.4	202.3	73.3	60.9	106.4	43.3	186.4
120	1033.89	72.13	.0	3835.7	30020.0	4845.6	4004.9	.0	675.2	3897.8	442.0	6999.9
		AUTO #13 E14-01	.0	425.5	421.0	829.0	182.0	.0	62.3	128.6	47.0	219.9
121	1113.52	76.22	775.1	3853.7	33675.9	6488.5	3851.7	.0	717.5	4526.5	595.2	6935.5
		AUTO #14 E14-01	211.7	340.7	439.9	1256.5	197.1	.0	65.1	142.9	47.1	203.6
122	1196.53	81.66	1183.8	4473.1	35552.2	5036.6	3715.1	.0	873.0	4431.9	742.1	7473.5
		AUTO #15 E14-01	289.6	385.4	467.0	961.3	205.9	.0	65.9	120.2	57.4	207.0
123	1283.64	81.66	.0	5022.2	37664.7	6236.1	4091.2	280.7	868.5	4423.7	714.9	7421.3
		AUTO #16 E14-01	.0	445.6	410.8	945.1	200.9	105.3	81.8	125.4	51.4	211.5
124	1371.42	83.02	283.3	3907.5	40129.2	4827.6	4907.3	362.0	805.3	4744.0	878.8	8046.5
		AUTO #17 E14-01	198.4	368.3	459.4	888.1	205.8	121.8	64.1	130.9	55.5	208.0

SPECTRUM I.D. GA.TAG NO.	CORE LOCATION PARAMETERS AXIAL CORE LOC. CP (MM)	SCAN INTERVAL / FUEL ELEMENT I.D.	CE-144 133 KEV	CE-141 145 KEV	PA-233 312 KEV	I-131 364 KEV	RU-103 497 KEV	RU-106 512 KEV	CS-137 661 KEV	ZR-95 724 KEV	CS-134 796 KEV	LA-140 1596 KEV
			NUCLIDE CPM +/- 1 SIGMA COUNTING ERROR									
125	1460.58	84.38	279.2	4933.0	42064.2	6642.2	4803.8	.0	1001.8	5131.8	896.6	8061.3
		AUTO #18 E14-01	188.9	479.2	446.5	1232.9	197.7	.0	93.0	160.5	55.4	213.1
126	1547.68	78.94	465.0	4769.9	41730.6	5503.3	4356.1	136.1	886.4	5020.5	962.2	8081.8
		AUTO #19 E14-01	211.4	344.9	469.3	916.9	210.2	108.4	79.2	131.3	58.4	213.4
127	1640.23	95.27	879.1	5475.4	42542.4	7782.4	4489.7	.0	1004.8	5005.7	967.5	8502.3
		AUTO #20 E14-01	229.5	433.3	448.6	1512.3	190.2	.0	71.6	135.8	60.1	236.3
128	1730.06	73.49	754.8	4153.2	43767.6	5159.9	4602.9	218.6	882.0	4801.2	937.4	8228.9
		AUTO #21 E14-01	159.4	472.1	482.7	870.9	207.3	134.5	79.7	133.7	54.6	209.8
129	1811.71	78.94	842.7	5152.7	41962.4	7729.5	4817.5	349.4	985.0	4921.1	1092.2	8506.3
		AUTO #22 E14-01	232.3	420.2	441.4	1077.3	212.7	110.6	70.6	126.7	79.3	216.2
130	1896.77	83.02	828.4	5052.8	42698.4	4532.6	4079.2	.0	862.2	5157.6	1035.1	8214.6
		AUTO #23 E14-01	206.3	406.9	462.2	824.4	190.2	.0	64.9	146.4	61.9	228.7
131	1985.25	83.02	308.5	4595.2	41399.0	6723.9	4777.5	.0	971.1	4850.7	894.5	8286.5
		AUTO #24 E14-01	270.4	463.1	486.9	988.4	195.4	.0	74.8	129.1	56.1	217.8
132	2075.07	85.74	1113.8	4829.0	41756.3	5450.3	3872.6	208.1	794.5	4947.3	859.8	7769.0
		AUTO #25 E14-01	350.8	463.1	504.8	1087.4	211.2	116.7	68.0	133.6	52.0	204.4
133	2169.90	83.02	438.9	4876.7	41424.1	7961.7	3769.3	340.8	833.2	4940.5	845.1	8265.8
		AUTO #26 E14-01	188.4	415.3	495.5	1542.0	209.4	105.5	67.7	139.1	51.8	217.4
134	2252.68	81.66	745.5	5003.8	40241.0	5283.3	4820.1	606.7	926.7	4955.8	894.3	8264.3
		AUTO #27 E14-01	253.6	530.1	496.2	1054.2	199.9	121.0	80.6	148.0	64.4	213.2
135	2341.14	84.38	.0	4422.4	37631.7	5440.0	4107.4	951.7	765.6	4478.6	643.4	7579.1
		AUTO #28 E14-01	.0	430.9	482.3	1176.8	217.5	133.7	69.2	125.1	51.2	207.4
136	2430.98	84.38	569.9	4143.1	35263.6	4143.0	4419.2	797.0	765.5	4525.3	801.8	7335.1
		AUTO #29 E14-01	235.4	431.9	434.0	892.5	192.5	147.4	73.6	148.2	65.3	215.3
137	2520.81	84.38	.0	4251.0	33438.4	3991.0	4091.0	879.1	836.7	4292.2	567.3	6727.5
		AUTO #30 E14-01	.0	393.5	469.2	1231.0	208.6	135.1	73.9	133.2	45.7	194.7
138	2611.99	87.11	712.7	3996.7	30675.8	3339.9	3976.8	787.8	664.6	3904.3	499.3	6561.5
		AUTO #31 E14-01	217.1	512.5	474.7	864.1	212.0	146.0	75.0	129.3	51.7	189.5
139	2701.81	81.66	464.1	3908.2	28433.0	4646.7	3949.4	940.6	746.7	3934.9	442.0	6613.7
		AUTO #32 E14-01	168.1	503.3	437.9	873.1	198.3	140.8	84.4	132.9	47.6	191.5
140	2789.60	83.02	.0	3524.1	26103.6	2845.0	3637.0	862.3	562.5	3588.7	376.9	5826.2
		AUTO #33 E14-01	.0	354.0	467.5	856.5	199.5	107.2	69.5	123.8	39.0	180.1
141	2873.98	77.58	1131.5	3496.0	21470.7	3284.1	3907.1	1193.6	454.0	3215.9	358.5	5520.4
		AUTO #34 E14-01	388.9	438.3	403.5	947.8	200.6	150.2	55.8	111.8	43.1	191.8

SPECTRUM I.D.	CORE LOCATION PARAMETERS	FUEL ELEMENT I.D.	NUCLIDE CPM + / - 1 SIGMA COUNTING ERROR									
GA.TAG NO.	AXIAL CORE LOC. CP (MM)	SCAN INTERVAL	CE-144 133 KEV	CE-141 145 KEV	PA-233 312 KEV	I-131 364 KEV	RU-103 497 KEV	RU-106 512 KEV	CS-137 661 KEV	ZR-95 724 KEV	CS-134 796 KEV	LA-140 1596 KEV
* * *	STRATA # 2 E14-01 TOTALS * * *											
MEAN =	1818.11	WT MEAN CPM =	666.0	4241.4	35093.0	5158.9	4056.8	565.7	783.2	4377.9	693.2	7292.0
RMS =	630.49	WT MEAN 1SIGMA=	241.8	414.7	448.8	1029.7	199.2	123.7	71.5	130.7	53.6	206.3
MIDPT=	1833.15	WT RMS =	283.8	769.5	7445.2	1450.2	573.8	335.2	153.9	655.5	254.8	1007.4
RANGE=	2159.25	WT ERROR =	55.6	83.1	93.0	207.3	39.9	30.9	14.3	26.2	10.7	41.3
142	2959.06	81.66	656.1	3256.1	19693.6	4653.9	3614.6	1014.7	652.6	3420.5	221.2	5647.7
		AUTO #35 E14-01	265.3	484.3	341.6	878.3	150.3	123.6	58.1	105.3	48.3	180.7
* * *	BEGIN STRATA # 3 * * *											
143	3048.21	85.74	.0	.0	.0	.0	.0	951.2	.0	.0	.0	.0
		AUTO #36 E14-01	.0	.0	.0	.0	.0	71.6	.0	.0	.0	.0
144	3134.63	76.22	.0	.0	.0	.0	.0	875.2	.0	.0	.0	.0
		AUTO #37 E14-01	.0	.0	.0	.0	.0	60.1	.0	.0	.0	.0
* * *	STRATA # 3 E14-01 TOTALS * * *											
MEAN =	3091.42	WT MEAN CPM =	.0	.0	.0	.0	.0	915.4	.0	.0	.0	.0
RMS =	43.21	WT MEAN 1SIGMA=	.0	.0	.0	.0	.0	66.5	.0	.0	.0	.0
MIDPT=	3091.42	WT RMS =	.0	.0	.0	.0	.0	38.0	.0	.0	.0	.0
RANGE=	162.64	WT ERROR =	.0	.0	.0	.0	.0	47.3	.0	.0	.0	.0
* * *	BEGIN STRATA # 4 * * *											
145	2516.76	1.00	481.3	4011.5	32374.7	4994.7	4185.1	859.0	677.4	4190.0	540.4	7050.2
		STAT #1 E14-01	85.1	220.3	195.3	495.9	82.4	50.6	28.3	53.3	21.6	80.6
146	1804.21	1.00	540.1	4829.5	41073.2	5116.3	4478.9	205.8	925.0	4696.1	961.1	7599.1
		STAT #2 E14-01	83.6	208.7	196.2	393.7	83.4	40.9	31.2	55.2	26.4	82.9
147	1820.67	1.00	664.6	4776.6	41587.5	6114.3	4642.7	127.7	923.3	4753.8	998.3	8134.0
		STAT #3 E14-01	129.9	149.9	195.5	437.5	83.8	32.7	30.8	54.2	24.7	86.5
148	1837.16	1.00	515.3	4524.9	41714.3	6136.1	4596.8	119.3	991.7	4674.6	940.1	7971.2
		STAT #4 E14-01	58.9	158.0	200.4	498.1	89.4	33.0	35.0	54.8	24.5	85.2
149	1853.64	1.00	741.0	5030.9	41206.0	5202.4	4713.5	234.5	970.4	4804.9	903.0	7725.8
		STAT #5 E14-01	80.5	178.2	196.5	397.5	79.9	42.3	36.0	55.0	25.9	85.7
150	1870.10	1.00	680.6	5286.1	47155.7	6178.8	5062.5	214.2	1132.2	5583.9	999.8	8703.1
		STAT #6 E14-01	86.4	181.1	210.2	393.8	88.3	40.4	36.0	61.6	24.7	89.3
151	996.90	1.00	503.2	3921.6	32543.2	5375.3	4337.2	195.4	765.0	4261.4	521.7	7227.1
		STAT #7 E14-01	65.4	125.2	174.7	408.6	77.2	43.1	30.2	49.9	22.4	80.4
152	239.04	1.00	.0	.0	.0	.0	.0	.0	28.1	.0	.0	.0
		TRAP E14-01	.0	.0	.0	.0	.0	.0	3.6	.0	.0	.0

SPECTRUM I.D.	CORE LOCATION PARAMETERS		FUEL ELEMENT I.D.	NUCLIDE CPM + / - 1 SIGMA COUNTING ERROR									
GA.TAG NO.	AXIAL CORE LOC. CP (MM)	SCAN INTERVAL		CE-144 133 KEV	CE-141 145 KEV	PA-233 312 KEV	I-131 364 KEV	RU-103 497 KEV	RU-106 512 KEV	CS-137 661 KEV	ZR-95 724 KEV	CS-134 796 KEV	LA-140 1596 KEV
* * *	STRATA # 4 E14-01 TOTALS		* * *										
MEAN =	1617.31		WT MEAN CPM =	589.4	4625.9	39664.9	5588.3	4573.8	279.4	801.6	4709.2	837.8	7772.9
RMS =	645.94		WT MEAN 1SIGMA=	86.9	177.2	195.8	434.3	83.6	40.8	30.5	55.0	24.4	84.4
MIDPT=	1377.90		WT RMS =	95.6	470.2	4960.3	492.1	261.8	240.0	319.9	422.2	196.5	519.3
RANGE=	-2276.72		WT ERROR =	32.8	67.0	74.0	164.2	31.6	15.4	10.8	20.8	9.2	31.9

T O T A L   S T R A T A   E 1 4 - 0 1

MEAN =	1818.11	WT MEAN CPM =	666.0	4241.4	35093.0	5158.9	4056.8	565.7	783.2	4377.9	693.2	7292.0
RMS =	630.49	WT MEAN 1SIGMA=	241.8	414.7	448.8	1029.7	199.2	123.7	71.5	130.7	53.6	206.3
MIDPT=	1833.15	WT RMS =	283.8	769.5	7445.2	1450.2	573.8	335.2	153.9	655.5	254.8	1007.4
RANGE=	2159.25	WT ERROR =	55.6	83.1	90.0	207.3	39.9	30.9	14.3	26.2	10.7	41.3

M I S C E L L A N E O U S   S C A N S

SPECTRUM I.D. / GA.TAG NO.	CORE LOCATION PARAMETERS / AXIAL CORE LOC. CP (MM)	FUEL ELEMENT I.D. / SCAN INTERVAL	CE-144 133 KEV	CE-141 145 KEV	PA-233 312 KEV	I-131 364 KEV	RU-103 497 KEV	RU-106 512 KEV	CS-137 661 KEV	ZR-95 724 KEV	CS-134 796 KEV	LA-140 1596 KEV
			NUCLIDE CPM + / - 1 SIGMA COUNTING ERROR									
106	.00	.00	12290.1	.0	343.6	.0	.0	521.6	3677.9	973.4	782.9	.0
		CAL.: ST E14-01	76.9	.0	65.3	.0	.0	38.4	36.4	30.9	23.3	.0
107	.00	.00	.0	.0	.0	.0	3.8	2.6	32.1	.0	.0	2.3
		BACKGROUND	.0	.0	.0	.0	3.7	2.5	4.1	.0	.0	1.4
153	.00	.00	13158.5	.0	285.5	.0	.0	589.9	3883.9	996.4	831.0	.0
		CAL.: MD E14-01	87.7	.0	63.1	.0	.0	40.4	43.9	39.4	33.6	.0
190	.00	.00	12488.7	.0	349.0	.0	.0	592.2	3699.8	932.5	865.7	.0
		CAL.:END E14-01	79.5	.0	47.1	.0	.0	34.5	36.5	27.1	24.8	.0
191	.00	.00	.0	.0	.0	.0	.0	26.7	71.7	.0	10.3	.0
		BACKGROUND	.0	.0	.0	.0	.0	5.5	5.6	.0	4.4	.0

SPECTRUM I.D. GA.TAG NO.	CORE LOCATION PARAMETERS AXIAL CORE LOC. CP (MM)	SCAN INTERVAL	FUEL ELEMENT I.D	CE-141 ZR-95	CE-144 ZR-95	I-131 ZR-95	RU-103 ZR-95	CS-137 ZR-95	RU-106 ZR-95	CS-134 CS-137
				NUCLIDE CPM RATIOS AND 1 SIGMA ERRORS						
* * *	BEGIN STRATA # 1 * * *									
108	49.21	81.66	AUTO #1 E14-01	.000	.000	.000	.000	.000	.000	.000
				.000	.000	.000	.000	.000	.000	.000
109	178.50	68.05	AUTO #2 E14-01	.000	.000	.000	.000	.000	.000	.000
				.000	.000	.000	.000	.000	.000	.000
110	254.72	68.05	AUTO #3 E14-01	.000	.000	.000	.000	.000	.000	.000
				.000	.000	.000	.000	.000	.000	.000
111	328.90	69.41	AUTO #4 E14-01	.000	.000	.000	.000	.000	.000	1.051
				.000	.000	.000	.000	.000	.000	1.739
112	416.00	93.91	AUTO #5 E14-01	.000	.000	.000	.000	.000	.000	.000
				.000	.000	.000	.000	.000	.000	.000
113	507.17	80.30	AUTO #6 E14-01	.000	.000	.000	.000	.000	.000	.068
				.000	.000	.000	.000	.000	.000	.072
114	556.86	68.05	AUTO #7 E14-01	.000	.000	.000	.000	.000	.000	.000
				.000	.000	.000	.000	.000	.000	.000
115	629.00	76.22	AUTO #8 E14-01	.000	.000	.000	3.408	3.675	.000	.000
				.000	.000	.000	3.080	2.581	.000	.000
* * *	STRATA # 1 E14-01 TOTALS * * *									
MEAN =	365.04		WT MEAN RATIO =	.000	.000	.000	3.408	3.675	.000	.524
RMS =	186.18		WT MEAN 1 SIGMA =	.000	.000	.000	3.080	2.581	.000	1.185
MIDPT=	339.11		WT RMS =	.000	.000	.000	.000	.000	.000	.490
RANGE=	656.00		WT ERROR =	.000	.000	.000	3.080	2.581	.000	.807
* * *	BEGIN STRATA # 2 * * *									
117	792.31	81.66	AUTO #10 E14-01	.881	.094	1.311	.927	.207	.000	.310
				.063	.060	.230	.063	.023	.000	.080
118	879.42	81.66	AUTO #11 E14-01	.924	.000	1.127	1.031	.166	.000	.526
				.084	.000	.230	.062	.020	.000	.096
119	946.78	91.19	AUTO #12 E14-01	.760	.169	1.002	.922	.152	.038	.725
				.075	.076	.237	.062	.017	.020	.112
120	1033.89	72.13	AUTO #13 E14-01	.984	.000	1.243	1.027	.173	.000	.655
				.114	.000	.217	.058	.017	.000	.092
121	1113.52	76.22	AUTO #14 E14-01	.851	.171	1.433	.851	.159	.000	.829
				.080	.047	.281	.051	.015	.000	.100
122	1196.53	81.66	AUTO #15 E14-01	1.009	.267	1.136	.838	.197	.000	.850
				.091	.066	.219	.052	.016	.000	.092
123	1283.64	81.66	AUTO #16 E14-01	1.135	.000	1.410	.925	.196	.063	.823
				.106	.000	.217	.052	.019	.024	.098
124	1371.42	83.02	AUTO #17 E14-01	.824	.060	1.018	1.034	.170	.076	1.091
				.081	.042	.189	.052	.014	.026	.111
125	1460.58	84.38	AUTO #18 E14-01	.961	.054	1.294	.936	.195	.000	.895
				.098	.037	.244	.048	.019	.000	.100

SPECTRUM I.D. GA.TAG NO.	CORE LOCATION PARAMETERS AXIAL CORE LOC. CP (MM)	SCAN INTERVAL	FUEL ELEMENT I.D	NUCLIDE CPM RATIOS AND 1 SIGMA ERRORS CE-141 / ZR-95	CE-144 / ZR-95	I-131 / ZR-95	RU-103 / ZR-95	CS-137 / ZR-95	RU-106 / ZR-95	CS-134 / CS-137
126	1547.68	78.94	AUTO #19 E14-01	.950	.093	1.096	.868	.177	.027	1.085
				.073	.042	.185	.048	.016	.022	.117
127	1640.23	95.27	AUTO #20 E14-01	1.094	.176	1.555	.897	.201	.000	.963
				.092	.046	.305	.045	.015	.000	.091
128	1730.06	73.49	AUTO #21 E14-01	.865	.157	1.075	.959	.184	.046	1.063
				.101	.033	.184	.051	.017	.028	.114
129	1811.71	78.94	AUTO #22 E14-01	1.047	.171	1.571	.979	.200	.071	1.109
				.090	.047	.223	.050	.015	.023	.113
130	1896.77	83.02	AUTO #23 E14-01	.980	.161	.879	.791	.167	.000	1.200
				.084	.040	.162	.043	.013	.000	.115
131	1985.25	83.02	AUTO #24 E14-01	.947	.064	1.386	.985	.200	.000	.921
				.099	.056	.207	.048	.016	.000	.091
132	2075.07	85.74	AUTO #25 E14-01	.976	.225	1.102	.783	.161	.042	1.082
				.097	.071	.222	.048	.014	.024	.113
133	2164.90	83.02	AUTO #26 E14-01	.987	.089	1.612	.763	.169	.069	1.014
				.089	.038	.315	.048	.014	.021	.103
134	2252.68	81.66	AUTO #27 E14-01	1.010	.150	1.066	.973	.187	.122	.965
				.111	.051	.215	.050	.017	.025	.109
135	2341.14	84.38	AUTO #28 E14-01	.987	.000	1.215	.917	.171	.213	.840
				.100	.000	.265	.055	.016	.030	.101
136	2430.98	84.38	AUTO #29 E14-01	.916	.126	.916	.977	.169	.176	1.047
				.100	.052	.199	.053	.017	.033	.132
137	2520.81	84.38	AUTO #30 E14-01	.990	.000	.930	.953	.195	.205	.678
				.097	.000	.288	.057	.018	.032	.081
138	2611.99	87.11	AUTO #31 E14-01	1.024	.183	.855	1.019	.170	.202	.751
				.136	.056	.223	.064	.020	.038	.115
139	2701.81	81.66	AUTO #32 E14-01	.993	.118	1.181	1.004	.190	.239	.592
				.132	.043	.225	.061	.022	.037	.092
140	2789.60	83.02	AUTO #33 E14-01	.982	.000	.793	1.013	.157	.240	.670
				.104	.000	.240	.066	.020	.031	.108
141	2873.98	77.58	AUTO #34 E14-01	1.087	.352	1.021	.935	.141	.371	.790
				.141	.122	.297	.070	.018	.048	.136
* * *	STRATA # 2 E14-01 TOTALS * * *									
MEAN =	1818.11		WT MEAN RATIO =	.967	.151	1.169	.932	.178	.137	.859
RMS =	630.49		WT MEAN 1 SIGMA =	.100	.057	.237	.055	.018	.030	.105
MIDPT=	1833.15		WT RMS =	.085	.072	.228	.078	.018	.096	.208
RANGE=	2159.25		WT ERROR =	.020	.013	.048	.011	.004	.007	.021
* * *	BEGIN STRATA # 3 * * *									
143	3048.21	85.74	AUTO #36 E14-01	.000	.000	.000	.000	.000	.000	.000
				.000	.000	.000	.000	.000	.000	.000

SPECTRUM I.D.	CORE LOCATION PARAMETERS		FUEL ELEMENT I.D	NUCLIDE CPM RATIOS AND 1 SIGMA ERRORS						
GA.TAG NO.	AXIAL CORE LOC. CP (MM)	SCAN INTERVAL		CE-141 ZR-95	CE-144 ZR-95	I-131 ZR-95	RU-103 ZR-95	CS-137 ZR-95	RU-106 ZR-95	CS-134 CS-137
144	3134.63	76.22	AUTO #37 E14-01	.000	.000	.000	.000	.000	.000	.000
				.000	.000	.000	.000	.000	.000	.000
* * *	STRATA # 3 E14-01 TOTALS * * *									
MEAN =	3091.42		WT MEAN RATIO =	.000	.000	.000	.000	.000	.000	.000
RMS =	43.21		WT MEAN 1 SIGMA =	.000	.000	.000	.000	.000	.000	.000
MIDPT=	3091.42		WT RMS =	.000	.000	.000	.000	.000	.000	.000
RANGE=	162.64		WT ERROR =	.000	.000	.000	.000	.000	.000	.000
* * *	BEGIN STRATA # 4 * * *									
145	2516.76	1.00	STAT #1 E14-01	.957	.115	1.192	.999	.162	.205	.798
				.054	.020	.119	.023	.007	.012	.046
146	1804.21	1.00	STAT #2 E14-01	1.028	.115	1.089	.954	.197	.044	1.039
				.046	.018	.085	.021	.007	.009	.045
147	1820.67	1.00	STAT #3 E14-01	1.005	.140	1.286	.977	.194	.027	1.081
				.034	.027	.093	.021	.007	.007	.045
148	1837.16	1.00	STAT #4 E14-01	.968	.110	1.313	.983	.212	.026	.948
				.036	.013	.108	.022	.008	.007	.042
149	1853.64	1.00	STAT #5 E14-01	1.047	.154	1.083	.981	.202	.049	.931
				.039	.017	.084	.020	.008	.009	.044
150	1870.10	1.00	STAT #6 E14-01	.947	.122	1.107	.907	.203	.038	.883
				.034	.016	.072	.019	.007	.007	.036
151	996.90	1.00	STAT #7 E14-01	.920	.118	1.261	1.018	.180	.046	.682
				.031	.015	.097	.022	.007	.010	.040
152	239.04	1.00	TRAP E14-01	.000	.000	.000	.000	.000	.000	.000
				.000	.000	.000	.000	.000	.000	.000
* * *	STRATA # 4 E14-01 TOTALS * * *									
MEAN =	1617.31		WT MEAN RATIO =	.982	.125	1.190	.974	.193	.062	.909
RMS =	645.94		WT MEAN 1 SIGMA =	.040	.019	.095	.021	.007	.009	.043
MIDPT=	1377.90		WT RMS =	.043	.015	.091	.033	.016	.059	.127
RANGE=	-2276.72		WT ERROR =	.015	.007	.036	.008	.003	.003	.016

TOTAL STRATA E14-01

MEAN =	1818.11	WT MEAN RATIO =	.967	.151	1.169	.932	.178	.137	.859
RMS =	630.49	WT MEAN 1 SIGMA =	.100	.057	.237	.055	.018	.030	.105
MIDPT=	1833.15	WT RMS =	.085	.072	.228	.078	.018	.096	.208
RANGE=	2159.25	WT ERROR =	.020	.013	.048	.011	.004	.007	.021

SPECTRUM I.D. GA.TAG NO.	CORE LOCATION PARAMETERS AXIAL CORE LOC. CP (MM)	SCAN INTERVAL	FUEL ELEMENT I.D	PA-233 MEAN	CE-141 MEAN	RU-106 MEAN	CS-137 MEAN	CS-134/137 MEAN	ZR-95 MEAN	LA-140 MEAN
				NORMALIZED NUCLIDE CPM RATIOS AND 1 SIGMA ERRORS						
* * *	BEGIN STRATA # 1	* * *								
108	49.21	81.66	AUTO #1 E14-01	.000	.006	.022	.027	.000	.000	.000
				.000	.005	.007	.022	.000	.000	.000
109	178.50	68.05	AUTO #2 E14-01	.001	.000	.000	.026	.000	.000	.000
				.000	.000	.000	.006	.000	.000	.000
110	254.72	68.05	AUTO #3 E14-01	.001	.000	.000	.032	.000	.000	.000
				.000	.000	.000	.007	.000	.000	.000
111	328.90	69.41	AUTO #4 E14-01	.000	.000	.000	.013	1.223	.000	.000
				.000	.000	.000	.022	.954	.000	.000
112	416.00	93.91	AUTO #5 E14-01	.000	.000	.009	.023	.000	.000	.000
				.000	.000	.005	.006	.000	.000	.000
113	507.17	80.30	AUTO #6 E14-01	.000	.000	.013	.023	.079	.000	.000
				.000	.000	.006	.006	.080	.000	.000
114	556.86	68.05	AUTO #7 E14-01	.001	.000	.000	.018	.000	.000	.000
				.001	.000	.000	.005	.000	.000	.000
115	629.00	76.22	AUTO #8 E14-01	.000	.000	.000	.022	.000	.001	.000
				.000	.000	.000	.008	.000	.001	.000
* * *	STRATA # 1 E14-01 TOTALS	* * *								
MEAN =	365.04		WT MEAN RATIO =	.001	.006	.015	.023	.609	.001	.000
RMS =	186.18		WT MEAN 1 SIGMA =	.001	.005	.006	.012	.652	.001	.000
MIDPT=	339.11		WT RMS =	.000	.000	.006	.005	.570	.000	.000
RANGE=	656.00		WT ERROR =	.000	.005	.003	.004	.445	.001	.000
* * *	BEGIN STRATA # 2	* * *								
117	792.31	81.66	AUTO #10 E14-01	.535	.612	.000	.780	.361	.673	.682
				.008	.053	.000	.079	.092	.025	.023
118	879.42	81.66	AUTO #11 E14-01	.647	.672	.000	.653	.612	.705	.783
				.010	.057	.000	.077	.110	.022	.027
119	946.78	91.19	AUTO #12 E14-01	.725	.650	.242	.703	.843	.829	.864
				.011	.061	.128	.077	.128	.024	.025
120	1033.89	72.13	AUTO #13 E14-01	.855	.904	.000	.862	.762	.890	.960
				.012	.098	.000	.078	.106	.029	.029
121	1113.52	76.22	AUTO #14 E14-01	.960	.909	.000	.916	.965	1.034	.951
				.012	.079	.000	.082	.114	.032	.027
122	1196.53	81.66	AUTO #15 E14-01	1.013	1.055	.000	1.115	.989	1.012	1.025
				.013	.089	.000	.083	.105	.027	.028
123	1283.64	81.66	AUTO #16 E14-01	1.073	1.184	.496	1.109	.958	1.010	1.018
				.012	.103	.182	.102	.112	.028	.028
124	1371.42	83.02	AUTO #17 E14-01	1.144	.921	.640	1.028	1.270	1.084	1.103
				.013	.085	.209	.081	.126	.029	.028
125	1460.58	84.38	AUTO #18 E14-01	1.199	1.163	.000	1.279	1.041	1.172	1.105
				.012	.110	.000	.115	.114	.036	.029

SPECTRUM I.D. | CORE LOCATION PARAMETERS | FUEL ELEMENT I.D | NORMALIZED NUCLIDE CPM RATIOS AND 1 SIGMA ERRORS

GA.TAG NO.	AXIAL CORE LOC. CP (MM)	SCAN INTERVAL	FUEL ELEMENT I.D	PA-233 MEAN	CE-141 MEAN	RU-106 MEAN	CS-137 MEAN	CS-134/137 MEAN	ZR-95 MEAN	LA-140 MEAN
126	1547.68	78.94	AUTO #19 E14-01	1.189	1.125	.241	1.132	1.263	1.147	1.108
				.013	.081	.189	.099	.133	.029	.029
127	1640.23	95.27	AUTO #20 E14-01	1.212	1.291	.000	1.283	1.120	1.143	1.166
				.013	.100	.000	.090	.105	.030	.032
128	1730.06	73.49	AUTO #21 E14-01	1.247	.979	.387	1.126	1.237	1.097	1.126
				.013	.109	.233	.099	.130	.030	.028
129	1811.71	78.94	AUTO #22 E14-01	1.196	1.215	.618	1.258	1.290	1.124	1.167
				.012	.097	.191	.089	.129	.028	.029
130	1896.77	83.02	AUTO #23 E14-01	1.217	1.191	.000	1.101	1.397	1.178	1.127
				.013	.094	.000	.082	.131	.033	.031
131	1985.25	83.02	AUTO #24 E14-01	1.180	1.083	.000	1.240	1.072	1.108	1.136
				.014	.106	.000	.093	.105	.029	.029
132	2075.07	85.74	AUTO #25 E14-01	1.190	1.139	.368	1.014	1.259	1.130	1.065
				.014	.106	.202	.085	.129	.030	.027
133	2164.90	83.02	AUTO #26 E14-01	1.180	1.150	.602	1.064	1.180	1.128	1.134
				.014	.096	.182	.085	.118	.031	.029
134	2252.68	81.66	AUTO #27 E14-01	1.147	1.180	1.072	1.183	1.123	1.132	1.133
				.014	.121	.207	.100	.124	.033	.029
135	2341.14	84.38	AUTO #28 E14-01	1.072	1.043	1.682	.977	.978	1.023	1.039
				.013	.099	.229	.087	.116	.028	.028
136	2430.96	84.38	AUTO #29 E14-01	1.005	.977	1.409	.977	1.219	1.034	1.006
				.012	.100	.249	.092	.149	.033	.029
137	2520.81	84.38	AUTO #30 E14-01	.953	1.002	1.554	1.068	.789	.980	.923
				.013	.091	.231	.092	.093	.030	.026
138	2611.99	87.11	AUTO #31 E14-01	.874	.942	1.392	.849	.874	.892	.900
				.013	.118	.246	.094	.131	.029	.026
139	2701.81	81.66	AUTO #32 E14-01	.810	.921	1.663	.953	.689	.899	.907
				.012	.116	.239	.105	.106	.030	.026
140	2789.60	83.02	AUTO #33 E14-01	.744	.831	1.524	.718	.780	.820	.799
				.013	.092	.190	.087	.123	.028	.024
141	2873.98	77.58	AUTO #34 E14-01	.612	.624	2.110	.580	.919	.735	.757
				.011	.101	.255	.070	.154	.025	.026
* * *	STRATA # 2 E14-01 TOTALS * * *									
MEAN =	1818.11		WT MEAN RATIO =	1.000	1.000	1.000	1.000	1.000	1.000	1.000
RMS =	630.49		WT MEAN 1 SIGMA =	.013	.096	.212	.089	.120	.029	.028
MIDPT=	1833.15		WT RMS =	.212	.181	.592	.197	.242	.150	.138
RANGE=	2159.25		WT ERROR =	.003	.019	.053	.018	.024	.006	.006
* * *	BEGIN STRATA # 3 * * *									
143	3048.21	85.74	AUTO #36 E14-01	.000	.000	1.661	.000	.000	.000	.000
				.000	.000	.050	.000	.000	.000	.000

SPECTRUM I.D. | CORE LOCATION PARAMETERS | FUEL ELEMENT I.D | NORMALIZED NUCLIDE CPM RATIOS AND 1 SIGMA ERRORS

GA.TAG NO.	AXIAL CORE LOC. CP (MM)	SCAN INTERVAL		PA-233 MEAN	CE-141 MEAN	RU-106 MEAN	CS-137 MEAN	CS-134/137 MEAN	ZR-95 MEAN	LA-140 MEAN
144	3134.63	76.22	AUTO #37 E14-01	.000	.000	1.547	.000	.000	.000	.000
				.000	.000	.031	.000	.000	.000	.000
* * *	STRATA # 3 E14-01 TOTALS		* * *							
MEAN =	3091.42		WT MEAN RATIO =	.000	.000	1.618	.000	.000	.000	.000
RMS =	43.21		WT MEAN 1 SIGMA =	.000	.000	.042	.000	.000	.000	.000
MIDPT=	3091.42		WT RMS =	.000	.000	.067	.000	.000	.000	.000
RANGE=	162.64		WT ERROR =	.000	.000	.030	.000	.000	.000	.000
* * *	BEGIN STRATA # 4		* * *							
145	2516.76	1.00	STAT #1 E14-01	.923	.946	1.518	.865	.928	.957	.967
				.005	.048	.107	.036	.051	.012	.011
146	1804.21	1.00	STAT #2 E14-01	1.170	1.139	.364	1.181	1.209	1.073	1.042
				.005	.046	.071	.040	.052	.012	.011
147	1820.67	1.00	STAT #3 E14-01	1.185	1.126	.226	1.179	1.258	1.086	1.115
				.005	.037	.057	.039	.052	.012	.012
148	1837.16	1.00	STAT #4 E14-01	1.189	1.067	.211	1.266	1.103	1.068	1.093
				.006	.037	.058	.044	.048	.012	.012
149	1853.64	1.00	STAT #5 E14-01	1.174	1.186	.414	1.239	1.083	1.098	1.059
				.005	.041	.074	.044	.050	.012	.012
150	1870.10	1.00	STAT #6 E14-01	1.344	1.246	.379	1.446	1.028	1.275	1.194
				.006	.042	.070	.045	.043	.014	.012
151	996.90	1.00	STAT #7 E14-01	.927	.925	.345	.977	.793	.973	.991
				.005	.031	.075	.038	.045	.011	.011
152	239.04	1.00	TRAP E14-01	.000	.000	.000	.036	.000	.000	.000
				.000	.000	.000	.005	.000	.000	.000
* * *	STRATA # 4 E14-01 TOTALS		* * *							
MEAN =	1617.31		WT MEAN RATIO =	1.130	1.091	.494	1.023	1.057	1.076	1.066
RMS =	645.94		WT MEAN 1 SIGMA =	.005	.041	.075	.038	.049	.012	.011
MIDPT=	1377.90		WT RMS =	.141	.111	.424	.408	.148	.096	.071
RANGE=	-2276.72		WT ERROR =	.002	.015	.028	.014	.018	.005	.004

T O T A L S T R A T A E 1 4 - 0 1

MEAN =	1818.11	WT MEAN RATIO =	1.000	1.000	1.000	1.000	1.000	1.000	1.000
RMS =	630.49	WT MEAN 1 SIGMA =	.013	.096	.212	.089	.120	.029	.028
MIDPT=	1833.15	WT RMS =	.212	.181	.592	.197	.242	.150	.138
RANGE=	2159.25	WT ERROR =	.003	.019	.053	.018	.024	.006	.006

ABSOLUTE NUCLIDE ACTIVITIES AND COMPOSITE BURNUP

FUEL IDENTIFICATION — NUCLIDE C(I) +/- 1 SIGMA ERROR — COMPOSITE FIMA

GA. TAG NO.	AXIAL CORE LOC.	SCAN INTERVAL	CE-144 133KEV	CE-141 145KEV	PA-233 312KEV	I-131 364KEV	RU-103 497KEV	RU-106 512KEV	CS-137 661KEV	ZR- 95 724KEV	CS-134 796KEV	LA-140 1596KEV	CS-137 MONITOR	RU-106 MONITO
* * * BEGIN STRATA # 1 * * *														
108	49.21	81.66	.0	.6	.0	.0	.1	.8	.4	.0	.0	.0	.000	.000
AUTO #1 E14-01			.0	.5	.0	.0	.0	.3	.3	.0	.0	.0	.000	.000
109	178.50	68.05	.0	.0	.5	.0	.1	.0	.4	.0	.0	.0	.000	.000
AUTO #2 E14-01			.0	.0	.3	.0	.1	.0	.1	.0	.0	.0	.000	.000
110	254.72	68.05	.0	.0	1.0	.0	.1	.0	.5	.0	.0	.0	.000	.000
AUTO #3 E14-01			.0	.0	.3	.0	.0	.0	.1	.0	.0	.0	.000	.000
111	328.90	69.41	.0	.0	.0	.0	.2	.0	.2	.0	.2	.0	.000	.000
AUTO #4 E14-01			.0	.0	.0	.0	.1	.0	.3	.0	.1	.0	.000	.000
112	416.00	93.91	.0	.0	.0	1.4	.0	.3	.3	.0	.0	.0	.000	.000
AUTO #5 E14-01			.0	.0	.0	.4	.0	.2	.1	.0	.0	.0	.000	.000
113	507.17	80.30	.0	.0	.0	.0	.1	.5	.3	.0	.0	.0	.000	.000
AUTO #6 E14-01			.0	.0	.0	.0	.1	.2	.1	.0	.0	.0	.000	.000
114	556.86	68.05	.0	.0	1.0	4.5	.0	.0	.3	.0	.0	.0	.000	.000
AUTO #7 E14-01			.0	.0	.7	1.7	.0	.0	.1	.0	.0	.0	.000	.000
115	629.00	76.22	.0	.0	.0	.0	.2	.0	.3	.2	.0	.0	.000	.000
AUTO #8 E14-01			.0	.0	.0	.0	.2	.0	.1	.1	.0	.0	.000	.000
* * * STRATA # 1 E14-01 TOTALS * * *														
	WT MEAN =		.0	.6	.8	2.7	.1	.5	.3	.2	.1	.0	.000	.000
	WT 1 SIGMA=		.0	.5	.4	1.2	.1	.2	.2	.1	.1	.0	.000	.000
	WT RMS =		.0	.0	.2	1.6	.1	.2	.1	.0	.1	.0	.000	.000
	WT ERROR =		.0	.5	.2	.8	.0	.1	.1	.1	.0	.0	.000	.000
* * * BEGIN STRATA # 2 * * *														
117	792.31	81.66	49.6	54.3	437.3	46.5	37.8	.0	10.9	108.9	3.8	146.8	6.505	.000
AUTO #10 E14-01			32.2	7.3	45.4	9.3	4.4	.0	1.6	11.9	1.0	15.9	2.121	.000
118	879.42	81.66	.0	59.6	528.5	41.9	44.1	.0	9.1	113.9	5.4	168.6	5.449	.000
AUTO #11 E14-01			.0	8.0	54.9	9.5	5.1	.0	1.4	12.2	.9	18.2	1.903	.000
119	946.78	91.19	109.8	57.7	592.8	43.8	46.4	8.2	9.8	134.1	8.0	186.1	5.865	5.881
AUTO #12 E14-01			50.5	8.0	61.5	11.2	5.5	4.5	1.5	14.3	1.2	19.9	1.978	1.677
120	1033.89	72.13	.0	80.2	699.0	58.4	55.5	.0	12.1	144.0	8.9	205.8	7.193	.000
AUTO #13 E14-01			.0	12.1	72.4	11.6	6.2	.0	1.7	15.5	1.3	22.2	2.235	.000
121	1113.52	76.22	138.5	80.6	764.1	78.1	53.3	.0	12.8	167.2	11.9	204.9	7.645	.000
AUTO #14 E14-01			40.4	10.9	81.0	17.1	6.1	.0	1.8	17.9	1.5	21.9	2.357	.000
122	1196.53	81.66	211.5	93.5	627.8	60.7	51.4	.0	15.6	163.7	14.9	227.8	9.301	.000
AUTO #15 E14-01			56.1	12.5	85.6	13.1	6.0	.0	2.0	17.4	1.9	23.5	2.644	.000
123	1263.64	81.66	.0	105.0	877.0	75.1	56.7	16.8	15.5	163.4	14.3	219.2	9.253	12.073
AUTO #16 E14-01			.0	14.2	90.5	13.7	6.4	6.5	2.2	17.4	1.8	23.3	2.901	3.236
124	1371.42	83.02	50.6	61.7	934.4	58.1	68.0	21.7	14.4	175.2	17.6	237.7	8.579	15.568
AUTO #17 E14-01			35.8	11.4	96.4	12.2	7.5	7.6	1.9	18.6	2.1	25.1	2.495	3.959
125	1460.58	84.38	99.9	103.1	979.4	80.0	66.5	.0	17.9	189.6	18.0	238.1	10.673	.000
AUTO #18 E14-01			34.1	14.6	101.0	17.0	7.4	.0	2.5	20.3	2.2	25.2	3.323	.000

ABSOLUTE NUCLIDE ACTIVITIES AND COMPOSITE BURNUP

FUEL IDENTIFICATION — NUCLIDE C(I) +/- 1 SIGMA ERROR — COMPOSITE FIMA

GA. TAG NO.	AXIAL CORE LOC.	SCAN INTERVAL	CE-144 133KEV	CE-141 145KEV	PA-233 312KEV	I-131 364KEV	RU-103 497KEV	RU-106 512KEV	CS-137 661KEV	ZR- 95 724KEV	CS-134 796KEV	LA-140 1596KEV	CS-137 MONITOR	RU-106 MONITOR
126	1547.68	76.94	83.1	99.7	971.7	66.3	60.3	8.1	15.8	185.4	19.3	238.7	9.444	5.854
AUTO #19 E14-01			38.7	12.5	100.3	13.0	6.8	6.5	2.2	19.6	2.3	25.3	2.891	2.270
127	1640.23	95.27	157.1	110.5	990.6	93.7	62.2	.0	17.9	184.9	19.4	251.2	10.705	.000
AUTO #20 E14-01			44.1	14.8	102.1	20.6	6.9	.0	2.2	19.6	2.3	26.7	2.968	.000
128	1730.06	73.49	134.9	66.8	1019.1	62.1	63.7	13.1	15.7	177.3	18.8	243.1	9.397	9.410
AUTO #21 E14-01			31.7	13.3	105.1	12.3	7.1	8.2	2.2	18.8	2.2	25.7	2.892	3.212
129	1811.71	78.94	150.6	107.7	977.1	93.1	66.7	20.9	17.6	181.8	21.9	251.3	10.494	15.027
AUTO #22 E14-01			44.3	14.1	100.7	16.1	7.4	7.0	2.2	19.2	2.7	26.6	2.917	3.710
130	1896.77	83.02	148.0	105.7	994.2	54.6	56.5	.0	15.4	190.5	20.7	242.7	9.186	.000
AUTO #23 E14-01			39.9	13.8	102.5	11.4	6.4	.0	2.0	20.3	2.5	25.8	2.608	.000
131	1985.25	83.02	55.1	96.1	963.9	81.0	66.2	.0	17.3	179.2	17.9	244.8	10.346	.000
AUTO #24 E14-01			48.7	13.8	99.5	14.5	7.3	.0	2.2	19.0	2.2	25.9	2.966	.000
132	2075.07	85.74	199.0	101.0	972.3	65.6	53.6	12.5	14.2	182.7	17.2	229.5	8.464	8.950
AUTO #25 E14-01			65.9	14.2	100.4	14.7	6.2	7.1	1.9	19.4	2.1	24.3	2.542	2.920
133	2164.90	83.02	78.4	102.0	964.5	95.9	52.2	20.4	14.9	182.5	16.9	244.2	8.877	14.656
AUTO #26 E14-01			34.6	13.6	99.6	21.0	6.1	6.7	1.9	19.4	2.0	25.9	2.606	3.580
134	2252.68	81.66	133.2	104.6	937.0	63.6	66.7	36.3	16.5	183.1	17.9	244.1	9.873	26.094
AUTO #27 E14-01			47.3	15.4	96.6	14.3	7.4	8.1	2.2	19.6	2.2	25.8	2.986	5.163
135	2341.14	84.38	.0	92.5	876.2	65.5	56.9	57.0	13.7	165.4	12.9	223.9	8.157	40.932
AUTO #28 E14-01			.0	13.1	90.6	15.7	6.6	9.9	1.9	17.6	1.7	23.8	2.510	6.871
136	2430.98	84.38	101.8	66.6	821.1	49.9	61.2	47.7	13.7	167.2	16.1	216.7	8.155	34.280
AUTO #29 E14-01			43.4	12.7	84.8	11.9	6.8	10.1	1.9	18.0	2.1	23.1	2.580	6.546
137	2520.81	84.38	.0	68.9	778.6	48.1	56.7	52.6	14.9	158.5	11.4	198.7	8.914	37.809
AUTO #30 E14-01			.0	12.3	80.6	15.6	6.5	9.7	2.0	17.0	1.5	21.2	2.715	6.619
138	2611.99	87.11	127.4	83.6	714.3	40.2	55.1	47.2	11.9	144.2	10.0	193.8	7.081	33.881
AUTO #31 E14-01			40.9	13.7	74.1	11.2	6.4	10.0	1.8	15.5	1.5	20.7	2.409	6.475
139	2701.81	81.66	82.9	61.7	662.0	56.0	54.7	56.3	13.3	145.3	8.9	195.4	7.955	40.452
AUTO #32 E14-01			31.2	13.5	68.7	12.0	6.2	10.2	2.0	15.7	1.3	20.8	2.708	6.994
140	2789.60	83.02	.0	73.7	607.8	34.3	50.4	51.6	10.0	132.6	7.6	172.1	5.993	37.086
AUTO #33 E14-01			.0	10.6	63.3	10.9	5.9	8.3	1.6	14.3	1.1	18.4	2.125	5.885
141	2873.98	77.58	202.2	73.1	499.9	39.6	41.6	71.5	8.1	118.8	7.2	163.1	4.837	51.336
AUTO #34 E14-01			72.5	11.8	52.1	12.1	5.1	11.6	1.3	12.9	1.1	17.7	1.711	8.191
* * * STRATA # 2 E14-01 TOTALS * * *														
WT MEAN =			119.0	88.7	817.1	62.1	56.2	33.9	14.0	161.7	13.9	215.4	8.345	24.332
WT 1 SIGMA=			45.2	12.7	86.3	14.1	6.4	8.4	1.9	17.5	1.9	23.1	2.594	5.202
WT RMS =			50.7	16.1	173.4	17.5	7.9	20.1	2.7	24.2	5.1	29.8	1.640	14.415
WT ERROR =			10.4	2.5	17.3	2.8	1.3	2.1	.4	3.5	.4	4.6	.520	1.301
* * * BEGIN STRATA # 3 * * *														
143	3048.21	85.74	.0	.0	.0	.0	.0	56.9	.0	.0	.0	.0	.000	.000
AUTO #36 E14-01			.0	.0	.0	.0	.0	7.2	.0	.0	.0	.0	.000	.000

ABSOLUTE NUCLIDE ACTIVITIES AND COMPOSITE BURNUP

FUEL IDENTIFICATION GA. TAG NO.	AXIAL CORE LOC.	SCAN INTERVAL	CE-144 133KEV	CE-141 145KEV	PA-233 312KEV	I-131 364KEV	RU-103 497KEV	RU-106 512KEV	CS-137 661KEV	ZR-95 724KEV	CS-134 796KEV	LA-140 1596KEV	COMPOSITE FIMA CS-137 MONITOR	COMPOSITE FIMA RU-106 MONITOR
144	3134.63	76.22	.0	.0	.0	.0	.0	52.4	.0	.0	.0	.0	.000	.000
AUTO #37 E14-01			.0	.0	.0	.0	.0	6.5	.0	.0	.0	.0	.000	.000
* * * STRATA # 3 E14-01 TOTALS * * *														
	WT MEAN =		.0	.0	.0	.0	.0	54.8	.0	.0	.0	.0	.000	.000
	WT 1 SIGMA=		.0	.0	.0	.0	.0	6.9	.0	.0	.0	.0	.000	.000
	WT RMS =		.0	.0	.0	.0	.0	2.3	.0	.0	.0	.0	.000	.000
	WT ERROR =		.0	.0	.0	.0	.0	4.9	.0	.0	.0	.0	.000	.003
* * * BEGIN STRATA # 4 * * *														
145	2516.76	1.00	86.0	87.9	753.8	60.2	58.0	51.4	12.1	154.8	10.8	209.3	7.217	36.944
STAT #1 E14-01			17.6	9.6	77.5	8.6	6.1	6.1	1.3	16.0	1.2	21.5	1.601	4.213
146	1804.21	1.00	96.5	101.0	956.4	61.6	62.0	12.3	16.5	173.5	19.3	224.5	9.854	8.849
STAT #2 E14-01			17.9	11.2	98.2	7.9	6.5	2.8	1.8	17.9	2.0	23.2	2.013	1.749
147	1820.67	1.00	118.8	99.9	968.3	73.6	64.3	7.6	16.5	175.6	20.0	240.3	9.836	5.494
STAT #3 E14-01			26.2	10.7	99.4	9.2	6.7	2.1	1.6	18.1	2.1	24.8	2.001	1.225
148	1837.16	1.00	92.1	94.6	971.3	73.9	63.7	7.1	17.7	172.7	16.8	235.5	10.566	5.129
STAT #4 E14-01			14.1	10.3	99.7	9.7	6.6	2.1	1.9	17.8	2.0	24.3	2.196	1.187
149	1853.64	1.00	132.4	105.2	959.4	62.7	65.3	14.0	17.3	177.5	18.1	228.2	10.336	10.084
STAT #5 E14-01			19.6	11.4	98.5	8.0	6.8	2.9	1.9	18.3	1.9	23.5	2.190	1.904
150	1870.10	1.00	121.6	110.5	1098.0	74.4	70.1	12.8	20.2	206.3	20.0	257.1	12.062	9.212
STAT #6 E14-01			19.9	12.0	112.7	9.0	7.3	2.8	2.2	21.3	2.1	26.5	2.409	1.775
151	996.90	1.00	89.9	82.0	757.7	64.7	60.1	11.7	13.7	157.4	10.4	213.5	8.150	8.405
STAT #7 E14-01			14.9	8.8	77.8	8.3	6.3	2.8	1.5	16.2	1.2	22.0	1.769	1.749
152	239.04	1.00	.0	.0	.0	.0	.0	.0	.5	.0	.0	.0	.300	.000
TRAP E14-01			.0	.0	.0	.0	.0	.0	.1	.0	.0	.0	.108	.000
* * * STRATA # 4 E14-01 TOTALS * * *														
	WT MEAN =		105.3	96.7	923.6	67.3	63.3	16.7	14.3	173.9	16.8	229.6	8.541	12.017
	WT 1 SIGMA=		19.0	10.6	95.6	8.7	6.6	3.3	1.7	18.0	1.8	23.7	1.910	2.189
	WT RMS =		17.1	9.8	115.5	5.9	3.6	14.4	5.7	15.6	3.9	15.3	3.409	10.324
	WT ERROR =		7.2	4.0	36.1	3.3	2.5	1.3	.6	6.8	.7	9.0	.675	.827

T O T A L   S T R A T A   E 1 4 - 0 1

		CE-144	CE-141	PA-233	I-131	RU-103	RU-106	CS-137	ZR-95	CS-134	LA-140	CS-137 MONITOR	RU-106 MONITOR
WT MEAN =		119.0	88.7	817.1	62.1	56.2	33.9	14.0	161.7	13.9	215.4	8.345	24.332
WT 1 SIGMA=		45.2	12.7	86.3	14.1	6.4	8.4	1.9	17.5	1.9	23.1	2.594	5.202
WT RMS =		50.7	16.1	173.4	17.5	7.9	20.1	2.7	24.2	5.1	29.8	1.640	14.415
WT ERROR =		10.4	2.5	17.3	2.8	1.3	2.1	.4	3.5	.4	4.6	.520	1.301

INTERPOLATED AXIAL CORE LOC. CP (MM)	INTERPOLATED NUCLIDE CPM AND 1 SIGMA ERRORS									
	CE-144 133 KEV	CE-141 145 KEV	PA-233 312 KEV	I-131 364 KEV	RU-103 497 KEV	RU-106 512 KEV	CS-137 661 KEV	ZR-95 724 KEV	CS-134 796 KEV	LA-140 1596 KEV
698.50	575.9	2324.1	14561.1	4282.7	2248.6	.0	717.3	2798.8	103.5	4177.0
	88.9	233.5	328.1	681.9	159.1	.0	62.0	102.6	41.0	183.2
774.70	333.4	2545.5	17987.7	3943.0	2641.5	.0	630.6	2919.3	173.1	4821.2
	88.9	233.5	328.1	681.9	159.1	.0	62.0	102.6	41.0	183.2
850.90	90.8	2766.8	21414.3	3603.4	3034.5	.0	543.9	3039.8	242.8	5465.3
	88.9	233.5	328.1	681.9	159.1	.0	62.0	102.6	41.0	183.2
927.10	434.7	2785.2	24651.5	3590.2	3298.9	96.8	539.1	3470.9	360.9	6127.4
	137.7	252.0	384.4	778.7	183.1	36.7	61.1	100.8	40.2	191.7
1003.30	215.7	3457.4	28418.0	4421.3	3774.0	48.0	631.4	3803.9	426.9	6754.5
	137.7	343.1	414.3	842.2	192.2	36.7	61.6	117.5	45.1	203.2
1079.50	444.0	3846.0	32113.9	5786.6	3917.1	.0	699.4	4257.9	529.7	6963.0
	105.8	393.1	425.9	1042.8	189.5	.0	63.7	135.7	47.0	211.8
1155.70	982.8	4168.4	34629.2	5750.8	3782.3	.0	796.5	4478.4	669.8	7208.9
	250.6	363.0	449.0	1108.9	201.5	.0	65.5	131.6	52.3	205.3
1231.90	703.1	4696.1	36409.9	5523.6	3867.8	114.0	871.2	4428.6	731.0	7452.3
	144.8	415.5	438.9	953.2	203.4	52.6	73.9	122.8	54.4	209.3
1308.10	79.0	4711.6	38351.5	5843.6	4318.6	303.4	850.9	4513.0	760.6	7595.5
	99.2	407.0	435.1	916.6	203.3	113.5	72.9	128.2	53.4	209.7
1384.30	282.8	4055.7	40408.8	5089.8	4892.4	309.7	833.7	4800.1	881.4	8048.7
	193.6	423.7	452.9	1060.5	201.7	60.9	78.5	145.7	55.4	210.6
1460.50	279.2	4932.1	42062.5	6640.6	4803.9	.3	1001.6	5131.4	896.6	8061.3
	193.6	423.7	452.9	1060.5	201.7	60.9	78.5	145.7	55.4	210.6
1536.70	441.6	4790.5	41772.7	5646.9	4412.5	119.0	900.9	5034.5	953.9	8079.2
	200.1	412.1	457.9	1074.9	204.0	54.2	86.1	145.9	56.9	213.3
1612.90	756.8	5267.1	42302.7	7109.4	4450.3	40.2	969.8	5010.1	965.9	8378.1
	220.5	389.1	458.9	1214.6	200.2	54.2	75.4	133.5	59.3	224.9
1689.10	811.4	4756.1	43208.9	6355.7	4551.3	119.0	938.0	4894.4	951.2	8353.6
	194.4	452.7	465.6	1191.6	198.8	67.3	75.7	134.7	57.4	223.0
1765.30	792.7	4584.5	42988.5	6268.6	4695.5	275.2	926.5	4852.9	1004.2	8348.6
	195.8	446.2	462.1	974.1	210.0	122.6	75.2	130.2	67.0	213.0
1841.50	837.7	5117.7	42220.1	6610.0	4559.0	227.0	942.0	5003.9	1072.2	8404.2
	219.3	413.6	451.8	950.9	201.4	55.3	67.8	136.6	70.6	222.5
1917.70	705.4	4944.6	42391.0	5050.9	4244.4	.0	888.0	5085.0	1001.8	8231.6
	238.4	435.0	474.5	906.4	192.8	.0	69.8	137.7	59.0	223.3
1993.90	386.1	4617.7	41433.4	6601.2	4690.3	20.0	954.1	4860.0	891.1	8236.6
	310.6	463.1	495.9	1037.9	203.3	58.4	71.4	131.3	54.1	211.1
2070.10	1069.2	4816.1	41736.6	5520.8	3922.9	196.6	804.2	4941.9	861.7	7797.7
	310.6	463.1	495.9	1037.9	203.3	58.4	71.4	131.3	54.1	211.1
2146.30	578.6	4866.8	41492.9	7441.7	3790.7	313.3	825.2	4941.9	848.1	8162.9
	269.6	439.2	500.1	1314.7	210.3	111.1	67.8	136.3	51.9	210.9

INTERPOLATED AXIAL CORE LOC. CP (MM)		CE-144 133 KEV	CE-141 145 KEV	PA-233 312 KEV	I-131 364 KEV	RU-103 497 KEV	RU-106 512 KEV	CS-137 661 KEV	ZR-95 724 KEV	CS-134 796 KEV	LA-140 1596 KEV
		INTERPOLATED NUCLIDE CPM AND 1 SIGMA ERRORS									
2222.50		640.1	4960.1	40647.8	6204.2	4458.8	515.3	894.5	4950.5	877.4	8264.8
		221.0	472.7	495.8	1298.1	204.7	113.2	74.1	143.5	58.1	215.3
2298.70		357.7	4701.3	38883.6	5364.8	4449.4	786.2	842.9	4707.6	763.8	7907.8
		126.8	480.5	489.2	1115.5	208.7	127.3	74.9	136.6	57.8	210.3
2374.90		214.1	4317.5	36741.9	4952.7	4224.5	893.6	765.6	4496.1	702.9	7487.4
		117.7	431.4	458.1	1034.6	205.0	140.5	71.4	136.6	58.2	211.4
2451.10		442.3	4167.3	34854.9	4108.9	4345.7	815.4	781.4	4473.1	749.3	7199.1
		117.7	412.7	451.6	1061.7	200.5	141.3	73.8	140.7	55.5	205.0
2527.30		50.7	4232.9	33241.9	3944.7	4082.9	872.6	824.4	4264.6	562.4	6715.7
		108.6	453.0	471.9	1047.5	210.3	140.5	74.5	131.3	48.7	192.1
2603.50		646.3	4020.4	30933.1	3400.5	3987.4	796.3	680.7	3940.4	505.6	6576.9
		108.6	453.0	471.9	1047.5	210.3	140.5	74.5	131.3	48.7	192.1
2679.70		525.3	3930.0	28985.2	4325.0	3956.2	902.9	726.5	3927.3	456.1	6600.8
		192.6	507.9	456.3	868.6	205.2	143.4	79.7	131.1	49.6	190.5
2755.90		178.2	3671.5	26997.9	3536.6	3756.9	892.3	633.2	3721.6	401.9	6128.5
		84.0	428.6	452.7	864.8	198.9	124.0	77.0	128.4	43.3	185.8
2832.10		569.9	3509.9	23770.3	3066.1	3319.7	1029.2	507.9	3400.9	367.7	5672.2
		194.4	396.2	435.5	902.2	200.1	128.7	62.6	117.8	41.0	185.9
2908.30		1591.7	3484.6	19586.6	3462.7	2750.9	1328.4	409.9	3064.3	351.0	5396.0
		194.4	396.2	435.5	902.2	200.1	128.7	62.6	117.8	41.0	185.9
ELEMENT TITLE: E14-01	MEAN CPM =	533.9	4168.2	34173.3	5114.9	3974.3	458.9	777.7	4307.1	668.8	7153.9
	MEAN 1 SIGMA =	183.7	408.4	446.3	1001.4	197.9	102.2	71.2	129.6	52.5	204.7
	RMS =	326.7	787.0	8410.5	1222.5	651.1	388.9	149.1	713.4	270.1	1154.0
	ERROR =	33.5	74.6	81.5	182.8	36.1	20.9	13.0	23.7	9.6	37.4

INTERPOLATED AXIAL CORE LOC. CP (MM.)	INTERPOLATED NUCLIDED CPM RATIOS AND 1 SIGMA ERRORS						
	CE-141 ZR-95	CE-144 ZR-95	I-131 ZR-95	RU-103 ZR-95	CS-137 ZR-95	RU-106 ZR-95	CS-134 CS-137
698.50	.830	.206	1.530	.803	.256	.000	.144
	.089	.033	.250	.064	.024	.000	.058
774.70	.872	.114	1.351	.905	.216	.000	.275
	.086	.031	.238	.063	.023	.000	.070
850.90	.910	.030	1.185	.998	.179	.000	.446
	.083	.029	.228	.062	.021	.000	.091
927.10	.802	.125	1.034	.950	.155	.078	.670
	.076	.040	.226	.060	.018	.011	.106
1003.30	.909	.057	1.162	.992	.166	.013	.676
	.094	.036	.224	.059	.017	.010	.097
1079.50	.903	.104	1.359	.920	.164	.000	.757
	.094	.025	.249	.053	.016	.000	.096
1155.70	.931	.219	1.284	.845	.178	.000	.841
	.086	.056	.250	.051	.016	.000	.095
1231.90	1.060	.159	1.247	.873	.197	.026	.939
	.098	.033	.218	.052	.018	.012	.095
1308.10	1.044	.017	1.295	.957	.189	.067	.894
	.095	.022	.206	.053	.017	.025	.099
1384.30	.845	.059	1.060	1.019	.174	.065	1.057
	.092	.040	.223	.052	.017	.013	.120
1460.50	.961	.054	1.294	.936	.195	.000	.895
	.087	.038	.210	.047	.016	.012	.089
1536.70	.952	.088	1.122	.876	.179	.024	1.059
	.086	.040	.216	.048	.018	.011	.119
1612.90	1.051	.151	1.419	.888	.194	.008	.996
	.083	.044	.245	.046	.016	.011	.099
1689.10	.972	.166	1.299	.930	.192	.024	1.014
	.096	.040	.246	.048	.016	.014	.102
1765.30	.945	.163	1.292	.968	.191	.057	1.084
	.095	.041	.204	.050	.016	.025	.114
1841.50	1.023	.167	1.321	.911	.188	.045	1.138
	.087	.044	.193	.047	.014	.011	.111
1917.70	.972	.139	.993	.835	.175	.000	1.128
	.090	.047	.180	.044	.015	.000	.111
1993.90	.950	.079	1.358	.965	.196	.004	.934
	.099	.064	.217	.049	.016	.012	.090
2070.10	.975	.216	1.117	.794	.163	.040	1.071
	.097	.063	.212	.046	.015	.012	.116
2146.30	.985	.117	1.506	.767	.167	.063	1.028
	.093	.055	.269	.048	.014	.023	.105

INTERPOLATED NUCLIDED CPM RATIOS AND 1 SIGMA ERRORS

INTERPOLATED AXIAL CORE LOC. CP (MM)		CE-141 / ZR-95	CE-144 / ZR-95	I-131 / ZR-95	RU-103 / ZR-95	CS-137 / ZR-95	RU-106 / ZR-95	CS-134 / CS-137
2222.50		1.002	.129	1.253	.901	.181	.104	.981
		.100	.045	.265	.049	.016	.023	.104
2298.70		.999	.076	1.140	.945	.179	.167	.906
		.106	.027	.239	.052	.017	.027	.106
2374.90		.960	.048	1.102	.940	.170	.199	.918
		.100	.026	.233	.054	.017	.032	.115
2451.10		.932	.099	.919	.972	.175	.182	.959
		.097	.027	.239	.054	.017	.032	.115
2527.30		.993	.012	.925	.957	.193	.205	.682
		.111	.025	.247	.057	.018	.034	.065
2603.50		1.020	.164	.863	1.012	.173	.202	.743
		.120	.028	.267	.063	.020	.036	.108
2679.70		1.001	.134	1.101	1.007	.185	.230	.628
		.134	.049	.224	.062	.021	.037	.097
2755.90		.987	.048	.950	1.009	.170	.240	.635
		.120	.023	.235	.064	.021	.034	.103
2832.10		1.032	.168	.902	.976	.149	.303	.724
		.122	.057	.267	.068	.019	.039	.120
2908.30		1.137	.519	1.130	.898	.134	.434	.856
		.136	.067	.298	.074	.021	.045	.165
ELEMENT TITLE: E14-01	MEAN RATIO =	.965	.128	1.184	.925	.181	.114	.833
	MEAN 1 SIGMA =	.099	.042	.235	.055	.018	.025	.105
	RMS =	.071	.092	.176	.066	.021	.111	.237
	ERROR =	.018	.008	.043	.010	.003	.005	.019

INTERPOLATED AXIAL CORE LOC. CP (MM)	NORMALIZED INTERPOLATED NUCLIDE CPM RATIOS AND 1 SIGMA ERRORS						
	PA-233 MEAN	CE-141 MEAN	RU-106 MEAN	CS-137 MEAN	CS-134/137 MEAN	ZR-95 MEAN	LA-140 MEAN
698.50	.426	.558	.000	.922	.173	.650	.584
	.010	.056	.000	.079	.070	.023	.025
774.70	.526	.611	.000	.811	.330	.678	.674
	.010	.056	.000	.079	.084	.023	.025
850.90	.627	.664	.000	.699	.536	.706	.764
	.010	.056	.000	.079	.108	.023	.025
927.10	.721	.668	.211	.693	.804	.806	.857
	.011	.060	.080	.078	.126	.023	.026
1003.30	.832	.829	.105	.812	.612	.883	.944
	.012	.081	.080	.078	.115	.027	.028
1079.50	.940	.923	.000	.899	.910	.989	.973
	.012	.091	.000	.081	.114	.031	.029
1155.70	1.013	1.000	.000	1.024	1.010	1.040	1.008
	.013	.086	.000	.083	.113	.030	.026
1231.90	1.065	1.127	.248	1.120	1.008	1.028	1.042
	.013	.098	.114	.093	.112	.028	.029
1308.10	1.122	1.130	.661	1.094	1.074	1.048	1.062
	.013	.096	.244	.092	.117	.029	.029
1384.30	1.182	.973	.675	1.072	1.270	1.114	1.125
	.013	.100	.133	.099	.141	.033	.029
1460.50	1.231	1.183	.001	1.298	1.075	1.191	1.127
	.013	.100	.133	.099	.106	.033	.029
1536.70	1.222	1.149	.259	1.158	1.272	1.169	1.129
	.013	.097	.118	.108	.140	.033	.029
1612.90	1.238	1.264	.088	1.247	1.196	1.163	1.171
	.013	.092	.118	.095	.117	.030	.031
1689.10	1.264	1.141	.259	1.206	1.218	1.136	1.168
	.013	.106	.146	.095	.121	.030	.031
1765.30	1.258	1.100	.600	1.191	1.302	1.127	1.167
	.013	.105	.263	.095	.134	.029	.029
1841.50	1.235	1.228	.495	1.211	1.367	1.162	1.175
	.013	.098	.121	.086	.131	.031	.030
1917.70	1.240	1.186	.000	1.142	1.355	1.181	1.151
	.014	.102	.000	.088	.131	.031	.031
1993.90	1.212	1.108	.044	1.227	1.122	1.128	1.151
	.014	.109	.127	.090	.107	.030	.029
2070.10	1.221	1.155	.428	1.034	1.287	1.147	1.090
	.014	.109	.127	.090	.137	.030	.029
2146.30	1.214	1.168	.683	1.061	1.234	1.147	1.141
	.014	.103	.239	.086	.124	.031	.029

NORMALIZED INTERPOLATED NUCLIDE CPM RATIOS AND 1 SIGMA ERRORS

INTERPOLATED AXIAL CORE LOC. CP (MM)		PA-233 MEAN	CE-141 MEAN	RU-106 MEAN	CS-137 MEAN	CS-134/137 MEAN	ZR-95 MEAN	LA-140 MEAN
2222.50		1.189	1.190	1.123	1.150	1.178	1.149	1.155
		.014	.111	.243	.094	.123	.032	.030
2298.70		1.138	1.128	1.713	1.084	1.088	1.093	1.105
		.014	.113	.272	.094	.125	.031	.029
2374.90		1.075	1.036	1.947	.984	1.103	1.044	1.047
		.013	.102	.299	.090	.135	.031	.029
2451.10		1.020	1.000	1.777	1.005	1.152	1.039	1.006
		.013	.097	.300	.093	.135	.032	.028
2527.30		.973	1.016	1.901	1.060	.819	.990	.939
		.014	.106	.299	.094	.101	.030	.026
2603.50		.905	.965	1.735	.875	.892	.915	.919
		.014	.107	.299	.094	.128	.030	.026
2679.70		.848	.943	1.967	.934	.754	.912	.923
		.013	.119	.305	.100	.115	.030	.026
2755.90		.790	.881	1.944	.814	.762	.864	.857
		.013	.101	.267	.097	.122	.029	.026
2832.10		.696	.642	2.242	.653	.869	.790	.793
		.013	.094	.278	.080	.142	.027	.026
2908.30		.573	.636	2.894	.527	1.029	.711	.754
		.013	.094	.284	.080	.192	.027	.026
ELEMENT TITLE: E14-01	MEAN RATIO =	1.000	1.000	1.000	1.000	1.000	1.000	1.000
	MEAN 1 SIGMA =	.013	.096	.219	.090	.124	.029	.028
	RMS =	.246	.189	.847	.192	.295	.166	.161
	ERROR =	.002	.018	.045	.016	.023	.005	.005

SPECTRUM I.D. GA.TAG NO.	CORE LOCATION PARAMETERS AXIAL CORE LOC. CP (MM)	FUEL ELEMENT I.D. SCAN INTERVAL	CE-144 133 KEV	CE-141 145 KEV	PA-233 312 KEV	I-131 364 KEV	RU-103 497 KEV	RU-106 512 KEV	CS-137 661 KEV	ZR-95 724 KEV	CS-134 796 KEV	LA-140 1596 KEV
* * *	STRATA # 1 E14-01	TOTALS * * *										
MEAN =	365.04	WT MEAN CPM =	.0	27.1	35.8	223.0	9.1	8.2	18.2	4.7	5.8	.0
RMS =	186.18	WT MEAN 1SIGMA=	.0	22.0	18.1	92.6	5.7	3.3	9.7	2.8	2.7	.0
MIDPT=	339.11	WT RMS =	.0	.0	9.6	129.9	4.3	3.2	4.0	.0	4.9	.0
RANGE=	656.00	WT ERROR =	.0	22.0	10.5	61.0	2.4	1.9	3.5	2.8	1.9	.0
* * *	STRATA # 2 E14-01	TOTALS * * *										
MEAN =	1818.11	WT MEAN CPM =	666.0	4241.4	35093.0	5158.9	4056.8	565.7	783.2	4377.9	693.2	7292.0
RMS =	630.49	WT MEAN 1SIGMA=	241.8	414.7	448.8	1029.7	199.2	123.7	71.5	130.7	53.6	206.3
MIDPT=	1833.15	WT RMS =	283.8	769.5	7445.2	1450.2	573.8	335.2	153.9	655.5	254.8	1007.4
RANGE=	2159.25	WT ERROR =	55.6	83.1	90.0	207.3	39.9	30.9	14.3	26.2	10.7	41.3
* * *	STRATA # 3 E14-01	TOTALS * * *										
MEAN =	3091.42	WT MEAN CPM =	.0	.0	.0	.0	.0	915.4	.0	.0	.0	.0
RMS =	43.21	WT MEAN 1SIGMA=	.0	.0	.0	.0	.0	66.5	.0	.0	.0	.0
MIDPT=	3091.42	WT RMS =	.0	.0	.0	.0	.0	38.0	.0	.0	.0	.0
RANGE=	162.64	WT ERROR =	.0	.0	.0	.0	.0	47.3	.0	.0	.0	.0
* * *	STRATA # 4 E14-01	TOTALS * * *										
MEAN =	1617.31	WT MEAN CPM =	589.4	4625.9	39664.9	5588.3	4573.8	279.4	801.6	4709.2	837.8	7772.9
RMS =	645.94	WT MEAN 1SIGMA=	86.9	177.2	195.8	434.3	83.6	40.8	30.5	55.0	24.4	84.4
MIDPT=	1377.90	WT RMS =	95.6	470.2	4960.3	492.1	261.8	240.0	319.9	422.2	196.5	519.3
RANGE=	-2276.72	WT ERROR =	32.8	67.0	74.0	164.2	31.6	15.4	10.8	20.8	9.2	31.9

NUCLIDE CPM + / - 1 SIGMA COUNTING ERROR

T O T A L S T R A T A E 1 4 - 0 1

			CE-144	CE-141	PA-233	I-131	RU-103	RU-106	CS-137	ZR-95	CS-134	LA-140
MEAN =	1818.11	WT MEAN CPM =	666.0	4241.4	35093.0	5158.9	4056.8	565.7	783.2	4377.9	693.2	7292.0
RMS =	630.49	WT MEAN 1SIGMA=	241.8	414.7	448.8	1029.7	199.2	123.7	71.5	130.7	53.6	206.3
MIDPT=	1833.15	WT RMS =	283.8	769.5	7445.2	1450.2	573.8	335.2	153.9	655.5	254.8	1007.4
RANGE=	2159.25	WT ERROR =	55.6	83.1	90.0	207.3	39.9	30.9	14.3	26.2	10.7	41.3

SPECTRUM I.D.	CORE LOCATION PARAMETERS	FUEL ELEMENT I.D	NUCLIDE CPM RATIOS AND 1 SIGMA ERRORS							
GA.TAG NO.	AXIAL CORE LOC. CP (MM)	SCAN INTERVAL			CE-141 ZR-95	CE-144 ZR-95	I-131 ZR-95	RU-103 ZR-95	CS-137 ZR-95	RU-106 ZR-95	CS-134 CS-137
* * *	STRATA # 1 E14-01 TOTALS * * *									
MEAN =	365.04		WT MEAN RATIO =	.000	.000	.000	3.408	3.675	.000	.524
RMS =	186.18		WT MEAN 1 SIGMA =	.000	.000	.000	3.080	2.581	.000	1.185
MIDPT=	339.11		WT RMS =	.000	.000	.000	.000	.000	.000	.490
RANGE=	656.00		WT ERROR =	.000	.000	.000	3.080	2.581	.000	.607
* * *	STRATA # 2 E14-01 TOTALS * * *									
MEAN =	1818.11		WT MEAN RATIO =	.967	.151	1.169	.932	.178	.137	.859
RMS =	630.49		WT MEAN 1 SIGMA =	.100	.057	.237	.055	.018	.030	.105
MIDPT=	1833.15		WT RMS =	.085	.072	.228	.078	.018	.096	.208
RANGE=	2159.25		WT ERROR =	.020	.013	.048	.011	.004	.007	.021
* * *	STRATA # 3 E14-01 TOTALS * * *									
MEAN =	3091.42		WT MEAN RATIO =	.000	.000	.000	.000	.000	.000	.000
RMS =	43.21		WT MEAN 1 SIGMA =	.000	.000	.000	.000	.000	.000	.000
MIDPT=	3091.42		WT RMS =	.000	.000	.000	.000	.000	.000	.000
RANGE=	162.64		WT ERROR =	.000	.000	.000	.000	.000	.000	.000
* * *	STRATA # 4 E14-01 TOTALS * * *									
MEAN =	1617.31		WT MEAN RATIO =	.982	.125	1.190	.974	.193	.062	.909
RMS =	645.94		WT MEAN 1 SIGMA =	.040	.019	.095	.021	.007	.009	.043
MIDPT=	1377.90		WT RMS =	.043	.015	.091	.033	.016	.059	.127
RANGE=	-2276.72		WT ERROR =	.015	.007	.036	.008	.003	.003	.016

TOTAL STRATA E14-01

MEAN =	1818.11	WT MEAN RATIO =	.967	.151	1.169	.932	.178	.137	.859
RMS =	630.49	WT MEAN 1 SIGMA =	.100	.057	.237	.055	.018	.030	.105
MIDPT=	1833.15	WT RMS =	.085	.072	.228	.078	.018	.096	.208
RANGE=	2159.25	WT ERROR =	.020	.013	.048	.011	.004	.007	.021

SPECTRUM I.D.	CORE LOCATION PARAMETERS		FUEL ELEMENT I.D	NORMALIZED NUCLIDE CPM RATIOS AND 1 SIGMA ERRORS						
GA.TAG NO.	AXIAL CORE LOC. CP (MM)	SCAN INTERVAL		PA-233 MEAN	CE-141 MEAN	RU-106 MEAN	CS-137 MEAN	CS-134/137 MEAN	ZR-95 MEAN	LA-140 MEAN
* * *	STRATA # 1 E14-01 TOTALS * * *									
MEAN =	365.04	WT MEAN RATIO	=	.001	.006	.015	.023	.609	.001	.000
RMS =	186.18	WT MEAN 1 SIGMA	=	.001	.005	.006	.012	.652	.001	.000
MIDPT=	339.11	WT RMS	=	.000	.000	.006	.005	.570	.000	.000
RANGE=	656.00	WT ERROR	=	.000	.005	.003	.004	.445	.001	.000
* * *	STRATA # 2 E14-01 TOTALS * * *									
MEAN =	1818.11	WT MEAN RATIO	=	1.000	1.000	1.000	1.000	1.000	1.000	1.000
RMS =	630.49	WT MEAN 1 SIGMA	=	.013	.096	.212	.089	.120	.029	.028
MIDPT=	1833.15	WT RMS	=	.212	.181	.592	.197	.242	.150	.138
RANGE=	2159.25	WT ERROR	=	.003	.019	.053	.018	.024	.006	.006
* * *	STRATA # 3 E14-01 TOTALS * * *									
MEAN =	3091.42	WT MEAN RATIO	=	.000	.000	1.618	.000	.000	.000	.000
RMS =	43.21	WT MEAN 1 SIGMA	=	.000	.000	.042	.000	.000	.000	.000
MIDPT=	3091.42	WT RMS	=	.000	.000	.067	.000	.000	.000	.000
RANGE=	162.64	WT ERROR	=	.000	.000	.030	.000	.000	.000	.000
* * *	STRATA # 4 E14-01 TOTALS * * *									
MEAN =	1617.31	WT MEAN RATIO	=	1.130	1.091	.494	1.023	1.057	1.076	1.066
RMS =	645.94	WT MEAN 1 SIGMA	=	.005	.041	.075	.038	.049	.012	.011
MIDPT=	1377.90	WT RMS	=	.141	.111	.424	.408	.148	.096	.071
RANGE=	-2276.72	WT ERROR	=	.002	.015	.028	.014	.018	.005	.004

T O T A L   S T R A T A   E 1 4 - 0 1

				PA-233	CE-141	RU-106	CS-137	CS-134/137	ZR-95	LA-140
MEAN =	1818.11	WT MEAN RATIO	=	1.000	1.000	1.000	1.000	1.000	1.000	1.000
RMS =	630.49	WT MEAN 1 SIGMA	=	.013	.096	.212	.089	.120	.029	.028
MIDPT=	1833.15	WT RMS	=	.212	.181	.592	.197	.242	.150	.138
RANGE=	2159.25	WT ERROR	=	.003	.019	.053	.018	.024	.006	.006

ABSOLUTE NUCLIDE ACTIVITIES AND COMPOSITE BURNUP

FUEL IDENTIFICATION GA. TAG NO.	AXIAL CORE LOC. / SCAN INTERVAL	CE-144 133KEV	CE-141 145KEV	PA-233 312KEV	I-131 364KEV	RU-103 497KEV	RU-106 512KEV	CS-137 661KEV	ZR- 95 724KEV	CS-134 796KEV	LA-140 1596KEV	COMPOSITE FIMA CS-137 MONITOR	COMPOSITE FIMA RU-106 MONITOR
		NUCLIDE C(I) +/- 1 SIGMA ERROR											
* * *	STRATA # 1 E14-01 TOTALS * * *												
	WT MEAN =	.0	.6	.8	2.7	.1	.5	.3	.2	.1	.0	.000	.000
	WT 1 SIGMA=	.0	.5	.4	1.2	.1	.2	.2	.1	.1	.0	.000	.000
	WT RMS =	.0	.0	.2	1.6	.1	.2	.1	.0	.1	.0	.000	.000
	WT ERROR =	.0	.5	.2	.8	.0	.1	.1	.1	.0	.0	.000	.000
* * *	STRATA # 2 E14-01 TOTALS * * *												
	WT MEAN =	119.0	83.7	817.1	62.1	56.2	33.9	14.0	161.7	13.9	215.4	8.345	24.332
	WT 1 SIGMA=	45.2	12.7	86.3	14.1	6.4	8.4	1.9	17.5	1.9	23.1	2.594	5.202
	WT RMS =	50.7	16.1	173.4	17.5	7.9	20.1	2.7	24.2	5.1	29.8	1.640	14.915
	WT ERROR =	10.4	2.5	17.3	2.8	1.3	2.1	.4	3.5	.4	4.6	.520	1.301
* * *	STRATA # 3 E14-01 TOTALS * * *												
	WT MEAN =	.0	.0	.0	.0	.0	59.6	.0	.0	.0	.0	.000	.000
	WT 1 SIGMA=	.0	.0	.0	.0	.0	6.9	.0	.0	.0	.0	.000	.000
	WT RMS =	.0	.0	.0	.0	.0	2.3	.0	.0	.0	.0	.000	.000
	WT ERROR =	.0	.0	.0	.0	.0	4.9	.0	.0	.0	.0	.000	.000
* * *	STRATA # 4 E14-01 TOTALS * * *												
	WT MEAN =	105.3	96.7	923.6	67.3	63.3	16.7	14.3	173.9	16.8	229.6	8.541	12.017
	WT 1 SIGMA=	19.0	10.6	95.6	8.7	6.6	3.3	1.7	18.0	1.8	23.7	1.910	2.189
	WT RMS =	17.1	9.8	115.5	5.9	3.6	14.4	5.7	15.6	3.9	15.3	3.409	10.324
	WT ERROR =	7.2	4.0	36.1	3.3	2.5	1.3	.6	6.8	.7	9.0	.675	.827
	T O T A L S T R A T A E 1 4 - 0 1												
	WT MEAN =	119.0	88.7	817.1	62.1	56.2	33.9	14.0	161.7	13.9	215.4	8.345	24.332
	WT 1 SIGMA=	45.2	12.7	86.3	14.1	6.4	8.4	1.9	17.5	1.9	23.1	2.594	5.202
	WT RMS =	50.7	16.1	173.4	17.5	7.9	20.1	2.7	24.2	5.1	29.8	1.640	14.915
	WT ERROR =	10.4	2.5	17.3	2.8	1.3	2.1	.4	3.5	.4	4.6	.520	1.301

SPECTRUM I.D.	CORE LOCATION PARAMETERS	FUEL ELEMENT I.D.	COMPARISIONS OF SELECTED VALUES & ITEMS									
GA.TAG NO.	AXIAL CORE LOC. CENTER POINT (MM)	SCAN INTERVAL	ZR-95 MEAN 'C'	LA140 MEAN 'M'	REL.DIF. Z=-1+C/M	COMPARISON TEST 1 D=Z/S(Z)	COMPARISON TEST 2 D**2	FIMA CS137 'C'	FIMA RU106 'M'	REL.DIF. Z=-1+C/M	COMPARISON TEST 1 D=Z/S(Z)	COMPARISON TEST 2 D**2
* * *	BEGIN STRATA # 1	* * *										
108	49.21	81.66	.000	.000	.000	.000	.000	.000	.000	.000	.000	.000
		AUTO #1 E14-01	.000	.000	.000	.000	.000	.000	.000	.000	.000	.000
109	178.50	68.05	.000	.000	.000	.000	.000	.000	.000	.000	.000	.000
		AUTO #2 E14-01	.000	.000	.000	.000	.000	.000	.000	.000	.000	.000
110	254.72	68.05	.000	.000	.000	.000	.000	.000	.000	.000	.000	.000
		AUTO #3 E14-01	.000	.000	.000	.000	.000	.000	.000	.000	.000	.000
111	328.90	69.41	.000	.000	.000	.000	.000	.000	.000	.000	.000	.000
		AUTO #4 E14-01	.000	.000	.000	.000	.000	.000	.000	.000	.000	.000
112	416.00	93.91	.000	.000	.000	.000	.000	.000	.000	.000	.000	.000
		AUTO #5 E14-01	.000	.000	.000	.000	.000	.000	.000	.000	.000	.000
113	507.17	80.30	.000	.000	.000	.000	.000	.000	.000	.000	.000	.000
		AUTO #6 E14-01	.000	.000	.000	.000	.000	.000	.000	.000	.000	.000
114	556.86	68.05	.000	.000	.000	.000	.000	.000	.000	.000	.000	.000
		AUTO #7 E14-01	.000	.000	.000	.000	.000	.000	.000	.000	.000	.000
115	629.00	76.22	.001	.000	.000	.000	.000	.000	.000	.000	.000	.000
		AUTO #8 E14-01	.001	.000	.000	.000	.000	.000	.000	.000	.000	.000
* * *	STRATA # 1 E14-01 TOTALS	* * *										
MEAN =	365.04	WT MEAN COMP. =	.001	.000	.000	.000	.000	.000	.000	.000	.000	.000
RMS =	186.18	WT MEAN 1SIGMA=	.001	.000	.000	.000	.000	.000	.000	.000	.000	.000
MIDPT=	339.11	WT RMS =	.000	.000	.000	.000	.000	.000	.000	.000	.000	.000
RANGE=	656.00	WT ERROR =	.001	.000	.000	.000	.000	.000	.000	.000	.000	.000
* * *	BEGIN STRATA # 2	* * *										
117	792.31	81.66	.673	.682	-.012	-.250	.063	6.505	.000	.000	.000	.000
		AUTO #10 E14-01	.025	.023	.049	.000	.000	2.121	.000	.000	.000	.000
118	879.42	81.66	.705	.783	-.100	-2.424	5.874	5.449	.000	.000	.000	.000
		AUTO #11 E14-01	.022	.027	.041	.000	.000	1.903	.000	.000	.000	.000
119	946.78	91.19	.829	.864	-.040	-1.026	1.053	5.865	5.881	-.003	-.006	.000
		AUTO #12 E14-01	.024	.025	.039	.000	.000	1.978	1.877	.463	.000	.000
120	1033.89	72.13	.890	.960	-.073	-1.753	3.072	7.193	.000	.000	.000	.000
		AUTO #13 E14-01	.029	.029	.041	.000	.000	2.235	.000	.000	.000	.000
121	1113.52	76.22	1.034	.951	.087	1.899	3.607	7.645	.000	.000	.000	.000
		AUTO #14 E14-01	.032	.027	.046	.000	.000	2.357	.000	.000	.000	.000
122	1196.53	81.66	1.012	1.025	-.012	-.326	.106	9.301	.000	.000	.000	.000
		AUTO #15 E14-01	.027	.028	.038	.000	.000	2.644	.000	.000	.000	.000
123	1283.64	81.66	1.010	1.018	-.007	-.183	.033	9.253	12.073	-.234	-.739	.546
		AUTO #16 E14-01	.028	.028	.039	.000	.000	2.901	3.236	.316	.000	.000
124	1371.42	83.02	1.084	1.103	-.018	-.494	.244	8.579	15.568	-.449	-2.109	4.446
		AUTO #17 E14-01	.029	.028	.036	.000	.000	2.495	3.959	.213	.000	.000
125	1460.58	84.38	1.172	1.105	.060	1.426	2.033	10.673	.000	.000	.000	.000
		AUTO #18 E14-01	.036	.029	.042	.000	.000	3.323	.000	.000	.000	.000

SPECTRUM I.D.	CORE LOCATION PARAMETERS		FUEL ELEMENT I.D.	COMPARISIONS OF SELECTED VALUES & ITEMS									
GA.TAG NO.	AXIAL CORE LOC. CENTER POINT (MM)	SCAN INTERVAL		ZR-95 MEAN 'C'	LA140 MEAN 'M'	REL.DIF. Z=-1+C/M	COMPARISON TEST 1 D=Z/S(Z)	COMPARISON TEST 2 D**2	FIMA CS137 'C'	FIMA RU106 'M'	REL.DIF. Z=-1+C/M	COMPARISON TEST 1 D=Z/S(Z)	COMPARISON TEST 2 D**2
126	1547.68	78.94		1.147	1.108	.035	.922	.850	9.444	5.854	.613	.769	.592
		AUTO #19 E14-01		.029	.029	.038	.000	.000	2.891	2.270	.797	.000	.000
127	1640.23	95.27		1.143	1.166	-.019	-.521	.271	10.705	.000	.000	.000	.000
		AUTO #20 E14-01		.030	.032	.037	.000	.000	2.968	.000	.000	.000	.000
128	1730.06	73.49		1.097	1.128	-.026	-.785	.616	9.397	9.410	-.001	-.003	.000
		AUTO #21 E14-01		.030	.028	.036	.000	.000	2.892	3.212	.459	.000	.000
129	1811.71	78.94		1.124	1.167	-.036	-1.065	1.134	10.494	15.027	-.302	-1.162	1.351
		AUTO #22 E14-01		.028	.029	.034	.000	.000	2.917	3.710	.260	.000	.000
130	1896.77	83.02		1.178	1.127	.046	1.129	1.276	9.186	.000	.000	.000	.000
		AUTO #23 E14-01		.033	.031	.041	.000	.000	2.608	.000	.000	.000	.000
131	1985.25	83.02		1.108	1.136	-.025	-.700	.490	10.346	.000	.000	.000	.000
		AUTO #24 E14-01		.029	.029	.036	.000	.000	2.966	.000	.000	.000	.000
132	2075.07	85.74		1.130	1.065	.061	1.549	2.398	8.464	8.950	-.054	-.130	.017
		AUTO #25 E14-01		.030	.027	.039	.000	.000	2.542	2.925	.419	.000	.000
133	2164.90	83.02		1.128	1.134	-.004	-.119	.014	8.877	14.656	-.394	-1.705	2.906
		AUTO #26 E14-01		.031	.029	.037	.000	.000	2.606	3.580	.231	.000	.000
134	2252.68	81.66		1.1[illegible]2	1.133	-.001	-.031	.001	9.873	26.094	-.622	-4.546	20.664
		AUTO #27 E14-01		.033	.029	.038	.000	.000	2.966	5.163	.137	.000	.000
135	2341.14	84.38		1.023	1.039	-.016	-.417	.174	8.157	40.932	-.801	-11.465	131.437
		AUTO #28 E14-01		.028	.029	.038	.000	.000	2.510	6.871	.070	.000	.000
136	2430.98	84.38		1.034	1.006	.028	.625	.391	8.155	34.280	-.762	-8.669	75.147
		AUTO #29 E14-01		.033	.029	.044	.000	.000	2.580	6.546	.088	.000	.000
137	2520.81	84.38		.980	.923	.063	1.418	2.009	8.914	37.809	-.764	-9.226	85.126
		AUTO #30 E14-01		.030	.026	.044	.000	.000	2.715	6.619	.083	.000	.000
138	2611.99	87.11		.892	.900	-.009	-.208	.043	7.081	33.881	-.791	-9.699	94.061
		AUTO #31 E14-01		.029	.026	.043	.000	.000	2.409	6.475	.082	.000	.000
139	2701.81	81.66		.899	.907	-.009	-.209	.044	7.955	40.452	-.803	-10.698	114.450
		AUTO #32 E14-01		.030	.026	.043	.000	.000	2.708	6.994	.075	.000	.000
140	2789.60	83.02		.820	.799	.026	.555	.308	5.993	37.086	-.838	-13.356	178.374
		AUTO #33 E14-01		.028	.024	.047	.000	.000	2.125	5.885	.063	.000	.000
141	2873.98	77.58		.735	.757	-.030	-.633	.401	4.837	51.336	-.906	-24.776	613.836
		AUTO #34 E14-01		.025	.026	.047	.000	.000	1.711	8.191	.037	.000	.000
* * *	STRATA # 2 E14-01 TOTALS * * *												
MEAN =	1818.11	WT. MEAN COMP. =		1.000	1.000	-.001	-.058	1.041	8.345	24.332	-.448	-6.073	81.110
RMS =	630.49	WT MEAN 1SIGMA=		.029	.028	.041	.000	.000	2.594	5.202	.310	.000	.000
MIDPT=	1833.15	WT RMS =		.150	.138	.042	1.018	1.382	1.640	14.415	.408	6.650	144.617
RANGE=	2159.25	WT ERROR =		.006	.006	.008	.000	.000	.520	1.301	.077	.000	.000
* * *	BEGIN STRATA # 3 * * *												
143	3048.21	85.74		.000	.000	.000	.000	.000	.000	.000	.000	.000	.000
		AUTO #36 E14-01		.000	.000	.000	.000	.000	.000	.000	.000	.000	.000

SPECTRUM I.D.	CORE LOCATION PARAMETERS		FUEL ELEMENT I.D.	COMPARISIONS OF SELECTED VALUES & ITEMS									
GA.TAG NO.	AXIAL CORE LOC. CENTER POINT (MM)	SCAN INTERVAL		ZR-95 MEAN 'C'	LA140 MEAN 'M'	REL.DIF. Z=-1+C/M	COMPARISON TEST 1 D=Z/S(Z)	TEST 2 D**2	FIMA CS137 'C'	FIMA RU106 'M'	REL.DIF. Z=-1+C/M	COMPARISON TEST 1 D=Z/S(Z)	TEST 2 D**2
144	3134.63	76.22		.000	.000	.000	.000	.000	.000	.000	.000	.000	.000
		AUTO #37 E14-01		.000	.000	.000	.000	.000	.000	.000	.000	.000	.000
* * *	STRATA # 3 E14-01 TOTALS * * *												
MEAN =	3091.42	WT MEAN COMP. =		.000	.000	.000	.000	.000	.000	.000	.000	.000	.000
RMS =	43.21	WT MEAN 1SIGMA=		.000	.000	.000	.000	.000	.000	.000	.000	.000	.000
MIDPT=	3091.42	WT RMS =		.000	.000	.000	.000	.000	.000	.000	.000	.000	.000
RANGE=	162.64	WT ERROR =		.000	.000	.000	.000	.000	.000	.000	.000	.000	.000
* * *	BEGIN STRATA # 4 * * *												
145	2516.76	1.00		.957	.967	-.010	-.609	.371	7.217	36.944	-.805	-16.511	272.609
		STAT #1 E14-01		.012	.011	.017	.000	.000	1.601	4.213	.049	.000	.000
146	1804.21	1.00		1.073	1.042	.029	1.811	3.280	9.854	8.849	.114	.359	.129
		STAT #2 E14-01		.012	.011	.016	.000	.000	2.013	1.749	.317	.000	.000
147	1820.67	1.00		1.086	1.115	-.027	-1.781	3.171	9.836	5.494	.790	1.463	2.140
		STAT #3 E14-01		.012	.012	.015	.000	.000	2.001	1.225	.540	.000	.000
148	1837.16	1.00		1.068	1.093	-.023	-1.529	2.337	10.566	5.129	1.060	1.655	2.738
		STAT #4 E14-01		.012	.012	.015	.000	.000	2.196	1.187	.641	.000	.000
149	1853.64	1.00		1.098	1.059	.036	2.220	4.930	10.338	10.084	.025	.087	.007
		STAT #5 E14-01		.012	.012	.016	.000	.000	2.190	1.904	.291	.000	.000
150	1870.10	1.00		1.275	1.194	.069	4.384	19.218	12.062	9.212	.309	.851	.725
		STAT #6 E14-01		.014	.012	.016	.000	.000	2.409	1.775	.363	.000	.000
151	996.90	1.00		.973	.991	-.018	-1.139	1.297	8.150	8.406	-.030	-.104	.011
		STAT #7 E14-01		.011	.011	.016	.000	.000	1.769	1.744	.291	.000	.000
152	239.04	1.00		.000	.000	.000	.000	.000	.300	.000	.000	.000	.000
		TRAP E14-01		.000	.000	.000	.000	.000	.108	.000	.000	.000	.000
* * *	STRATA # 4 E14-01 TOTALS * * *												
MEAN =	1617.31	WT MEAN COMP. =		1.076	1.066	.008	.480	4.944	8.541	12.017	.209	-1.743	39.765
RMS =	645.94	WT MEAN 1SIGMA=		.012	.011	.016	.000	.000	1.910	2.189	.398	.000	.000
MIDPT=	1377.90	WT RMS =		.096	.071	.034	2.171	5.984	3.409	10.324	.561	6.060	95.063
RANGE=	-2276.72	WT ERROR =		.005	.004	.006	.000	.000	.675	.827	.150	.000	.000

T O T A L   S T R A T A   E 1 4 - 0 1

MEAN =	1818.11	WT MEAN COMP. =		1.000	1.000	-.001	-.058	1.041	8.345	24.332	-.448	-6.073	81.110
RMS =	1818.11	WT MEAN 1SIGMA=		.029	.028	.041	.000	.000	2.594	5.202	.310	.000	.000
MIDPT=	1818.11	WT RMS =		.150	.138	.042	1.018	1.382	1.640	14.415	.408	6.650	144.617
RANGE=	1818.11	WT ERROR =		.006	.006	.008	.000	.000	.520	1.301	.077	.000	.000

SPECTRUM I.D. — CORE LOCATION PARAMETERS — FUEL ELEMENT I.D.

COMPARISIONS OF SELECTED VALUES & ITEMS

GA.TAG NO.	AXIAL CORE LOC. CENTER POINT (MM)	SCAN INTERVAL	CS137 MEAN 'C'	CS4/7 MEAN 'M'	REL.DIF. Z=-1+C/M	COMPARISON TEST 1 D=Z/S(Z)	TEST 2 D**2	'C'	'M'	REL.DIF. Z=-1+C/M	COMPARISON TEST 1 D=Z/S(Z)	TEST 2 D**2
* * *	BEGIN STRATA # 1	* * *										
108	49.21	81.66	.027	.000	.000	.000	.000					
		AUTO #1 E14-01	.022	.000	.000	.000	.000					
109	178.50	68.05	.026	.000	.000	.000	.000					
		AUTO #2 E14-01	.006	.000	.000	.000	.000					
110	254.72	68.05	.032	.000	.000	.000	.000					
		AUTO #3 E14-01	.007	.000	.000	.000	.000					
111	328.90	69.41	.013	1.223	-.989	-50.157	2515.698					
		AUTO #4 E14-01	.022	.954	.020	.000	.000					
112	416.00	93.91	.023	.000	.000	.000	.000					
		AUTO #5 E14-01	.006	.000	.000	.000	.000					
113	507.17	80.30	.023	.079	-.710	-2.337	5.461					
		AUTO #6 E14-01	.006	.089	.304	.000	.000					
114	556.86	68.05	.018	.000	.000	.000	.000					
		AUTO #7 E14-01	.005	.000	.000	.000	.000					
115	629.00	76.22	.022	.000	.000	.000	.000					
		AUTO #8 E14-01	.008	.000	.000	.000	.000					
* * *	STRATA # 1 E14-01 TOTALS	* * *										
MEAN =	365.04	WT MEAN COMP. =	.023	.609	-.839	-24.508	1169.294					
RMS =	186.16	WT MEAN 1SIGMA=	.012	.652	.223	.000	.000					
MIDPT=	339.11	WT RMS =	.005	.570	.139	23.847	1251.790					
RANGE=	656.00	WT ERROR =	.004	.445	.163	.000	.000					
* * *	BEGIN STRATA # 2	* * *										
117	792.31	81.66	.780	.361	1.162	1.953	3.812					
		AUTO #10 E14-01	.079	.092	.595	.000	.000					
118	879.42	81.66	.653	.612	.067	.293	.086					
		AUTO #11 E14-01	.077	.110	.229	.000	.000					
119	946.78	91.19	.703	.843	-.166	-1.069	1.142					
		AUTO #12 E14-01	.077	.128	.156	.000	.000					
120	1033.89	72.13	.862	.762	.132	.702	.492					
		AUTO #13 E14-01	.078	.106	.188	.000	.000					
121	1113.52	76.22	.916	.965	-.051	-.362	.131					
		AUTO #14 E14-01	.082	.114	.141	.000	.000					
122	1196.53	81.66	1.115	.989	.127	.867	.751					
		AUTO #15 E14-01	.063	.105	.147	.000	.000					
123	1283.64	81.66	1.109	.958	.158	.919	.844					
		AUTO #16 E14-01	.102	.112	.172	.000	.000					
124	1371.42	83.02	1.028	1.270	-.190	-1.858	3.454					
		AUTO #17 E14-01	.081	.126	.102	.000	.000					
125	1460.58	84.38	1.279	1.041	.228	1.312	1.720					
		AUTO #18 E14-01	.115	.114	.174	.000	.000					

SPECTRUM I.D. — CORE LOCATION PARAMETERS — FUEL ELEMENT I.D. — COMPARISIONS OF SELECTED VALUES & ITEMS

GA.TAG NO.	AXIAL CORE LOC. CENTER POINT (MM)	SCAN INTERVAL	CS137 MEAN 'C'	CS4/7 MEAN 'M'	REL.DIF. Z=-1+C/M	COMPARISON TEST 1 D=Z/S(Z)	COMPARISON TEST 2 D**2	'C'	'M'	REL.DIF. Z=-1+C/M	COMPARISON TEST 1 D=Z/S(Z)	COMPARISON TEST 2 D**2
126	1547.66	78.94	1.132	1.263	-.104	-.849	.721					
		AUTO #19 E14-01	.099	.133	.122	.000	.000					
127	1640.23	95.27	1.283	1.120	.145	1.084	1.175					
		AUTO #20 E14-01	.090	.105	.134	.000	.000					
128	1730.06	73.49	1.126	1.237	-.089	-.716	.513					
		AUTO #21 E14-01	.099	.130	.125	.000	.000					
129	1811.71	78.94	1.258	1.290	-.025	-.213	.045					
		AUTO #22 E14-01	.089	.129	.119	.000	.000					
130	1896.77	83.02	1.101	1.397	-.212	-2.246	5.046					
		AUTO #23 E14-01	.082	.131	.094	.000	.000					
131	1985.25	83.02	1.240	1.072	.157	1.097	1.203					
		AUTO #24 E14-01	.093	.105	.143	.000	.000					
132	2075.07	85.74	1.014	1.259	-.195	-1.824	3.327					
		AUTO #25 E14-01	.085	.129	.107	.000	.000					
133	2164.90	83.02	1.064	1.180	-.099	-.855	.731					
		AUTO #26 E14-01	.085	.118	.115	.000	.000					
134	2252.68	81.66	1.183	1.123	.054	.365	.133					
		AUTO #27 E14-01	.100	.124	.147	.000	.000					
135	2341.14	84.38	.977	.978	-.000	-.002	.000					
		AUTO #28 E14-01	.087	.116	.148	.000	.000					
136	2430.98	84.38	.977	1.219	-.198	-1.602	2.567					
		AUTO #29 E14-01	.092	.149	.124	.000	.000					
137	2520.81	84.38	1.068	.789	.354	1.785	3.185					
		AUTO #30 E14-01	.092	.093	.198	.000	.000					
138	2611.99	87.11	.849	.874	-.029	-.161	.026					
		AUTO #31 E14-01	.094	.131	.181	.000	.000					
139	2701.81	81.66	.953	.689	.384	1.467	2.151					
		AUTO #32 E14-01	.105	.106	.262	.000	.000					
140	2789.60	83.02	.718	.780	-.079	-.431	.186					
		AUTO #33 E14-01	.087	.123	.183	.000	.000					
141	2873.98	77.58	.580	.919	-.369	-2.831	8.017					
		AUTO #34 E14-01	.070	.154	.130	.000	.000					
* * *	STRATA #.2 E14-01 TOTALS * * *											
MEAN =	1818.11	WT MEAN COMP. =	1.000	1.000	.047	-.121	1.659					
RMS =	630.49	WT MEAN 1SIGMA=	.089	.120	.194	.000	.000					
MIDPT=	1833.15	WT RMS =	.197	.242	.289	1.282	1.870					
RANGE=	2159.25	WT ERROR =	.018	.024	.039	.000	.000					
* * *	BEGIN STRATA # 3 * * *											
143	3048.21	85.74	.000	.000	.000	.000	.000					
		AUTO #36 E14-01	.000	.000	.000	.000	.000					

SPECTRUM I.D. | CORE LOCATION PARAMETERS | FUEL ELEMENT I.D.

COMPARISIONS OF SELECTED VALUES & ITEMS

GA.TAG NO.	AXIAL CORE LOC. CENTER POINT (MM)	SCAN INTERVAL	CS137 MEAN 'C'	CS4/7 MEAN 'M'	REL.DIF. Z=-1+C/M	COMPARISON TEST 1 D=Z/S(Z)	COMPARISON TEST 2 D**2	'C'	'M'	REL.DIF. Z=-1+C/M	COMPARISON TEST 1 D=Z/S(Z)	COMPARISON TEST 2 D**2
144	3134.63	76.22	.000	.000	.000	.000	.000					
		AUTO #37 E14-01	.000	.000	.000	.000	.000					
* * *	STRATA # 3 E14-01 TOTALS * * *											
MEAN =	3091.42	WT MEAN COMP. =	.000	.000	.000	.000	.000					
RMS =	43.21	WT MEAN 1SIGMA=	.000	.000	.000	.000	.000					
MIDPT=	3091.42	WT RMS =	.000	.000	.000	.000	.000					
RANGE=	162.64	WT ERROR =	.000	.000	.000	.000	.000					
* * *	BEGIN STRATA # 4 * * *											
145	2516.76	1.00	.865	.928	-.068	-1.060	1.123					
		STAT #1 E14-01	.036	.051	.064	.000	.000					
146	1804.21	1.00	1.181	1.209	-.023	-.436	.190					
		STAT #2 E14-01	.040	.052	.053	.000	.000					
147	1820.67	1.00	1.179	1.258	-.063	-1.266	1.602					
		STAT #3 E14-01	.039	.052	.050	.000	.000					
148	1837.16	1.00	1.266	1.103	.148	2.314	5.353					
		STAT #4 E14-01	.044	.048	.064	.000	.000					
149	1853.64	1.00	1.239	1.083	.144	2.158	4.656					
		STAT #5 E14-01	.044	.050	.067	.000	.000					
150	1870.10	1.00	1.446	1.028	.407	5.538	30.674					
		STAT #6 E14-01	.045	.043	.073	.000	.000					
151	996.90	1.00	.977	.793	.231	2.724	7.423					
		STAT #7 E14-01	.038	.045	.085	.000	.000					
152	239.04	1.00	.036	.000	.000	.000	.000					
		TRAP E14-01	.005	.000	.000	.000	.000					
* * *	STRATA # 4 E14-01 TOTALS * * *											
MEAN =	1617.31	WT MEAN COMP. =	1.023	1.057	.111	1.425	7.289					
RMS =	645.94	WT MEAN 1SIGMA=	.038	.049	.066	.000	.000					
MIDPT=	1377.90	WT RMS =	.408	.148	.162	2.293	9.844					
RANGE=	-2276.72	WT ERROR =	.014	.018	.025	.000	.000					

T O T A L   S T R A T A   E 1 4 - 0 1

MEAN =	1818.11	WT MEAN COMP. =	1.000	1.000	.047	-.121	1.659
RMS =	1818.11	WT MEAN 1SIGMA=	.089	.120	.194	.000	.000
MIDPT=	1818.11	WT RMS =	.197	.242	.289	1.282	1.870
RANGE=	1818.11	WT ERROR =	.018	.024	.039	.000	.000

ABSOLUTE NUCLIDE ACTIVITIES +/- 1 SIGMA ERROR E14-01

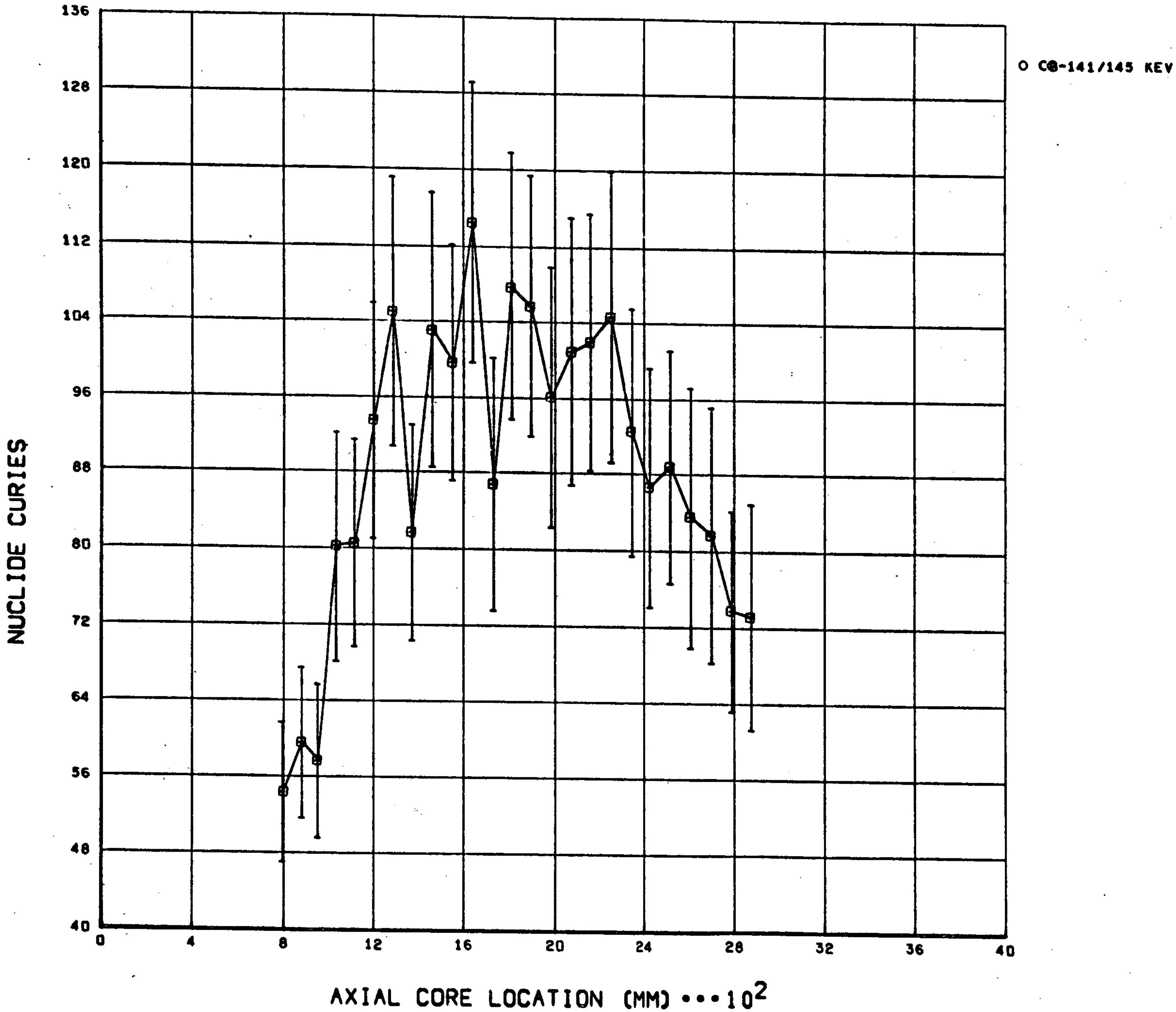

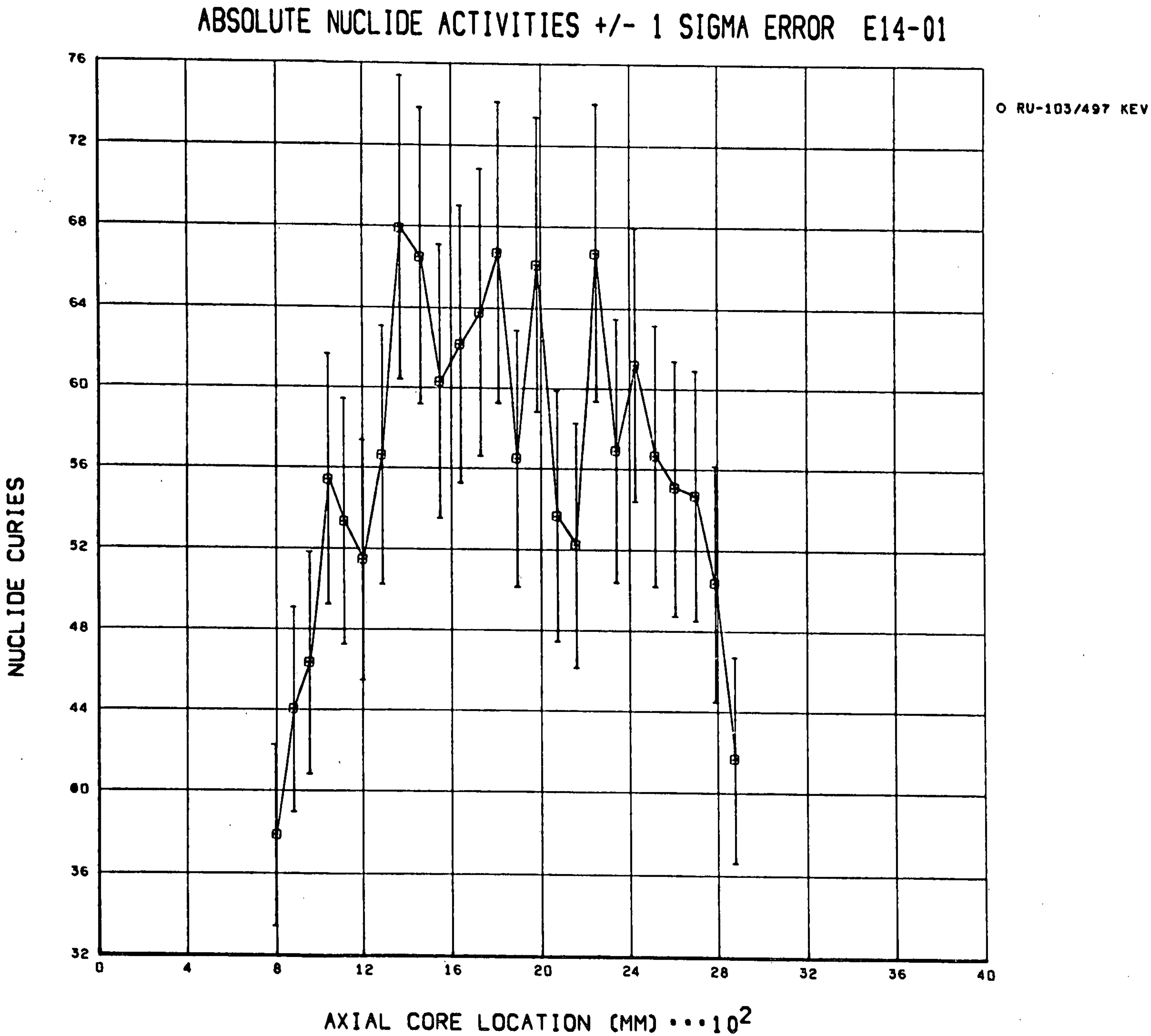

ABSOLUTE NUCLIDE ACTIVITIES +/- 1 SIGMA ERROR E14-01
O RU-103/497 KEV
NUCLIDE CURIES
AXIAL CORE LOCATION (MM) •••10^2
76
72
68
64
60
56
52
48
44
40
36
32
0
4
8
12
16
20
24
28
32
36
40

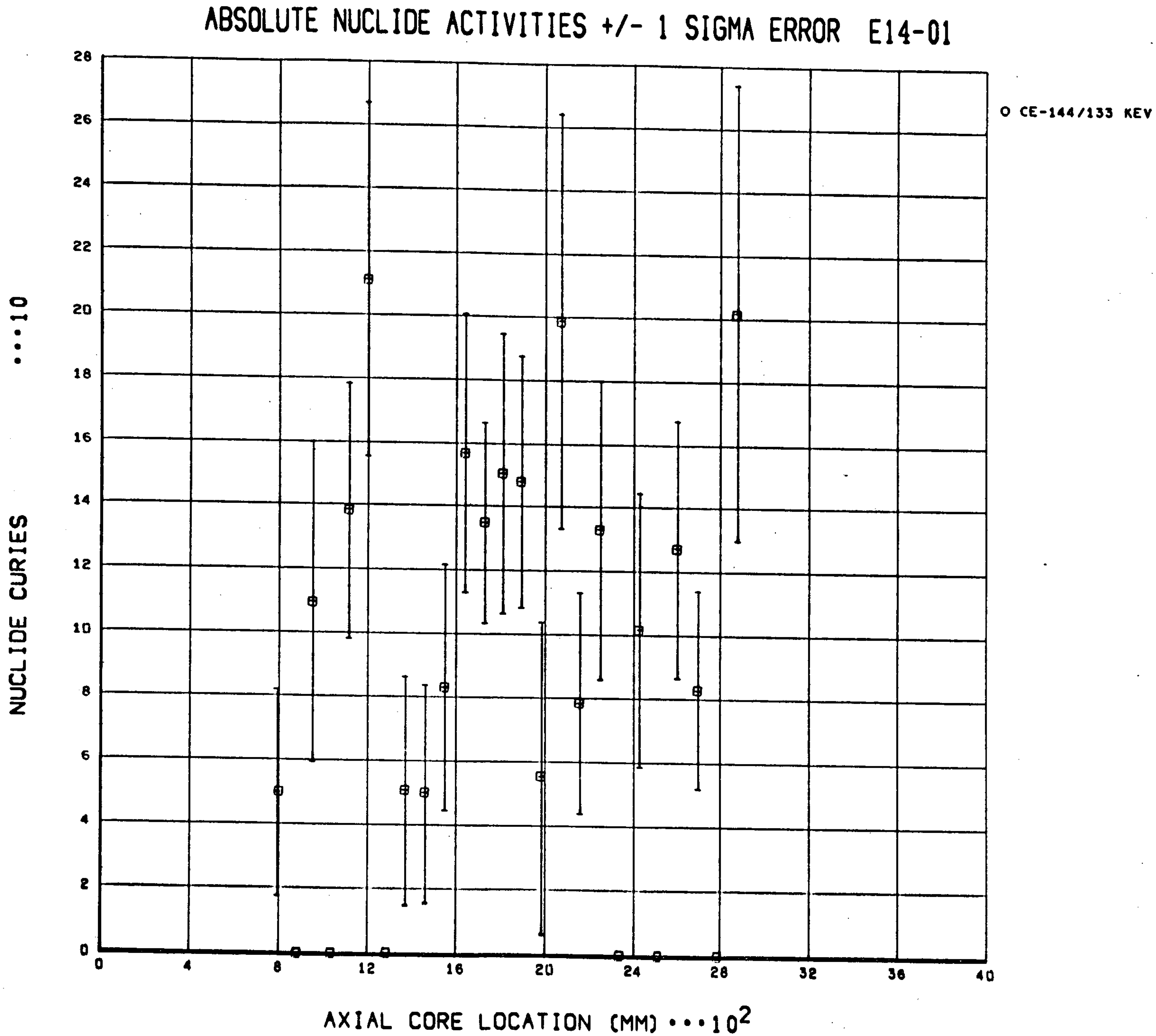
ABSOLUTE NUCLIDE ACTIVITIES +/- 1 SIGMA ERROR E14-01
O CE-144/133 KEV
NUCLIDE CURIES •••10
AXIAL CORE LOCATION (MM) •••10²
0
2
4
6
8
10
12
14
16
18
20
22
24
26
28
32
36
40

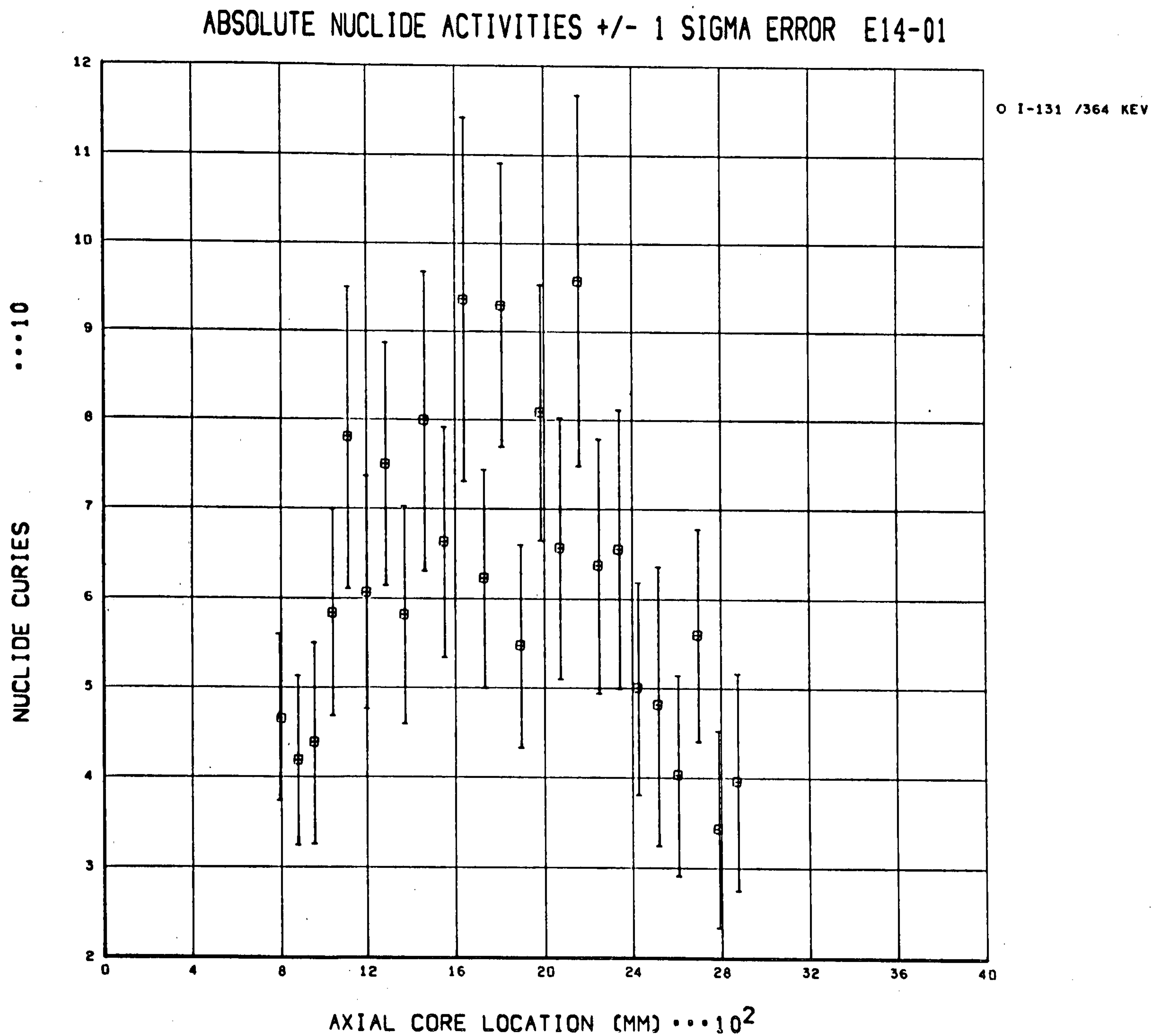
ABSOLUTE NUCLIDE ACTIVITIES +/- 1 SIGMA ERROR E14-01
O I-131 /364 KEV
NUCLIDE CURIES •••10
AXIAL CORE LOCATION (MM) •••10^2
12
11
10
9
8
7
6
5
4
3
2
0
4
8
12
16
20
24
28
32
36
40

NUCLIDE COUNTS PER MINUTE RATIOS +/- 1 SIGMA ERROR E14-01

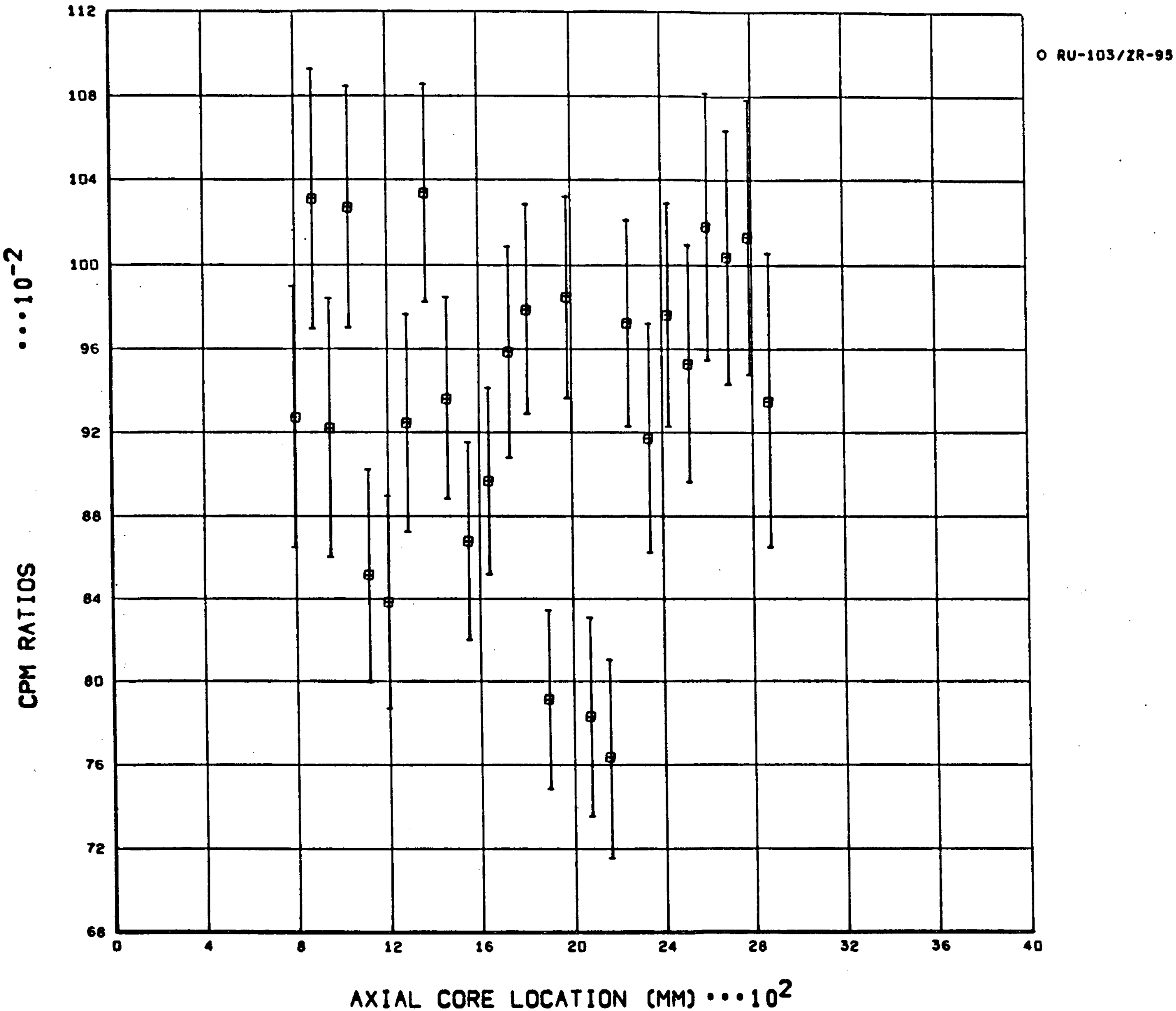

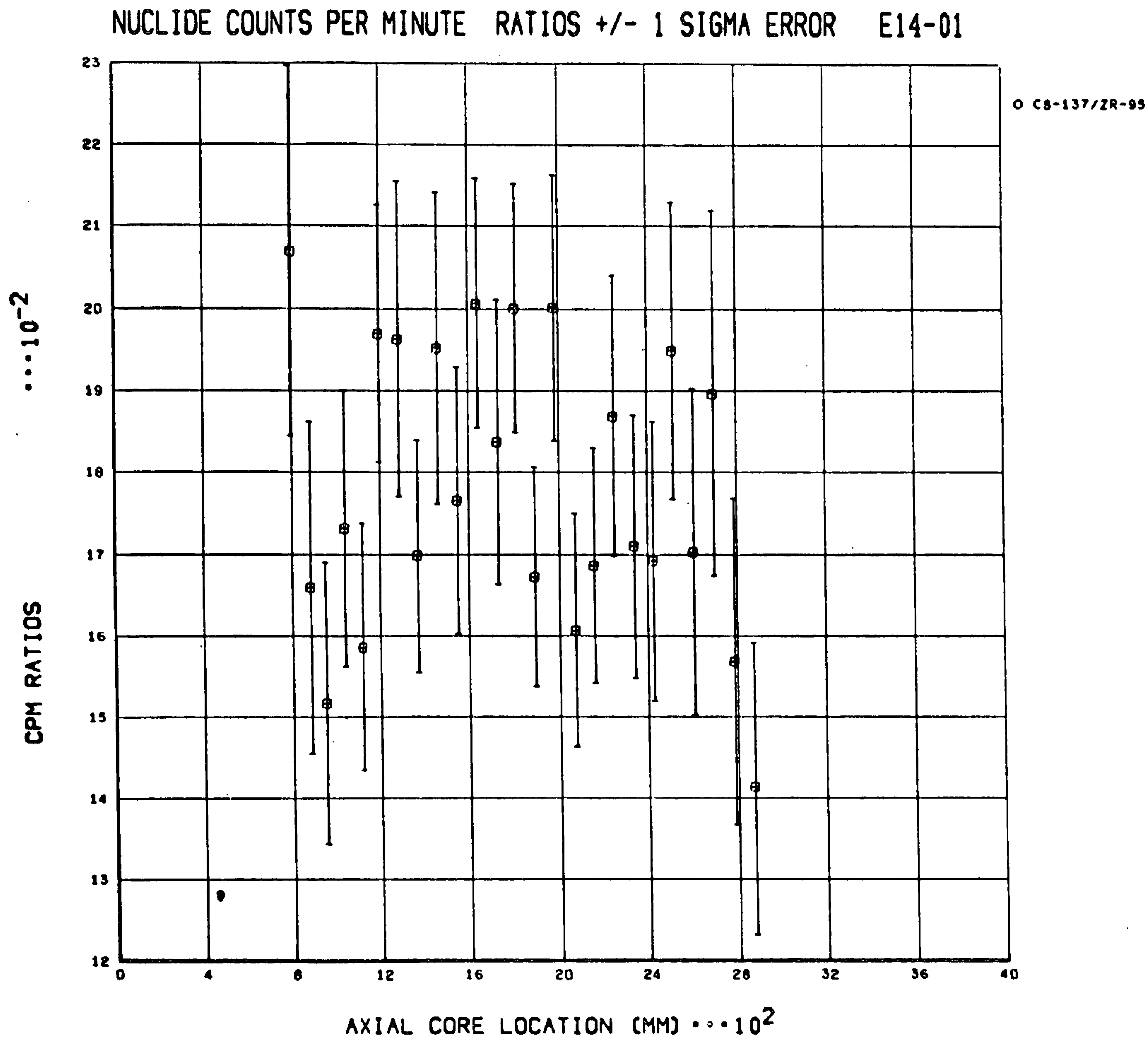
NUCLIDE COUNTS PER MINUTE RATIOS +/- 1 SIGMA ERROR E14-01
O CS-137/ZR-95
CPM RATIOS ••• 10^-2
AXIAL CORE LOCATION (MM) ••• 10^2
23
22
21
20
19
18
17
16
15
14
13
12
0
4
8
12
16
20
24
28
32
36
40

C-39

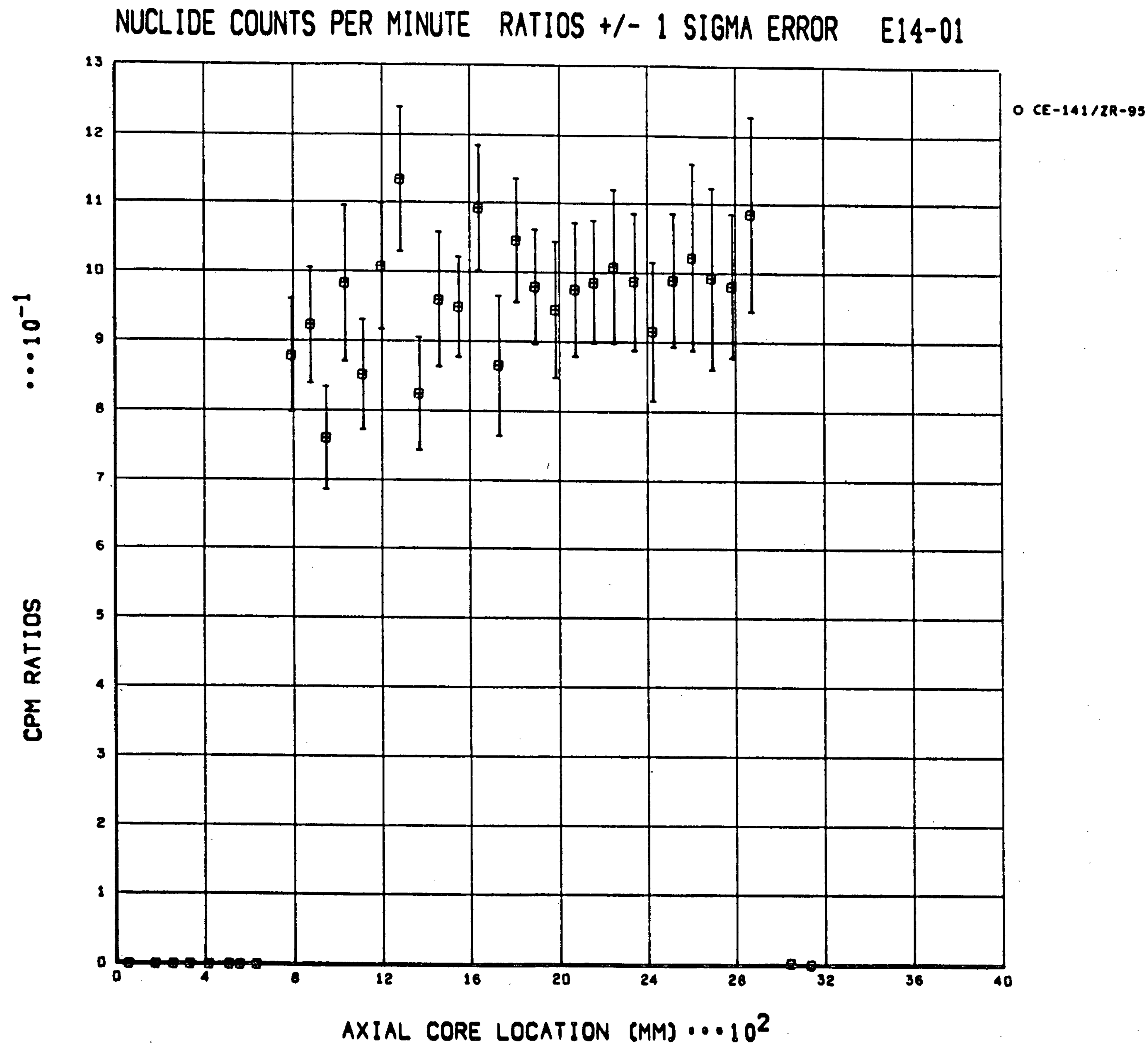
NUCLIDE COUNTS PER MINUTE RATIOS +/- 1 SIGMA ERROR E14-01
O CE-141/ZR-95
CPM RATIOS •••10^-1
AXIAL CORE LOCATION (MM) •••10^2
0
1
2
3
4
5
6
7
8
9
10
11
12
13
0
4
8
12
16
20
24
28
32
36
40

NUCLIDE COUNTS PER MINUTE RATIOS +/- 1 SIGMA ERROR E14-01

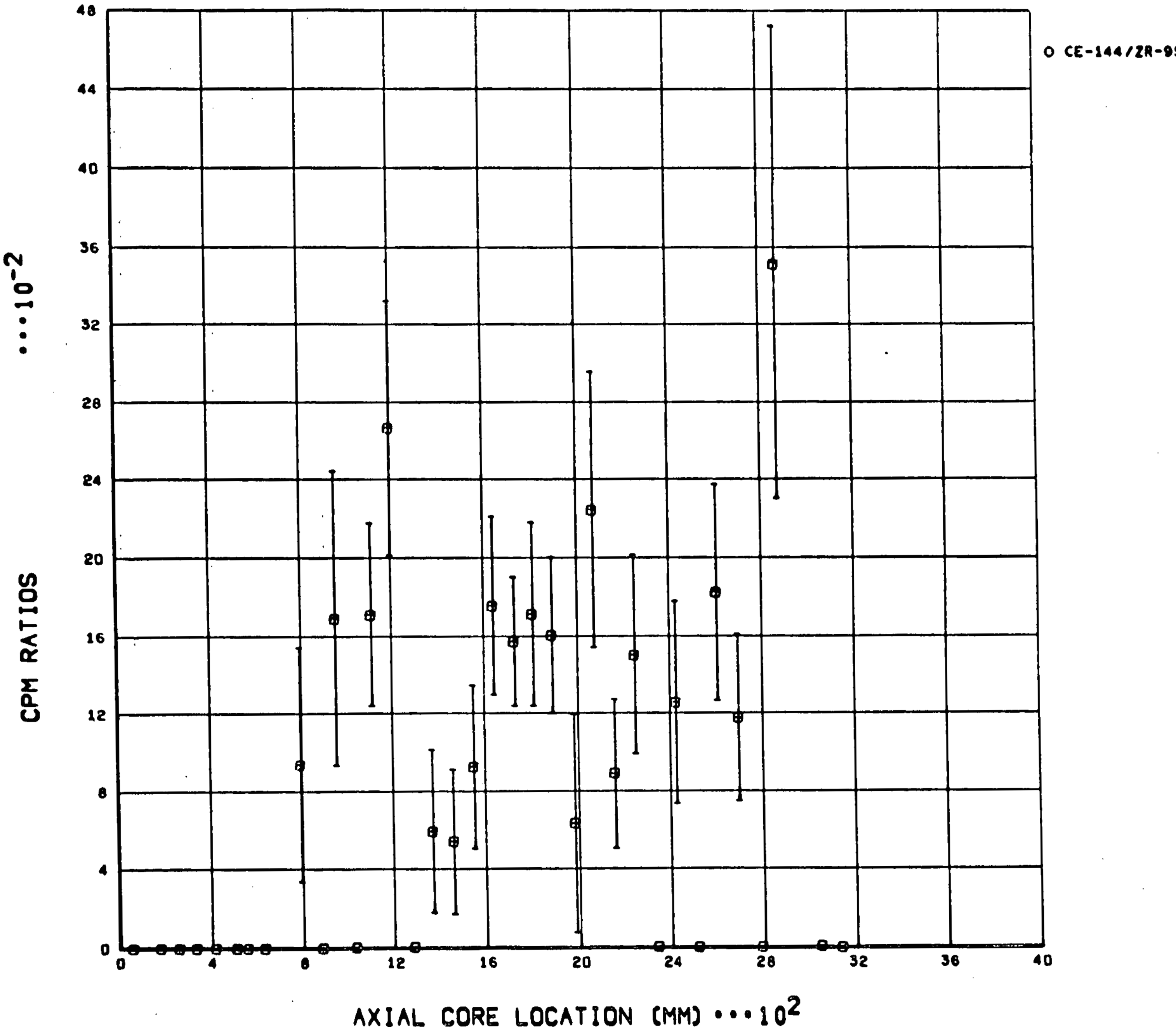

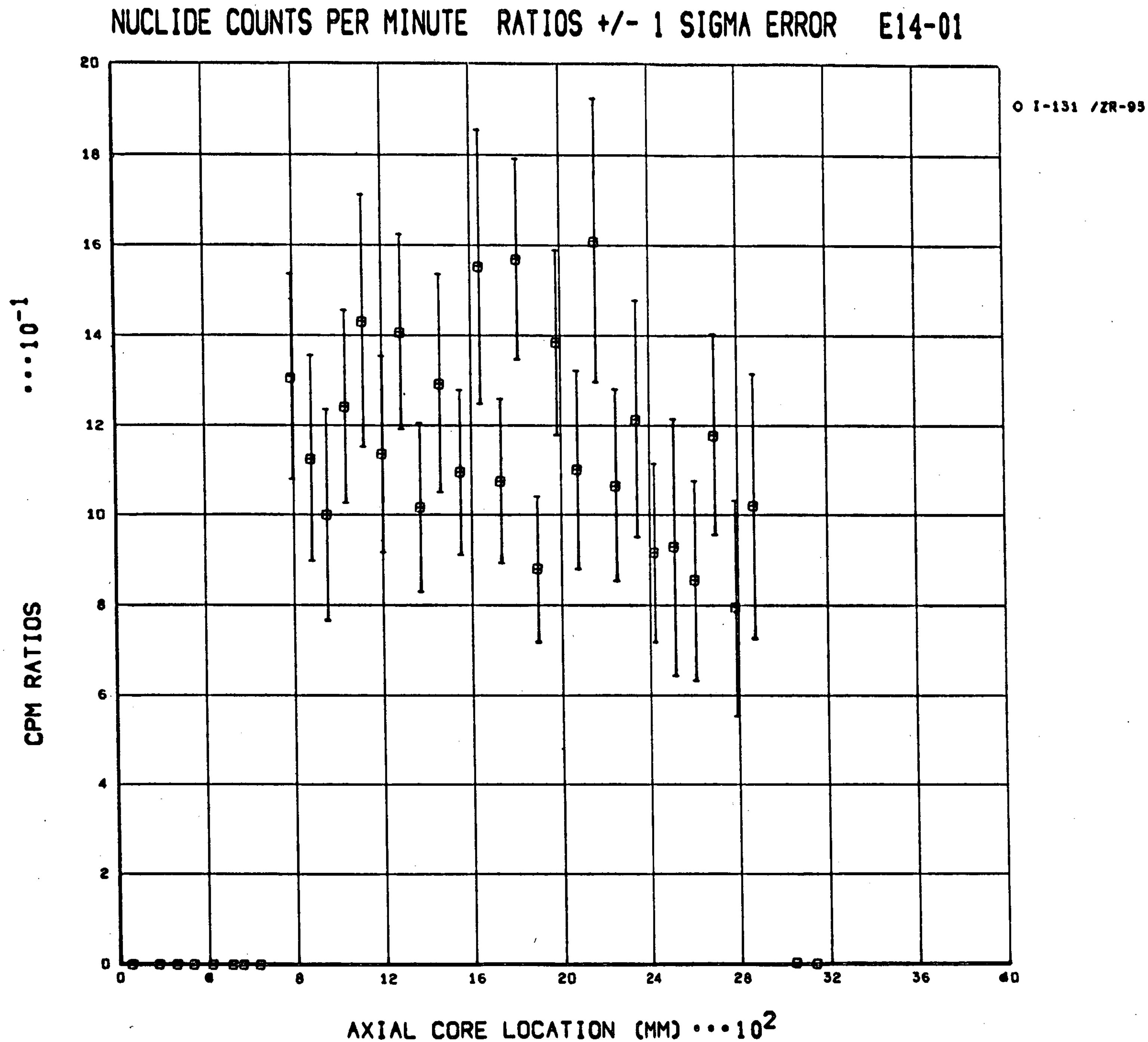
NUCLIDE COUNTS PER MINUTE RATIOS +/- 1 SIGMA ERROR E14-01
O I-131 /ZR-95
CPM RATIOS •••10⁻¹
AXIAL CORE LOCATION (MM) •••10²
0
2
4
6
8
10
12
14
16
18
20
0
4
8
12
16
20
24
28
32
36
40

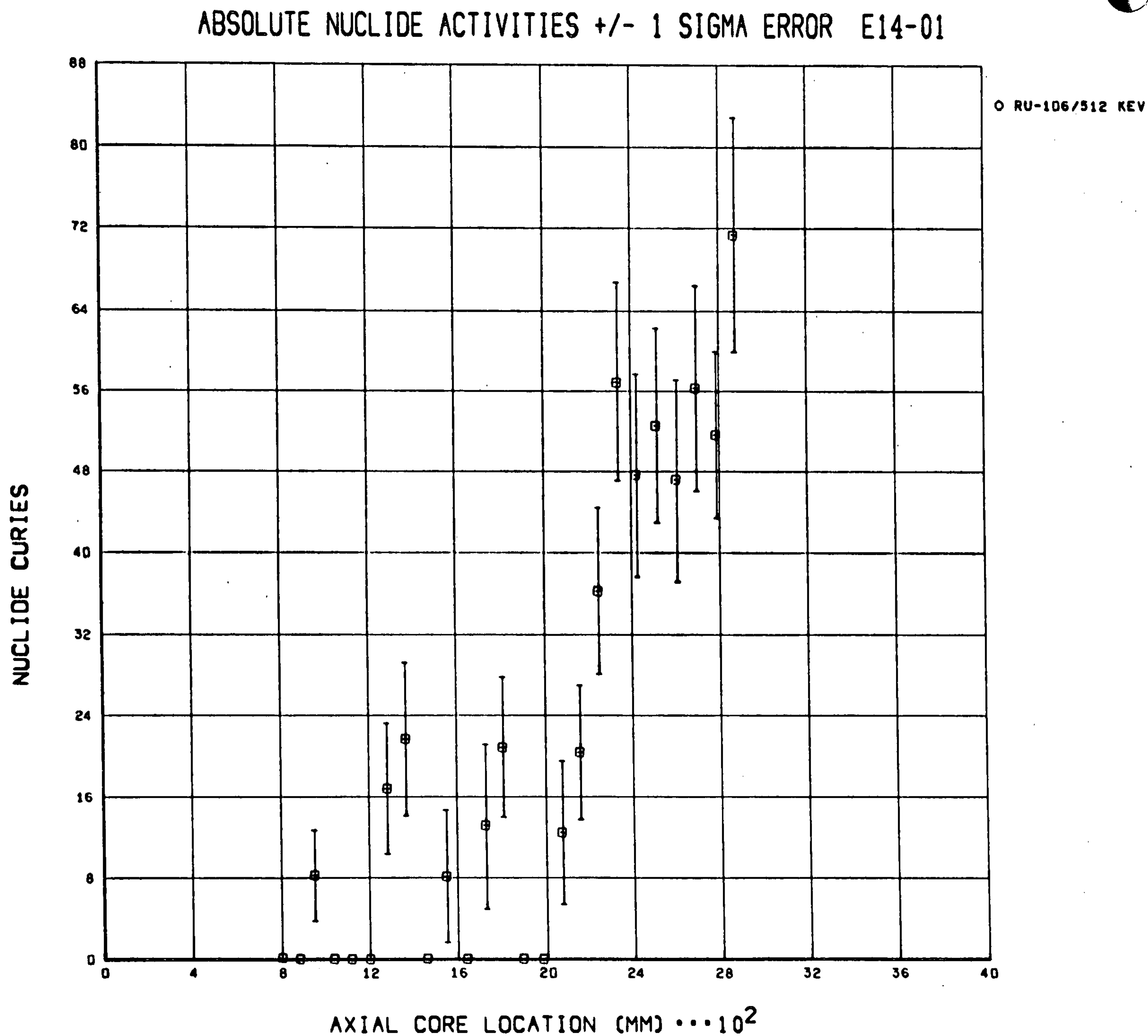
ABSOLUTE NUCLIDE ACTIVITIES +/- 1 SIGMA ERROR E14-01
O RU-106/512 KEV
NUCLIDE CURIES
0
8
16
24
32
40
48
56
64
72
80
88
0
4
8
12
16
20
24
28
32
36
40
AXIAL CORE LOCATION (MM) •••10^2

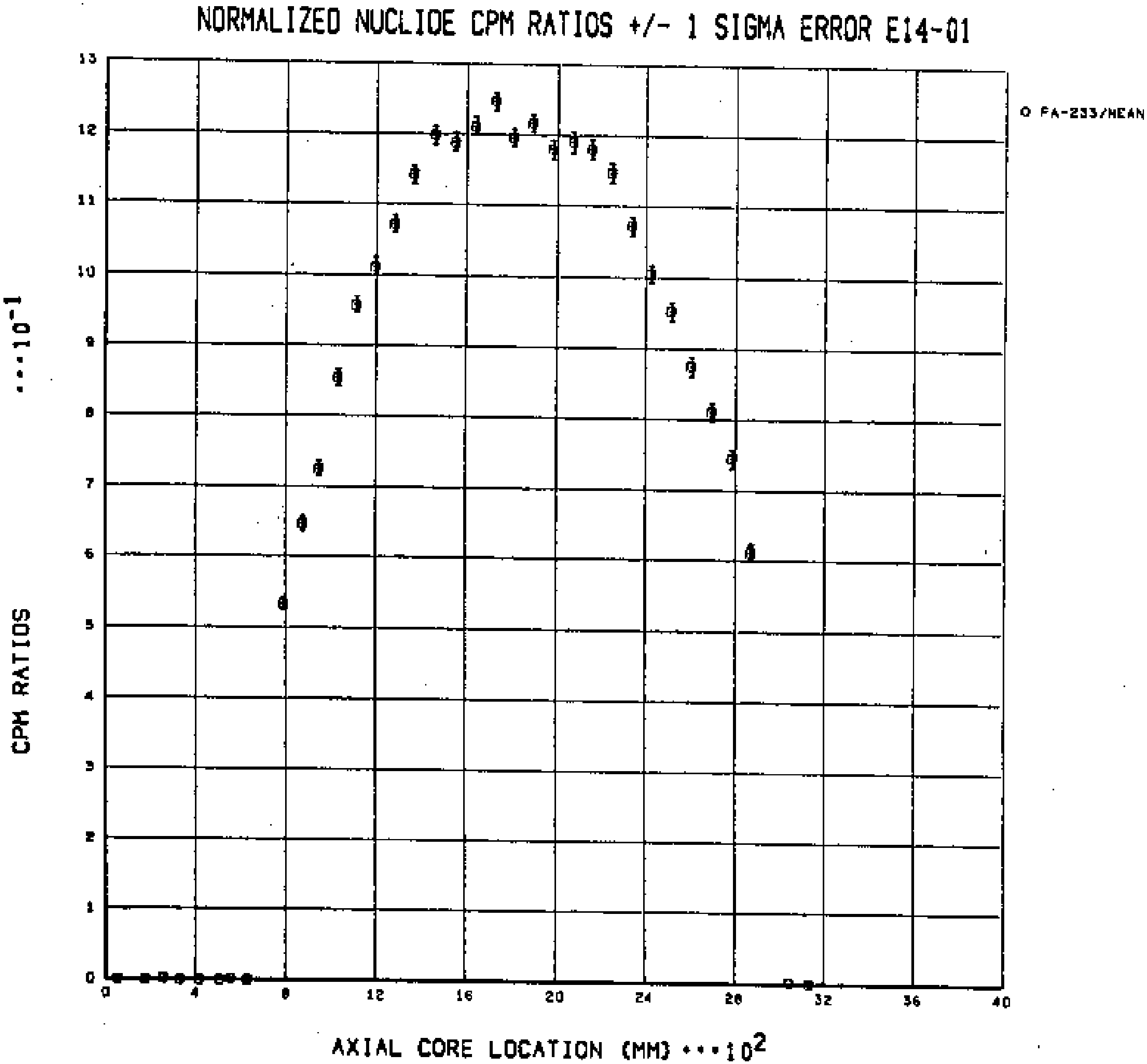
NORMALIZED NUCLIDE CPM RATIOS +/- 1 SIGMA ERROR E14-01
O PA-233/MEAN
CPM RATIOS
***10^-1
AXIAL CORE LOCATION (MM) ***10^2
0
4
8
12
16
20
24
28
32
36
40
1
2
3
4
5
6
7
8
9
10
11
12
13

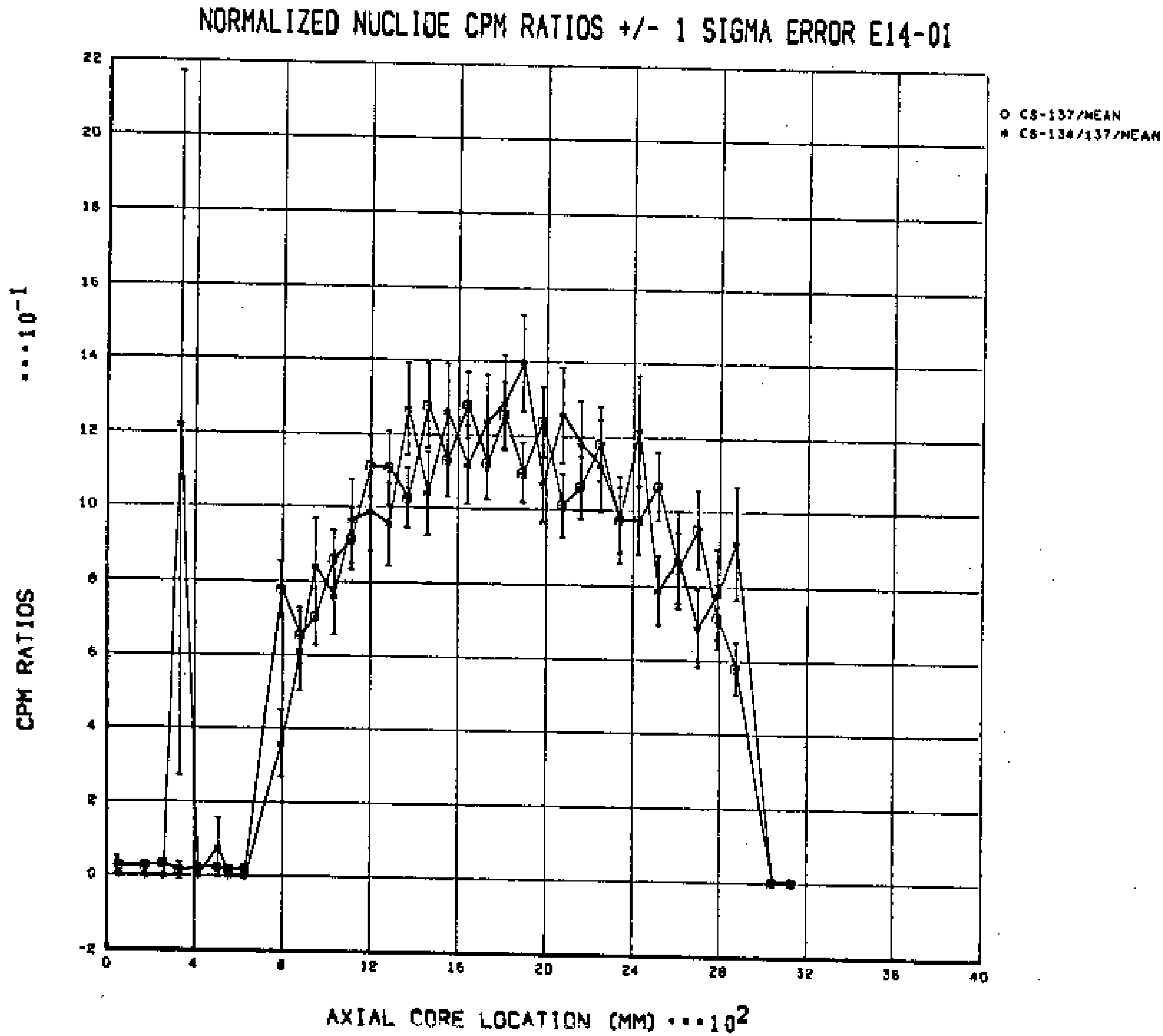
NORMALIZED NUCLIDE CPM RATIOS +/- 1 SIGMA ERROR E14-01
O CS-137/MEAN
* CS-134/137/MEAN
CPM RATIOS
***10^-1
AXIAL CORE LOCATION (MM) ***10^2

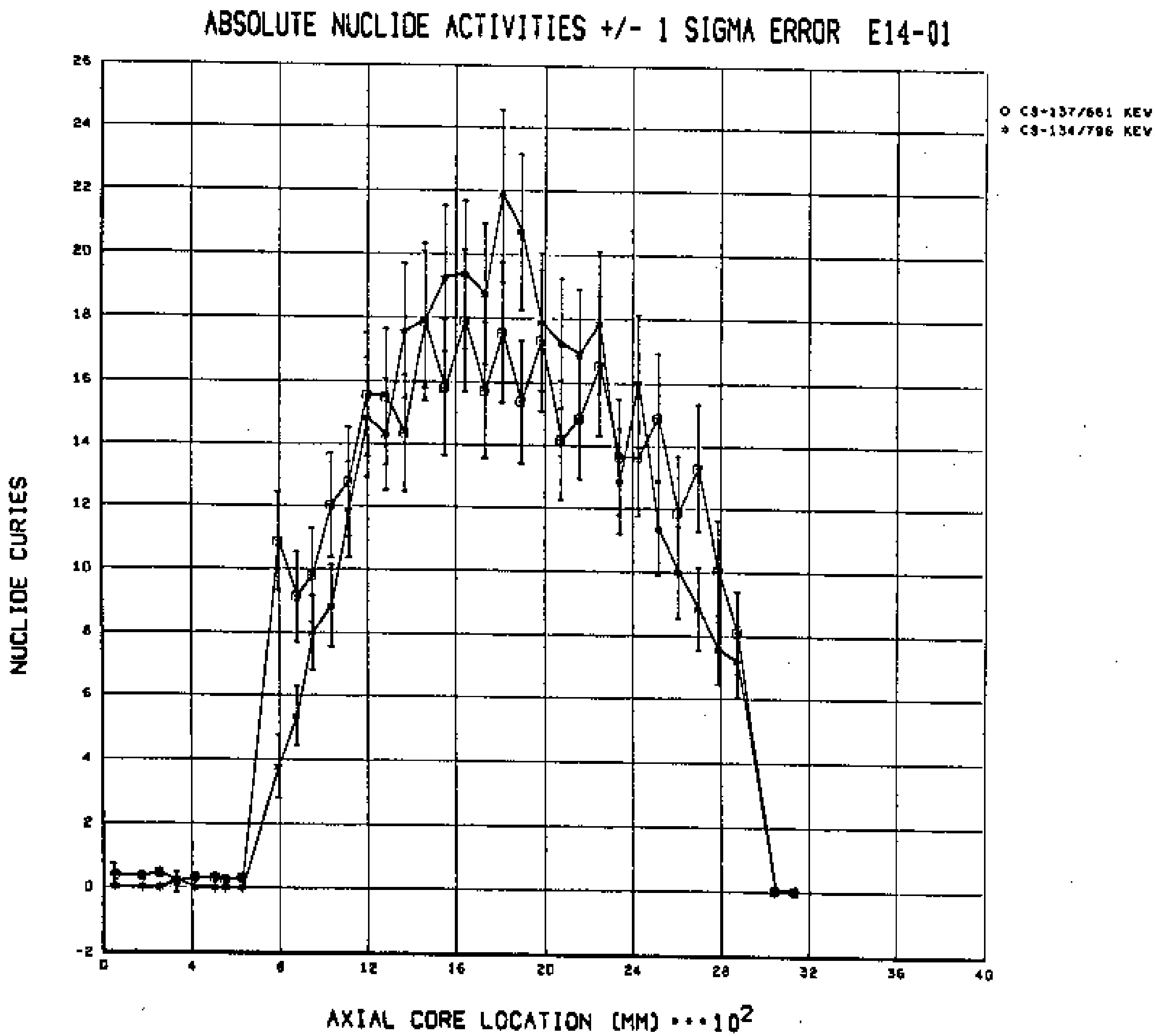
ABSOLUTE NUCLIDE ACTIVITIES +/- 1 SIGMA ERROR E14-01
O CS-137/661 KEV
* CS-134/796 KEV
NUCLIDE CURIES
AXIAL CORE LOCATION (MM) ***10²
-2
0
2
4
6
8
10
12
14
16
18
20
22
24
26
0
4
8
12
16
20
24
28
32
36
40

NORMALIZED NUCLIDE CPM RATIOS +/- 1 SIGMA ERROR E14-01

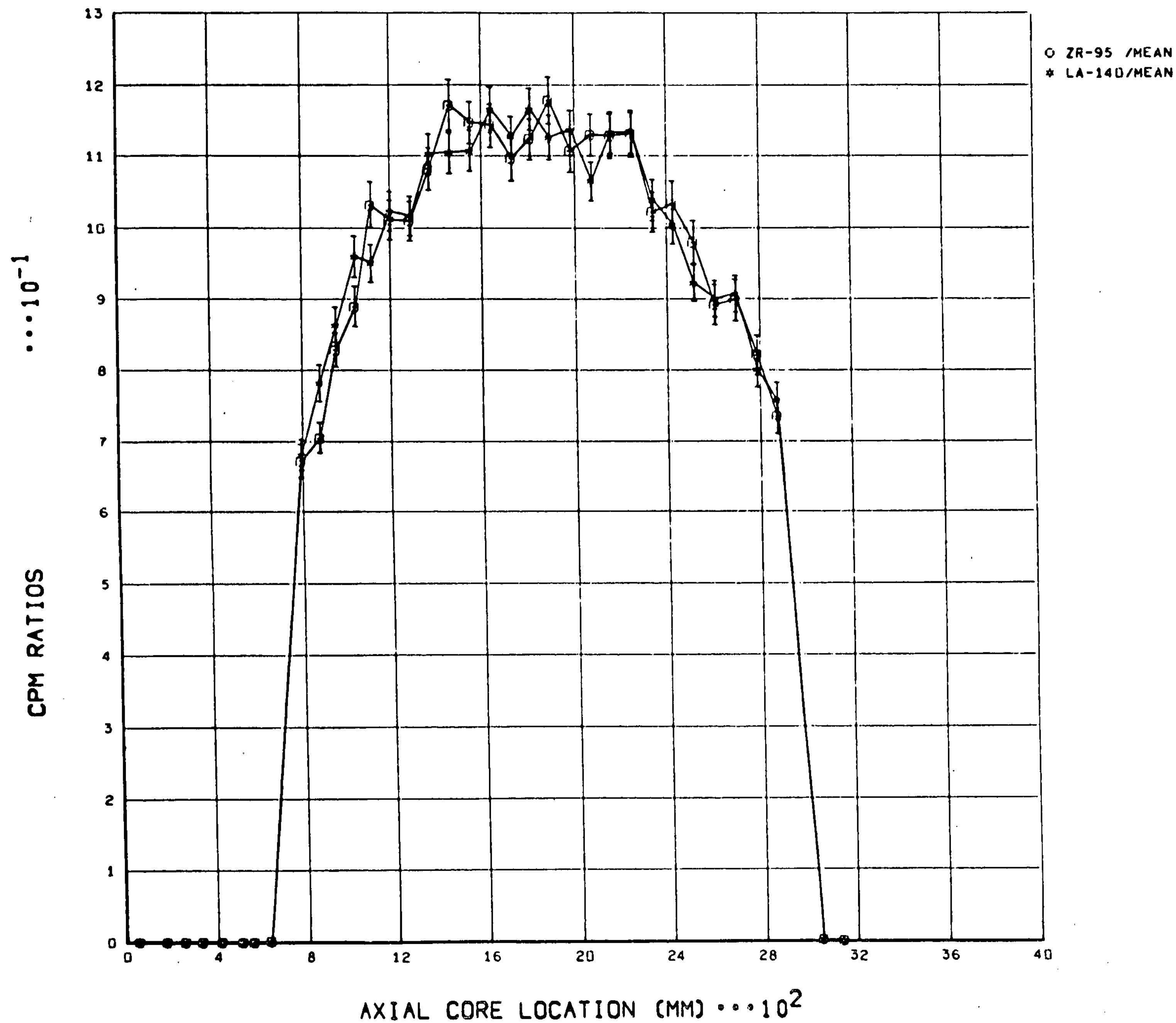

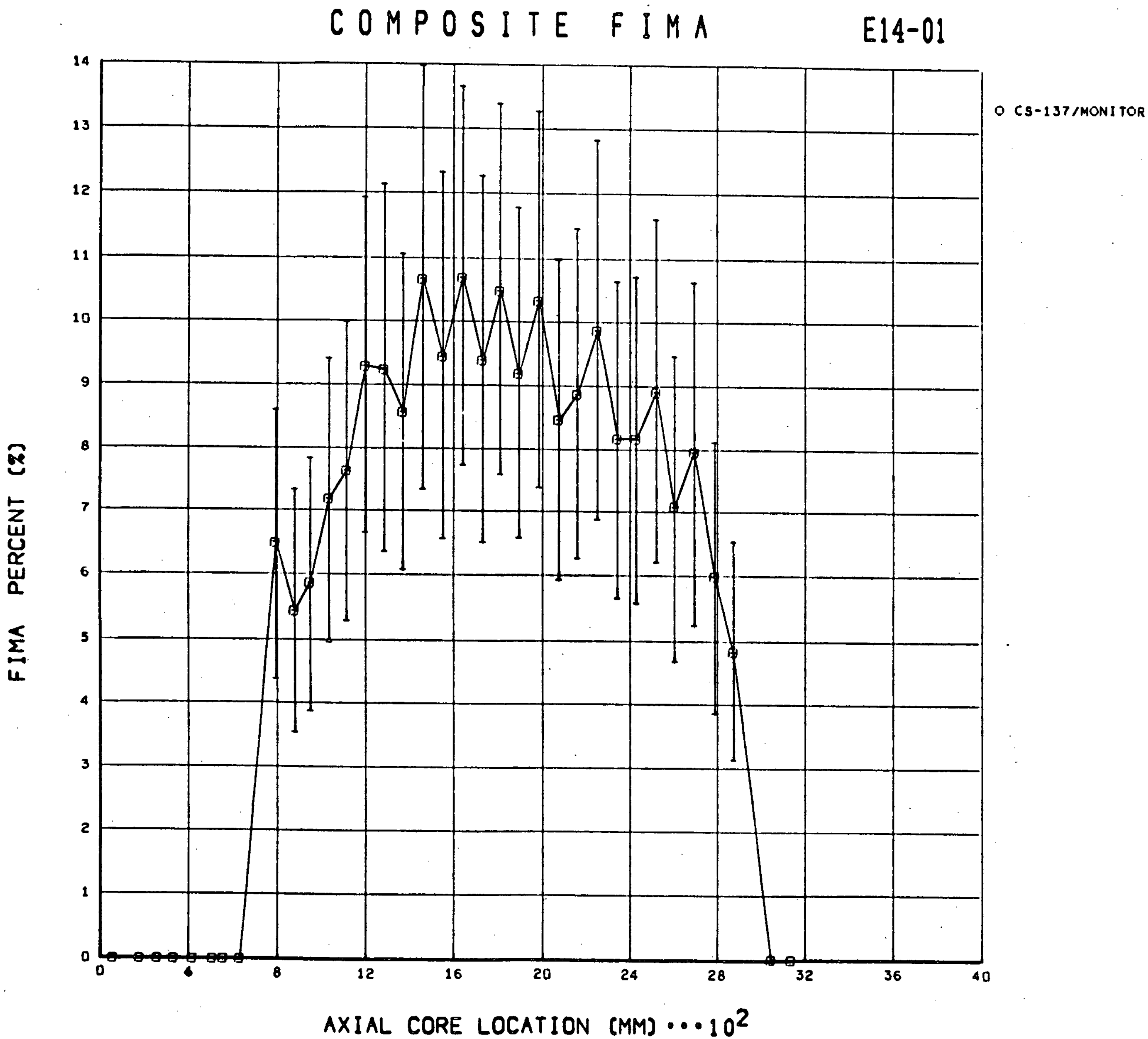
COMPOSITE FIMA
E14-01
O CS-137/MONITOR
FIMA PERCENT (%)
AXIAL CORE LOCATION (MM) •••10^2
0
1
2
3
4
5
6
7
8
9
10
11
12
13
14
0
4
8
12
16
20
24
28
32
36
40